uOttawa

L'Université canadienne
Canada's university

FACULTÉ DES ÉTUDES SUPÉRIEURES ET POSTOCTORALES

uOttawa

L'Université canadienne
Canada's university

FACULTY OF GRADUATE AND POSDOCTORAL STUDIES

Mary-Luyza Avramescu
AUTEUR DE LA THÈSE / AUTHOR OF THESIS

Ph.D. (Biology)
GRADE / DEGREE

Department of Biology
FACULTÉ, ÉCOLE, DÉPARTEMENT / FACULTY, SCHOOL, DEPARTMENT

Biogeochemical Factors Influencing Net Mercury Methylation in Freshwater Systems

TITRE DE LA THÈSE / TITLE OF THESIS

Danielle Fortin
DIRECTEUR (DIRECTRICE) DE LA THÈSE / THESIS SUPERVISOR

CO-DIRECTEUR (CO-DIRECTRICE) DE LA THÈSE / THESIS CO-SUPERVISOR

Tamar Barkay (Rutgers University)

Jules Blais

Alexandre Poulain

Tony Scheuhammer

Gary W. Slater
Le Doyen de la Faculté des études supérieures et postdoctorales / Dean of the Faculty of Graduate and Postdoctoral Studies

BIOGEOCHEMICAL FACTORS INFLUENCING NET MERCURY METHYLATION IN FRESHWATER SYSTEMS

Mary-Luyza Avramescu

Thesis submitted to the

Faculty of Graduate and Postdoctoral Studies

In partial fulfillment of the requirements for the

Ph.D. degree in

Chemical and Environmental Toxicology

Ottawa-Carleton Institute of Biology

and

University of Ottawa

Ottawa, Canada

Thèse soumise à la

Faculté des études supérieures et postdoctorales

en vue de l'obtention du doctorat en

Toxicologie Chimique et Environnementale

L'Institut de biologie d'Ottawa-Carleton

and

Université d'Ottawa

Ottawa, Canada

Your file Votre référence
ISBN: 978-0-494-69128-1
Our file Notre référence
ISBN: 978-0-494-69128-1

ABSTRACT

Mercury methylation in aquatic systems has been linked to the activity of various anaerobic microbes, including sulfate-reducers (SRB), iron-reducers (FeRP) and methanogens (MPA). This study focuses on the biogeochemical factors, i.e., the relative importance of the diverse groups of anaerobic microbes, that affect net methyl mercury formation in freshwater. Methylation and demethylation were measured separately using enriched stable isotopes of mercury in microcosms treated with specific microbial inhibitors and abiotic control systems. Non-contaminated sediments from the Mer Blue wetland in Ottawa, Ontario, were used to test the proper set up and methods to be used for future experiments. Mercury-contaminated sediments of the St. Lawrence River (SLR) in Cornwall (Zone 1), Ontario, were investigated because they have been found to be a potential source of MeHg in the food web and the river system.

In the Zone 1 SLR sediments, strong positive correlations were observed between methylation rate constants and sulfate reducing rates, as well as demethylation rates constants and methane production rates, indicating that SRB are primary methylators and MPA have the leading role in methylmercury demethylation. The inhibition of both SRB and MPA enhanced iron-reduction while MeHg production was not completely stopped, indicating that iron-reduction might however be another important process in MeHg production in the Zone 1 SLR sediments, probably by decreasing demethylation rather than favouring methylation, as shown by the strong negative correlation between Kd and iron-reduction rates. Similar findings were obtained for the Mer Bleue sediments, with the exception that SRB were involved in both methylation and demethylation.

A new modified procedure for measuring mercury isotopes in sediment samples was also proposed. The procedure uses acid leaching-ion exchange-thiosulfate extraction (TSE) to isolate and purify the methylated mercury from the matrix. Major advantages of the TSE procedure include the extraction and analysis of a large number of samples in a short time, excellent analyte recoveries, and the lack of artefact formation. Recoveries between 94 and 106% were obtained for the standards CRMs, BCR 580 and IAEA 405.

Comparisons between TSE and other procedures (distillation, acid-leaching) have shown good agreement of methylmercury values.

SOMMAIRE

La méthylation du mercure dans les environnements aquatiques dépend en partie de l'activité des bactéries anaérobiques, principalement les bactéries sulfato-reductrices, les bactéries ferro-reductrices et les méthanogènes. Le but de cette étude est de déterminer les facteurs biogéochimiques affectant la méthylation du mercure, plus précisément, l'importance relative de chaque groupe de bactéries dans la methylation nette du mercure. La méthylation et la déméthylation du Hg ont été mesurées lors d'incubations contenant des sédiments injectés avec des isotopes stables du Hg et des inhibiteurs microbiens spécifiques. Les sédiments non contaminés du marais Mer Bleue, près d'Ottawa, en Ontario, ainsi que les sédiments contaminés du fleuve St Laurent, près de Cornwall en Ontario, ont été le sujet de cette thèse.

Nos résultats indiquent que pour les sédiments contaminés du fleuve St Laurent, une forte corrélation a été observée entre la constante du taux de methylation et celle du taux de réduction de sulfates, ainsi qu'entre la constante du taux de demethylation (Kd) et celle du taux de production de méthane, indiquant que les bactéries sulfato-réductrices sont les bactéries responsables de la méthylation, alors que les méthanogènes sont impliqués dans la déméthylation. L'inhibition des bactéries sulfato-réductrices et des méthanogènes a eu pour effet d'augmenter l'activité des bactéries ferro-reductrices. La methylation du Hg n'a toutefois pas été complètement inhibée, ce qui suggère que la réduction des oxydes de fer dans les sédiments du fleuve St Laurent représente un processus important associé à la methylation du Hg. Des résultats similaires ont été observés pour les sédiments du marais Mer Bleue.

Cette thèse inclut aussi une modification de la méthode utilisée pour la détermination des isotopes du Hg. La nouvelle procédure utilise une extraction acide combinée à un échange d'ions afin d'isoler et de purifier le mercure méthylé dans la matrice. Les avantages majeurs de cette nouvelle méthode incluent l'extraction et l'analyse d'un grand nombre d'échantillons sur une courte période de temps, ainsi que l'absence d'artéfacts. Nos résultats indiquent aussi que nous pouvons récupérer des standards, tels CRM, BCR 580 et IAEA 405, à des taux se situant entre 94 et 106 %.

AKNOWLEDGEMENTS

During the course of my Ph.D. thesis, I have benefited a lot from the mentorship of numerous outstanding individuals both from within and outside the university. My heartfelt gratitude and thanks go out to all of them since this thesis would not have seen its completion without their help.

First and foremost, I would like to express my deepest gratitude to my supervisors, Dr. Danielle Fortin and Dr. David Lean, for their scientific and moral support throughout my research years and the completion of this thesis. I am very grateful for their steady encouragement and the way they have always found the time to discuss my ideas, helping shape and push the writing process forward through its completion. I feel privileged to have been allowed to get to know and learn from them.

I would also like to extend my most sincere thanks to all my committee members, Dr. Jules Blais, Dr. Nimal de Silva, Dr. Scot Findlay and Dr. Anton Scheuhammer for their guidance and advice.

A very special "thank you" to Dr. Holger Hintelmann for welcoming me to his laboratory at Trent University, as well as for his insightful advice and feedback during critical analytical moments. My research would not have been possible without his collaboration. I would also like to express my gratitude to Dr. Jeff Ridal and the St. Lawrence River Institute in Cornwall, for their technical and sampling support during my study.

This research was also carried out with the support of an NSERC Discovery Grant awarded to Dr. David Lean, and a Best in Science Grant from the Ontario Ministry of the Environment, Canada, along with an NSERC and Excellence Scholarship awarded to Luyza Avramescu.

I have received assistance from many researchers, technicians, graduate and undergraduate students: i.e., Emmanuel Yumvihoze, Jutta Meyer, Susan Winch, Vanessa Mongeon, Jonathan Mayo, Willy de Wit, Paul Middlestead, Katrina, Sean Langley, Andrew Gault, Anu Ananth, Ping Zhang, Monika Wilk, Kristen Feige, Raphael Lavöi, Tamar Bodek, Serena Maharadjah, Tania Delongchamp, Linda Kimpe, Ogo Nwobu, Jenifer Gibson, John Holmes, Nelson O'Driscoll, Tulita Seminario, and many others from

the Fortin and Lean's laboratories. I thank all of them for their kind support and friendship along the way. My sincere thanks are also extended to Joy Zhu from Trent University for her assistance with the isotope analyses.

Finally, I wish to thank my mother for her unconditional support, love and understanding through this whole experience. My special appreciation goes to my long-time friend Claudia Taraibuta for her true friendship, encouragement and for believing in me. My final and greatest thanks are for my husband Cornel Avramescu for putting up with me through the good and the bad, and always helping me move forward; you are my emotional base and partner in every sense. I am also grateful to my daughter Andrea for the amazing joy and love she is bringing to my everyday life.

Thank you all so much for your support!

Sincerely,
Luyza Avramescu
Ottawa, May 2010

TABLE OF CONTENTS

LIST OF FIGURES

CHAPTER 2

CHAPTER 3

CHAPTER 4

LIST OF TABLES

CHAPTER 2

CHAPTER 3

CHAPTER 4

LIST OF ABBREVIATIONS

CRM	certified reference material
CVAFS	cold-vapor atomic fluorescence spectrometry
DL	detection limit
DOC	dissolved organic carbon
DOM	dissolved organic matter
DMeHg	dimethylmercury
GC-AFS	gas chromatography - atomic fluorescence spectrometry
GC-ICP-MS	gas chromatography -inductively coupled plasma mass spectrometry
FeRP	iron reducing prokariots
FeRR	Iron reduction rates
MDL	Method detection limit
MeHg	methylmercury
$Me^{199}Hg$	methylmercury containing the ^{199}Hg isotope (used to trace demethylation)
$Me^{200}Hg$	methylmercury containing the ^{200}Hg isotope (used to trace methylation)
Amb-MeHg	ambient methylmercury content in the sample (^{202}Hg isotope)
ΣMeHg	Sum of all methylmercury isotopes in the samples ($Me^{199}Hg + Me^{200}Hg + Me^{202}Hg$)
MPA	methane producing archaea or methanogens
OD	oxidative demethylation
RD	reductive demethylation
RSE	relative standard error (SE/mean)
SE	standard error (standard deviation/square root of n)
SRB	sulphate-reducing bacteria
SRR	sulphate reducing rates
SSIDA	species specific isotopes dilution analysis
THg	total mercury
HFO	Ferrihydrite (six line)

CHAPTER 1. INTRODUCTION

1.1. Thesis Rationale

Monomethylmercury (MeHg) is the most toxic form of mercury (Hg) present in the environment because it is the only mercury compound that is bioaccumulated and biomagnified in the food web [Scheuhammer et al. 2007, Hammerschmidt et al., 2002; Morel, 1998]. High concentrations of monomethylmercury in fish have led to increasing health concerns that have resulted in health advisories and to the avoidance of many traditional and nutritious foods. It is now clear that the pathways leading to mercury methylation are of highest scientific priority. This study focuses on the biogeochemical factors that affect net methyl mercury formation in freshwater systems. In aquatic environment, the net methylation represents the balance between MeHg formation and MeHg demethylation (Ullrich et al., 2001).

Previous studies on mechanisms and factors that affect methylation of mercury in the aquatic environment have focused on mercury methylation by sulfate-reducing bacteria (SRB) [i.e. King et al., 2000; Compeau and Bartha, 1985; Gilmour and Henry, 1991]. However, despite the generally accepted view that some SRB are the primary methylators in anoxic freshwater and estuarine sediments, not all SRB are capable of mercury methylation [King et al., 2000] and other microorganisms may also be important. The ability to convert mercury to methyl mercury might be a protective mechanism during the early evolution of those microbes some 3 billion years ago [Clarkson, 1998]. Methanogens or methane producing archaea (MPA) are also thought to be involved in Hg methylation [Pak and Bartha, 1998; Wood et al., 1968].

Moreover, iron reducing microbes (FeRP) found in many sub-oxic to anoxic habitats might also be involved in Hg methylation. They can use many different organic carbon compounds as metabolic energy sources and are involved in degradation of organic pollutants [Lovely 1993]. Fleming et al. [2006] and Kerin at al. [2006] have shown that FeRP may be able to methylate mercury at environmentally significant rates comparable to SRB. This is in agreement with the findings of Warner et al. [2003]. Recent studies have also reported that macrophyte and sediment associated periphyton [Achá et al., 2005; Mauro,

2002; Cleckner et al., 1999] are also important sites for the production and accumulation of methylmercury in aquatic environments.

1.2. Methylated mercury species in aquatic environments

Methylated mercury species, mono- and dimethylmercury, are considered the most toxic mercury species present in the environment [Grigal, 2002; Morel, 1998]. Monomethylmercury is by far the most toxic mercury compound present in aquatic environments because it bioaccumulates and biomagnifies in aquatic food web [Scheuhammer et al., 2007; Hammerschmidt et al., 2002]. It is the ionic form (CH_3Hg^+), monomethylmercury, that is present in aquatic environment and complexed with different anions, such as Cl^- (seawaters) or OH^- (freshwaters), or with reduced sulfur functional groups of dissolved natural organic matter (NOM) in oxic waters [Skyllberg et al., 2006, Hintelmann et al., 1995; Morel, 1998]. In contrast, in anoxic sulfidic waters and sediments, MeHg is mainly bound to sulphur, but NOM has also been shown to influence the complexation [Skyllberg et al.,, 2006; Ravichandran, 2004; Morel, 1998]. In its complexed form, MeHg is easily taken up by the organisms at the bottom of the food chain (bacteria and phytoplankton) and through the process of biomagnification, it leads to high levels in animals and humans that occupy the top of the food chain [Hammerschmidt et al., 2002; Morel, 1998].

The average proportion of MeHg to total mercury (THg) in aquatic environments is 10% in the water column (but a range from 0.1 to 60% in water samples has been observed in Lean's lab in the past 2 years), 15% in phytoplankton, 30% in zooplankton, and up to 95% in fish [Morel, 1998]. In fish, most of mono methylmercury is covalently bound to the sulphydryl groups of proteins [Harris, 2003; Morel, 1998], which explains the high biomagnification factor in fish at higher trophic levels.

Dimethylmercury (DMeHg) never accumulates to detectable levels in freshwater systems and is not considered to be available for accumulation in aquatic organisms, because it is readily lost by evaporation or photolytic degradation to MeHg or to elemental mercury (Hg^0) [Mason et al., 1995; Baldi et al., 1995]. In addition, acidification of freshwater lakes results in more rapid decomposition of DMeHg [Morel, 1998; Mason et al., 1995].

For the rest of the thesis, monomethylmercury will be addressed as methylmercury or MeHg.

1.3. Sources and sites of Methylmercury to Freshwater Systems

There are three main sources of methylmercury to remote lakes: direct precipitation, watershed runoff (especially from wetlands), and in-lake methylation of inorganic Hg, but the relative importance of these sources varies with the rates of MeHg deposition from the atmosphere, lake type and catchment hydrology [Munthe et al., 2007; Rudd 1995]. Wetlands can be particularly active zones of MeHg production (i.e., Florida Everglades), therefore providing MeHg to receiving waters via runoff [Munthe et al., 2007; Branfireun et al., 1999; St. Louis et al., 1994]. A recent small-scale Hg loading experiment of Branfireun and co-workers [2005] in the Experimental Lakes Area wetland also demonstrated the link between Hg deposition, methylation, and transport to surface waters. It is generally accepted that *in situ* production is the dominant MeHg source to watersheds [Munthe et al., 2007], even when wetlands play a dominant hydrologic role [Eckley et al., 2005; Watras et al., 2005]. In addition, Loseto et al., [2004] found that wetlands in the Canadian Arctic produce MeHg, but the yield from snowmelt was much greater. Sellers et al., [2001] found that in lakes production of MeHg was the most important source based on a mass balance for known inputs and losses, and while degradation rates were lower than what the authors concluded, inflow from a brown-water lake with riparian wetlands may be more important than originally thought.

The methylation of inorganic mercury can take place in both remote and impacted environments. Several studies have demonstrated that Hg methylation occurs mostly in surface sediments [i.e. Martin-Doimeadios et al., 2004; Gilmour et al., 1992; Choi and Bartha, 1994; Compeau and Bartha, 1985] and to a lesser extent, in the water column [Watras et al., 1995a; Eckley et al., 2005]. The root zone of floating macrophytes [Mauro, 1999], the macrophyte and sediments associated periphyton [Clekner et al., 1999; Mauro 2002] and epilithic biofilms [Desrosiers et al., 2006] were also found as important sites of methylation.

It is generally recognized that freshwater aquatic ecosystems, warm, shallow and organic rich lake sediments are often important zones of net methylation [Hammerschmidt et al., 2004; Krabbenhoft et al., 1998; Munthe et al., 2007]. Elevated concentrations of both total Hg and MeHg are frequently found in anoxic waters. MeHg concentrations up to 4 ng/l (37% of total Hg), were found in the anoxic bottom waters of a stratified pristine lake [Bloom, 1989]. In many freshwater systems, the anoxic conditions develop in June at the sediment–water interface, and this has been thought to be the zone of highest methylation potential [Watras et al., 2005; Rudd, 1995]. The maximum methylation rates have been observed at the redox boundary and found to decrease with increasing sediment depth [Rudd, 1995; Matilainen and Verta, 1995; Drott et al., 2008]. Eckley et al. [2005] suggested that Hg methylation begins in the sediments and moves into the water column as summer progresses and as the redox boundary moves into the water column. Migration into the water column brings sulfate-reducing bacteria and other microbes closer to the source of important substrates (like sulfate) that have significant atmospheric sources.

Overall environmental concentrations of MeHg reflect net methylation rather than actual rates of MeHg synthesis. The combined effect of production and degradation of MeHg leads to a steady state with a near constant level of MeHg, in sediments rarely exceeding 1 to 1.5% of THg. Estimated rates of MeHg production in freshwater lakes are 0.5 to 5 g MeHg/km^2/yr [Watras et al., 1995b]. Few studies provide information about simultaneous methylation and demethylation processes and about which organisms are responsible. The few investigations with such information have concluded that both processes are very rapid and that the net formation of methyl mercury may be near zero even though rates may be high in both cases [Eckley et al., 2005; 2006; Hintlemann et al., 2000; 2004]. Recent studies of Drott al. [2008] and Hammerschmidt et al. [2004; 2008] give more insights on either methylation or demethylation by using an enriched stable isotope approach (discussed in sub-chapter 1.6.).

In summary, the sites of methylation are complex and the mechanism of NET formation is not known. Most researchers have worked on a small part of a very complex process. Many studies have provided insights on each pathway, but the integration of the steps in the overall process is key in identifying the relative contribution of each pathway.

1.4. Mechanism of Methylation and Demethylation

The mechanism of formation of methyl mercury is confusing, as each study promotes its specific interests without an appreciation for all of the interacting factors. For example, Jensen and Jernelov [1969] were the first to demonstrate the natural conversion of inorganic mercury to MeHg in bottom sediments from a freshwater aquarium, as well as from Lake Landsjen near Stockholm, Sweden. Although many studies confirmed the natural conversion of mercury, the mechanism of the process is still speculative. Below is a review of our current state of knowledge for mercury methylation pathways in aquatic environments. It is also becoming clear that we must distinguish between biotic (microbial) and abiotic (chemical) processes.

1.4.1. Mercury methylation

1.4.1.1. Biological Methylation

Microorganisms play a key role in aquatic mercury cycling. Even though mercury compounds are acutely toxic to freshwater microorganisms, many microbes have developed resistance mechanisms [Barkay et al., 2003]. Conversion of Hg^{2+} to elemental mercury, which is then removed through volatilization is also considered a detoxification mechanism. From a microbial perspective, Hg methylation is also a detoxification mechanism, the microorganisms convert the potentially toxic forms of mercury to a form that can be excreted and lost by diffusion from their immediate environment [Wood, 1974]. Alternatively, other authors have proposed that it is an accidental process [Robinson and Tuovinen, 1984].

Organisms capable of Hg methylation *in vitro* have been found among anaerobes, aerobes, and facultative anaerobes [i.e., Wood et al., 1968; King et al., 2000; Kerin et al., 2006], but it is not known if these microbes are responsible for Hg methylation in natural aquatic environments. Contrary to earlier assumptions [Wood et al., 1968], methanogens seem to play a minor role in MeHg production, sulfate-reducing bacteria (SRB) being identified as the primary methylators in anoxic freshwaters and estuarine sediments [Compeau and Bartha, 1985; Gilmour and Henry, 1991; Choi and Bartha, 1994a]. However, not all SRB are capable of Hg methylation. King et al. [2000] have demonstrated that members of the family *Desulfobacteriaceae* (acetate oxidizers) have a greater potential to

methylate Hg than members of the family *Desulfovibrionaceae*. *Desulfobacter* populations are generally more abundant in lake sediments than the *Desulfovibrio* group [Benoit et al., 2001b].

Moreover, Mehrotra and Sedlak [2005] showed that the addition of low concentrations of iron (0.3 and 3.0 mM) stimulated Hg methylation and suggested that methylation by iron-reducing microbes (FeRP) is important in marine sediments. An alternative explanation however, may be that the increased methylation rates were due to a general increase in the bioavailability of mercury for methylators, as a result of the dissolution of iron colloids or via electron acceptor stimulation of methylation by metal-reducing microbes [Gagnon et al., 1997; Warner et al., 2003; Farrel et al., 1998]. Warner et al. [2003] demonstrated that freshwater sediments with iron reduction as a dominant process, had methylation potentials similar to those of sediments in which sulfate reduction was the dominant terminal electron accepting process. Since both activities go on simultaneously, it is hard to determine which is more important in net MeHg formation.

Fleming et al. [2006] showed that an iron-reducing bacterium, *Geobacter* sp. strain CLFeRP, was able to methylate mercury at environmentally significant rates comparable to those of SRB. In their study, anoxic sediments of lakes in California which showed evidence of iron reduction continued to produce MeHg even in the presence of a molybdate inhibitor of sulfate reduction. In pure cultures, the rate of Hg methylation was 0.076 attomol/cell/day with the *Geobacter sp.* strain CLFeRP which is more than the rate measured for the *D. propionicus* strain, i.e., 1pr3, 0.043 attomol/cell/day. Fleming et al. (2006) concluded that the methylation pathway by iron-reducing microbes represents a previously unidentified and potentially significant source of MeHg in iron-rich freshwater sediments. They [Fleming et al. 2006] also suggested that ferric oxyhydroxides are at least as effective as soluble ferric iron at promoting methylation in pure cultures, emphasizing the potential importance of solid-phase electron acceptor in studies of methylation by natural populations of microbes.

Kerin at al. [2006] examined the ability of different strains in the genera of dissimilatory iron-reducing prokariots (DIRP) to methylate mercury and found that all of the *Geobacter* and *Desulfuromonas* strains (closely related to known Hg-methylating SRB within the *Deltaproteobacteria)* methylated mercury while reducing ferric iron, nitrate or

fumarate, while none of the *Shewanella* strains produced methylmercury at higher levels than abiotic controls under similar culture conditions. The authors concluded that Hg methylation by FeRP may be important in sediments and soils where these organisms are dominant, e.g., iron-rich sediments with low concentrations of sulfate which is in agreement with the findings of Pak and Bartha [1998]. In conclusion iron can affect methylation by altering the availability of Hg [Warner et al., 2003; Mehrotra and Sedlak, 2005] or by changing the activity of FeRP versus other groups of organisms, particularly SRB [Flemming et al., 2006; Kerin et al., 2006; Warner et al., 2003].

It is also important to consider some of the cellular processes that researchers have thought to be important for Hg methylation. Some have considered the process to be enzymatic (i.e., requiring the presence of an actively metabolizing organism) while others have suggested a nonenzymatic reaction (i.e., requiring only the methylated products of active metabolism). Ridley et al. [1977] suggested that the process involves the nonenzymatic transfer of methyl group of methylcorrinoid (Me-B12) to Hg^{2+}, while Bertilsson et al. [1971] showed that metabolically formed Me-B12 can spontaneously methylate Hg^{2+} in aqueous solutions. More recent studies of Chen et al. [2007] also suggested that the methylation could occur in the absence of enzymes, in which Hg(II) acts as an electrophile to attack methylcobalamin with a subsequent transfer of carbanion methyl group to the higher oxidized state of Hg(II). The same authors also found that the reaction was fast with a first-order kinetic for Hg(II) and dependent on salinity and pH, which alter the electron density of the methyl donor and the electrophilicity of the metal ion in the reaction system. In contrast, Choi and Bartha [1994b] showed that Hg^{2+} was also methylated by *Desulfovibrio desulfuricans* within the cell and that the process appeared to be enzyme-catalyzed (rather than chemical) and oxygen sensitive, with optimum conditions at 35^0C and pH=7. Cellular uptake also appeared to play a key role in methylation.

Methylation requires the presence of a suitable methyl donor molecule. In biological systems, the methylating agents (coenzymes) available for methyl transfer are: S-adenosylmethionine, N5-methyltetrahydrofolate derivatives, and Vitamin B12 derivatives (methylcorrinoid, Me-B12) [Ridley et al., 1977]. The only known methylating agents capable of transferring methyl groups as CH_3^- to Hg^{2+} are methylcorrinoids [Chen, 2007; Ridley et

al., 1977]. Choi and Bartha [1994c] suggested that Me-B12 is the methyl group donor when Hg^{2+} is methylated by *Desulfovibrio desulfuricans*, but other studies suggested that the amino acid serine [Berman et al., 1990] provides the methyl moiety. Two possible enzymatic pathways have been shown to be involved: acetylcoenzyme A pathway (eq.1), with methyltransfer group from methyltetrahydrofolate in conjunction with Me-B12 [Choi and Bartha, 1994c] and methyltransferase pathway, similar to the biological synthesis of methionine by homocysteine [Siciliano and Lean, 2002]. More recent studies have demonstrated some incomplete oxidizers in contrast with complete oxidizers that can methylate Hg via different pathways independent of the acetyl-coenzyme A [Ekstrom et al., 2003].

$$^{14}CH_3 - THF + Co\text{-}protein \xrightarrow{\text{Methyltransferase I}} {}^{14}CH_3 - Co - protein$$
$$^{14}CH_3 - Co - protein + Hg^{2+} \xrightarrow{Me\text{-}transferaseII} Co - protein + CH_3 - Hg^{+} \qquad [1]$$

1.4.1.1. Abiotic Methylation

Chemical reagents thought to lead to abiotic methylmercury formation include small organic molecules, such as methyl iodide and dimethylsulfide, and larger organic components of dissolved organic matter, such as fulvic and humic acids.

Transmethylation reactions involving organometallic compounds, such as methylcobalamin, methyllead or methyltin compounds, have also been considered as possible pathways for chemical methylation of mercury in the aquatic environment [Chen, 2007; Celo et al., 2006; Weber, 1993; Morel, 1998].

The environmental alkylation of mercuric ions by organocobalt complexes was first demonstrated in by Wood et al. [1968], and methyl transfer from methylcobalamin to mercury was proposed to occur as a result of both enzymatic and non-enzymatic processes. Both MeHg and DMeHg can be synthesized from methyl-B12 (see eq. 2, 3 below) [Wood, 1974, Chen et al., 2007].

$$CH_3 - B12 + Hg^{2+} + H_2O \rightarrow CH_3Hg^{+} + H_2O - B12 \qquad [2]$$

$$CH_3 - B12 + CH_3Hg^{+} \rightarrow (CH_3)_2Hg + H_2O - B12 \qquad [3]$$

The optimum pH for synthesis of MeHg was found to be 3-5 [Chen et al., 2007]. This may be a factor in explaining why low pH systems such as the Kejimkkujik National Park (Nova Scotia) or lakes on the Canadian Shield, have higher levels of MeHg [O'Driscoll et al., 2003].

There is however a considerable uncertainty regarding the pathways of MeHg and DMeHg formation. Baldi et al., [1995] have demonstrated that the initial product of the reaction between methylcobalamin and Hg^{2+} is MeHg, which is then further transformed into DMeHg. The reaction is pH and temperature dependent with low pH values giving rise to the production of MeHg, while DMeHg formation is found under neutral and basic (pH>7) conditions [Jensen and Jernelöv, 1969]. In general, aquatic systems, not located on igneous rocks, are circumneutral or basic with a pH range from 6 to 8.5.

Celo et al., [2006] examined the plausibility of abiotic mechanisms, as pathways for mercury methylation in the water column, and found that the methylation of mercury by methylcobalamin, which is strongly dependent on pH and the presence of complexing agents, such as chloride, could be a source of methylmercury formation in freshwaters, which have low pH and low chloride concentration, but not in seawater. In contrast, the methylation pathway by methyltin compounds is expected to be more important in seawater than in freshwaters since methyltin species are more abundant in high salinity waters and the reaction is faster at higher pH and requires the presence of chloride. In addition, Celo et al., [2006] found that methyliodide (MeI), a naturally occurring compound in aquatic environments, slowly methylates Hg^0 at room temperature in the dark, presumably by oxidative addition, with a yield based on Hg(0) of 1.1%, which is similar to the yields reported for methylation by SRB [Celo et al., 2006].

Fulvic and humic acids have a major effect on the distribution and mobility of Hg in freshwaters. Formation of MeHg by humic matter was observed at pH 4 and 6 and depended of Hg^{2+} speciation: $Hg(NO_3)_2$ (pH=4)>> $Hg(NO_3)_2$ (pH 6)>>$HgCl_2$ (pH 4 or 6) [Weber, 1993]. The methylation mechanism is however unknown [Weber, 1993].

The addition of ferric oxyhydroxides has also been shown to increase methylation rates in certain lacustrine sediments [Farrel et al., 1998; Falter, 1999]. In organic rich

surficial sediments, Matilainen et al. [1991] discovered that mercury was methylated under aerobic conditions and the authors concluded that the process was slower than anaerobic and abiotic methylation. The methylation was shown to increase with increasing mineral content, especially the iron and manganese content.

1.4.2. Methylmercury Demethylation

Methylmercury degradation process may also proceed as a result of a number of abiotic and biotic pathways in the natural environment.

Abiotic demethylation pathways include photodegradation [Sellers at al., 1996] and the reaction with sulfide to form dimethylmercury (DMeHg) and HgS [Baldi et al., 1995]. Abiotic degradation of MeHg can be affected by sunlight (UV-A and UV-B, 280-400 nm) and elemental Hg(0) was identified as the major product of photodegradation in wetlands [Selers at al., 1996; Barkay et al., 2003]. In light-exposed environments, such as wetlands and lakes, and especially at low total Hg concentrations, photodegradation may be the major mechanism for MeHg degradation [Sellers at al., 1996]. In addition, Baldi et al. [1995] found abiotic degradation in alkaline anoxic sediments where MeHg reacts with microbially produced sulfide (by *Desulfovibrio desulfuricans)* to form DMeHg and HgS [eq. 4]. DMeHg is volatile and easily evade from the sediments being degraded to MeHg and CH_4 or further to Hg(0).

$$2CH_3Hg^+ + H_2S \Rightarrow (CH_3Hg)_2S \Rightarrow (CH_3)_2Hg_{(g)} + HgS_{(s)} \qquad [4]$$

There are two known **pathways for microbial MeHg demethylation**: reductive demethylation [Robinson and Tuovinen, 1984; Schaefer et al., 2002,; Barkay et al., 2003] and oxidative demethylation [Oremland et al., 1995; Marvin-Diapsquale et al., 2000]. **Reductive demethylation (RD)** is found in a "broad-spectrum" of Hg-resistant microbes which have the ability to detoxify both inorganic Hg^{2+} and organomercurials (including MeHg), by sequential action of two enzymes [eq 5]: organomercurial-lyase (OML, encoded by *mer*-B gene) and mercuric reductase (MR, encoded by *mer*-A gene) [Barkay et al., 2003; Schaefer et al., 2002]. All Hg-resistant microbes are resistant to Hg^{2+}. The *mer*-detoxification pathway is induced or regulated by ambient MeHg concentrations.

$$CH_3Hg^+ \xrightarrow{OML} Hg(II) + CH_4 \uparrow \xrightarrow{MR} Hg^0 \uparrow \qquad [5]$$

The broad-spectrum of mercury resistant microbes, gram negative and gram-positive bacteria that contain both *mer*-B and *mer*-A gene, are able to detoxify MeHg (aerobic or anaerobic) by converting it to a form that may readily evade from the immediate environment (Hg^0 and CH_4) [Barkay et al., 2003].

Oxidative demethylation (OD) is mediated by anaerobic microbes and occurs with the oxidation of the MeHg methyl group to CO_2, with or without concurrent CH_4 production [Oremland et al., 1995]. The mechanism is currently unknown, but may be analogous to methanol or monomethylamine degradation by methanogens (eq. 6) or to acetate oxidation by SRB (eq. 7), and thus does not represent an active detoxification response [Oremland et al., 1995; Marvin-Diapsquale and Oremland, 1998; Marvin-Diapsquale et al., 2000].

$$4CH_3Hg^+ + 2H_2O + 4H^+ \rightarrow 3CH_4 + CO_2 + 4Hg^{2+} + 4H_2 \qquad [6]$$

$$SO_4^{2-} + CH_3Hg^+ + 3H^+ \rightarrow H_2S + CO_2 + Hg^{2+} + 2H_2O \qquad [7]$$

Oremland et al. [1995] and Marvin-Diapasquale et al. [2000] suggested that both methanogens and SRB can simultaneously degrade MeHg via OD, since it is proposed that MeHg is simply cometabolized along with primary substrates (small organic substrates e.g., C1 compounds) and does not represent an energy-yielding substrate for either group. It was suggested by Oremland et al. [1995] that an increase of MeHg concentration may induce a shift from methanogen dominated demethylation at low concentrations to SRB dominated demethylation at higher concentrations, with constant contributions of both groups at MeHg concentrations ~800 ng/g d.w. sediments.

Barkay et al. [2003] concluded that in sediments and bottom waters, where MeHg accumulates following methylation, photodegradation may have little impact on demethylation and either reductive or oxidative microbial processes will most likely dominate. However, it is unknown under which environmental conditions either RD or OD dominates at *in situ* MeHg concentrations.

1.5. Biogeochemical Factors Influencing NET Mercury Methylation

Formation of methylmercury in aquatic systems is influenced by a wide range of environmental factors, which interact to form a complex system of synergistic and antagonistic effects [Benoit et al., 2003; Ulrich et al., 2001]. The efficiency of biotic mercury methylation depends on microbial community structure and activity, and on the concentration of bioavailable mercury (Hg^{2+}) rather than the total mercury pool. These in turn are influenced by temperature, pH, redox potential (i.e., iron redox chemistry), the concentration and character of dissolved inorganic and organic complexing agents, sulfur cycling (sulfate reduction, sulfide production) [Benoit et al., 2003; Munthe et al., 2007].

It appears that enhanced rates of MeHg production are linked with higher bioavailable Hg concentration, low pH, low salinity, and the presence of decomposable organic matter in reducing environments [Benoit et al., 2003], while DMeHg formation is favoured under neutral and basic (pH>7) conditions in the presence of H_2S or when Hg concentration is low [Baldi et al., 1995]. DMeHg is thermodynamically unstable and decomposes below pH 5 to form MeHg, which may be one of the reasons why DMeHg has not been detected in freshwaters, where the pH is typically low compared with estuarine and marine systems [DeSimone, 1973]. Alternatively, Mason et al. [1995] suggested that DMeHg forms directly from Hg^{2+}, but it is rapidly decomposed to MeHg in freshwaters and does not accumulate to detectable levels. Since researchers normally acidify samples for preservation, all DMeHg would normally be degraded. Recently, Kirk et al., [2008] found DMeHg levels equivalent to MeHg in the deep waters of Hudson Bay.

1.5.1. Microbial Activity

The efficiency of microbial MeHg production appears to depend chiefly on the activity and structure of the microbialcommunity, Hg availability, temperature, the availability of nutrients and the abundance of electron acceptors, such as sulphate and iron redox chemistry [Munthe et al., 2007].

Gilmour and Henry [1991] proposed an optimal sulfate concentration range of 0.2 to 0.5 mM SO_4^{2-} for Hg methylation by SRB in sediments. Sulfate concentrations above that range inhibit methylation, whereas lower concentrations limit the methylation and sulfate-

reduction processes [Compeau and Bartha, 1994; Gilmour et al., 1991; Benoit et al., 1999; 2001a,b]. At high sulfate concentrations, the accumulation of sulfide generated by sulfate respiration interferes with Hg methylation, thereby limiting MeHg production. Sulfide inhibition was previously ascribed to HgS precipitation, but is now thought to be linked with charged Hg-S complexes [Benoit et al., 1999; 2001].

The growth phase of bacteria can also affect the speciation and fate of Hg, but available data appear contradictory. Ramamoorthy et al. [1982] observed that growing bacterial cells promoted Hg^0 formation, whereas living, but non-growing ones, caused demethylation, and dead cells led to the formation of MeHg. In contrast, Ebinghaus et al. [1996 as cited by Ullrich, 2001] observed active methylation during the phase of exponential growth of sediment bacteria, whereas demethylation became dominant when the bacterial population began to die off.

Hg concentrations also affect the methylation process, i.e., the percentage of total Hg converted to MeHg decline significantly with increasing spiking levels of mercury [Drott et al., 2008; Hammerschmidt et al., 2004; Compeau and Bartha, 1985; Robinson and Tuovinen, 1984]. Hg spikes concentrations exceeding 15.3 μg $HgCl_2$/g d.w also appear to inhibit microbial methylation activity [Chen et al., 1996]. The results suggest that high concentrations of inorganic Hg may depress MeHg production or may favor demethylation in pure cultures, possibly due to the toxic effect of inorganic mercury on microorganisms. In addition, sediments containing high levels of Hg have also shown higher rates of demethylation compared with less contaminated sediments [Gilmour et al., 1991; Oremland et al., 1995].

Microbial uptake of Hg involves diffusive transport of Hg across microbial membranes, which are known to have higher permeability for uncharged molecules than for ionic species [Benoit et al., 1999; 2001]. As a result, the availability of Hg to methylating microbes is controlled by the concentration of neutral dissolved Hg complexes [Drott et al., 2007; Benoit et al., 1999, 2001; Barkay et al., 1997]. $HgCl_2$ may be the key chemical species determining cellular uptake of inorganic Hg in oxic waters [Morel, 1998], while uncharged HgS^0, bisulfide $Hg(SH)_2^0$, or polysulfide $HgSn^0$ complexes may be important for

microbialuptake in anoxic waters [Benoit et al., 1999; 2001; Jay et al., 2000; Drott et al., 2007].

Methylation and sulfate reduction rates are generally at their highest in the upper layers of sediments, where microbial activity and nutrient supply are the greatest. Because of the generally stimulating effect of organic matter on microbial activity, a positive correlation was found between sediment organic matter content and MeHg production [Hammerschmidht et al., 2004; 2009, Drott et al., 2008; Choi and Bartha, 1994; Pak and Bartha, 1998] and demethylation [Ramlal et al., 1986; Pak and Bartha, 1998]. In addition, it is influencing the structure of microbial community present in the system [Macalady et al., 2000].

1.5.2. Temperature

Seasonal variations in MeHg production and decomposition generally have been attributed to temperature effects, correlated with seasonal changes in productivity, nutrient supply and redox conditions [Ullrich et al., 2001]. For instance, Siciliano and Lean [2002] found the highest levels of MeHg in the Mer Bleue sediments in early May along with the highest levels of methyltransferase. Hg methylation rates in aquatic systems tend to peak during the summer months, with maximum methylation activity during mid or late summer [Eckley et al., 2006; Hintelmann et al., 1995; Watras et al., 1995a,b]. It is thought that in the late summer season, water column MeHg formation results from oxygen depletion in the water column with redox conditions moving up as well [Eckley et al., 2005; 2006].

Temperature is an important factor controlling both methylation and demethylation. It appears that moderately high temperatures have a stimulating effect on Hg methylation, which is most likely due to increased microbial activity. Together with seasonal changes in oxygen levels and organic content/primary production, this seems to account for the increased MeHg production rates usually observed in the summer [Oremland et al., 1991].

Interestingly, Loseto et al., [2004a] found that methylmercury can be produced in Arctic wetlands at 4^0C or less, even though SRB were not detected. This implies that Hg methylation was either not driven by SRB activity or that the SRB enumeration technique used in the study was not sensitive enough for these environments. The results for Hg

demethylation are however contradictory. It is generally observed that Hg demethylation is favoured at lower temperatures, possibly because the rate of methylation increases faster than the rate of demethylation with increasing temperature [Oremland et al., 1991; Martın-Doimeadios et al., 2004; Eckley et al., 2005].

1.5.3. pH

The effect of pH on Hg methylation varies between waters and sediments. MeHg concentrations in lake water and at the sediment-water interface have been found to generally increase with decreasing pH [Gilmour and Henry, 1991], but in anaerobic sediments, low pH values generally decrease the net MeHg production [Ramlal et al., 1986; Steffan et al., 1988]. The decrease in Hg methylation with decreasing pH in anaerobic sediments appears to be linked to the reduction of available inorganic Hg^{2+} in the sediment porewater, which may be due to increased sorption to particles at low pH [Ramlal et al., 1986] or increased demethylation activity at low pH [Steffan et al., 1988; Matilainen et al., 1991]. Moreover, the uptake of Hg by micro-organisms that use facilitated transport for Hg uptake is enhanced with decreasing pH [Winfrey and Rudd, 1990].

In general, demethylation rates in both sediments and lake water are less affected by pH than methylation rates, indicating that the changes observed in net MeHg production are largely due to an effect of pH on methylation rather than demethylation [Ramlal et al., 1986; Steffan et al., 1988; Matilainen et al., 1991]. It is not clear whether the stimulation of methylation in lake water is a direct effect of low pH on the methylation process, or whether it is related to other factors that are influenced by pH, such as the loss of volatile Hg species from water surfaces [Watras et al., 2005; Eckley et al., 2005] or changes in Hg solubility and partitioning [Grigal, 2002].

The solubility and mobility of Hg^{2+} and MeHg are however pH dependent. At low pH conditions, solubility of MeHg and its desorption from surficial sediments are increased [Grigal, 2002]. Lake water acidification probably affects the overall partitioning of MeHg [Gilmour and Henry, 1991]. In addition, in the water column, low pH values may stimulate methylation by promoting Hg^{2+} binding directly onto microbial cells as a result of the decrease in DOC binding sites due to the protonation of functional groups [Winfrey and

Rudd, 1990]. Watras et al. [1995] observed an increase in Hg^0 volatilization and a corresponding decrease in MeHg with increasing pH values. Abiotic methylation of Hg^{2+} by organic substances was also found to be pH dependent [Falter, 1999; Celo et al., 2006]. In summary, the observed differences in the effect of pH on mercury methylation in waters and sediments may be related to differences in redox conditions.

1.5.4. Organic Matter

Natural organic matter interacts with mercury in several different ways, affecting its transport, transformation and bioavailability. High levels of organic matter in sediments were related to higher methylation rates in water and sediments [i.e., Hammerschmidt et al., 2008; Benoit 2003; Ullrich et al., 2001] due to a stimulating effect of organic nutrients on microbial methylation activity and to a minor extent, to the direct abiotic methylation by humic and fulvic acids [Falter 1999; Siciliano et al., 2004]. In contrast, Hg methylation may also be inhibited at high DOC concentrations due to the increased complexation of Hg by organic ligands, therefore reducing Hg bioavailability to microbes, particularly in the neutral pH range [Ravichandran et al., 1999].

In microbial methylation, complexation with DOC generally limits the amount of inorganic mercury available for uptake by methylating microbes [Gilmour and Henry, 1991; Gilmour et al., 1992; Choi and Bartha, 1994; Barkay et al., 1997] because DOC molecules are generally too large to cross the cell wall of microbes. At neutral and alkaline pH, DOC-mediated reduction of Hg^{2+} to volatile Hg^0 [O'Driscoll et al., 2004; Siciliano et al., 2002] species can also reduce the bioavailability of mercury for methylation and the subsequent biological uptake [Ullrich et al., 2001]. At low pH, DOC is less negatively charged, and therefore less likely to complex mercury, making it more available to the methylating microbes [Barkay et al., 1997].

The degradation of organic matter in aquatic environments has been shown to lead to the production of low-molecular weight sulphur compounds that can potentially form complexes with Hg^{2+} [O'Driscoll et al., 2004; Hill et al., 2005]. Organic matter degradation can also increase oxygen consumption, making the sediment/water interface more anoxic, which may lead to the mobilization and potential methylation of inorganic Hg [Gagnon et al.,

1997; Ullrich et al., 2001]. Watras et al. [1995b] observed an increase in the MeHg fraction in Wisconsin lake waters with increasing levels of DOC (>5 mg/l), while the Hg^0 fraction decreased, and they concluded that high DOC conditions in lakes favor either methylation (at low pH) or evasion (at high pH), whereas low pH and low DOC conditions favor sedimentation processes. The role of humic matter in the methylation of Hg is however still unclear.

1.5.4. Redox Conditions

Mercury methylation occurs in both aerobic and anaerobic environments, but both methylation rates and the stability of MeHg in sediments appear to be enhanced under anaerobic conditions [Compeau and Bartha, 1985]. Methylation rates are low under aerobic conditions, probably because of the reduced activity of anaerobic SRB. On the other hand, the demethylation of MeHg appears to be generally favored by aerobic-high pH conditions [Compeau and Bartha, 1985; Ramlal et al., 1986; Oremland et al., 1991].These observations clearly illustrate the need (see experimental design of this thesis) to measure both methylation and demthylation processes independent of each other, as well as net changes in MeHg formation.

Ullrich et. al. [2001] suggested that different mechanisms may be responsible for Hg methylation under aerobic and anaerobic conditions. Anaerobic methylation was found to be enhanced by high concentrations of organic matter, presumably due to stimulated microbial growth [Compeau and Bartha, 1985]. Aerobic methylation is frequently observed to be suppressed by high organic matter or particulate concentrations, and does not appear to be microbially mediated [Matilainen et al., 1995]. The same authors reported that aerobic methylation and the methylation/demethylation ratio correlated positively with the Fe and Mn content of the sediments. Gagnon et al. [1997] found that high dissolved Fe concentrations in sediment porewaters seem to limit the amount of dissolved H_2S that may potentially interfere with the methylation process and suggested that sediments with high metal content may have more bioavailable Hg, owing to the interaction of these metals with sulfide. Iron can also have a catalytic effect, increasing Hg methylation in lake waters in the presence of fulvic acid [Weber, 1993].

Generally speaking, MeHg concentrations in aquatic sediments are highest in the moderately anaerobic surface sediments and rapidly decline with increasing sediment depth. Microbially mediated methylation is generally favored by anaerobic conditions, while demethylation can take place in both aerobic or anaerobic consitions but is largely favored by aerobic conditions. Sediment redox state also affects the partitioning of Hg species between the sediment and water phases. Other environmental factors can interact significantly with redox effects, especially organic matter and pH.

1.5.5. Sulfide

Hydrogen sulfide, originating from microbial sulfate reduction, plays an important role in the chemistry of anaerobic sediments. High sulfide concentrations typically develop in anoxic, organic-rich sediments that are rich in sulfate, but they can also occur in surface waters, as a result of industrial or domestic wastewater discharges [Ullrich et al., 2001].

It is speculated that the inhibitory effect of sulfide on Hg methylation is the result of decreased solubility and bioavailability of Hg^{2+} due to HgS precipitation [i.e. Benoit et al., 1999, 2001, Winfrey and Rudd, 1990; Gilmour and Henry, 1991]. However, high dissolved Hg^{2+} concentrations in the porewater of sulfidic sediments indicate that the solubility of Hg is actually increased in the presence of excess sulfide, most likely due to the formation of soluble sulfide complexes [Gagnon et al., 1996; 1997; Benoit et al., 2001]. The optimal sulfide concentration is quite low, about 10 μM [Drott et al., 2008; Benoit et al., 1999; 2001]. Those ranges are also affected by iron, as well as organic matter concentration due to their effect on Hg and S complexation [Munthe et al., 2007]. Furthermore, a recent study of Drott et al. [2007] demonstrated that Hg methylation rates in contaminated sediments from Sweden are largely controlled by concentrations of neutral inorganic mercury sulfide species, as well as by the availability of energy-rich organic matter. In addition, those authors suggested that in organic-rich sediments without formation of HgS(s), the dominant species taken up by MeHg producing microbes is $Hg(SH)_2$. In a more recent study, Drott et al. [2008b] found that in all freshwater and brackish waters investigated in their study, the dominant MeHg species in the sediment pore water were MeHgSH(aq), $MeHgS^-$(aq) and MeHg–thiol complexes [MeHgSR(aq)] associated to dissolved organic matter.

1.6. Use of enriched mercury isotope in Hg methylation studies

In the recent years, a new technique that allows monitoring opposite processes, like simultaneously Hg^{2+} methylation and MeHg demethylation at ambient tracer levels in the same sample that use mercury-enriched isotopes with subsequent detection by ICP-MS, has been developed. This method, called in literature as either double tracer technique or isotope enriched multilabeling technique [Hintelmann and Evans, 1997; Bjorn et al., 2007], has been used to study different transformations in the biogeochemical cycle of mercury. For example, this technique offers the possibility to determine the mercury species transformation rates (i.e. Hg^{2+} methylation and MeHg demethylation rates, absorption and desorption dynamics of Hg^{2+} and MeHg in sediments) in water and sediment samples, and to identify which of the two processes controls the actual levels of methylmercury in the aquatic environment [Hintelmann and Evans, 1997]. This stable isotope enriched approach [Hintelmann et al., 1995; 1997; 2000; Bjorn et al., 2007] consists of adding different isotopically enriched Hg species (i.e. $^{200}Hg^{2+}$ and $Me^{202}Hg^{+}$) to the sample to study the transformation rates during an incubation period. A third different isotope is added as an internal standard before sample extraction to calculate the isotope ratios based on a modified isotope dilution analysis (IDA). The isotope enriched Hg spikes (i.e., $^{200}Hg^{2+}$ and $Me^{202}Hg^{+}$) are added in sufficient quantities in such as way that the generated $Me^{200}Hg$ and the remaining $Me^{202}Hg$ (after demethylation) are greater than or at least equal to 1% of the ambient MeHg [Dr. Hintelmann, personal communication]. The additions increase by 10-100% the concentrations of total Hg and methylmercury in the samples with respect to environmental levels depending on the type of sediments [Martin-Doimeadios et al., 2004 ; Hintelmann et al., 1997 ; 2000 ; Drott et al., 2008 ; 2007 ; Hammerschmidt et al., 2004; 2006]. The method offers the advantage that we can follow not only at the behavior of the added tracers, but at the same time, we are able to monitor the fate of the ambient metal already present in the system and allows to calculate the specific methylation and demethylation rate constants (Km and Kd).

With this method, Hintelmann et al. [2000] calculated mercury methylation and demethylation rate constants and observed that the inorganic mercury tracer was methylated at a faster rate compared to the ambient inorganic mercury, and concluded that the added

tracer Hg^{2+} is more available for transformation reaction than the ambient Hg^{2+}. In contrast, the degradation of tracer and ambient methylmercury proceeded at a similar rate.

Martin-Doimeadios et al. [2004] used the same technique, and was able to show that the levels of methylmercury in estuarine sediments investigated (Adour River estuary, France) are controlled by competing and simultaneous methylation and demethylation reactions, mercury methylation being enhanced under anaerobic non-sterile conditions in contrast with other environmental conditions investigated (i.e. aerobic). Furthermore, the authors found that the production of total gaseous mercury was found to be minimal throughout the experimental time course. In more recent studies, Drott and co-workers successfully applied this mercury-enriched isotopes approached, but with just one tracer at a time, to determine either potential Hg methylation [Drott et al., 2007] or MeHg demethylation rates [Drott et al., 2008a; b] in brackish waters and freshwater contaminated sediments from Sweden and study their correlation with different geochemical characteristics (i.e. sulfides). Drott et al. [2008b] found significant correlation between the specific methylation rate constant (Km, day^{-1}) in just two of the brackish and freshwater sediments investigated and the sum of neutral mercury sulfides [$Hg(SH)_2$ + HgS], but no significant correlation between Km and total Hg, total mercury sulfides or $Hg(SR)_2(aq)$ in pore waters. In contrast, significant positive relationship [Drott et al., 2008a] between Kd and ambient MeHg concentrations in sediments was observed across all sites, but no significant relationship between Kd and ambient Hg and concluded that variations in Kd among and within sites were related to ambient concentrations of mercury and MeHg and to pore water speciation of MeHg. Moreover, Kd was significantly correlated with porewater MeHg speciation at the sites with low ambient Hg concentrations, in contrast with the high concentration ones. The same authors suggested that the sites were dominated by oxidative demethylation process which may be dependent on a passive uptake of inorganic MeHgSH molecules. It was shown that additions of different amounts of MeHg and Hg tracers, in relation to the ambient concentrations of MeHg and Hg, could result in dramatically different kd values within and between sites.

Examining temporal differences in sedimentary production of monomethylmercury (MMHg) at three sites in Long Island Sound, Hammerschmidt and coworkers [2004] used

the isotopic tracer technique to measure Hg methylation potentials. The authors observed enhanced Km in August relative to May and June and concluded that a principal control on MeHg production in low-sulfide coastal marine sediments is partitioning of Hg(II) between particle and dissolved phases, which regulates the availability of Hg substrate to methylating microbes.

Hammerschmidt et al. [2008] using a mercury-enriched isotopes approach, determined the potential rates of Hg methylation in sediments from New York/New Jersey Harbor and found that Km, as well as the solid-phase MeHg concentrations, differed by a factor of two between summer and winter conditions, and were able to link the production and efflux of methylmercury from sediments to the availability of dissolved Hg^{2+} (as HgS), to methylating microbes which in turn are largely controlled by organic material and dissolved sulfide.

Rodrigues-Gonzales et al. [2009] showed that the methylation of Hg^{2+} (NIST-3133) in the presence of the pure bacterial strain *Desulfobulbus propionicus* under fermentative conditions caused mass-dependent fractionation of the Hg isotopes for both Hg^{2+} substrates and production of MeHg occurred under the exponential growth of the bacteria which preferentially methylated the lighter isotopes of Hg, after 96 h of continuous culture and 140 h for the single sampling cultures. Those findings need further investigations in order to identify their implications for the mercury-enriched isotopes approach. Finally, the above examples illustrate that the mercury-enriched isotopes approach is a useful and advanced technique which allows the study of complex and simultaneous transformations in the biogeochemical cycle of mercury in aquatic environments.

1.7. Limitations of previous research

Although progress has been made, the mechanisms for mercury methylation are still unclear. The biological methylation of mercury, the specific microorganisms involved and the forms of mercury that are being methylated have only been vaguely identified. Furthermore, the biological methylation has likely been overestimated as abiotic methylation has been ignored. Considering that mercury methylation can be a biological process, the type of microorganisms involved in the processes and the factors that stimulate them need to be

elucidated. It is not clear if FeRP are involved in mercury methylation in aquatic environments. Some of the confusion stems from the lack of data for the two competing processes of methylation and demethylation that go on simultaneously. Consequently, net methylation has likely never been quantified nor the principal pathways identified.

1.8. Objectives and hypotheses

The main objectives of this study are to assess the contribution of the different groups of anaerobic microbes (FeRP, SRB, MPA) to rates of methylation and demethylation relative to abiotic methyl mercury processes. The main hypothesis is that iron-reducing prokariots do play an important role in Hg methylation in freshwater sediments since from a redox point of view, iron reduction is favoured over sulfate reduction and methanogenesis in surface sediments. The specific objectives and hypotheses are described in chapters 2, 3 and 4.

1.9. Authorship of research

Chapters 2, 3 and 4 are co-authored by several authors, but L. Avramescu remains the leading author of all chapters. L. Avramescu carried out the analytical work and its entire interpretation. This project was a collaborative project, involving Dr. Holger Hintelmann from Trent University, who greatly helped with the analytical methods, along with Dr. Emmanuel Yumvihoze of the University of Ottawa.

1.10. References

Achá D, Iñiguez V, Roulet M, Guimarães JRD, Luna R, Alanoca L, Sanchez S, 2005. Sulfate-reducing bacteria in floating macrophyte rhizospheres from an Amazonian floodplain lake in Bolivia and their association with Hg methylation. Appl. Environ. Microbiol., 71 (11), 7531-7535

Baldi F, Parati F, Filipelli M, 1995. Dimethylmercury and dimethylmercury-sulfide of microbial origin in the biogeochemical cycle of Hg, Water Air Soil Pollut., 80, 805-815.

Barkay T, Gillman M, Turner RR, 1997. Effects of dissolved organic carbon and salinity on bioavailability of mercury. Appl. Environ. Microbiol., 63, 4267-4271.

Barkay T, Miller SM, Summers AO, 2003. Bacterial mercury resistance from atoms to ecosystems. FEMS Microbiology Reviews, 27, 355-384.

Benoit JM, Gilmour CC, Heyes A, Mason RP, Miller CL, 2003. Geochemical and biological controls over methylmercury production and degradation in aquatic ecosystems. ACS Symposium Series 835, 262–297.

Benoit JM, Gilmour CC, Mason RP, 2001. The influence of sulfide on solid-phase mercury bioavailability for methylation by pure cultures of *Desulfobulbus propionicus* (1p3). Environ. Sci.Technol. 35, 127-132.

Benoit JM, Gilmour CC, Mason RP, Heyes A, 1999. Sulfide controls on mercury speciation and bioavailability to methylating bacteria in sediment pore waters, Environ. Sci. Technol., 33, 951-957.

Benoit JM, Gilmour CC, Mason RP, 2001a. The influence of sulfide on solid-phase mercury bioavailability for methylation by pure cultures of *Desulfobulbus propionicus* (1p3). Environ. Sci.Technol., 35, 127-132.

Benoit JM, Gilmour CC, Mason RP, 2001b. Aspects of bioavailability of mercury for methylation in pure cultures of *Desulfobulbus propionicus* (1pr3). Applied Environ. Microbiol., 67, 51-58.

Berman M, Chase T, Bartha R, 1990. Carbon flow in mercury biomethylation by *Desulfovibrio desulfuricans*. Applied and Environ. Microbiol. 56, 298-300.

Bertilsson L, Neujahr HY, 1971. Methylation of mercury compounds by methylcobalamin, Biochemistry, 10, 2805-2808.

Bjorn E, Larsson T, Lambertsson L, Skyllberg U, Frech W, 2007. Recent advances in mercury speciation analysis with focus on Spectrometric methods and enriched stable isotope applications. Ambio, 3,443-451.

Bloom N, 1988. Determination of picogram levels of methylmercury by aqueous phase ethylation, followed by cryogenic gas chromatography with cold vapour atomic fluorescence detection. Can. J. Fish. Aquat. Sci., 46, 1131-1140.

Branfireun BA, Roulet NT, Kelly CA, Rudd JWM. 1999. Toward a link between acid rain and methylmercury contamination in remote environments. Global Biogeochemical Cycles 13, 743-750.

Branfireun BA, Krabbenhoft DP, Hintelmann H, Hunt RJ, Hurley JP, Rudd JWM, 2005. Speciation and transport of newly deposited mercury in a boreal forest wetland: a stable isotope approach. Water Resource Res., 41, 1-11.

Celo V, Scott S, Lean DRS, 2006. Abiotic pathways of mercury methylation in the aquatic environment. Science of the Total Environment, 368, 126-137.

Chen B, Wang T, Yin Y, He B, Jiang G, 2007. Methylation of inorganic mercury by methylcobalamin in aquatic systems. Appl. Organometal. Chem., 21, 462–467.

Chen Y, Bonzongo JC, Miller GC, 1996. Levels of methylmercury and controlling factors in surface sediments of the Carson River system. Nevada. Environ. Poll., 92, 281-287.

Choi SC, Bartha R, 1994a. Environmental factors affecting mercury methylation in estuarine sediments. Bull Environ Contam Toxicol., 53, 805-812.

Choi SC, Chase T, Bartha R, 1994b. Enzymatic catalysis of mercury methylation by *Desulfovibrio desulfuricans* LS. Appl. Environ. Microbiol., 60,1342-1344.

Choi SC, Chase T, Bartha R, 1994c. Metabolic pathways leading to mercury methylation in *Desulfovibrio desulfuricans* LS. Appl. Environ. Microbiol., 60, 4072-4077.

Clarkson TW, 1998. Human toxicology of mercury. J. Trace Elem. Exp. Med., 11, 303-317.

Cleckner L, Gilmour C, Hurley JP, Krabbenhoft DP, 1999. Mercury methylation in periphyton of Florida Everglades. Limnology and Oceanography, 47, 1815-1825.

Compeau GC, Bartha R, 1985. Sulfate-reducing bacteria: principal methylators of mercury in anoxic estuarine sediments. Appl. Environ. Microbiol., 50, 498-502.

DeSimone RE, Penley MW, Charbonneau L, Smith SG, Wood JM, Hill HAO, Pratt JM, Ridsdale S, Williams RJP, 1973. The kinetics and mechanisms of cobalamin-

dependent methyl and ethyl transfer to mercuric ion. Biochim. Biophys. Acta, 304,851-863.

Desrosiers M, Planas D, Muccia A, 2006. Mercury methylation in the epilithon of boreal shield aquatic ecosystems. Environ. Sci. Technol., 40, 1540-1546.

Drott A, Lambertsson L, Björn E, Skyllberg U. 2007. Importance of dissolved neutral mercury sulfides for methyl mercury production in contaminated sediments. Environ. Sci. Technol., 41, 2270-2276.

Drott A, Lambertsson L, Björn E, Skyllberg U. 2008a. Do Potential Methylation Rates Reflect Accumulated Methyl Mercury in Contaminated Sediments? Environ. Sci. Technol., 42, 153–158.

Drott A, Lambertsson L, Björn E, Skyllberg U. 2008b. Potential demethylation rate determinations in relation to concentrations of MeHg, Hg and pore water speciation of MeHg in contaminated sediments. Marine Chemistry, 112, 93–101.

Eckley CS, Hintelmann H, 2006. Determination of mercury methylation potentials in the water column of lakes across Canada. Science of the Total Environment, 368, 111-125.

Eckley CS, Watras CJ, Hintelmann H, Morrison K, Kent AD, Regnell O, 2005. Mercury methylation in the hypolimnetic waters of lakes with and without connection to wetlands in northen Wisconsin. Can. J. Fish Aquat. Sci., 62, 400-411.

Ekstrom EB, Morel FMM, Benoit JM, 2003. Mercury methylation independent of the acetyl-coenzyme a pathway in sulfate-reducing bacteria. Appl. Environ. Microbiol. 69, 5414-5422.

Falter R, 1999. Experimental study on the unintentional abiotic formation of inorganic mercury during analysis: Part 1: Localisation of the compounds effecting the abiotic mercury methylation. Chemosphere, 39, 1051-1073.

Farrell RE, Huang PM, Germida JJ, 1998. Biomethylation of mercury(II) adsorbed on mineral colloids common in freshwater sediments. Appl. Organomet. Chem., 12, 613-620.

Flemming EJ, Marck EE, Green PG, Nelson DC, 2006. Mercury methylation from unexpected sources: molybdate-inhibited freshwater sediments and an iron-reducing bacterium. Appl. Environ. Microbiol., 72, 457–464.

Gagnon C, Pelletier E, Mucci A, Fitzgerald WF, 1996. Diagenetic behaviour of methylmercury in organic-rich coastal sediments. Limnol. Oceanogr., 41, 428-434.

Gagnon C, Pelletier E, Mucci A, 1997. Bihaviour of antropogenic mercury in costal marine sediments. Mar. Chem., 59, 159-176.

Gilmour CC, Henry EA, Mitchell R, 1992. Sulfate simulation of mercury methylation in freshwater sediments. Environ. Sci. Technol., 26, 2281-2287.

Gilmour, CC, EA Henry, 1991. Mercury methylation in aquatic systems affected by acid deposition. Environ. Pollut., 71, 131-169.

Grigal NF, 2002. Inputs and outputs of mercury from terrestrial watersheds: a review. Environ. Rev., 10, 1–39.

Hammerschmidt CR, Fitzgerald WF, 2006. Methylmercury cycling in sediments on the continental shelf of southern NewEngland. Geochim. Cosmochim. Acta, 70, 918–930.

Hammerschmidt CR, Fitzgerald WF, Balcom PH, Visscher PT, 2008. Organic matter and sulfide inhibit methylmercury production in sediments of New York/New Jersey Harbor. Marine Chemistry, 109, 165–182.

Hammerschmidt CR, Fitzgerald WF, 2004. Geochemical Controls on the Production and Distribution of Methylmercury in Near-Shore Marine Sediments. Environ. Sci. Technol., 38, 1487-1495.

Hammerschmidt CR, Sandheinrich MB, Wiener JG, Rada RG, 2002. Effects of dietary methylmercury on reproduction of fathead minnows. Environ, Sci. Technol., 36, 877-883.

Harris H, Pickering IJ, George GN, 2003. The Chemical Form of Mercury in Fish. Science, 301, 1203.

Hill J, O'Driscoll NJ, Lean DRS, 2009. Size distribution of methylmercury associated with particulate and dissolved organic matter in freshwaters. Science of the Total Environment 408, 408-414.

Hintelmann H, Evans RD, 1997. Application of stable isotopes in environmental tracer studies—Measurement of monomethylmercury (CH3Hg1) by isotope dilution ICP-MS and detection of species transformation. Fresenius J. Anal. Chem., 358, 378–385.

Hintelmann H, Harris R, 2004. Application of multiple stable mercury isotopes to determine the adsorption and desorption dynamics of Hg(II) and MeHg to sediments. Marine Chemistry, 90 (1-4 SPEC. ISS.), 165-173.

Hintelmann H, Keppel-Jones K, Evans RD, 2000. Constants of mercury methylation and demethylation rates in sediments and comparison of tracer and ambient mercury availability. Environ. Toxicol. Chem.,. 19, 2204– 2211.

Hintelmann H, Wilken RD, 1995. Levels of total mercury and methylmercury compounds in sediments of the polluted Elbe River: influence of seasonally and spatially varying environmental factors. Science of the Total Environment, 166, 1-10.

Jay JA, Morel FMM, Hemond HF, 2000. Mercury speciation in the presence of polysulfides. Environ. Sci. Technol., 34, 2196-2200.

Jensen S, Jernelöv A, 1969. Biological methylation of mercury in aquatic organisms. Nature, 223, 753-754.

Kerin EJ, Gilmour CC, Roden E, Suzuki MT, Coates JD, Mason RP, 2006. Mercury Methylation by Dissimilatory Iron-Reducing Bacteria. Appl. Environ. Microbiol., 72, 7919–7921

King JK, Kostka JE, Frischer, ME, Saunders FM, 2000. Sulfate-reducing bacteria methylate mercury at variable rates in pure culture and in marine sediments. Appl. Environ. Microbiol., 66, 2430-2437.

King JK, Kostka JE, Frisher ME, Saunders FM, Jahnke RA, 2001. A quantitative relationship that demonstrates mercury methylation rates in marine sediments are based on the community composition and activity of sulfate bacteria. Environ. Sci. Technol., 35, 2492-2496.

Kirk JL, St. Louis VL, Hintelmann H, Lehnherr I, Else B, Poissant L, 2008. Methylated mercury species in marine waters of the Canadian high and sub arctic. Environ. Sci. Technol., 42, 8367-8373.

Krabbenhoft DP, Gilmour CC, Benoit JM, Babiarz CL, Andren AW, Hurley JP, 1998. Methylmercury dynamics in littoral sediments of a temperate seepage lake. Can. J. Fish Aquat. Sci., 55, 835–844.

Loseto L, Siciliano SD, Lean DRS, 2004. Methylmercury production in high Arctic wetlands. Environ. Toxicol. Chem., 23, 17-23.

Lovley DR, 1993. Dissimilatory Metal Reduction. Ann. Rev. Microbiol, 47, 263-290.

Macalady JL, Mack EE, Nelson DC, Scow KM, 2000. Sediment microbial community structure and mercury methylation in mercury-polluted Clear Lake, California. Appl. Environ. Microbiol., 66, 1479-1488.

Martin-Doimeadios R, Tessier E, Amouroux D, Guyoneaud R, Duran R, Caumette P, Donard OFE, 2004. Mercury methylation/demethylation and volatilization pathways in estuarine sediment slurries using species-specific enriched stable isotopes. Marine Chemistry, 90, 107– 123.

Marvin-Diapsquale MS and Oremland RS, 1998. Bacterial Methylmercury Degradation in Florida Everglades Peat Sediment. Environ. Sci. Technol., 32, 2556-2563

Marvin-Diapsquale MC, Agee J, McGowan C, Oremland RS, Thomas M, Krabbenhoft D, Gilmour CC, 2000. Methylmercury degradation pathways: a comparison among three mercury-impacted ecosystems. Environ. Sci. Technol., 34, 4908-4917.

Mason RP, Rolfhus, KR, Fitzgerald WF, 1995. Methylated and elemental mercury cycling in surface and deep ocean waters of the North Atlantic. Water Air Soil Pollut., 80, 665-677.

Matilainen T, Verta M, 1995. Mercury methylation and demethylation in aerobic surface waters. Can. J. Fish Aquat. Sci., 52, 1597-1608.

Matilainen T, Verta M, Korhonen H, Niemi, M 1991. Specific rates of methylmercury production in lake sediments. Water Air Soil Pollut., 56, 595-605.

Mauro J, Guimarães JRD, Hintelmann H, Watras CJ, Haack EA, Coelho-Souza SA, 2002. Mercury methylation in macrophytes, periphyton, and water –comparative studies with stable and radio-mercury additions. Anal. Bioanal. Chem., 374, 983–989.

Mauro J, Guimarães JRD, Melamed R, 1999. Mercury methylation in a tropical macrophyte: Influence of abiotic parameters. Appl. Organomet. Chem., 13, 631-636.

Mehrotra AS, Sedlak DL, 2005. Decrease in net mercury methylation rates following iron amendment to anoxic wetland sediment slurries. Environ. Sci. Technol., 39, 2564–2570.

Morel FMM, 1998, The chemical cycle and bioaccumulation of mercury. Annu. Rev. Ecol. Syst., 29, 543–566.

Munthe J, Bodlay RA, Branfireun BA, Driscoll CT, Gilmour CG, Harris R, Horvat M, Lucotte M, Malm O, 2007. Recovery of Mercury-Contaminated Fisheries. Ambio, 36, 33-44.

O'Driscoll NJ, Lean DRS, Loseto L, Carignan R, Siciliano SD, 2004. Effect of Dissolved Organic Carbon on the Photoproduction of Dissolved Gaseous Mercury in Lakes: Potential Impacts of Forestry. Environ. Sci. Technol., 38, 2664-2672.

O'Driscoll NJ, Beauchamp S, Siciliano SD, Rencz AN, Lean DRS, 2003. Continuous analysis of dissolved gaseous mercury (DGM) and mercury flux in two freshwater lakes in Kejimkujik Park, Nova Scotia: Evaluating mercury flux models with quantitative data. Environ. Sci. Technol., 37, 2226-2235.

Oremland RS, Culbertson CW, Winfrey MR, 1991. Methylmercury decomposition in sediments and bacterial cultures-involvement of methanogens and sulfate reducers in oxidative demethylation. Appl. Environ. Microbiol., 57, 130-137.

Oremland RS, Miller LG, Dowdle P, Connell T, Barkay R, 1995 Methylmercury oxidative degradation potentials in contaminated and pristine sediments of the Carson River, Nevada. Appl. Environ. Microbiol., 61, 2745-2753.

Praharaj T, Fortin D. 2004. Indicators of microbial sulfate reduction in acidic sulfide-rich mine tailings. Geomicrobiology J., 21, 457-467.

Ramamoorthy S, Cheng TC, Kushner DJ, 1982. Effect of microbial life stages on thefate of methylmercury in natural waters. Bull. Environ. Contam. Toxicol., 29, 167-173.

Ramlal PS, Rudd JWM, Hecky RE, 1986. Methods for measuring specific rates of mercury methylation and degradation and their use in determining factors controlling net rates of mercury methylation. Appl. Environ. Microbiol,, 51, 110-114.

Ravichandran M, Aiken, GR, Ryan, JN, Reddy MM, 1999. Inhibition of precipitation and aggregation of metacinnabar (mercuric sulfide) by dissolved organic matter from the Florida Everglades. Environ. Sci. Technol., 33, 1418-1423.

Ravichandran M. 2004. Interactions between mercury and dissolved organic matter - a review. Chemosphere, 55, 319-331.

Ridley WP, Dizikes LJ, Wood JM, 1977. Biomethylation of toxic elements in the environment, Science, 197, 329-332.

Robinson JB, Tuovinen OH, 1984. Mechanisms of microbial resistance and detoxification of mercury and organomercury compounds-physiological, biochemical and genetic analyses. Microbiol. Reviews, 48, 95-124.

Rodŕiguez-Gonźalez P, Epov VN, Bridou R, Tessier E, Guyoneaud R, Monperrus M, Amouroux D, 2009. Species-specific stable isotope fractionation of mercury during Hg(II) methylation by an anaerobic bacteria (*Desulfobulbus propionicus*) under dark conditions. Environ. Sci. Technol., 43, 9183-9188.

Rudd JWM, 1995. Sources of methyl mercury to freshwater ecosystems: a review. Water Air and Soil Pollution, 80, 697-713.

Schaefer J, Latowski J, Barkay T, 2002. Mer-mediated resistance and volatilization of Hg(II) under anaerobic conditions. Geomicrobiol. J. 19, 87-102.

Scheuhammer AM, Meyer MW, Sandheinrich MB, Murray MW, 2007. Effects of environmental methylmercury on the health of wild birds, mammals, and fish. Ambio, 36, 12-18.

Sellers P, Kelly CA, Rudd JWM, MacHutchon AR. 1996 Photodegradation of methylmercury in lakes. Nature, 380, 694-697.

Sellers P, Kelly CA, Rudd JWM, 2001. Fluxes of methylmercury to the water column of a drainage lake: Relative importance of internal and external sources. Limnol. Oceanogr., 46, 623-631.

Siciliano SD, Lean DRS, 2002. Methyltransferase: an enzyme assay for microbial methylmercury formation in acidic soils and sediments. Environ. Toxicol. Chem., 21, 1184-1190.

Siciliano SD, O'Driscoll N, Lean D, 2004. Microbial reduction and oxidation of mercury in freshwater lakes. Environ. Sci. Technol., 36, 3064-3068.

Skyllberg U, Bloom PR, Qian J, Lin CM, Bleam WF, 2006. Complexation of mercury (II) in soil organic matter: EXAFS evidence for linear two coordination with reduced sulfur groups. Environ. Sci. Technol., 40, 4174–4180.

St. Louis VL, Sharp M, Steffen A, May M, Barker J, Kirk J, Kelly DJA, Arnott, SE, Keatly B, Smol JP, 2004. Some sources and sinks of monomethyl and inorganic mercury on Ellesmere Island in the Canadian High Arctic. Environ. Sci. Technol., 39, 2686-2701.

St. Louis VL, Rudd JWM, Kelly CA, Beaty KG, Bloom NS, Flett RJ, 1994. Importance of wetlands as sources of methyl mercury to boreal forest ecosystems. Can. J. Fish Aquat. Sci., 51, 1065-1076.

Steffan RJ, Korthals ET, Winfrey MR, 2003. Effect of acidification on mercury methylation, demethylation, and volatilization in sediments from an acid-susceptible lake. Appl. Environ. Microbiol., 54, 2003-2009.

Ullrich SM, Tanton TW, Abdrashitova SA, 2001 Mercury in the aquatic environment: A review of factors affecting methylation. Critical Rev. Environ. Sci. Technol., 31, 241–293.

Warner KA, Roden EE, Bonzongo JC, 2003. Microbial mercury transformation in anoxic freshwater sediments under iron-reducing and other electron-accepting conditions. Environ. Sci. Technol., 37, 2159–2165.

Watras CJ, Bloom NS, Claas SA, Morrison KA, Gilmour CC, Craig SR, 1995a. Methylmercury production in the anoxic hypolimnion of a dimictic seepage lake. Water Air Soil Pollut., 80, 735-745.

Watras CJ, Morrison KA, Host JS, Bloom NS, 1995b. Concentration of mercury species in relationship to other site-specific factors in the surface waters of northern Wisconsin lakes. Limnol. Oceanogr., 40, 556-565.

Watras CJ, Morrison KA, Kenta A, Price N, Regnell O, Eckley C, Hintelmann H, Hubacher T, 2005. Sources of Methylmercury to a Wetland-Dominated Lake in Northern Wisconsin. Environ. Sci. Technol., 39, 4747-4758.

Weber JH, 1993. Review of possible paths for abiotic methylation of mercury in the aquatic environment. Chemosphere, 26, 2063-2077.

Winfrey MR, Rudd JWM, 1990. Environmental factors affecting the formation of methylmercury in low pH lakes: a review. Environ. Tox. Chem., 9, 853–869.

Wood JM, 1974. Biological cycles for toxic elements in environment. Science, 183, 1049-1052.

Wood JM, Kennedy PS, Rosen CG, 1968. Synthesis of methylmercury compounds by extracts of a methanogenic bacterium. Nature, 220, 173-174.

CHAPTER 2. A SIMPLIFIED SAMPLE PREPARATION PROCEDURE FOR MEASURING ISOTOPE ENRICHED METHYLMERCURY[1]

[1] Adapted from Avramescu ML, Zhu J, Yumvihoze E, Hintelmann H, Fortin D, Lean DRS, 2010. A simplified sample preparation procedure for measuring isotope enriched methylmercury. Environmental Toxicology and Chemistry, (in press)

Abstract

Many procedures have been developed to measure the concentration of monomethylmercury (MeHg) from different sample matrices and the use of stable isotopes of mercury now provides opportunities to determine its formation and degradation rates. Here, a modified procedure for measuring mercury isotopes in sediment samples that uses acid leaching-ion exchange-thiosulfate extraction (TSE) to isolate and purify the methylated mercury from the matrix is proposed. The latter is followed by aqueous-phase ethylation, purge and trap on Tenax, gas chromatography separation of ethylated mercury compounds, and inductively coupled plasma mass spectrometry detection. The new TSE procedure bridges together two well known methods, the acid-leaching and distillation-derivatization procedures, offering the advantages of artefact-free formation of the first, and low detection limits and the possibility of quantification of individual isotopes of mercury of the second. The modified procedure retains the derivatization, purge and trap, and GC-ICP-MS detection steps from the distillation-derivatization procedure and eliminates the distillation step which is not only laborious but also expensive due to the high cost of installation and time consuming cleaning process. Major advantages of the TSE procedure proposed include the extraction and analysis of a large number of samples in a short time, excellent analyte recoveries and the lack of artefact formation. Sediment certified reference materials (CRMs), BCR 580 and IAEA 405, were used to test the TSE procedure accuracy. Recoveries between 94 to 106% and 95 to 96% were obtained for CRMs and spiked samples (Milli-Q® water), respectively. Comparisons among thiosulfate extraction, distillation, and acid-leaching procedures have shown good agreement of methylmercury values.

Keywords– Methylmercury, Sediment, Isotopes, Thiosulfate extraction, Artefacts.

2.1. Introduction

Known as a powerful neurotoxin that bioaccumulates and biomagnifies in the food chain, methylmercury (MeHg) is naturally produced in the environment, especially in marine, freshwater and estuarine sediments [Benoit et al., 2003; Munthe et al., 2007]. In order to better understand the environmental toxicology of MeHg, reliable and accurate data regarding the rates of MeHg formation and degradation in soils and sediments are required. This is a first step in understanding the transport, persistence and bioavailability of MeHg and is critical to evaluating and identifying ecosystems at risk from MeHg and its impact on human health. The complexity of sediment mineralogy combined with the high organic matter content of many samples generally makes the determination of MeHg concentrations challenging. Accurate, rapid, and less laborious analytical methods are therefore needed for the determination of MeHg concentrations in such matrices, which when combined with isotope enriched mercury experiments, provide estimates of kinetics about MeHg formation and degradation in sediments.

Traditional methods for mercury speciation analyses in sediment/slurry samples are multistep sample treatment procedures. They generally consist of the separation/extraction of mercury species from the matrix, subsequent cleanup/separation of analytes from the interfering matrix compounds, then derivatization and detection by instrumental analysis [Jackson et al., 2009; Bjorn et al., 2007; Hintelmann et al., 1995; Cai et al., 1997; Horvat et al., 1993]. High sensitivity is necessary for mercury speciation analysis, hence different hyphenated analytical techniques have been developed over the years, including cold vapor atomic absorption spectrometry (CVAAS), gas chromatography and atomic fluorescence spectroscopy (GC-AFS), and gas chromatography and inductively coupled plasma mass spectrometry (GC-ICP-MS). Only the latter provides isotopic information.

The most widely used method for the analysis of MeHg in sediment/soil samples consists of a combination of distillation and aqueous-phase ethylation, purge and trap pre-collection followed by GC separation and cold-vapor atomic fluorescence spectrometry (CVAFS) detection ([US EPA Method 1630, 1998; Bloom et al., 1983]). This protocol is popular due to its low detection limit and high efficiency for isolation of MeHg from

complex matrices. In recent years, it has been frequently used in combination with ICP-MS detection (e.g., [Bjorn et al., 2007; Hintelmann et al., 1995; 1997; Hintelmann and Evans, 1997; Heyes et al., 2007]), which provides the lowest detection limits and permits isotope-selective detection [Hintelmann et al., 1995; 2000]. The major inconvenience of the distillation method is the high cost of installation and Teflon® accessories, as well as the time consuming and laborious post-distillation cleaning steps, which limit sample throughput. Moreover, extra attention is required to prevent artefact formation, as well as the temperature and duration of distillation, which can also affect the results [US EPA Method 1630, 1998; Hintelmann et al., 1997; Hintelmann, 1999]. Amongst all the techniques evaluated for isolating MeHg from sediment/soils during the Wiesbaden/Mainz 1998 Workshop [Hintelmann, 1999; Falter et al., 1999], the acid leaching-ion exchange followed by solvent extraction [Cai et al., 1997] was identified as a step not known to produce species transformation (artefactual formation of MeHg) at any concentration of inorganic Hg in the sample, which makes this procedure an attractive alternative to the distillation process.

Recently, new extraction approaches [Lambertsson et al., 2001; Liang et al., 2004] have been developed for MeHg isotope analysis to replace the distillation step. They employ solvent extraction and back extraction in water prior to derivatization and detection. However, the back extraction step using water baths and/or solvent removal via nitrogen purging is also time consuming and costly and considered a limiting step during MeHg analysis.

Here, we propose a new procedure (P1) for the isolation and quantification of MeHg from soil and sediment samples. The method is free of artefact formation that allowed us to quantify not only the total concentration of MeHg, but also the stable isotopic composition of MeHg that is key to the determination of mercury species transformation rates (e.g., methylation and demethylation rates) in sediment samples. This new procedure combines the extraction/separation method based on acid leaching-ion exchange-solvent extraction [6] with derivatization and GC-ICP-MS detection. The proposed procedure is compared with the distillation procedure [Hintelmann et al., 1995; 1997; 2000; US EPA Method 1630, 1998] for reliable MeHg enriched stable isotope determination, and with

distillation and acid leaching procedures for total methylmercury (ΣMeHg – sum of all isotopes) determination.

2.2. Materials and methods

2.2.1. Samples used for investigation

Eleven wet sediment samples and two certified reference materials (CRMs; listed in Table 2-1) were used for the experiments performed in this study. The wet samples were collected from two time series incubation experiments with sediments from the St. Lawrence River near Cornwall, Ontario, Canada sampled in July and August 2007. Six samples from the July 2007 experiment and five samples from the August 2007 were used for the artefact formation test. The mercury species used were enriched with $^{200}Hg^{+}$ and $Me^{199}Hg^{+}$. The samples were collected at -24, 0, 24, and 48h with respect to the time of isotopically enriched mercury species spike, frozen in liquid nitrogen to stop the methylation reaction and kept frozen until analysis. Prior to freezing and analysis, samples were acidified with hydrochloric acid to prevent any methylation during handling. All samples were analyzed in triplicate (duplicate if limited by sample size) using the proposed (P1) and acid-leaching (P3) procedures, except for the distillation (P2) method for which one sample per batch was chosen to be analyzed in duplicate due to the high cost of analysis. These procedures (P1-3) are described in the method section. Multiple analyses (n=7-8) were performed for both CRMs (BCR 580, IAEA 405) presented through all three methods for evaluation and comparison. The sample relative standard errors (RSE; standard error/mean) varied between 1 and 6%. Recoveries of MeHg were determined using the internal standard ($Me^{201}Hg$) peak area for each sample and reference materials. Methylmercury concentration in reagent blanks was below the detection limit of 1 pg of MeHg (as Hg) for the proposed procedure (P1) and distillation (P2), and 20 pg MeHg (as Hg) for the acid leaching procedure (P3). Methylmercury concentrations in all samples were measured as wet weight and normalized to dry weight based on the water content of the sample to avoid sample loss and alteration during the drying process.

2.2.2. Reagents

Stock solutions of 706 μg ml^{-1} of $Me^{199}HgCl$ in 2-propanol and 911 μg ml^{-1} $^{200}Hg^{2+}$ in 10% nitric acid were diluted appropriately on the day of spiking, using anoxic overlaying water from the sampling site, and their concentration was checked by GC-ICP-MS (Platform-ICP-MS, Micromass [Hintelmann and Ogrinc, 2003]) at Trent University (Peterborough, ON, Canada). The solutions were equilibrated for two hours before being added to the incubation bottles. Internal standards were prepared from a 100 ng ml^{-1} $Me^{201}HgCl$ (as Hg) stock solution in 2-propanol diluted to 1 ng ml^{-1} $Me^{201}HgCl$ (as Hg) in Mili-Q® water before spiking the samples. All standards were handled in dark vials. The isotope abundance of spike solutions together with the natural mercury abundance is listed in Table 2-2.

The KBr, $CuSO_4$, H_2SO_4, $Na_2S_2O_3$ and CH_2Cl_2 reagents (analytical purity grade) were obtained from Fisher Scientific or Sigma Aldrich (Canada). Sediment reference materials IAEA 405 and BCR 580 were obtained from the International Atomic Energy Agency (IAEA) and the Institute for Reference Materials and Measurements (IRMM, European Commission – Directorate General Joint Research Centre, Geel, Belgium,), respectively.

2.2.3. Procedures

2.2.3.1. Thiosulfate extraction of MeHg (P1)

The thiosulfate extraction (TSE) procedure consists of two major parts: the extraction and purification steps modified/adapted from the procedure of Cai et al. [1997] as described below; and the aqueous-phase ethylation and detection, consistent with the published procedure of Hintelmann et al. [1995; 1997] that allows isotope enriched MeHg determination.

Wet sediments consisting of 0.5 to 2.0 g were weighed into a 50 ml polypropylene centrifuge tube. The sample was spiked with 50 pg of 1ng ml^{-1} $Me^{201}HgCl$ (100 pg for CRMs) as an internal standard for the isotope dilution quantification. After homogenization, 5 ml of acidic KBr-$CuSO_4$ (5:1) mixture was added and after vigorous

mixing (with vortex), 10 ml of CH_2Cl_2 was added quantitatively. The tube was tightly capped and left to react for 1 h in the dark, followed by 2 h of vigorous mixing with a shaker (330 rpm). The sample was centrifuged at 5000 rpm for 15 min to break the emulsion that may have formed. An exact known amount (by weight) of the extract was transferred to clean 7 ml glass vials and 2 ml of 0.0001 M sodium thiosulfate ($Na_2S_2O_3$) was added to each sample for purification. Samples were shaken for 45 minutes at 330 rpm, vortexed for 30s and then centrifuged for 5 min at 3000 rpm. At this point, two phases could be observed in the vials. An exact known volume from the top aqueous phase ($Na_2S_2O_3$) was then transferred into an extraction vial (microcentrifuge tube), and stored at 4 °C until ethylation and detection.

An appropriate aliquot (0.5 - 1 ml) of the extract was then taken for derivatization by aqueous-phase ethylation with sodium tetraethylborate, and the volatile organomercury compounds (e.g., methylethylmercury) were purged and trapped on a Tenax absorber, thermodesorbed onto the GC column, isothermally separated at 105°C and quantified by ICP-MS as mercury [Hintelmann et al., 1995; 1997; Hintelmann and Ogrinc, 2003]. Details of the procedure are summarized in Figure 2-1. The aqueous-phase ethylation and detection were performed at Trent University. Chromatographic peak areas of the isotopes (generated by the ICP-MS) were used to calculate methylmercury concentrations using a programmed spreadsheet that accounts for procedural blanks and isotope abundance (as in Hintelmann and Ogrinc [2003]).

2.2.3.2. Distillation of MeHg (P2)

The procedure of Hintelmann et al. [Hintelmann et al., 1995; Hintelmann and Evens, 1997] was used for sample preparation (distillation), followed by aqueous-phase ethylation (derivatization) and detection (GC-ICP-MS) as per the P1 procedure shown in Figure 2-1 (steps 3-5). During MeHg analysis, special attention was paid to sample aliquots to be distilled to maintain the original species distribution and avoid species transformation (formation of MeHg artefacts [Hintelmann et al., 1997; Liang et al., 2004; Bloom et al. 1997]); aliquots containing 1 to 2 g sediment (MeHg fraction 0.28%) were taken for distillation. The results were used as a method comparison for isotopically enriched MeHg quantification, as well as for total methylmercury (ΣMeHg – all isotopes) values.

2.2.3.3. Acid extraction of MeHg (P3)

Samples were prepared (H_2SO_4-KBr-$CuSO_4$ leaching /CH_2Cl_2 extraction) and analyzed (GC-AFS) according to Cai et al. [1997]. The procedure generates total methylmercury (ΣMeHg - all isotopes) values of the samples since the MeHg after extraction and $Na_2S_2O_3$ purification (as in P1) undergoes solvent extraction (CH_2Cl_2) and GC-AFS detection.

2.3.4. Statistical analyses

The statistical analysis used both parametric and non-parametric analyses [Millard and Neerchal, 2001; Otto, 2007; Zar, 2006]. Linear regressions, two-sample t-tests, Wilcoxon rank-sum test, and analysis of variances (ANOVA) were used to assess procedure differences in ΣMeHg and MeHg isotopes ($Me^{200}Hg$, $Me^{199}Hg$, Amb-MeHg) concentrations with S-Plus® 8.0 software (Insightful Corporation) for Windows®. Data were tested for normality and homogeneity of variance with the Kolmogorov-Smirnov test of composite normality and ANOVA. Where normality and/or homoscedasticity assumptions of residuals were not met, non-parametric analyses were performed.

2.3. Results and discussion

2.3.1. Comparison of Methylmercury Results by P1, P2, and P3 Procedures

Two certified reference materials and six wet sediment (slurry) samples were analyzed using the thiosulfate extraction (P1), distillation (P2), and acid extraction (P3) procedures for MeHg content (ΣMeHg and MeHg isotopes: $Me^{200}Hg$, $Me^{199}Hg$, Amb-MeHg). The sample characteristics are listed in Table 2-1.

Statistical correlations between the results acquired for each procedure are reported in the Supplemental Data, Table S2-1and S2-2. The ΣMeHg data obtained with the P1 procedure strongly correlate with results obtained with the P2 (r^2=0.83, p<0.05) and P3 (r^2=0.97, p<0.05) procedures. The relationships between sample MeHg isotope concentrations (ng g^{-1}) obtained by the P1 and P2 procedures are shown in Figure 2-2. For both $Me^{200}Hg$ and $Me^{199}Hg$, the results obtained with the P1 procedure are strongly

correlated to those obtained with the P2 procedure ($Me^{200}Hg$: r^2=0.93, p<0.05; $Me^{199}Hg$: r^2=0.906, p<0.05). In contrast, for ambient MeHg-(amb-$Me^{202}Hg$), the results of the two P1 and P2 procedures show a poor correlation (r^2=0.09, p>0.05); however, we believe that the observed differences are not caused by the analytical process. The sediment samples (Zone 1, St. Lawrence River, Cornwall, ON, Canada) used in the present study were highly heterogeneous, being a composite of brown-black clayed mud with wood fibres and oil patches resulting from the historical industrial contamination of the site [Ridal et al., 2009; Delongchamp et al., 2009; Biberhofer and Rukavina, 2002] and microbialdecay. The sediment heterogeneity therefore influenced the high variability of ambient mercury concentrations (MeHg: 2.6±0.53 ng g^{-1}, n=24 and total Hg: 1212±489.4 ng g^{-1}, n=35) in the samples. For future analyses of highly heterogeneous samples, we recommend a greater amount of sample (at least 2 g of wet sediments) to be taken for analysis to reduce the sample heterogeneity. For the analyzed samples (Figure 2-2), the statistical analyses (Supplemental Data, Table S2-1 and S2-2) indicate that there is no significant difference between MeHg isotope results obtained with the P1 and P2 procedures.

The purpose of this method development was to establish an easy procedure to analyze samples containing isotope enriched mercury resulting from incubation experiments with river sediments. For rate calculations (methylation and demethylation), it was necessary to analyze the samples wet (slurry) in order to minimize species interconversions during drying. Based on the data and statistical analyses, we can conclude that the thiosulfate (P1) procedure can replace the distillation (P2) procedure for MeHg isotope analyses. The P1 procedure offers reliable and accurate results for quantification of the added isotope tracers.

Figure 2-3 shows the comparison among the concentrations (± SE) obtained with the P1, P2, and P3 procedures; MeHg values as well as the average results of the three procedures (± SE) are listed in Supplemental Data, Table S2-3. Statistical analysis showed that there was no significant difference (p > 0.05) between the results, with P1 and P2 having the highest mean concentrations (Supplemental Data, Table S2-2).

Analysis of procedural blanks consisting of deionized water (Milli-Q water) revealed no mercury contamination during MeHg extraction and analysis. The detection limit was estimated to be 1 pg for ICP-MS [Hintelmann et al., 1997; Hintelmann and Evans 1997; Hintelmann and Ogrinc, 2003]. The P1 method recoveries for spiked samples (Milli-Q water) were 95-96% (n=2), whereas for certified reference materials (IAEA 405 and BCR 580), it was between 94 to 106% (BCR 580: 97.1%, n=6, RSD=0.43; IAEA 405: 98.2%, n=8, RSD=2.69). The accuracy of the CRM measurements calculated as percent error for the mean of the measurements was 0.26% for BCR 580 and 1.8% for IAEA 405.

2.3.2. Formation of MeHg artefacts

The proposed TSE procedure (P1) generated results similar to the other two procedures (P2 and P3) for both the samples and the reference materials (Figure 2-2 and 2-3). Knowing that the distillation procedure (P2) produces artefacts which are significant for soil and sediment samples having a low MeHg fraction (i.e., 0.1-1%) [Hintelmann and Evans 1997; Hintelmann, 1999; Falter et al., 1999], the TSE procedure (P1) was evaluated for artefact formation (i.e., undesired production of MeHg during the extraction procedure). Since the purpose of this method development was to analyze samples containing isotope enriched methylmercury derived from microbial methylation of inorganic Hg, we spiked the river sediment incubation microcosms with $^{200}Hg^{2+}$. Five different samples (Table 2-3) from the August 2007 experiment with the St. Lawrence River (Cornwall, ON, Canada) sediments were spiked with 200 µl of 9.9 ng ml^{-1} $^{200}Hg^{2+}$ (1.98 ng $^{200}Hg^{2+}$) solution and analyzed with the TSE procedure (P1). Non-spiked samples were also run with the P1 procedure and the difference between spiked and non-spiked MeHg concentrations of samples was accounted for as an artefact. The MeHg values were found to be independent of the spiked $^{200}Hg^{2+}$ standard suggesting no artefact formation (Table 3). Also, ΣMeHg values (not-spiked: 7.80-10.02 ng g^{-1}, spiked: 7.78-10.30, SE=0.01-0.36) showed no additional formation of MeHg; spiked samples were in general lower than the calculated ones (8.88-11.4 ng g^{-1}) (Supplemental Data, Table S2-4 and S2-5).

Moreover, the excess $Me^{200}Hg$ in the spiked samples was calculated as the difference between the measured $Me^{200}Hg$ and the expected $Me^{200}Hg$ if no artefact was present, where:

$$\text{expected } Me^{200}Hg = Me^{202}Hg * \frac{\text{abundance } 200Hg}{\text{abundance } 202Hg} \qquad (1)$$

The calculated excess $Me^{200}Hg$ was negative for all the samples tested, further indicating that no artefact was formed (Supplemental Data, Table S2-5).

While comparing the distillation and the acid leaching (HCl) extraction for artefact formation, Hintelmann et al. [1997] observed that in the case of acid leaching, the artefactual MeHg was only formed when the stable isotope was directly added to the sediments before the acid addition. Using an acid extracting procedure (HNO_3 leaching), Liang et al. [2004] observed no artefact formation, and noted that the measured MeHg was independent of the naturally occurring Hg(II) content in the aliquots of the analyzed sediment samples. In our tests, the stable isotope spike ($^{200}Hg^{2+}$) and the internal standard ($Me^{201}Hg$) were added just before the acid KBr-$CuSO_4$ mixture and no additional MeHg formation was noticed (Table 2-3) for all samples, except F4 for which a small increase was measured. Taking into account the high heterogeneity of the river sediments, we conclude that the proposed method (P1) does not produce artefactual MeHg.

2.3.3. Procedure optimization

During the extraction procedure, the acidic KBr-$CuSO_4$ mixture was used as the extractant to release organomercury compounds from the sediment matrix. Cupric ions promote the release of the organomercury compounds from the matrix while keeping the volume of organic solvent small, thus reducing the extraction time. Organomercury compounds are then transformed to organomercury bromide derivatives (RHgBr) that are extracted into the CH_2Cl_2 (methylene chloride) layer. Due to their greater nucleophilic character, RHgBr compounds have more affinity for the organic (CH_2Cl_2) phase than other halides [Cai et al., 1997; Cai et al., 1996; Cappon and Smith, 1977]. The cleanup of the organic (CH_2Cl_2) extract is quantitatively achieved with sodium thiosulfate which rapidly complexes methylmercury. Since sodium thiosulfate has a high complexing affinity for

organic mercury [Cappon and Smith, 1977], the optimization of the TSE procedure (P1) was necessary to improve the recovery of Hg species (internal standard, IS) during the ethylation step. The high affinity of Hg for thiosulfate makes Hg species less available for ethylation, consequently affecting the ethylation step efficiency and producing low recoveries of the internal standard (IS: $Me^{201}Hg$). The critical factor that impacts the efficiency of ethylation is the thiosulfate concentration in the ethylation vessel. Its influence was checked in two ways by varying: the volume of extract considered for ethylation; and the concentration of thiosulfate used for Hg species extraction from the organic phase (CH_2Cl_2).

In order to test the first factor, two different samples (BH 21 and BH 30) and one CRM (BCR 580) were extracted using 10 mM thiosulfate, as in Cai et al. [1997], and three different volumes of extract (0.2, 0.5, and 1 ml) were taken for ethylation (Figure 2-4A). The test showed that by decreasing the extract volume from 1 to 0.2 ml, the internal standard recovery increased from 16 to 59.1% for the given thiosulfate concentration (10 mM). A 50% recovery was attained for the 0.5 ml extract analyzed for both CRM and the sample tested. In order to avoid too much dilution of the IS in the ethylation vessel, the 0.5 ml extract was considered optimum for the analysis.

The second factor, i.e., thiosulfate concentration, strongly influences the ethylation step efficiency and IS recovery, as shown in Figure 2-4b; consequently more diluted concentrations of thiosulfate (i.e., 1 mM and 0.1 mM) were tested. The thiosulfate solutions were spiked with 50µl of a 5 ng g^{-1} MeHg standard solution (natural abundance), ethylated, and the recovery was calculated. Figure 2-5 shows the recovery of the internal standard as a function of the thiosulfate concentration. The lower the thiosulfate concentration of the extraction reagent and consequently in the ethylation vessel, the higher the recovery, and for concentrations less than 0.1 mM, recoveries increased from 66 to 106% (Figure 2-4b). Also, for 1 ml and 0.5 ml of the 0.1 mM thiosulfate solution tested, high recoveries of 87.6 and 99.7%, respectively, were obtained. Based on the optimization tests, we conclude that 0.1 mM thiosulfate should be used for extraction and an extract volume of 0.5 ml for ethylation.

2.3.4. Procedure validation

The validation of the method was performed with two different reference materials IAEA 405 and BCR 580, described in Table 2-1. Replicates (n=8) of the two CRMs were run using the TSE procedure (P1) and, for comparison, with the P3 procedure. Figure 2-5 shows the mean values for both CRMs (±SD) obtained with P1 and P3. The null hypothesis that the difference between the measured values (CRMs) and the certified values is random was tested by using the student t-test (95% confidence interval) after the data sets were checked for outliers with the Dixon's Q outlier test and Grubb's outlier test (Supplemental Data, Table S2-6 and S2-7). No significant difference (p<0.05) was found between the mean values determined with the P1 procedure and the certified values for both CRM tested. Recoveries of 94 to 109% were obtained for BCR 580 with both procedures, while for IAEA 405, the P1 procedure generated improved recoveries of 94 to 105% (P3: 78-96%).

2.4. Conclusions

The new TSE procedure (P1) not only produces accurate results, but also combines the major advantages of the other two procedures evaluated (P2 and P3): low detection limits and possibility of isotope quantification with the use of ICP-MS detection from the distillation procedure (P2) and the absence of artefact formation during sample extraction from the acid-leaching procedure (P3). Another major advantage of the TSE procedure proposed here is that a large number of samples can be extracted and analyzed in a short time with excellent recoveries and without artefact formation. Moreover, the high sensitivity of the ethylation step and use of ICP-MS offer the advantage of a low detection limit which allows the application of this new method to analyze samples bearing trace levels of MeHg as presented in this present study.

2.5. References (reference style according to Env. Toxicol. Chem.)

Benoit JM, Gilmour CC, Heyes A, Mason RP, Miller CL. 2003. Geochemical and biological controls over methylmercury production and degradation in aquatic ecosystems. *ACS Symposium Series* 835: 262-297.

Biberhofer J, Rukavina NA. 2002. Data on the distribution and stability of St. Lawrence River sediments at Cornwall, Ontario. Environment Canada, National Water Research Institute, Burlington/ Saskatoon, NWRI Contribution No. 02–195.

Bjorn E, Larsson T, Lambertsson L, Skyllberg U, Frech W. 2007. Recent advances in mercury speciation analysis with focus on Spectrometric methods and enriched stable isotope applications. *Ambio* 3: 443-451.

Bloom NS, Colman JA, Barber L. 1997. Artefact formation of methyl mercury during aqueous distillation and alternative techniques for the extraction of methyl mercury from environmental samples *Fresen J Anal Chem* 358: 371-377.

Bloom NS, Crecelius EA. 1983. Determination of mercury in seawater at sub-nanogram per liter levels. *Mar Chem* 14: 49-59.

Cai Y, Jaff R, Allia A, Jones RD. 1996. Determination of organomercury compounds in aqueous samples by capillary gas chromatography-atomic fluorescence spectrometry following solid-phase extraction. *Anal Chim Acta* 334: 25 l-259.

Cai Y, Tang G, Jaffé R, Jones R. 1997. Evaluation of some Isolation Methods for Organomercury Determination in Soil and Fish Samples by Capillary Gas

Chromatography – Atomic Fluorescence Spectrometry. *Int J Environ An Ch* 68: 331-345.

Cappon C J and Smith JC. 1977. Gas-chromatographic determination of inorganic mercury and organomercurials in biological materials. *Anal Chem* 49: 365-369.

Delongchamp, T M, Lean D R S, Ridal JJ, Blais J M. 2009. Sediment mercury dynamics and historical trends of mercury deposition in the St. Lawrence River area of concern near Cornwall, Ontario, Canada. *Sci Total Environ* 407: 4095-4104.

Falter R, Hintelmann H, Quevauviller P. 1999. Conclusion of the workshop on "Sources of error in methymercury determination during sample preparation, derivatization and detection". *Chemosphere* 39: 1039-1049.

Heyes A, Mason R, Kim E-H, Sunderland E. 2006. Mercury methylation in estuaries: Insights from using measuring rates using stable mercury isotopes. *Mar Chem* 102: 134-147.

Hintelmann H, Evans RD, Villeneuve JY. 1995. Measurement of mercury methylation in sediments by using enriched stable mercury isotopes combined with methylmercury determination by gas chromatography-inductively coupled plasma mass spectrometry. *J Anal Atom Spectrom* 10: 619–624.

Hintelmann H, Falter R, Ilgen G, Evans RD. 1997a. Determination of arifactual formation of monomethylmercury (CH_3Hg^+) in environmental samples using stable Hg2+ isotopes with ICP-MS detection: Calculation of contents applying species specific isotopes addition. *Fresen J Anal Chem* 358: 363–370.

Hintelmann H, Evans RD. 1997b. Application of stable isotopes in environmental tracer studies – Measurement of monomethylmercury (CH_3Hg^+) by isotope dilution ICP-MS and detection of species transformation. *Fresen J Anal Chem* 358: 378–385.

Hintelmann H. 1999. Comparison of different extraction techniques used for methylmercury analysis with respect to accidental formation of methylmercury during sample preparation. *Chemosphere* 39: 1093-1105.

Hintelmann H, Keppel-Jones K, Evans RD. 2000. Constants of mercury methylation and demethylation rates in sediments and comparison of tracer and ambient mercury availability. *Environ Toxicol Chem* 19: 2204–2211.

Hintelmann H, Ogrinc N. 2003. Determination of Stable Mercury Isotopes by ICP-MS and Their Application in Environmental Studies ACS Symposium Series 835: 321-338

Horvat http://www.scopus.com.proxy.bib.uottawa.ca/search/submit/author.url?author=Horvat%2c+M.&origin=resultslist&authorId=7004953937&src=sM, Bloom NS, Liang L. 1993a. Comparison of distillation with other current isolation methods for the determination of methyl mercury compounds in low level environmental samples. Part 1. Sediments. *Anal Chim Acta* 28: 135-152

Jackson B, Taylor V, Baker RA, Miller E. 2009. Low-level mercury speciation in freshwaters by isotope dilution GC-ICP-MS. *Environ Sci Technol* 43: 2463-2469.

Lambertsson L, Lundberg E, Nilsson M, Frech W. 2001. Applications of enriched stable isotope tracers in combination with isotope dilution GC-ICP-MS to study mercury

species transformation in sea sediments during in situ ethylation and determination. *J Anal Spectrum* 16:1296-1301.

Liang L, Horvat M, Feng X, Shang L, Li H, Pang P. 2004. Re-evaluation of distillation and comparison with HNO_3 leaching /solvent extraction for isolation of methylmercury compounds from sediment/soil samples. *Appl Organomet Chem* 18: 264-270

Millard SP, Neerchal NK. 2001. *Environmental Statistics with S-Plus.* CRC Press LLC, Bocca Raton, Florida.

Munthe J, Bodlay RA, Branfireun BA, Driscoll CT, Gilmour CG, Harris R, Horvat M, Lucotte M, Malm O. 2007. Recovery of Mercury-Contaminated Fisheries. *Ambio* 36: 33-44.

Otto M. 2007. Chemometrics, Statistics and Computer Application in Analytical Chemistry, 2nd ed. Wiley-VCH Verlag GmbH & Co. KgaA.

Ridal JJ, Yanch E, Fowlie A, Razavi NR, Delongchamp T, Choy E, Fathi M, Hodson P, Campbell LM, Blais JM, Hickey MBC, Yumvihoze E, Lean DRS. 2009. Potential Causes of Enhanced Transfer of Mercury to St. Lawrence River Biota: Implications for Sediment Management Strategies at Cornwall, Ontario, Canada. *Hydrobiology* DOI 10.1007/s10750-009-9951-1.

US EPA. Method 1630: Methyl Mercury in water by distillation, aqueous ethylation, purge and trap, and cold vapor atomic fluorescence spectrometry. Draft, August 1998.

Zar JH. 2006. *Biostatistical Analysis,* 5th ed. Prentice-Hall, Upper Saddle River, New Jersey.

Tables

Table 2-1. Samples used for method comparison

Sample ID	Description	Status	Comments
IAEA[a] 405	Estuarine sediment, intertidal mudflats of the Tagus estuary, Portugal	Dry	Certified Reference Material THg : 0.81 ± 0.04 μg g^{-1} MeHg : 5.49 ± 0.53 ng g^{-1} as Hg
BCR[a] 580	Estuarine sediment	Dry	Certified Reference Material THg : 132 ± 3 μg g^{-1} MeHg : 75.5 ±3.7 ng g^{-1} as Hg
BH 21	River sediment, St Lawrence River (Cornwall, ON, Canada)	Wet (slurry)	t = -24 h (before spiking with $^{200}Hg^{2+}$ and $Me^{199}Hg^{+}$)
BH 24	River sediment, St Lawrence River	Wet (slurry)	t = 0 h (treated with $^{200}Hg^{2+}$ and $Me^{199}Hg^{+}$)
BH 27	River sediment, St Lawrence River	Wet (slurry)	t = 24 h (treated with $^{200}Hg^{2+}$ and $Me^{199}Hg^{+}$)
BH 33	River sediment, St Lawrence River	Wet (slurry)	t = 96 h (treated with $^{200}Hg^{2+}$ and $Me^{199}Hg^{+}$)
E 24	River sediment, St Lawrence River	Wet (slurry)	t = 0 h (treated with $^{200}Hg^{2+}$ and $Me^{199}Hg^{+}$, and SRB inhibitor)[b]
F 27	River sediment, St Lawrence River	Wet (slurry)	t = 24 h (treated with $^{200}Hg^{2+}$ and $Me^{199}Hg^{+}$, and MPA inhibitor)[a]

The t represents the sampling time during the 96 h incubation experiment.

[a] Community Bureau of Reference (BCR); International Atomic Energy Agency (IAEA)

[b] sulfate reducing bacteria (SRB); methane producing archaea (MPA)

Table 2-2. Natural and enriched Hg solution abundances used in this study. Values are given as the percentage of the total Hg concentration.

Hg isotope	Natural abundance	$Me^{199}HgCl$ (706 μg ml^{-1})	$^{200}Hg(NO_3)_2$ (911 μg ml^{-1})	$Me^{201}HgCl$ (100 μg ml^{-1})
196	0.15	0.02	0.07	0.01
198	10.02	1.63	4.00	0.12
199	16.84	91.95	3.57	0.10
200	23.13	4.92	79.60	0.45
201	13.22	0.66	3.96	98.11
202	29.8	0.73	7.34	1.18
204	6.85	0.11	1.46	0.03

Table 2-3. MeHg results (ng g^{-1} dry wt) obtained with non-spiked and spiked (2 ng of $^{200}Hg^{2+}$) samples for the artefact formation test.

Sample ID	Description	$Me^{200}Hg$ (ng g^{-1})		
		non spiked	spiked	average
BH4	St Lawrence River (Cornwall, ON, Canada) sediment treated with $^{200}Hg^{2+}$ and $Me^{199}Hg^{+}$ (t=0 h)	0.52	0.51	0.51 ± 0.00
B4	St Lawrence River sediment treated with $^{200}Hg^{2+}$ and $Me^{199}Hg^{+}$and HFO (t=0 h)	0.63	0.57	0.60 ± 0.05
E4	St Lawrence River sediment treated with $^{200}Hg^{2+}$ and $Me^{199}Hg^{+}$, HFO, and SRB inhibitor (t=0 h)	0.45	0.46	0.46 ± 0.01
F4	St Lawrence River sediment treated with $^{200}Hg^{2+}$ and $Me^{199}Hg^{+}$, HFO, and MPA inhibitor (t=0 h)	0.46	0.44	0.45 ± 0.02
G4	St Lawrence River sediment treated with $^{200}Hg^{2+}$ and $Me^{199}Hg^{+}$, HFO, SRB and MPA inhibitor (t=0 h)[a]	0.37	0.39	0.38 ± 0.01

[a] Ferrihydrite (HFO); sulfate reducing bacteria (SRB); methane producing archaea (MPA)

Figures

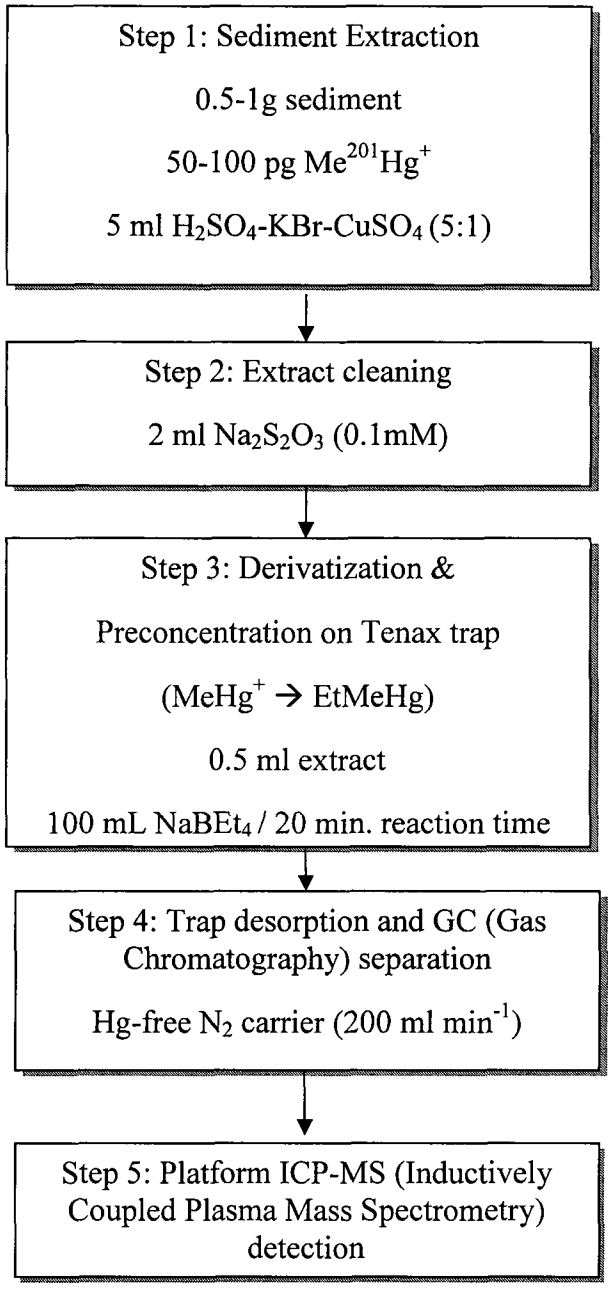

Figure 2-1. Schematic description of the thiosulfate extraction of methylmercury procedure ([TSE], P1).

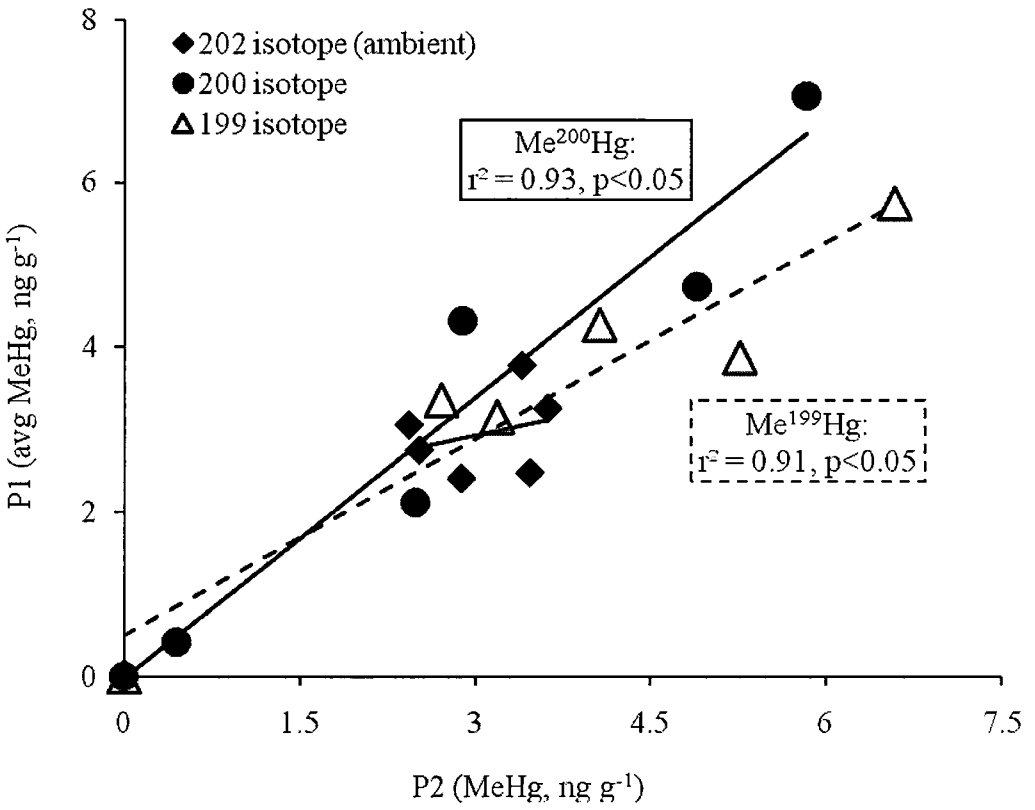

Figure 2-2. Methylmercury (MeHg) isotope concentrations ($Me^{200}Hg$, $Me^{199}Hg$, and ambient-MeHg, ng g^{-1} dry wt) generated by thiosulfate (P1, n=3 replicates) and distillation procedures (P2, n=1 replicates). St. Lawrence River (Cornwall, ON, Canada) sediment samples as in Table 2-2.

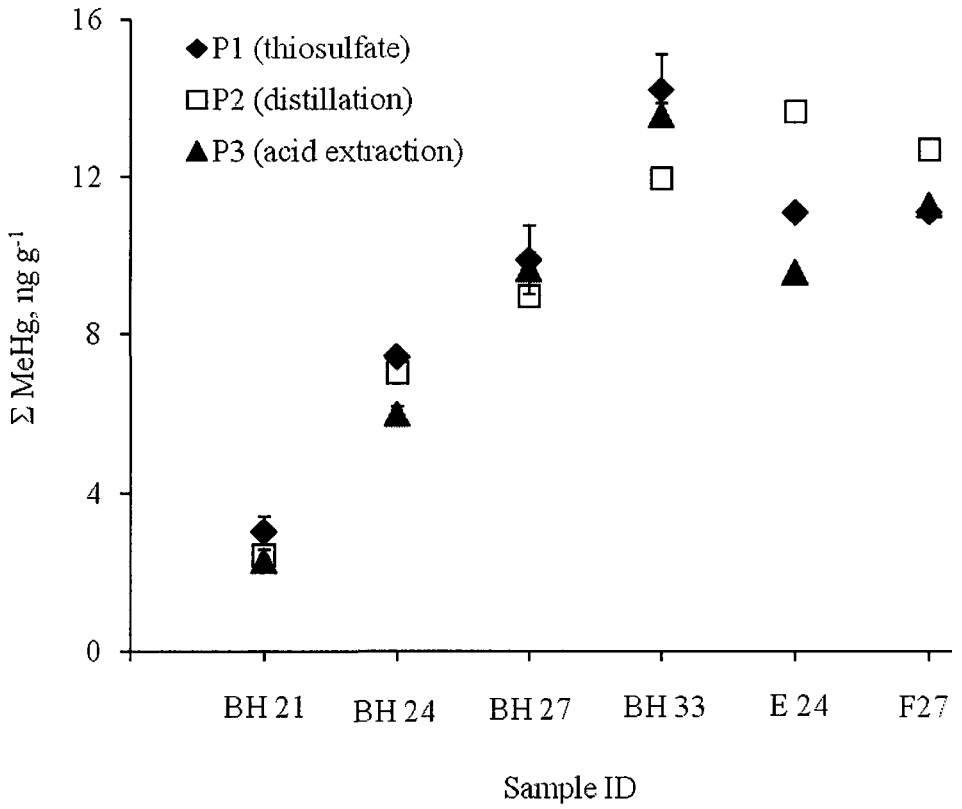

Figure 2-3. Comparison of methylmercury results (ΣMeHg, ng g^{-1} dry wt) generated by thiosulfate (P1, n=3), distillation (P2), and acid extraction (P3, n=3) procedures. Error bars represent standard deviation. (ΣMeHg =sum of all Hg isotopes).

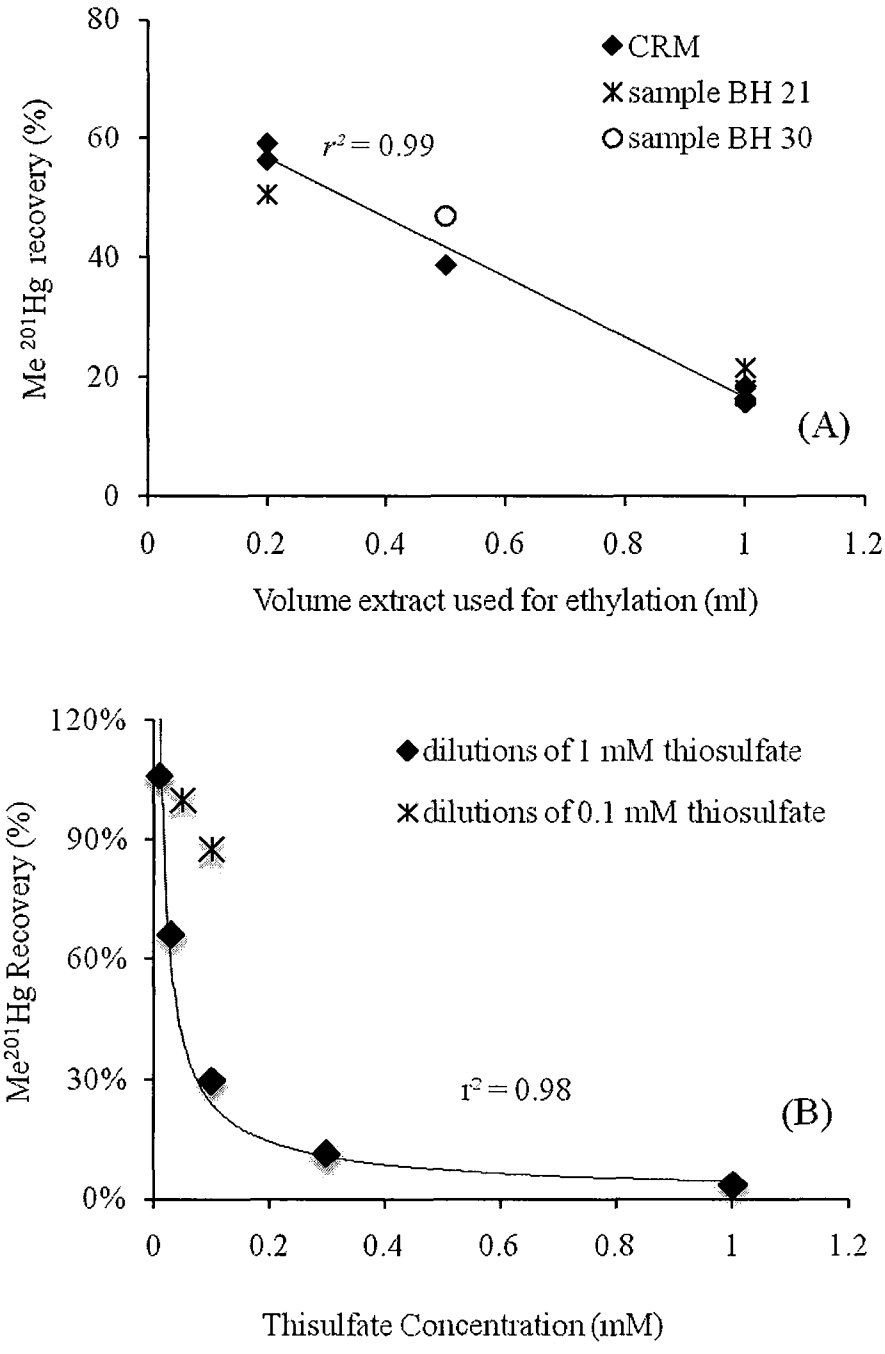

Figure 2-4. Recovery of internal standard (IS: $Me^{201}Hg$) as a function of the volume of extract used for ethylation (A) and the concentration of thiosulfate solution added to the ethylation vessel (B). The certified reference material (CRM) was BCR 580 (BCR = Community Bureau of Reference).

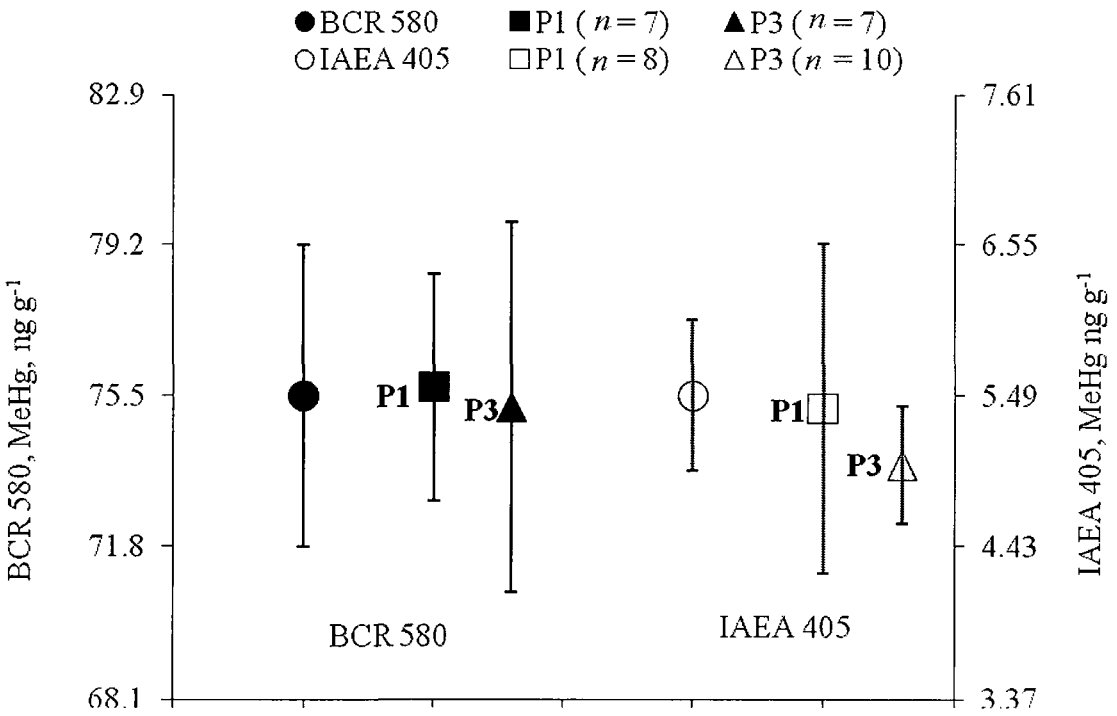

Figure 2-5. Certified reference materials (CRM) methylmercury (MeHg) concentrations obtained for the procedures P1 and P3: BCR 580 (black symbols; 75.5 ± 3.7 ng g^{-1}) and IAEA 405 (white symbols; 5.49 ± 0.53 ng g^{-1}). The certified values (circles) are given for both CRMs tested. Error bars represent the standard deviation.

Supporting information

Seven tables (Table S2-1 to S2-7) are presented as supporting information containing details of the statistical analyses, MeHg results obtained by P1, P2, and P3 procedures, and artefact formation test results.

Table S2-1. Simple Regression model to check the relationship among methylmercury (MeHg) concentrations obtained by thiosulfate (P1), distillation (P2), and acid-leaching (P3) procedures (H0: there is no relationship between P1 and P2 results; $y=a*x+b$).

MeHg isotopes	Procedure	*df*	*a*	*b*	*se*	*t* value	*f*	r^2	*p*-value	Correlation of coefficients	Statistical signification
200	P1 vs P2	4	1.138	-0.035	0.15	7.54	56.82	0.934	0.0017	-0.79	reject H0
199	P1 vs P2	4	0.797	0.501	0.13	6.19	38.37	0.906	0.0035	-0.87	reject H0
Amb(202)	P1 vs P2	4	0.301	2.034	0.48	0.62	0.39	0.088	0.5671	-0.99	accept H0
All	P1 vs P2	4	0.821	1.702	0.19	4.37	19.12	0.827	0.0120	-0.93	reject H0
All	P1 vs P3	4	1.021	-0.899	0.08	11.80	139.33	0.972	0.0003	-0.92	reject H0

Simple model I regression assumptions were checked using the plots obtained from regression procedure (ANOVA): residuals vs fit plot (for any value of X, the Y's are independently and normally distributed - residuals are normally distributed); normal QQ plot of residuals (the variances of Y for fixed X is independent of X).

Table S2-2. Parametric Pooled-Variance Two-Sample *t*-test for comparison methylmercury concentrations (ΣMeHg-sum of all isotopes) obtained by P1, P2, and P3 procedures (H0: mean X = mean Y). Assumption of normally distributed residuals and equal variances were tested with ANOVA (fixed effects), Kolmogorov-Smirnov Test of Composite Normality, and by examining the mean differences in the absolute values of the residuals (*t* test).

MeHg isotopes	Procedure	mean X	mean Y	*t*	*p*	Statistical signification	normality of residuals	homoscedasticity of residuals
200	P1 vs P2	3.11	2.76	0.237	0.82	accept H0	yes	yes
* 199	* P1 vs P2				0.60	accept H0	no	yes
Amb(202)	P1 vs P2	2.95	3.05	0.341	0.74	accept H0	yes	yes
All	P1 vs P2	9.46	9.45	0.004	1.00	accept H0	yes	yes
* All	* P1 vs P3				0.70	accept H0	no	yes

* non-parametric Exact Wilcoxon rank-sum test was used.

Table S2-3. ΣMeHg concentration (ng g^{-1} dry weight) obtained with all three procedures.

Time* (h)	Sample ID	ΣMeHg (ng g^{-1})			
		P-1 (n=3)	P-2	P-3 (n=3)	Avg. P1-P3
-24	BH 21	2.43 ± 0.34	3.05	2.5 ± 0.02	2.65 ± 0.35
0	BH 24	7.03 ± 0.07	7.44	6.0 ± 0.16	6.82 ± 0.74
24	BH 27	8.96 ± 0.86	9.87	9.7 ± 0.42	9.50 ± 0.48
96	BH 33	11.94 ± 0.93	14.19	13.6 ± 0.27	13.23 ± 1.16
0	E 24	13.64 ± 0.10	11.08	9.6 ± 0.003	11.43 ± 2.05
24	F27	12.69	11.10	11.3	11.69 ± 0.87

* Time (h) represents the sampling time during the 96 h incubation experiment.

Table S2-4. Artefact formation test results (ng g^{-1} dry weight) obtained with thiosulfate (TSE, P1) procedure- non-spiked. Spiked sample results presented in Table S2-5.

Description	ID	Measured (non-spiked) (ng g^{-1})			[Spiked - (non-Spiked)] (ng g^{-1})
		ΣMeHg	amb-MeHg	$Me^{200}Hg$	$Me^{200}Hg$
BH4	37	8.69	2.19	0.516	0.00
B4	39	10.30	2.99	0.633	-0.07
E4	41	8.80	2.18	0.450	0.01
F4	43	9.50	2.66	0.464	-0.03
G4	45	7.78	2.04	0.373	0.01

Table S2-5. Artefact formation test results (ng g^{-1} dry weight) obtained with thiosulfate (TSE, P1) procedure: spiked samples with 0.2 mL of 9.9 ng mL^{-1} ^{200}Hg.

Description	ID	Measured (ng g^{-1})			Expected $Me^{200}Hg$ (ng g^{-1})	Excess $Me^{200}Hg$ (ng g^{-1})
		ΣMeHg	amb-MeHg	$Me^{200}Hg$		
BH4	37	9.07	2.69	0.51	29.17	-28.66
B4	39	9.58	2.56	0.57	27.73	-27.16
E4	41	9.22	2.20	0.46	23.86	-23.40
F4	43	10.02	3.98	0.44	43.15	-42.71
G4	45	7.80	1.86	0.39	20.20	-19.81

The excess $Me^{200}Hg$ was calculated as:

$$\textbf{excess}\ Me^{200}Hg = \textbf{measured}\ Me^{200}Hg - \textbf{expected}\ Me^{200}Hg \quad (1)$$

where,

$$\text{expected}\ Me^{200}Hg = Me^{202}Hg * \frac{\text{abundance } 200Hg}{\text{abundance } 202Hg} \quad (2)$$

Table S2-6. Student *t* test for comparison of measured CRM methylmercury concentrations (P1 and P3 procedures) with certified values (ng g^{-1} dry weight)

	P1 Procedure		P3 Procedure	
	BCR 580	IAEA 405	BCR 580	IAEA 405
Certified Value	75.5 ± 3.7	5.49 ± 0.53	75.5 ± 3.7	5.49 ± 0.53
Mean	75.70	5.39	75.19	4.98
STDEV	2.78	1.16	4.53	0.41
n	7	8	7	9
f = n-1	6	7	6	8
α	0.05	0.05	0.05	0.05
t	0.188	0.244	0.182	3.697
$t(1-\alpha/2, f)$	2.447	2.365	2.447	2.262
$t < t(1-\alpha/2, f)$	accept H0*	accept H0*	accept H0*	accept H0*
	no significant difference			

* H0: the difference between the sample and the true value is random (mean = certified value)

Table S2-7 Outlier tests for methylmercury CRM measurements (ng g^{-1} dry weight) obtained with P1 and P3 procedures

Dixon's Q outlier test	P1 procedure		P3 procedure	
	BCR 580	IAEA 405	BCR 580	IAEA 405
Mean	75.70	5.39	75.19	5.22
STDEV	2.78	1.16	4.53	0.86
n	7	8	7	10
Q1	0.0016	0.3682	0.0481	0.1008
Qn	0.2599	0.4822	0	0.6003
α	0.01	0.01	0.01	0.01
$Q(1-\alpha, n)$	0.54	0.59	0.54	0.53
$Q1 < Q(1-\alpha, n)$	not outlier	not outlier	not outlier	not outlier
$Qn < Q(1-\alpha, n)$	not outlier	not outlier	not outlier	outlier
Grubb's outlier test	P1 procedure		P3 procedure	
	BCR 580	IAEA 405	BCR 580	IAEA 405
T1	1.02	1.55	0.90	1.09
T2	1.43	2.08	1.62	2.54
α	0.01	0.01	0.01	0.01
$T(1-\alpha, n)$	2.22	2.22	2.22	2.41
$T1 < Q(1-\alpha, n)$	not outlier	not outlier	not outlier	not outlier
$T2 < Q(1-\alpha, n)$	not outlier	not outlier	not outlier	not outlier

CHAPTER 3. METHYLATION AND DEMETHYLATION IN WETLAND SEDIMENTS: INITIAL EXPERIMENT AND VALIDATION OF THE EXPERIMENTAL DESIGN

Abstract

High concentrations of monomethylmercury (MMHg) in fish have led to increasing scientific research and political interest regarding the various pathways leading to mercury methylation. Previous studies on mechanisms and factors that affect mercury methylation in aquatic environments have shown that microorganisms play a role in mercury methylation, especially sulfate-reducing bacteria (SRB). However, despite the generally accepted view that some SRB are the primary methylators in anoxic sediments, not all SRB are capable of mercury methylation and other microorganisms (methanogens - MPA and iron-reducing prokariots - FeRP) may also be important. Our study focuses on the biogeochemical factors, i.e., the relative importance of the diverse groups of anaerobic microbes (FeRP, SRB, MPA), that affect net methyl mercury formation in freshwater. Methylation and demethylation were measured separately by using enriched stable isotopes of mercury $^{200}Hg^{2+}$ and $Me^{202}Hg$ in microcosms treated with specific microbial inhibitors. Sediments from the Mer Bleue wetland in Ottawa, Ontario, were sampled in May and July 2006 and incubated in the dark at room temperature in an anaerobic chamber for 72h. The amount of $Me^{200}Hg$ produced and the amount of $Me^{202}Hg$ remaining were measured. During the first 24 h, MeHg concentrations increased linearly for all treatments containing microbial inhibitors, but not for the control system (with only Hg spikes). In that system, a linear increase could only be assumed (based on the available data) for the first 4 hours. This preliminary experiment allowed us to establish the proper set up and methods to be used for future experiments.

Keywords: methylmercury, methylation, Demethylation, SRB, MPA, FERP, wetland.

3.1. Introduction

High concentrations of monomethylmercury (MeHg) in fish have triggered a large number of scientific studies and led to major policy decisions related to safe fish consumption. It is now clear that pathways leading to mercury methylation are of a highest scientific priority, because methylation of inorganic mercury can take place in both pristine and impacted environments. The major pathways of Hg methylation have however not been resolved. Several studies have demonstrated that Hg methylation occurs mostly in surface sediments [e.g., Martin-Doimeadios 2004; Gilmour et al., 1992; 1998; Choi and Bartha, 1994; King et al., 2001; Compeau and Bartha, 1985] and to a lesser extent, in the water column [e.g., Eckley et al., 2005; Watras et al., 1995; Robinson et al., 1984]. Elevated concentrations of both total mercury (THg) and MeHg are frequently found in anoxic waters. In many freshwater systems, the highest methylation rates have been observed at the sediment–water interface [Watras et al., 2005; Rudd, 1995], where anoxic conditions occur (usually in June), but they decrease with increasing sediment depth [Rudd, 1995; Matilainen, 1995].

In temperate environments, wetlands are considered to be the principal source of MeHg, as they contribute significant amounts of MeHg to receiving waters via surface runoff [St. Louis et al., 1994; 2004]. In addition, Loseto et al. [2004] found that wetlands in the Canadian Arctic can produce large amounts of MeHg, with apparently no microbial (SRB) activity, which suggest that SRB may not the dominant mercury methylators in some systems. Moreover, different studies propose that *in situ* production of MeHg can be an important process, even when wetlands play a dominant hydrologic role [Eckley et al., 2005; Watras et al., 2005; Sellers et al., 2001].

Although many studies have confirmed the natural conversion of inorganic mercury to methyl mercury, the mechanism itself remains elusive. Previous studies have shown that microbes play a role in mercury methylation, especially sulfate-reducing bacteria (SRB) [Compeau and Bartha, 1985; Gilmour and Henry, 1991], however not all SRB are capable of mercury methylation [King et al., 2000; Ullrich, 2001] and other microorganisms (methanogens - MPA and iron-reducing prokariots - FeRP) may also be important [Wood

et al., 1969; Pak and Bartha, 1998; Fleming et al., 2006; Kerin at al., 2006]. This ability to convert mercury to methyl mercury may well have been a protective mechanism during the early evolution of those microbes some 3 billion years ago [Clarkson 1998]. It is becoming clear that we must distinguish biotic (microbial) from abiotic (chemical) processes.

The environmental concentrations of MeHg reflect net methylation rather than actual rates of MeHg synthesis leading to a near constant level of MeHg, which rarely exceeds 1 to 1.5% of THg in the sediments. Few studies provide information about both simultaneous methylation and demethylation processes, nor do we know which organisms, if any, are responsible. Previous investigations have concluded that both processes are very rapid, and the net formation of methyl mercury may be near zero even though reaction rates may be high in both directions [Eckley et al., 2005; 2006; Hintelmann et al., 2000; Hintelmann and Harris, 2004].

Our study focuses on the biogeochemical factors that affect net methylmercury formation, more specifically the role played by methanogens (MPA), iron- (FeRP) and sulfate- (SRB) reducing bacteria in freshwater sediments. To test and validate the experimental design, sediments from Mer Bleue, a pristine wetland near Ottawa, Ontario, were sampled during the summer 2006 and the experimental results are the subject of this paper. The main objectives of the initial experiment with Mer Bleue sediments were: (a) to determine the rates of biotic methyl mercury formation and demethylation and (b) to assess the relative contribution of the different groups of anaerobic microbes (FeRP, SRB, MPA) in methyl mercury formation and demethylation in freshwater sediments. Hypothesis and predictions tested in this chapter are:

H1: MeHg production and degradation are influenced by interspecific competition among SRB, MPA and FeRP for electron donors.

P1: MeHg production and degradation rates that can be related to microbial iron reduction should be higher in microcosms where sulfate reduction and/or methanogenesis are inhibited

3.2. Materials and Methods

3.2.2. Site Description

The Mer Bleue Conservation Area is part of the Greenbelt land owned by the National Capital Commission. Located 10 km east of Ottawa, ON, Canada (latitude 45.40°N, longitude 75.50°W), the Mer Bleue wetland was designated as an international protected site by Ramsar in 1995 [http://www.wetlands.org/reports/ris/4CA033en.pdf, Canada 33: Mer Bleue Conservation Area. Information Sheet on Ramsar Wetlands]. The Mer Bleue Conservation Area includes three zones: the marshes, the bog (peatland) and the sand ridges. The Mer Bleue peatland is a large, open low-shrub, raised bog, having a small moss called Sphagnum as the dominant plant [Moore et al., 2002]. In contrast, the marsh areas are populated by plants, such as cattails, alders (*Alnus rugosa*), willows (*Salix* sp.), and a variety of sedges (*Cyperaceae*) [Bilette and Moore, 2008].

3.2.3. Sample Collection

Surface water and sediment samples were collected from the Mer Bleue wetland (MB) in May and July 2006. Surface sediments from Mer Bleue were sampled using plastic tubes (10 cm in diameter and 1 m in length) sealed (to prevent oxygen contact) on site and kept cold during handling. Cores were taken at the same location and sliced (0-5, 5-10, 10-15 cm) in the field and transferred into in 500 mL pre-acid washed high density polyethylene (HDPE) bottles under nitrogen in order to prevent contact with oxygen and kept cold during their transport to the laboratory.

In the laboratory, subsequent handling of the anoxic sediments was conducted in an anaerobic chamber. Sediment sub-samples were transferred into sterile centrifuge tubes under nitrogen atmosphere and used for geochemical parameter analyses, microbial analyses, and total Hg (THg) and MeHg analyses. The rest of the sediments was used for the microcosm incubations with enriched Hg isotopes and microbial inhibitors. The time lag between the sampling and the start of incubation was 5 days, during which time the samples were stored in the dark at 4^0C.

Surface water from the wetland and from above the sediment-water interface were also sampled and collected in acid pre-washed high density polyethylene (HDPE) bottles. *In situ* pH and Eh measurements were performed on site using a VWR portable pH meter with a VWR pH probe and Corning redox probe. Correction with respect to the hydrogen reference electrode was performed for each reading. Water conductivity and dissolved oxygen were measured on site with a VWR conductivity and YSI 54 oxygen meters. In the laboratory, water samples used for the determination of MeHg were filtered (0.45μm) and acidified with ultrapure HCl to a final concentration of 0.5% (v/v), while another sub-set of samples was preserved with 1% BrCl for total mercury (THg) analysis. Another sub-set of water samples was used for the analysis of dissolved organic carbon (DOC), dissolved inorganic carbon (DIC), sulfate, sulfides, ferrous and ferric iron. Samples were kept refrigerated and analyzed within one week of sampling.

3.2.4. Sample Analysis

Two categories of samples were analyzed: (a) water and sediment samples preserved in the field and (b) sediments and porewater samples taken from the microcosm incubation experiments designed to determine the potential Hg methylation and MeHg demethylation rates. Analyses performed on the samples preserved in the field include sediment THg, MeHg, water and organic carbon content (as loss on ignition (LOI)), porewater sulfate, sulfide, Fe^{2+} and Fe^{3+}. The analytical measurements associated with the samples originating from the microcosm incubations included sediment THg and MeHg isotopic analyses, sulfate reduction rate (SRR), water and organic carbon content (as LOI), pH and Eh, as well as pore water THg and MeHg isotopic analyses, sulfate, sulfide, ferrous iron (Fe^{2+}), ferric iron (Fe^{3+}).

3.2.4.1. Mercury Analyses

Total Hg isotopic analyses of the sediment samples were carried out at Trent University (Ontario, Canada) after acid digestion by flow injection analysis with hydride generation, and subsequent detection by ICP-MS as described in Hintelmann et al. (2003).

Methylmercury isotope analysis of wet sediments and porewater samples was measured after water vapour distillation and aqueous phase ethylation using NaBEt4.

Volatile ethylated Hg species were purged and trapped onto Tenax and MeHg quantified after thermodesorption at 105^0C and GC separation using ICP/MS detection (Micromass Platform) [Hintelmann and Ogrinc, 2003]. To correct for procedural recoveries, each sample was spiked with $^{201}Hg^{2+}$ and $Me^{201}Hg$, respectively, prior to digestion or distillation. The isotopes of Hg measured: ^{199}Hg (to calculate ambient MeHg concentrations), ^{200}Hg (methylation spike), ^{202}Hg (demethylation spike), and ^{201}Hg (internal standard). Peak areas were used to calculate concentrations of individual isotopes using a programmed Excel spreadsheet used in Dr. Hintelmann's laboratory that accounts for procedural blanks and the purities of the isotopes as described in Hintelmann and Ogrinc (2003).

Total Hg and MeHg concentrations in all sediment samples were measured as wet weight and normalized to dry weight based on the water content of the sample to avoid sample loss and alteration during the drying process.

THg in surface sediment samples was measured using the Nippon SP-3D Hg analyzer (CV-AAS) by thermal decomposition with gold amalgamation method (UOP Method 938-00, detection limit of 0.01 ng Hg and range up to 1000 ng Hg).

MeHg was extracted from the sediment (core) samples using the acid leaching procedure-solvent extraction-GC-AFS method described in Cai et al. (1997). All samples were analyzed in duplicate with a Relative Standard Error (RSE) of 1-10%. Recoveries of certified reference material (CRM), BCR 580, was between 94-109% (n=8). MeHg concentration in reagent blanks was below the detection limit of 0.02 ng L^{-1} MeHg (as Hg). The CRM measurement accuracy, calculated as percent error for the mean of the measurements, was 0.41% for BCR 580. MeHg analysis of surface water samples was conducted by solid-phase extraction onto sulfhydryl cotton columns and acidic potassium bromide elution followed by GC-AFS detection [Cai et al., 1996]. Recoveries were 95-103% and MeHg concentration in reagent and travel blanks were below the detection limit of 0.02 ng L^{-1} MeHg (as Hg) [Avramescu et al., 2010].

3.2.4.2. Geochemical Analyses

The pore water samples from the incubation experiment were extracted by centrifugation at 5000 rpm for 20 min, immediately transferred to a clean syringe, and filtered through 0.2μm syringe filters. All samples were immediately stored in the dark at 4^0C for THg and MeHg analyses. All porewater analyses (i.e. Fe^{2+}, Fe^{3+}, sulfates, sulfides) were conducted during the day of sampling.

In the laboratory, pH and Eh measurements were performed with a portable pH meter with a VWR pH probe and Corning redox probe. Correction with respect to the hydrogen reference electrode was performed for each reading.

The water content of the sediment samples was determined by drying the sediments for 24 hours at 105°C, and the organic carbon content was estimated by loss on ignition (LOI) by heating the samples at 400 °C for 8 hours.

Dissolved Organic Carbon (DOC) in porewater samples was measured with an IO Analytical 1010 total organic carbon analyzer using the persulfate oxidation method (range of 2 – 125 ppb organic carbon) and potassium biphtalate standards. When necessary, some samples were diluted with Mili-Q water in order to obtain a sufficient volume for the analysis.

Total sulfate concentrations in porewater samples were determined with the $BaSO_4$ turbidimetric method [Rodier, 1975], while sulfides were analyzed with the Cline's colorimetric method (method range: 0-2.5μM) [Cline, 1969].

Fe^{2+} and Fe^{3+} concentrations in porewater were determined using the revised ferrozine method [Viollier et al., 2000], using a Cary 100 UV-Vis spectrophotometer (562 nm, DL=0 – 5.5 mg L^{-1}). Sulfate, sulfide and iron analyses were performed within minutes after the pore waters were extracted in order to prevent oxidation of sulfides and ferrous iron. Sulfate reduction rates (SRR) were determined in triplicate for all microcosms (t=0h) according to Jørgensen (1978a) as described in Praharaj and Fortin (2004). 20μL $^{35}S\text{-}SO_4^{-2}$ (2.66μCi) radioisotope was used to spike a 5 mL sediment slurry and the samples were incubated at ambient sediment temperature in the dark for 6 hours. In order to stop the

reaction and fix the free sulfides as ZnS, 20 mL of 20% Zn-acetate was added and the samples were frozen until analysis. The sulfide precipitates were distilled with HCl and reduced chromium chloride, the produced H_2S was trapped in Zn-acetate and measured by liquid scintillation. As described in Meier et al. (2000), SRR (nmol SO_4^{2-} cm^{-3} d^{-1}) were calculated based on reactivity and taking into account the porosity values.

The metabolic activity of iron reducing prokariots (FeRP) in sediments was determined by measuring the *in situ* iron reduction rates (FeRR) [Wendt-Potthoff et al., 2002]. FeRR (nmol Fe^{2+} cm^{-3} d^{-1}) were determined in triplicate by linear regression from time courses of porewater Fe^{2+}.

All chemical analyses run for each of the treatments with reference to the method used are given in Table 3-1.

3.2.5. Mercury Methylation and MeHg Demethylation Experiments

Environmental concentrations of MeHg reflect net methylation, which is the result of two simultaneous reactions: Hg methylation and MeHg degradation. Our experiments were designed to measure the rates of MeHg formation and demethylation by combining the isotope enriched multilabeling technique [Hintelmann et al., 1995; 1997; 2000] with microbial inhibitors (SRB and MPA).

The isotope enriched multilabeling technique using stable mercury-enriched isotopes allows us to determine the mercury species transformation rates (i.e. Hg methylation and MeHg demethylation rates) in water and sediment samples, and to identify which of the two processes controls the actual levels of methylmercury in the aquatic environment [Hintelmann et al., 1997]. This stable isotope enriched approach [Hintelmann et al., 1995; 1997; 2000; Bjorn et al., 2007] consists of adding different isotopically enriched Hg species to the sample to study the transformation rates during an incubation period. A third different isotope is added as an internal standard before sample extraction to calculate the isotope ratios based on a modified isotope dilution analysis (IDA). The additions increase by 50-100% the concentrations of total Hg and methylmercury in the samples with respect to environmental levels depending on the type of sediments. The

method offers the advantage that we can look not only at the behavior of the added tracers, but at the same time, we are able to monitor the fate of the ambient metal already present in the system.

In order to assess the relative contribution of different types of anaerobic microbes to methylmercury formation and demethylation, specific inhibitors of SRB (sodium molybdate, $NaMoO_4$) and MPA (sodium 2-bromoethane sulfonate, BES) were added prior to the addition of Hg enriched isotopes. There is no known inhibitor for iron reducing microbes (FeRP).

In the summer 2006, an initial series of experiments were conducted with Mer Bleue sediments in order to validate the described experimental design. Microcosms containing the Mer Bleue sediment slurry (0-5cm), treated with specific microbial inhibitors and inoculated with stable mercury-enriched isotopes were incubated in triplicate, in HDPE bottles containing cca. 500 g of homogenized sediments per treatment. The mercury species used were enriched with $^{200}Hg^{+}$ and $Me^{202}Hg^{+}$. Their abundances are presented in Table 3-2 along with the natural Hg abundance. The additions of isotope enriched spikes of $^{200}Hg^{2+}$ and $Me^{202}Hg^{+}$ were: 0.5 mL of 20 $\mu g\ mL^{-1}$ inorganic ^{200}Hg solution to a give a final concentration of cca. 20 ng g^{-1} ^{200}Hg and 0.4mL of 214.6 ng mL^{-1} $Me^{202}Hg$ solution to a final concentration of cca.150 pg g^{-1} $Me^{202}Hg$ in the incubation slurry. Isotope-enriched ^{200}HgO and $Me^{202}HgCl$ were kindly provided by Dr. Hintelmann (Trent University). $Me^{202}HgCl$ was prepared at Trent University from enriched ^{202}HgO.

Four microcosms treated with isotopes enriched Hg and microbial inhibitors were incubated: one just contained the Hg spiked slurry, the second with a SRB-inhibited slurry, a third one with a MPA-inhibited slurry, and a fourth one with both SRB and MPA inhibited (FeRP active). Natural samples (N) containing no inhibitors and/or no mercury spikes, were run in parallel. Inhibitors of SRB and MPA were added in the microcosms prior to the mercury spikes. All the microcosms incubated were biotic active; no abiotic microcosms were incubated at this stage in the project. Table 3-3 presents the experimental set up and the description of the five microcosms.

The slurries were incubated in the dark at room temperature in an anaerobic chamber for 72 hours. Sub-samples were removed from triplicate systems at regular time intervals (0, 4, 12, 24, 48, 72h) to measure the amount of $Me^{200}Hg$ produced and the amount of $Me^{202}Hg$ removed [Hintelmann et al., 1997; Martin-Doimeadios et al., 2004]. Temperature, pH, Eh, water (LOW) and organic matter content (LOI), along with sulfate reduction rates (SRR) were determined on separate sub-samples. The pore water was extracted immediately after sampling; subsequent analyses of Fe^{2+}, Fe^{3+}, sulfates, sulfides were conducted within minutes after the extraction in the anaerobic chamber, and sub-samples for Hg isotopic analyses were acidified and kept frozen until analysis. Sulfate reduction rates (SRR) were determined in parallel in triplicates for all microcosms according to Jørgensen (1978).

3.2.5.1. Inhibitory Effect of Sodium Molybdate and Sodium 2-Bromoethane Sulfonate

Naturally occurring SRB activity was inhibited by treating the sediment slurries with 1 mL of 1M sodium molybdate ($NaMoO_4$) to a final concentration of 2mM. This inhibitor also prevents FeS formation. FeS formation may lead to an underestimation of iron reduction rates if rates are determined from the increase of dissolved Fe(II) concentrations. The efficiency of $NaMoO_4$ to inhibit sulfate reduction was determined by comparison of SRR in triplicate sub-samples (t=0h) from amended and not amended sediments. The molybdate concentration was chosen taking into account the direct inhibitory effect of group VI anions on MeHg production [Chen et al., 1996] and recommendations of Fleming et al. (2006). Researchers have suggested that the appropriate concentration for molybdate application to sediments should be equimolar to that of ambient sulfate [Oremland and Capone, 1988].

Naturally occurring methanogens were inhibited by treating the sediment slurries with 0.5 mL of 10mM of sodium 2-bromoethane sulfonate (BES, $BrCH_2CH_2SO_3Na$) [Pak and Bartha, 1998] to give a final concentration of 10μM. The efficiency of BES to inhibit methane production was later tested by measuring methane concentrations in the headspace during the experiment (see chapter 4). BES is considered to be a "specific" inhibitor for methanogens because it is a structural analog of mercaptoehanesulfonic acid, the cofactor

known as "HS-coenzyme M", which is found in all methanogens but not in other bacteria or Archaea (*Halobacterium halobium* or *Sulfolobus aidocaldarius*) [Oremland and Capone, 1988; Balch et al., 1979]. The BES concentration was chosen based on the study by Oremland (1988) and Pak and Bartha (1998).

More details about the two specific inhibitors, sodium molybdate and BES and their path of action is given in the Supporting information.

3.2.6. Specific Potential Methylation Rates Constants Calculation

Pseudo-first order reactions were used to describe the potential methylation and demethylation rates following the procedure outlined in Hintelmann et al. (2000). The equation describing the net production of methylmercury is:

$$d[CH_3\,^{200}Hg^+]/dt = k_m\,[^{200}Hg^{2+}] - k_d\,[CH_3\,^{200}Hg^+] \quad (1)$$

Considering that for the first 24h the contribution from the newly produced methylmercury ($CH_3\,^{200}Hg^+$) is negligible, equation 1 is reduced to:

$$d[CH_3\,^{200}Hg^+]/dt = k_m\,[^{200}Hg^{2+}] \quad (2)$$

Integration of this equation gives us the specific methylation rate constant (Km):

$$k_m = [CH_3\,^{200}Hg^+] / [^{200}Hg^{2+}] * t \text{ , where } t=2d. \quad (3)$$

In addition, considering the fact that $^{199}Hg^{2+}$ resulting from the demethylation of $Me^{199}Hg^+$ is virtually zero at the beginning of the experiment and very low during the 72h incubation, the specific demethylation rate constant (Kd) was calculated by reducing the equation 1 written for $Me^{199}Hg^+$ to:

$$d[Me^{199}Hg^+]/dt = - k_d\,[Me^{199}Hg^+]_0 \quad (4)$$

which integrated form is:

$$[Me^{199}Hg^+]_t = [Me^{199}Hg^+]_{t=0} * e^{-kd*t} \quad (5)$$

The Kd was calculated as:

$$Kd = - \ln ([Me^{199}Hg+]_t / [Me^{199}Hg+]_{t=0}) / t \quad (6)$$

where t=2d, $[Me^{199}Hg^+]_t$ is the concentration of $Me^{199}Hg^+$ at the end of the incubation, and $[Me^{199}Hg^+]_{t=0}$ is the initial concentration of $CH_3{}^{199}Hg^+$ in the sediments. Plotting ln $[Me^{199}Hg^+]_t$ or ln $([Me^{199}Hg^+]_t / [Me^{199}Hg^+]_{t=0})$ versus time (t) gives a straight line with a slope of $-Km(d^{-1})$. The plot should be linear for up to a 80-90% conversion, which is the point at which 80-90% of the concentration of the limiting reactant is consumed. The half-life ($t_{½}$) of methylmercury in sediment can be calculated as: $t_{½} = \ln 2 / Kd$ (7).

Equation 1 can be written for the ambient species and integrated, considering the inorganic $[Hg^{2+}]$ stays constant for the duration of the experiment:

$$[MeHg^+] / [Hg^{2+}] = (Km/Kd) * (1-e^{-Kd*t}) \quad (8)$$

The rate of demethylation of methylmercury in sediment can be expressed in pmol of Me202Hg demethylated per gram per hour [Ramlal et al.,1986] and it is used to calculate the specific rate of demethylation (SpD), i.e., the percentage of the added mercury demethylated per gram per hour (Eq. 9). Specific rates of mercury methylation were calculated similarly to demethylation calculations.

$$SdD = 100 * \text{demethylation rate}/(\text{added pmol of Me202Hg}) \quad (9)$$

3.2.7. Statistical Analyses

Simple linear regression was used to calculate FeRR for different microcosms over a 72h incubation period as well as the relationships between the porewater characteristics and different MeHg isotope concentrations using the S-Plus 8.0 software for Windows [Morin and Findlay 2006; Otto 2007; Zar 2006]. Student t-test was performed to asses if the differences among the SRR and FeRR were significant. The XLfit software was also used to determine ambient Km and Kd values by curve fitting of ambient MeHg data (199 isotope).

3.3. Results and Discussion

3.3.1. Field Data Results

The physico-chemical characteristics of the Mer Bleue sampling site are presented in Figure 3-1. Mer Bleue water is weakly acidic (pH = 5.6 – 6.0) and soft (conductivity = 300 - 303 μS cm^{-1}, n=3) and contains low levels of sulfate (55±3.1 μM (±SE, n=5)) and total phosphorous (42.68±0.5 μgP L^{-1} (±SE, n=2)). The surface sediments (0-5 cm) have a density of 1.013 g cm^{-3} and a porosity of 0.94 g cm^{-3} and contain on average ~55% of organic carbon content (as LOI). Our results for pH, sulfate, etc. are in agreement with previous geochemical studies of Mer Bleue [Goldhammer and Blodau 2008; Heitmann et al., 2007; Blodau et al., 2002]. Total mercury (THg) and methylmercury concentrations of the sediments vary between 25.6 – 30.8 ng g^{-1} wet wt. and 0.070 – 0.086 ng g^{-1} wet wt. (n= 5), respectively. Pore waters (n=6) contain low levels of sulfate (73±17 μM), sulfides (0.48±0.06 μM), ferrous iron (0.62±0.19 μM) and ferric iron (0.114±0.01 μM), as well as THg (0.25±0.06 ng L^{-1}) which are in agreement with other Mer Bleue studies [Blodau et al., 2002; Goldhammer and Blodau 2008].

3.3.2. Methylation - Demethylation Experiments Results

The porewater characteristics, along with the sulfate- and iron reduction rates in the 5 systems tested (i.e., natural (N), Hg spiked only (T1), Hg spiked and SRB inhibited (T2), Hg spiked and MPA inhibited (T3), and Hg spiked and SRB and MPA inhibited (T4), see Table 3-3) are presented in Figures 3-2 and 3-3. The statistics for the FeRR calculation by linear regression are shown in Table S3-1 (Supporting information) and the statistical tests results for SRR and FeRR comparison among microcosms in Table S3-2. Geochemical analyses are presented as an average of the three replicates (±SE), but only one replicate was analyzed for the mercury isotopes due to the high cost of the isotope analyses and because this was considered a preliminary experiment for testing the experimental design. It is also noteworthy to mention here that for all microcosms, the time zero samples were frozen 4 hours after sampling because of the time it took to sample and process all samples. As a result, the time zero samples are considered t = 4 hours in the rate calculations. For the rate calculations, the initial values (t=0h) for $Me^{200}Hg$ (produced from the $^{200}Hg^{2+}$ spike)

were considered zero and the initial concentration of the $Me^{199}Hg$ (demethylation spike) was calculated.

3.3.2.1. Aqueous geochemistry of the various microcosms

The determined density and porosity of the pooled sediment slurries used for the batch systems were 1.013 ± 0.01g cm^{-3} (n=6) and 0.94 ± 0.01g cm^{-3} (n=12), respectively. In the natural system (N) (Figure 3-2), pH slightly increased from 6.15 to 6.23 over 72 h after an initial decrease after the first 24h, while the redox potential slightly declined over time indicating the development of more reducing conditions in the system. Sulfide concentrations remained very low and fairly constant throughout the experiment, never exceeding 0.33 µM. Ferrous iron (Fe^{2+}) concentrations increased constantly (from 0.12 µM to 5.74 µM) over 72h with a slower increase during the first 24h. The iron reduction rate (FeRR = 1.9 ± 0.7 nmol cm^{-3} d^{-1}) was calculated from the linear increase of Fe^{2+} over 72 hours (Figure 3-3). Saturation index calculations (see Supporting Information Table S3-5) did show that the systems were undersaturated with respect to FeS and mackinawite throughout the course of the experiment, indicating that the iron reduction rates were likely not biased by the precipitation of iron sulfides. However, the calculations indicated that the microcosms were saturated with respect to more stable iron sulfides, such as pyrite. Their formation cannot be ascertained here, because kinetics are not taken in account in the thermodynamics calculations. The relatively high SRR (109.9 ± 18.3 nmol cm^{-3} d^{-1}) (Figure 3-3) determined with the ^{35}S incubation technique indicates the existence of an active SRB population (109.9 ± 18.3 nmol cm^{-3} d^{-1}) in the Mer Bleue sediments.

The Hg spiked only system (T1) showed the same pH, Eh, sulfide and ferrous iron trends as the natural system (N) (Figure 3-2). The SRR (111.7 ± 21.3 nmol cm^{-3} d^{-1}) was slightly higher when compared with the natural system (N), but the FeRR (1.3 ± 0.3 nmol cm^{-3} d^{-1}) was lower (i.e., decrease of ~33%) than in the system N (Figure 3-3).

For the Hg spiked and SRB inhibited system (T2), the pH remained fairly stable over time (despite a slight drop at 24 h), but the initial pH was slightly higher than that in the N and T1 systems (Figure 3-2). The redox potential decreased steadily over 72 hours, as observed in the other systems, while both sulfide and Fe^{2+} concentrations increased

during the course of the experiment, ranging from 0.50 to 1.72 μM and 0.02 to 8.22 μM, respectively. The increase of sulfide over time is however inconsistent with the measured SRR of 0.2 nmol cm^{-3} d^{-1}, which indicates the complete inhibition (99.8 %) of the sulfate reducing activity by sodium molybdate. It is likely that the production of sulfides in the microcosm was caused by the dissolution of pre-existing iron sulfide minerals, as shown by the saturation index calculations (see Supporting Information, Table S3-5). In comparison with the other two systems, N and T1, the FeRR (2.3 ± 0.2 nmol cm^{-3} d^{-1}) increased by 19 and 79%, respectively, but the difference was not statistically significant (Table S3-2).

The Hg spiked and MPA inhibited system (T3) featured the same pH and Eh trends as the N and T1 systems (Figure 3-2). Sulfide concentrations were very low and remained fairly constant over 72 hours, ranging from 0.38 to 0.55 μM, whereas Fe^{2+} concentrations increased from 0.25 to 5.32 μM (Figure 3-2). The SRR of the system (130.7 ± 4.8 nmol cm^{-3} d^{-1}) was the highest among all microcosms (Figure 3-3), with a 19% increase when compared with the natural system (N), which proves that the BES inhibitor of MPAs activity did not affect the activity of SRB. The differences between SRR values of microcosms N, T1 and T3 were statistically significant ($p < 0.05$, Table S3-2). FeRR (1.8 ± 0.13 nmol cm^{-3} d^{-1}) was higher (38%) than that for the T1 assay, but slightly lower (8%) than the one for the natural system (N), but the differences were not statistically significant ($p < 0.05$, Table S3-2).

The last system, i.e., Hg spiked, SRB and MPA inhibited (T4), behaved very similarly to the T2 system which also contained molybdate. The pH slightly increased over time, despite an initial pH that was higher than the N, T1 and T3 systems (Figure 3-2). Eh decreased correspondingly from -124.5 to -184 mV with a peak of -207.3 mV after 24h. The initial sulfide concentration of this system was higher than that of the other systems, ranging from 1.08 to 2.08 μM in 48h and slightly decreased after that (Figure 3-2), whereas soluble ferrous iron concentrations steadily increased from 0.65 to 9.08 μM over 72 hours. The inhibition of sulfate reducing activity was complete (99.7%) and similar to the other molybdate inhibited treatment (T2). By contrast, FeRR was stimulated by the inhibition of the other two microbial groups (SRB and MPA), with a 2.3 and 1.5 time increase when compared with the T2 and natural (N) systems, respectively (Figure 3-3). Table S3-2 shows

the statistical tests results for SRR and FeRR comparison among microcosms. Moreover, the one-way ANOVA with multiple comparison for SRR and FeRR among treatments gave the same results as in Table S3-2.

In summary, all systems developed anoxic conditions during the course of the experiment, which represent suitable conditions for either iron or sulfate reduction, as shown by the measured iron- and sulfate reduction rates. In addition, SRR values reported here are similar to those measured in aquatic environments, such as lake sediments (50-600 nmol cm^{-3} d^{-1}; Ingvorsen et al., 1981). Regarding the calculated FeRR for the various microcosms, they are in agreement with the values reported by Blodau et al. [2002] (<0.1 μmol g^{-1} d^{-1}) for experiments carried out with Mer Bleue peat. The study showed that the rates were independent of sulfate and acetate availability in the slurries.

It is clear that the chosen inhibitors, especially molybdate which completely stopped microbial sulfate reduction, enhanced iron reduction in the T2 and T4 systems, as seen in Figure 3-3. It is known that iron reducers and sulfate reducers often compete for the same electron donors under environmental conditions [Fortin and Praharaj, 2005; Kusel et al., 1999]. The efficiency of BES on methanogen activity was not assessed in this preliminary study but our results indicate that it increased the iron and sulfate reduction rates with respect to the N and T1 systems, indicating that there might have been a slight competition between these microbes and iron and sulfate reducers. Both SRB and FeRP can couple either iron or sulfate reduction to methane oxidation [Boetius et al., 2000; Beal et al., 2009].

Future experiments should however quantify iron sulfide formation in the systems by determining the AVS (acid volatile sulfide fraction) and CRS (chromium reducible sulfide fraction), as they can provide more information about microbial sulfate reduction [e.g., Blodau et al., 2007; Fortin and Praharaj, 2005]. The AVS and CRS fractions can also give information about the formation of iron sulfides which can affect the dissolved iron concentrations and in return, the calculated FeRR. In addition, the H_2S gas (short-term end product of sulfate reduction) should be measured because it can rapidly react with organic matter, producing carbon-bonded sulfur (CBS) (i.e., organic matter containing a C–S bond)

fractions [e.g., Vile et al., 2003]. SRR therefore include the reduced inorganic sulfur (H_2S, FeS, FeS_2) and the carbon bonded-sulfur (CBS) [Vile et al., 2003]. Incorporation of H_2S into dissolved organic matter (as CBS) was observed in the porewaters from the Mer Bleue peatland [Blodau et al., 2007]. The authors also showed that deeper into the peat, the sulfate pool was apparently replenished from the peat matrix (sulfate became enriched in ^{32}S), likely stemming from TRIS (total reducible inorganic sulfur) or CBS (organic ester-bound sulfate hydrolysis) in the peat. Sulfur was thus anaerobically cycled between oxidized and reduced pools but the electron acceptor driving this cycle could not be conclusively identified.

3.3.2.2. Isotope Enriched Hg Analyses Results

The analysis of the isotopes enriched THg and MeHg in one set of the triplicate samples (pore waters and sediments) was conducted in Dr. Hintelmann's laboratory at Trent University using the methods described previously.

The minimum amount of isotope spikes was determined by backward calculation considering the initial THg and MeHg contents of tested sediments and the detection limit for the isotope MeHg (approx. 1% of the ambient MeHg). The isotope enriched Hg spikes ($^{200}Hg^{2+}$ and $Me^{202}Hg^{+}$) used in this study were sufficient, i.e., the generated $Me^{200}Hg$ and the remaining $Me^{202}Hg$ (after demethylation) were ≥ 1% of the ambient MeHg. The spike additions did however increase the concentration of total Hg and methylmercury by a factor of two, when compared to the background ambient concentrations. Moreover, the addition of the enriched isotope spikes increased the % MeHg to THg by 17-31%. The ambient background concentrations of the Mer Bleue wetland sediments used for the incubation experiments along with the concentrations after the isotope addition are shown in Table 3-4.

Changes in the relative abundance of isotope 199 followed the evolution of natural mercury (ambient), those of the 200 isotope followed the evolution of spiked enriched inorganic mercury (methylation), whereas changes in the 202 isotope followed the evolution of the spiked enriched methylmercury (demethylation) (Figure 3-4). The amount of methylated mercury derived from inorganic ^{200}Hg spike and demethylated mercury

derived from $Me^{202}Hg$ spike were calculated using Equations 3 and 6, respectively. Net mercury methylation rates can be calculated directly using data from the methylation assay, but only when MeHg increases linearly over time and demethylation activity is insignificant. From the outset, it was not known for how long it would be necessary to measure changes or over which time period methylation would proceed at a constant rate in the batch assays.

The trend of MeHg produced from the isotope enriched mercury spikes (^{200}Hg and $Me^{202}Hg$) along with the ambient MeHg trend during the 72h incubation time are presented in Figure 3-4. The microcosms behaved differently with respect to the 199, 200, and 202 isotopes. A linear decrease over 72h was observed for the $Me^{202}Hg$ concentrations (Figure 3-4c) but the slope was different: T1 and T4 assays had the highest decrease when compared to the very small decrease in T2 and T3. In contrast, the $Me^{200}Hg$ produced from the inorganic mercury spike had a linear increase for the first 24h in all treatments, after which steady state levels were achieved in T1 and T3 microcosms, and a continuing linear increase occurred in the SRB inhibited treatments T2 and T4 (Figure 3-4 b). The observed decrease in MeHg production (steady state) was possible because once sufficient MeHg was produced, demethylation may have slowed down the net increase in MeHg. In some cases, an equilibrium or steady state developed after 24 hours, but other samples showed a slower but continuous increase throughout the experiment period. The T1 and T3 microcosms showed the highest methylmercury values (ng g^{-1}dw), but also the highest demethylation rates (Table 3-6), which can explain the equilibrium reached after 24h. The 199 isotope results showed a linear increase for 24h in the T1 microcosm and for 72h, in the T3 microcosm, but no increase was observed for the T2 and T4 microcosms. A similar trend for the 199 and 200 isotopes was observed during the incubation, which suggests that methylation of ambient mercury and isotope enriched methylation tracer followed the same pathway. The different order of magnitude might however be due to the different availability of the two isotopes (ambient and tracer). No increase in native MeHg was observed in the natural microcosm compared with the spiked microcosms (T1-T4), suggesting that the addition of spikes also increased the availability of ambient Hg for methylation [Hintelmann et al., 2000; Drott et al., 2008].

The total percentage of mercury methylated and methylmercury demethylated from the tracer spikes in the different microcosms is presented in Table 3-5. The highest methylation percentage was observed in the T1 microcosms (6.17%). For a 24 hour incubation period, the T3 microcosms (MPA inhibited) showed almost the same methylation percentage (6.01%), which can be explained by either an incomplete inhibition of MPA due to the applied concentration of BES or to the elimination of the competition for organic substrate through the inhibition of methanogens favoring the SRB and other microorganisms. For this specific experiment, the BES efficiency to inhibit methane production was not tested, but it was in the other experiments (see Chapter 4). With respect to the microcosms containing the SRB inhibitor (T2 and T4), both systems had comparable methylating potential (2.54% and 2.18%, respectively), but slightly different demethylating potential (7.87% for T2 compared with 10.2% for T4) (see Table 3-5). For all microcosms, the demethylation of $Me^{202}Hg$ took place very quickly with a linear decrease over the 72 hour incubation period. The percent methylated of the ambient (199 isotope) mercury (% [MeHg] / $[Hg^{2+}]$, where Hg^{2+} = [THg] – [ΣMeHg]) varied from 0.42% for the natural microcosm (N) to 0.55% and 1.21% for the T1 and T3 microcosms, respectively. The addition of sodium molybdate inhibited not only the methylation of the mercury tracer (200 isotope) but also the methylation of ambient mercury (Table 3-5 and Figure 3-4). The percent $Me^{202}Hg$ demethylated varied with the type of microbes inhibited from 7.87% (T2) to 24.72% (T1). The values reported here are however lower than those reported by Hintelmann et al. [2000], i.e., ~ 40%. The high percentage of Hg methylated and MeHg demethylated in the Mer Bleue microcosms may be due to the high availability of electron donors (from DOM) and electron acceptors in this system ([Heitmann et al., 2007; Blodau et al., 2002] which influences microbial activity and in turn Hg methylation in the sediments [Lambertsson et al., 2006]. Drott et al. (2007) obtained higher methylation rates in the surface layer of lake sediments where the availability of energy-rich organic matter (e-donors for SRB) was higher than in deeper sediments. The same authors concluded that Hg methylation rates in contaminated sediments are largely controlled by the concentration of neutral inorganic mercury sulfide species, together with the availability of energy-rich organic matter.

Dissolved organic matter (DOM) strongly affects the mobility and bioavailability of Hg in aquatic ecosystem [Ravichandran et al., 2004]. Heitmann et al. (2007) found that DOM (humic substances) served as electron acceptors for the oxidation of organic substrates and reduced sulfur in Mer Bleue peat soils. In their experiments, Mer Bleue DOM chemically oxidized H_2S to thiosulfate and reduced dissolved ferric iron which explained their low *in situ* concentrations of H_2S. According to the same study, DOM transferred more electrons to ferric iron when it had previously gained electrons by reaction with H_2S. Moreover, the thiosulfate may partly replace the sulfate as an electron acceptor in peat soils and even re-supply the sulfate pool when disproportionated into H_2S and sulfate by microbial mediation [Widdell, 1991; Habicht et al., 1998]. Since peatlands undergoe oxic and anoxic periods, DOM can be oxidized under unsaturated oxic conditions and reduced under saturated anoxic conditions. They [Heimann et al., 2007] concluded that in peatlands, electron transfer of DOM may thus significantly contribute to the oxidation of reduced organic substrates by anaerobic heterotrophic respiration, or by maintaining the respiratory activity of sulfate reducers via the provision of thiosulfate.

Finally, for this experiment, the isotope enriched spikes were prepared in DIW and not equilibrated with the overlaying water or porewater due to time constraints. For future experiments, the added tracers need to be equilibrated in overlaying/porewater before addition to the incubation vessels in order to achieve the same speciation as the ambient Hg(II) [Hintelmann et al., 2000; Drott et al., 2008b].

3.3.2.3. Potential Rates of Methylation and Demethylation

Mercury methylation and methylmercury demethylation rates (pmol g^{-1} h^{-1}) along with the specific transformation rates (SpM, SpD) calculated for the 24h incubation period with the isotope enriched tracers ($^{200}Hg^{2+}$ and $Me^{202}Hg^{+}$) are presented in Table 3-6.

The process of $^{200}Hg^{2+}$ methylation varied with the type of microbes inhibited, i.e., the highest calculated rate (among the inhibited assays) was in the microcosms where methanogenesis was inhibited (T3: 1.46 pmol g^{-1} h^{-1}). Specific methylation rate, calculated as the proportion of added isotope enriched tracers methylated or demethylated in 24h, was the highest in the T3-MPA inhibited microcosm ; followed by the T1 and T2-SRB inhibited

and T4-SRB and MPB inhibited microcosms, with rates twice as lower as the other ones (see Table 3-6). In contrast, the specific demethylation rate ($Me^{202}Hg$) was the highest for the T1 microcosm and lower for the T3 microcosm, which was in agreement with the methylation rates, i.e. higher methylation and lower demethylation due to the inhibition of MPA. In the case of the T2 and T4 microcosms, the specific rates decreased when compared to the T1 assay. Moreover, the addition of inhibitors influenced not only the methylation and demethylation of tracers in the four microcosms, but also the evolution of native MeHg. Higher rates were calculated in the T1 and T3 assays in comparison with the SRB inhibited microcosms T2 and T4 where no methylation was observed.

Ramlal et al. (1986) suggested that the methylation/demethylation (M/D) ratios (see methods for description) are a good indicator of how environmental perturbations affect the net rate of mercury methylation and hence, MeHg concentrations in aquatic environments. The M/D ratios are a direct measure of the relative balance of methylating or demethylating activity in a specific system. Based on the M/D ratio shown in Table 3-6, we can conclude that all microcosms favored demethylation over methylation but the degree of magnitude of the ratios indicates that it varied with the type of active microbes. We observed that the inhibition of SRB (T2) alone increased the M/D ratio due to a large decrease of the demethylation rate over the methylation one. The inhibition of MPA (T3) alone also increased the M/D ratio, by increasing methylation rate (22%) and decreasing demethylation one (22%) comparing with T1. In contrast, the inhibition of both microbial groups (T4) did not change the M/D ratios, but reduced by half (53%) the magnitude of both processes. These findings suggest that sulfate-reducers and methanogens play an important role in MeHg demethylation in Mer Bleue system and that the inhibition of one microbial group stimulated net methylation by either inhibition of demethylation or stimulation of methylation, or both.

The decrease of net methylation caused by the inhibition of SRB, MPA or both is conceivable if we consider that oxidative demethylation takes place in the Mer Bleue sediments. Sulfate-reducing and methanogenic archaea have been identified as primary agents in oxidative demethylation (OD) of MeHg in anoxic environments [Oremland et al., 1995; Marvin-Dipasquale and Oremland, 1998] in studies using (^{14}C)MeHg.

Our experiments showed that demethylation was responsible for maintaining the MeHg level in the Mer Bleue sediment microcosms, even in the SRB and MPA inhibited microcosms (T2 and T4). In these microcosms, the methylation proceeded at lower rates (T2: 0.52 pmol g^{-1} h^{-1}, T4: 0.54 pmol g^{-1} h^{-1}) as well as demethylation (T2: 0.009 pmol g^{-1} h^{-1}, T4: 0.018 pmol g^{-1} h^{-1}), in contrast with the T1 and T3 systems. Moreover, the decrease of the demethylation ratios alone resulted in an increase of the M/D ratios, which are the highest in these two microcosms (T2 and T3). Consequently, changes in the natural overall microbial activity through inhibition of one microbial group and stimulation of other groups favoured the increase in MeHg production in the long run. Also, by liberating Hg^{2+} through demethylation, more available mercury ready to be re-methylated will be produced, which in turn may induce more methylation and increase the MeHg pool in the Mer Bleue anoxic sediments, as also observed for other systems (Marvin-Dipasquale and Oremland, 1998]. In addition, the supply of nutrients and electron acceptors should favour one microbial group over another, which can be critical for the levels of MeHg production in anoxic sediments. Further investigations aimed at identifying whether there is a symbiotic pattern between SRB and MPA in which the SRB supply the carbon source for the MPA and the MPA supply the available Hg for SRB methylation in the system are necessary.

The M/D ratios show that the activity of SRB and MPA is important for the demethylation process, but for methylation, there might be other processes (either biotic or abiotic) that should be considered. The inhibition of both SRB and MPA might have enhanced the activity of iron reducing prokariots (FeRP) as seen by the increase of FeRR in the inhibited microcosms (Figure 3-3). It is known that iron can affect mercury methylation either by altering the availability of Hg [Warner et al., 2003; Mehrotra et al., 2005] or by enhancing the activity of FeRP with respect to other microorganisms, particularly SRB [Flemming et al., 2006; Kerin et al., 2006; Warner et al., 2003]. Hg methylation by FeRP may be important in sediments and soils where these organisms are dominant, e.g., iron-rich freshwater sediments (Fleming et al., 2006) and iron-rich sediments with low concentrations of sulfate [Kerin et al., 2006]. Moreover, Oremland et al. (1995) detected substantial oxidative demethylation at a site where sulfate reduction and methanogenesis rates were low, and suggested that other respiratory anaerobes (e.g., denitrifiers and Fe^{3+}

and Mn^{4+} reducers) may also carry out oxidative demethylation, which can be an explanation for the higher demethylation rate measured in the T4 (SRB and MPA inhibited) microcosm when compared with the T2 microcosm.

Alternatively, in the SRBs inhibited microcosms (T2 and T4), the increased sulfides production (Figure 3-2a), caused by the dissolution of pre-existing iron sulfide minerals (as shown by the saturation index calculations, Table S3-5), might stimulate the formation of charged Hg polisulfides complexes which are not available for bacterial uptake (diffusive transport across microbial membranes), therefore decreasing methylation. It is also possible the increased production of ferrous iron (likely as a result of iron oxide reduction) help destabilize the iron sulfides (by changing the ion acitivty product), rendering them more soluble.

3.3.2.4. Specific Methylation and Demethylation Rate Constants

In order to verify if the methylation or demethylation rates were dependent on the amount of tracers added, as previously suggested by Hintelmann et al. (1995; 2000), we calculated the rate constants, which by definition are independent of the amount spiked.

Potential Hg methylation rate constants (Km and Kd) calculated from isotope enriched tracer trends over 24 hours are presented in Table 3-7, along with data from other studies. Potential methylation rate constants (Km) differed among microcosms, the MPA inhibited microcosm (T3) having the highest rate constant (0.057 d^{-1}), followed by the T1 microcosm (0.046 d^{-1}). The SRB inhibited microcosms had comparable specific methylation rate constants (T2: 0.025 $d^{-1}$and T4: 0.022 d^{-1}). The trends observed for Km values in all microcosms are in agreement with the calculated potential methylation rates (M) presented in Table 3-6. Our results therefore indicate the importance of SRB in Hg methylation in freshwater systems, as reported in other studies [Compeau and Bartha, 1985; King et al., 2000; 2002; Fleming et al., 2006; Oremland et al., 1995]. For instance, Matilainen et al. (1995) observed that molybdate inhibited methylation in sediments from four lakes in Finland, and suggested that acetate-utilizing SRB were the main methylators under sulfate limiting conditions. In addition, in anoxic estuarine sediments, inhibition of methanogenesis stimulated the SRB activity and Hg methylation when sulfate was limiting

[Compeau and Bartha, 1985]. Finally, Lovely and Klug (1983) showed that SRB were able to outcompete methanogens, even in sulfate limited freshwater sediments.

With respect to the demethylation rate constants (Kd), the highest value (0.289 d^{-1}) was in the T1 microcosm followed closely by the MPA inhibited microcosm (T3: 0.219 d^{-1}), which may indicate an inhibition of methanogenesis (but the efficiency of the inhibitor was not tested here, as mentioned earlier). Kd values for the SRB inhibited microcosms were however completely different (T2: 0.063 d^{-1} and T4: 0.120 d^{-1}) from the Km values calculated from the linear increase over 24 hours. This difference can be explained by either an incomplete inhibition of methanogenesis or to the stimulation of other anaerobic reducers. The measurement of methane production rates in future experiments is therefore needed. In contrast with methylation, demethylation evolved linearly for 72h, and the Kd values calculated for the whole period were lower, but of the same magnitude (T2: 0.023 d^{-1} and T4: 0.034 d^{-1}), which is in agreement with the Km values (T2: 0.025 d^{-1} and T4: 0.022 d^{-1}). The Kd values were also in agreement with the potential methylation rates (D) presented in Table 3-6.

The ambient rate constants (Km, Kd) were obtained by fitting the experimental data ($Me^{199}Hg$) to the curve derived from Equation 8 [Hintelmann et al., 2000]. The XLfit software was used for fitting the curve, and the results are presented in Table S3-3. The ambient MeHg concentrations in the microcosms were predicted by applying the calculated rate constants. Other tracer studies [Hintemann et al., 2000] concluded that the tracers were more bioavailable than the ambient mercury since the discrepancies observed between the predicted and measured ambient MeHg concentrations were assumed to be due to differences in Km (Kd values were similar). However, as shown in Table 3-7, this was not observed in our study where a good agreement was obtained between the predicted and measured values of ambient methylmercury (199 isotope).

The demethylation rate constants translated into a very short half-life ($t_{1/2}$) of the native MeHg in sediments (i.e., 1.6 d^{-1}), which is very similar to that obtained by Hintelmann et al. (2000) (i.e., 1.8 d^{-1}). The half-life of the added tracers varied from 2.5 d^{-1} (T1) to 10.9 d^{-1} (T2: SRB inhibited). The fraction of Hg present as MeHg is slightly higher

for the tracer isotope (202 isotope: 0.29 – 0.33%) when compared to ambient Hg (199 isotope: 0.21 – 0.25%), which supports the fact that the tracers are more available than the native Hg [Hintemann et al., 2000]. We also observed that the inhibition of SRB and MPA may increase the residence time of MeHg in sediments, which in turn may increase the availability of MeHg for bioaccumulation. Considering the decrease in demethylation rate constants in all microcosms (T2, T3, T4) when compared to T1, we can conclude that oxidative demethylation (OD) may be an important pathway for MeHg demethylation in Mer Bleue sediments. Barkay (2003) stated that a methylation-demethylation cycle may exist in environments lacking the mer-mediated process [Schaefer et al., 2002], and that oxidative demethylation prevails at lower Hg concentrations in anaerobic settings [Marvin-Dipasquale et al., 2000; Marvin-Dipasquale and Oremland, 1998; Oremland et al., 1991; 1995]. Whether the mer-mediated demethylation takes place at the same time in Mer Bleue sediments has yet to be determined.

3.3.3. Relationship between the rate constants, SRR, FeRR, % MeHg and porewater geochemistry

We evaluated the relationship between the rate constants (Km and Kd) calculated under laboratory conditions and the %MeHg (100*[MeHg]/[THg]) in sediments, the sulfate reduction rates (SRR) and iron reduction rates (FeRR), as well as the pore water characteristics. Figure 3-5 presents the relationship between Km or Kd and % MeHg, SRR, and FeRR.

In all incubated microcosms (Figure 3-5a), a stronger negative relationship was observed between Kd and % MeHg ($r^2 = 0.71$) than between Km and % MeHg ($r^2 = 0.67$). Our results (based on Figure 3-5a) therefore indicate that the magnitude of Km and Kd decreases with the increasing of % MeHg in the sediments. Drott and co-workers (2008a) reported positive significant correlations ($r^2 = 0.67 – 0.88$) between Km and % MeHg in surface freshwater sediments and no relationship for brackish sediments from Finland. The authors suggested that Km rates reflected a short term MeHg production, whereas % MeHg was an indication of the normalized long-term production of MeHg, and found that Km can be used to estimate long-term MeHg production in the contaminated freshwater system

investigated. In marine surface sediments, Hammerschmit and Fitzgerald (2006) also reported a positive relationship between Km and the ratio [MeHg] to [Hg^{2+}], whereas Sunderland et al. (2004) concluded that % MeHg could be used to approximate the rate of methylation in estuarine sediments. Our negative relationship in contrast to the published studies mentioned above might be related to the fact that our data (i.e., Figure 3-5a) represent five microcosms, each equivalent to a different system (with different microbial activity), which are likely different from the ones reported in other studies [Drott et al., 2008a; b; Hammerschmit and Fitzgerald, 2006]. Considering that Km and Kd reflect the long-term buildup of MeHg (as % MeHg) and can be linked to factors operating at the level of microbial metabolism (i.e., donor availability and bioavailability of mercury sulfides), as suggested by Drott et al (2008a) and our findings, we conclude that the Km and Kd respectively were low in microcosms with higher % MeHg and inactive SRB, and higher in the microcosms with active SRB and low % MeHg.

Figure 3-5b shows that both Km and Kd are positively correlated with SRR (r^2 = 0.97 and 0.81, respectively), i.e., the higher the SRR is, the higher the Km and Kd values are, which indicates that SRB are involved in both Hg methylation and MeHg demethylation in Mer Bleue sediments. In contrast, the relationship between Km or Kd and FeRR (Figure 3-5c) is negative (r^2 = 0.67 for Km and r^2 = 0.66 for Kd). The increase in FeRR therefore corresponds to a decrease in methylation and demethylation, but to an increase in M/D ratios (Table 3-6, Figure 3-3b), showing that the iron reduction may influence net methylation in Mer Bleue sediments in the long term. This fact is supported by the strong positive relationship obtained in all microcosms between MeHg concentrations (200 isotope) and porewater Fe^{2+} concentrations (Figure S3-1) (T1: slope= 6.9, r^2= 0.9216, p=0.18; T2: slope= 4.91, r^2=0.8029, p=0.29; T3: slope=11.55 , r^2=0.4616, p=0.53; T4: slope=7.42, r^2=0.7038, p=0.37), as well as for the 199 isotope (r^2 = 0.6022 - 0.9411), with the exception of the T4 slurry. Higher variability was however observed in the relationship between the 202 isotope and dissolved iron (r2 = 0.3804 – 0.9594). There was also a strong negative relationship between MeHg isotopes and Eh for all microcosms (r^2=0.5018 – 0.9833), except for the T2 microcosm where no relationship was observed between the 202 isotope and Eh (Figure S3-1). The relationship between the MeHg

isotopes and sulfides concentrations in porewater was however highly variable (Figure S3-1), with strong relationships (r^2=0.8165- 0.969) in T1 and T2 for all isotopes (except for the 202 isotope in the T2 slurry: r^2=0.366, p=0.59) and no relationship for the T3 and T4 microcosms (except for the 200 isotope in the T4 slurry: r^2=0.828, p=0.27). This variation may be explained if some sulfides in the various systems were not produced through biotic reactions (i.e., from SRB), but rather from the dissolution of pre-existing metal sulfides, as shown by the saturation index calculations (Support information, Table S3-5). In general pH did not show a good correlation with MeHg concentrations, except for 202 isotope (demethylation) in the T2 (r^2=0.950, p=0.14) and T4 systems (r^2= 0.8615, p=24) and for 200 isotope (methylation) in the T1 system (r^2=0.315, p=0.62) and T3 (r^2= 0.635, p=0.41). The natural MeHg (199 isotope) was however correlated with the pH in the T4 microcosm (r^2=0.959, p=0.13). Statistical analysis results are given in Table S3-4, Support information. Previous studies [Ramlal et al., 1985; Steffan et al., 1988; Gilmour and Henry, 1991] found that demethylation was relatively insensitive to pH changes but acidification of the anoxic lake sediments to pH 5.0 or lower essentially stopped net methylation rates, apparently because of the reduction of available Hg^{2+} in the sediment porewater, which may have been due to increased sorption to particles at low pH. Low pH also increases aerobic methylation at the sediment-water interface [Ullrich et al., 1991]. Demethylation rates in both sediments and water are less affected by pH than methylation rates, indicating that the changes observed in net MeHg production are largely due to an effect of pH on methylation rather than demethylation [Ramlal et al., 1986; Steffan et al., 1988; Matilainen et al.1991]. The low pH variation in our microcosms, as shown previously, can be an explanation for the little correlation observed.

Based on the results above, we conclude that methylation and demethylation are dependent of the type of microbial inhibition treatment, which determines the type of microbes that are active in the specific systems, and the availability of Hg^{2+} for methylation. Demethylation and methylation are related to SRB and MPA activity, but another process might also be important in determining net Hg methylation levels and defining the MeHg concentration level in Mer Bleue sediments. Further investigations are

clearly needed to determine in which way those changes are critical for the long-term production of MeHg in aquatic systems.

3.4. Conclusions and Future Work

In conclusion, this initial experiment illustrates that both methylation and demethylation processes proceed very fast, in some cases reaching an equilibrium or steady state within 24 hours. With both SRB and MPA inhibited, methylmercury production proceeded more slowly, but continued throughout the 72h period and was still increasing at the end of the experiment. Other processes (FeRP, abiotic, or dissolution of iron sulfides/oxides) may also be very important. Our results also showed that newly added tracers are more available for transformation than ambient species, and that low spike concentrations (<100% increase in THg) should be used in future experiments to be closer to natural conditions.

This initial experiment also showed that specific inhibitors are a useful tool to study the role of various microbes in Hg methylation. The combined use of specific inhibitors (molybdate and BES) indicated that iron reducing microbes may be responsible for some Hg methylation although future experiments are necessary. The inhibition of methanogens increased iron reduction rates as well, but to a lesser extent, suggesting that either the competition between methanogens and iron reducing microbes is not strong or that methanogens were not completely inhibited.

Our preliminary study did not however allow us to determine which process, i.e., methylation or demethylation, was the most important in the Mer Bleue microcosms. In the future, sterile gamma-radiated microcosms should also be set up to assess the contribution of abiotic processes on methylmercury formation or demethylation. In addition, in order to assess the importance of iron-reducers in Hg methylation, iron oxides should be added to the microcosms to stimulate the microbial populations. Finally, in order to avoid the sampling delay for the samples taken at time zero, the samples should be immediately frozen in liquid nitrogen in order to avoid unwanted methylation/demethylation reactions in the samples. The samples can be kept frozen until analysis and acidified before thawing (1 mL of concentrated HCl; Ramal et al., 1986).

3.5. References

Avramescu ML, Zhu J, Yumvihoze E, Hintelmann H, Fortin D, Lean DRS, 2010. A simplified sample preparation procedure for measuring isotope enriched methylmercury by GC-ICP/MS. Environ Toxicol Chem (in press).

Balch WE, Wolfe RS, 1979. Specific and biological distribution of coenzyme M (2-mercaptoethane sulfonic acid). J Bacteriol, 137, 264-273.

Barkay T, Miller SM, Summers AO, 2003. Bacterial mercury resistance from atoms to ecosystems. FEMS Microbiol Rev, 27, 355-384.

Beal EJ, House CH, Orphan VJ, 2009. Manganese- and Iron-Dependent Marine Methane Oxidation. Science, 325, 184-187.

Billett MF, Moore TR. 2008. Supersaturation and evasion of CO_2 and CH_4 in surface waters at Mer Bleue peatland, Canada. Hydrol Process, 22, 2044-2054.

Bjorn E, Larsson T, Lambertsson L, Skyllberg U, Frech W, 2007. Recent advances in mercury speciation analysis with focus on Spectrometric methods and enriched stable isotope applications. Ambio, 36, 443-451.

Blodau C, Mayer B, Peiffer S, Moore TR, 2007. Support for an anaerobic sulfur cycle in two Canadian peatland soils. J Geophs Res-Biogeo, 112, G02004, doi:10.1029/2006JG000364.

Blodau C, Roehm CL and Moore TR, 2002. Iron, sulfur and dissolved carbon dynamics in a northern peatland. Arch Hydrobiol, 154, 561-583.

Boetius A, Ravenschlag K, Schubert CJ, Rickert D, Widdel F, Gleseke A, Amann R, Jørgensen BB, Witte U, Pfannkuche O, 2000. A marine microbial consoprtion apparently mediating anaerobic methane oxidation. Nature, 407, 623-626.

Cai Y, Jaff R, Allia A, Jones RD, 1996. Determination of organomercury compounds in aqueous samples by capillary gas chromatography-atomic fluorescence spectrometry following solid-phase extraction. Anal Chim Acta, 334, 25 l-259,

Cai Y, Tang G, Jaffé R, Jones R, 1997. Evaluation of some Isolation Methods for Organomercury Determination in Soil and Fish Samples by Capillary Gas Chromatography – Atomic Fluorescence Spectrometry. Intl J Environ An Ch, 68, 331-345.

Chen Y, Bonzongo JC, Miller GC, 1996. Y.Inhibition of mercury methylation in anoxic freshwater sediment by group VI anions. ACS Div Environ Chem, Preprints, 36, 55-57.

Choi S-C, Bartha R, 1994a. Environmental factors affecting mercury methylation in estuarine sediments. Bull Environ Contam Toxicol 53, 805-812.

Clarkson TW. 1998. Human toxicology of mercury. J. Trace Elem. Exp. Med. 11, 303-317.

Cline JD, 1969, Spectrophotometric determination of hydrogen sulfide in natural waters. Limnol Oceanogr, 14, 454-458.

Compeau G, Bartha R, 1985. Sulfate-reducing bacteria: principal methylators of mercury in anoxic estuarine sediments. App Environ Microbiol, 50, 498-502.

Drott A, Lambertsson L, Björn E, Skyllberg U. 2007. Importance of dissolved neutral mercury sulfides for methyl mercury production in contaminated sediments. Environ Sci Technol, 41, 2270-2276.

Drott A, Lambertsson L, Björn E, Skyllberg U. 2008a. Do Potential Methylation Rates Reflect Accumulated Methyl Mercury in Contaminated Sediments? Environ Sci Technol, 42,153–158.

Drott A, Lambertsson L, Björn E, Skyllberg U. 2008b. Potential demethylation rate determinations in relation to concentrations of MeHg, Hg and pore water speciation of MeHg in contaminated sediments. Mar Chem, 112, 93–101

Eckley CS and Hintelmann H. 2006. Determination of mercury methylation potentials in the water column of lakes across Canada. Sci Tot Environ, 368, 111-125.

Eckley CS, Watras CJ, Hintelmann H, Morrison K, Kent AD and Regnell O, 2005. Mercury methylation in the hypolimnetic waters of lakes with and without connection to wetlands in northen Wisconsin. Can J Fish Aquat Sci, 62, 400-411.

Flemming EJ, Marck EE, Green PG, Nelson DC, 2006. Mercury methylation from unexpected sources: molybdate-inhibited freshwater sediments and an iron-reducing bacterium. App Environ Microbiol, 72, 457–464.

Fortin D, Praharaj T, 2005. Role of microbial activity in Fe and S cycling in sub-oxic to anoxic sulfide-rich mine tailings: a mini-review. J Nucl Radiochem Sci, 6, 39-42.

Gilmour CC, Henry EA, 1991. Mercury methylation in aquatic systems affected by acid deposition. Environ Pollut, 71, 131-169.

Gilmour CC, Henry EA, Mitchell R. 1992, Sulfate simulation of mercury methylation in freshwater sediments. Environ SciTechnol, 26,2281-2287.

Gilmour CC, Riedel GS, Ederington MC, Bell JT, Benoit JM, Gill GA, Stordal MC, 1998. Methylmercury concentrations and production rates across a trophic gradient in the northern Everglades. Biogeochemistry, 40, 327-345.

Goldhammer T, Blodau C, 2008. Desiccation and product accumulation constrain heterotrophic anaerobic respiration in peats of an ombrotrophic temperate bog, Soil Biol Biochem, 40: 2007-2015.

Habicht KS, Canfield, DE, Rethmeier J, 1998. Sulfur isotope fractionation during bacterial reduction and disproportionation of thiosulfate and sulfite. Geochim Cosmochim Acta, 62, 2585-2595.

Hammerschmidt CR, Fitzgerald WF, 2006. Methylmercury cycling in sediments on the continental shelf of southern NewEngland. Geochim Cosmochim Acta, 70, 918–930.

Heitmann T, Goldhammer T, Beer J, Blodau C, 2007. Electron transfer of dissolved organic matter and its potential significance for anaerobic respiration in a northern bog. Glob Change Biol, 13,1771-1785.

Hintelmann H, Harris R, 2004. Application of multiple stable mercury isotoes to determine the adsorption and desorption dynamics of Hg (II) and MeHg to sediments. Mar Chem, 90, 165-173.

Hintelmann H, Ogrinc N. 2003. Determination of stable mercury isotopes by ICP/MS and their application in environmental studies. In: Cai, Y., Braids, C.O. (Eds.), Biogeochemistry of Environmentally Important Trace Elements. ACS Symp. Ser., 504, vol. 835, 321–338. American Chemical Society, Washington, DC.

Hintelmann H, Keppel-Jones K, Evans RD. 2000. Constants of mercury methylation and demethylation rates in sediments and comparison of tracer and ambient mercury availability. Environ Toxicol Chem, 19, 2204– 2211.

Hintelmann H, Evans RD, 1997. Application of stable isotopes in environmental tracer studies—Measurement of monomethylmercury (CH_3Hg^+) by isotope dilution ICP-MS and detection of species transformation. Fresen J Anal Chem, 358,378–385.

Hintelmann H, Evans RD, Villeneuve JY, 1995. Measurement of mercury methylation in sediments by using enriched stable mercury isotopes combined with methylmercury determination by gas chromatography-inductively coupled plasma mass spectrometry. J Anal Atomic Spectrom, 10,619–624.

http://www.wetlands.org/reports/ris/4CA033en.pdf, Information Sheet on Ramsar Wetlands, Canada 33: Mer Bleue Conservation Area.

Ingvorsen K, Zeikus JG, Brock TD, 1981. Dynamics of Bacterial Sulfate Reduction in a Eutrophic Lake. App Environ Microbiol, 42,1029-1036.

Jørgensen BB. 1978. A comparison of methods for the quantification of bacterial sulfate reduction in coastal marine sediments. I. Measurement with radiotracer techniques. Geomicrobiol J, 1,11–27.

Kerin EJ, Gilmour CC, Roden E, Suzuki MT, Coates JD, Mason RP. 2006. Mercury Methylation by Dissimilatory Iron-Reducing Bacteria. Appl Environ Microbiol, 72, 7919–7921.

King JK, Harmon S, Michele S, Fu TT, Gladden JB. 2002. Mercury removal, methylmercury formation, and sulfate-reducing bacteria profiles in wetland mesocosms. Chemosphere, 46, 859-870.

King JK, Kostka JE, Frischer ME, Saunders FM. 2000. Sulfate-reducing bacteria methylate mercury at variable rates in pure culture and in marine sediments. Appl Environ Microbiol, 66, 2430-2437.

King JK, Kostka JE, Frisher ME, Saunders FM and Jahnke RA. 2001. A quantitative relationship that demonstrates mercury methylation rates inmarine sediments are based on the community composition and activity of sulfate bacteria. Environ Sci Technol, 35, 2492-2496.

Kusel K, Dorsch T, Acker G, Strackebrandt E, 1999. Microbial Reduction of Fe(III) in Acidic Sediments: Isolation of *Acidiphilium cryptum* JF-5 Capable of Coupling the Reduction of Fe(III) to the Oxidation of Glucose. Appl Environ Microbiol. 65, 3633-3640.

Lambertsson L, Nilsson M, 2006. Organic material: the primary control on mercury methylation and ambient methyl mercury concentrations in estuarine sediments. Environ Sci Technol, 40, 1822-1829.

Loseto L, Siciliano SD, Lean DRS. 2004. Methylmercury production in high Arctic wetlands. Environ Toxicol Chem, 23, 17-23.

Lovley DR, Klug MJ, 1983. Sulfate reducers can outcompete methanogens at freshwater sulfate concentrations. Appl Environ Microbiol, 45,187–192.

Martin-Doimeadios R, Tessier E, Amouroux D, Guyoneaud R, Duran R, Caumette P, Donard OFE, 2004. Mercury methylation/demethylation and volatilization pathways in estuarine sediment slurries using species-specific enriched stable isotopes. Mar Chem, 90, 107-123.

Marvin-Diapasquale MC, Oremland RS, 1998. Bacterial methylmercury degradation in Florida Everglades peat sediment. Environ Sci Technol, 32, 2556-2563.

Marvin-Diapasquale MC, Agee J, McGowan C, Oremland, RS, Thomas M, Krabbenhoft D, Gilmour CC, 2000, Methylmercury degradation pathways: a comparison among three mercury- impacted ecosystems. Environ Sci Technol, 34, 4908-4917.

Matilainen T, Verta M, Korhonen H, Niemi M, 1991. Specific rates of methylmercury production in lake sediments. Water Air Soil Poll, 56, 595-605.

Matilainen T, Verta M, 1995. Mercury methylation and demethylation in aerobic surface waters. Can J Fish Aquat S, 52, 1597-1608.

Mehrotra AS, Sedlak DL, 2005. Decrease in net mercury methylation rates following iron amendment to anoxic wetland sediment slurries. Environ Sci Technol, 39, 2564–2570.

Meier J, Voigt A, Babenzien H-D, 2000. A comparison of $^{35}S\text{-}SO_4^{2-}$ radiotracer techniques to determine sulfate reduction rates in laminated sediments. Journal of Microbiol Meth, 41, 9–18.

Moore T, Bubier JL, Frolking S, Lafleur, P.M., Roulet, N.T. 2002. Plant biomass and production and CO_2 exchange in an ombrotrophic bog. J Ecol, 90, 25–36.

Morin A, Findlay CS, 2006. Course notes for BIO 4158 Applied Biostatistics. University of Ottawa, Ottawa, On., Canada.

Oremland RS, Miller LG, Dowdle P, Connell T, Barkay R, 1995. Methylmercury oxidative degradation potentials in contaminated and pristine sediments of the Carson River, Nevada, Appl Environ Microbiol, 6, 2745-2753.

Oremland RS, Capone DG, 1988. Use of specific inhibitors in biogeochemistry and microbial ecology. Adv. Microb. Ecol. 10, 285–383.

Oremland, RS, Culbertson, CW, Winfrey MR, 1991. Methylmercury decomposition in sediments and bacterial cultures: involvement of methanogens and sulfate reducers in oxidative demethylation. Appl Environ Microbiol, 57,130-137.

Otto M, 2007. Chemometrics. Statistics and Computer Application in Analytical Chemistry. Second Edition. Wiley-VCH Verlag GmbH & Co. KgaA.

Pak KR, Bartha R, 1998. Mercury methylation and demethylation in anoxic lake sediments and by strictly anaerobic bacteria, Appl Environ Microbiol, 64, 1013-1017.

Praharaj T, Fortin D. 2004. Indicators of microbial sulfate reduction in acidic sulfide-rich mine tailings. Geomicrob J, 21,457-467.

Ramlal PS, Rudd JWM andHecky RE, 1986. Methods for measuring specific rates of mercury methylation and degradation and their use in determining factors controlling net rates of mercury methylation, Appl Environ Microbiol, 51, 110-114.

Ramlal PS, Rudd JWM, Furutani A, Xun L, 1985. The effect of pH on methyl mercury production and decomposition in lake sediments. Can. J. Fish. Aquat. Sci., 42, 685-692.

Ravichandran M,. 2004. Interactions between mercury and dissolved organic matter - A review. Chemosphere 55, 319-331.

Robinson JB, Tuovinen OH. 1984. Mechanisms of microbial resistance and detoxification of mercury and organomercury compounds-physiological, biochemical and genetic analyses, Microbiol Rev, 48, 95-124.

Rodier J, 1975. L'analyse de l'eau. 5^{em} ed., Paris-Dunod, pp. 176-177.

Rudd JWM, 1995. Sources of methyl mercury to freshwater ecosystems: a review. Water Air Soil Poll, 80, 697- 713.

Schaefer J, Latowski J, Barkay T, 2002. mer-mediated resistance and volatilization of Hg(II) under anaerobic conditions. Geomicrobiol J, 19, 87-102.

Sellers P, Kelly CA, Rudd JWM, 2001. Fluxes of methylmercury to the water column of a drainage lake: Relative importance of internal and external sources. Limnol Ocean, 46, 623-631.

St. Louis V, Sharp M, Steffen A, May M, Barker J, Kirk J, Kelly DJA, Arnott, SE, Keatly B, Smol JP, 2004 Some sources and sinks of monomethyl and inorganic mercury on Ellesmere Island in the Canadian High Arctic. Environ Sci Technol, 39, 2686-2701.

St. Louis V L, Rudd JW, Kelly M, Beaty CA, Bloom NS, Flett, RJ, 1994 Importance of wetlands as sources of methyl mercury to boreal forest ecosystems. Can J Fish Aquat Sci, 51, 1065-1994.

Steffan RJ, Korthals ET, Winfrey MR, 1988. Effect of acidification on mercury methylation, demethylation, and volatilization in sediments from an acid-susceptible lake, Appl Environ Microbiol, 54, 2003-2009

Sunderland EM, Gobas FAPC, Heyes A, Branfireun BA, Bayer AK, Cranston RE, Parsons MB, 2004. Speciation and bioavailability of mercury in well-mixed estuarine sediments. Mar Chem 90, 91–105.

Ullrich SM, Tanton TW and Abdrashitova SA, 2001 Mercury in the aquatic environment: A review of factors affecting methylation. Crit Rev Environ Sci Technol, 31, 241–293.

Vile MA, Bridgham SD, Kelman H and Wieder R, 2003. Response of anaerobic carbon mineralization to sulfate amendments in boreal peatland. Ecol Appl, 13, 720–734.

Viollier E, Inglett PW, Hunter K, Roychoudhury AN, Van Cappellen P, 2000. The ferrozine method revisted: Fe(II)/Fe(III) determination in natural waters. Appl Geochem, 15, 785-790.

Warner KA, Roden EE, Bonzongo JC, 2003. Microbial mercury transformation in anoxic freshwater sediments under iron-reducing and other electron-accepting conditions. Environ Sci Technol, 37,2159–2165.

Watras CJ, Bloom NS, Claas SA, Morrison KA, Gilmour CC, Craig SR, 1995. Methylmercury production in the anoxic hypolimnion of a dimictic seepage lake. Water Air Soil Poll, 80,735-745.

Watras CJ, Morrison KA, Kenta A, Price N, Regnell O, Eckley C, Hintelmann H, Hubacher T, 2005. Sources of Methylmercury to a Wetland-Dominated Lake in Northern Wisconsin. Environ Sci Technol, 39, 4747-4758.

Wendt-Potthoff K, Frommichen R, Herzprung P, Koschorreck M, 2002. Microbial Fe(III) reduction in acidic mining lake sediments after addition of an organic substrate and lime. Water Air Soil Poll, Focus 2, 81-85.

Widdel F, 1988. Microbiology and ecology of sulfate- and sulfurreducing bacteria. In: Biology of Anaerobic Microorganisms (eds Zehnder A, Stumm W), pp. 469–586. Wiley, New York.

Wood JM, Kennedy PS, Rosen CG, 1968. Synthesis of methylmercury compounds by extracts of a methanogenic bacterium, Nature 220, 173-174.

Zar JH 2006. Biostatistical Analysis (5^{th} edition). Prentice-Hall, Upper saddle River, New Jersey.

Tables

Table 3-1. Summary of the analytical methods used in the methylation/demethylation experiments

Type of analysis	Preservation method	Method description (Reference)
Total mercury - isotopic composition	Frozen	Flow injection analysis with hydride generation and subsequent detection by ICP-MS (Hintelmann et al. 1995)
Methylmercury – isotopic composition	Frozen	Steam distillation, aqueous phase ethylation , purge and trap on a Tenax adsorber, isothermally GC separation (105°C), and ICP-MS detection (Hintelmann et al. 1995)
Total mercury (THg)	Frozen	SP3D mercury analyzer (CV-AAS) by thermal decomposition with gold amalgamation method
Net methylmercury	Frozen	Acid digestion successive extraction in DCM, acidic KBr-$CuSO_4$, and DCM , capillary GC-AFS (Cai et al. 1997)
Microbial sulfate reducing rates (SRR)	Frozen after fixing with zinc acetate	^{35}S incubation technique; reduced ^{35}S recovered by distillation with HCl and boiling acidic $CrCl_2$ (Fossing and Jørgensen 1989)
Microbial iron reducing rates FeRR		Linear regression from time courses of HCl-soluble Fe(II) (Wendt-Potthoff et al. 2000)
Metane producing rates (MPR)	Koschorreck M, 2000	50 µL sample headspace taken with a gas tight syringe is injected in a GC equipped with thermal conductivity detector (TCD) to analyze CH_4. MPR determined by linear regression from time courses
LOW and LOI	fresh	24h at 100^0C, then 8h at 400^0C
pH, Eh porewater		VWR portable meter and pH and Eh probes
DIC porewater	filtered (0.45um)	Acidification, CO_2 purged, NDIR detection (1010 Total Organic Carbon OI Analyzer)
DOC porewater	filtered (0.45um)	Persulfate oxidation, CO_2 purged, NDIR detection (1010 Total Organic Carbon OI Analyzer)
Fe(II), Fe(III), porewater	immediately	Immediately after filtration with the colorimetric ferrozine method (Stookey 1970; Viollier et al. 2000)
Sulfides (HS-), porewater	immediately	Cline colorimetric method (Cline 1969)
Sulfate, porewater	HCl immediately	$BaSO_4$ turbidimetric (Rodier 1975)

Table 3-2. Natural and enriched Hg solution abundances used in this study. Values are given as the percentage of total Hg concentration.

Hg isotope	Natural abundance	$^{200}Hg(NO_3)_2$ (22.8 μg mL^{-1})	$Me^{201}HgCl$ (100 μg mL^{-1})	$Me^{202}HgCl$ (0.22 μg mL^{-1})
196	0.15	0.07	0.01	N/A
198	10.02	3.87	0.12	N/A
199	16.84	3.97	0.10	0.10
200	23.13	79.52	0.45	0.10
201	13.22	4.22	98.11	0.10
202	29.8	6.63	1.18	99.2
204	6.85	1.72	0.03	N/A

Table 3-3. Mer Bleue experimental design set up and microcosm description.

ID	Microcosm description (n=3 replicate bottles)	Treatment		
		* $^{200}Hg^{2+}$ and $Me^{202}Hg^{+}$ spikes	**SRB inhibitor	***MPA inhibitor
N	Mer Bleue sediment slurry (Natural -unspiked control)	no	no	no
T1	Mer Bleue sediment slurry (Hg spiked control)	Yes	no	no
T2	Mer Bleue sediment slurry (SRB inhibited)	Yes	yes	no
T3	Mer Bleue sediment slurry (MPA inhibited)	Yes	no	yes
T4	Mer Bleue sediment slurry (SRB and MPA inhibited, FERP active)	Yes	yes	yes

* isotope enriched Hg solutions were added to give a final concentration of cca. 20 ng g^{-1} $^{200}Hg^{2+}$ (0.5 mL of 20 µg mL^{-1} $^{200}Hg^{2+}$) and ca.150 pg g^{-1} $Me^{202}Hg^{+}$ (0.4 mL of 214.6 ng mL^{-1} $Me^{202}Hg$) in the sediment slurry.

** 2mM final concentration in sediment (1 mL of 1M $NaMoO_4$)

***10µM final concentration in sediment (0.5 mL of 10mM sodium 2-bromoethane Sulfonate)

Table 3-4. Sediment ambient background concentrations and percent increases due to isotope enriched Hg ($^{200}Hg^{2+}$ and $Me^{202}Hg^{+}$) additions in the Mer Bleue incubation experiments

Parameter	N	T1	T2	T3	T4
Organic content (±SE), (%) n=3	53.5±1.6	53.7±0.2	54.3±1.6	53.1±0.2	55.0±0.5
Water content (±SE), (%) n=3	92.9±0.2	92.9±0.1	92.9±0.3	92.8±0.2	93.1±0.1
Ambient total mercury, ng g^{-1} d.w, n=1	129.0	118.2	125.1	140.9	128.4
Ambient methylmercury, ng g^{-1} d.w, n=1	0.585	0.527	0.562	0.559	0.494
THg after spikes additions, ng g^{-1} d.w, n=1	129.0	228.6	223.3	265.1	249.0
MeHg after $Me^{202}Hg$ additions, ng g^{-1} d.w, n=1	0.585	0.752	0.810	0.825	0.820
Increase in THg due to the addition of $^{200}Hg^{2+}$ and $Me^{202}Hg^{+}$	-	93%	79%	88%	94%
Increase in MeHg due to the addition of $Me^{202}Hg^{+}$	-	43%	44%	48%	66%

Table 3-5. Total percentage of mercury methylated and methylmercury demethylated from the spikes in the different systems (calculated by dividing the amount measured by the amount spiked x100).

Microcosm	^{200}Hg methylated (%)		$Me^{202}Hg$ demethylated (%)		^{199}Hg methylated (%)	
	4h	24h	4h	24h	4h	24h
N	n/a	n/a	n/a	n/a	0.37	0.42
T1	4.98	6.17	4.67	24.72	0.45	1.21
T2	0.50	2.57	5.98	7.87	0.38	0.36
T3	1.86	6.01	11.85	22.27	0.32	0.55
T4	0.39	2.18	1.56	10.19	0.37	0.32

Table 3-6. Comparison of specific mercury methylation (SpM) and methylmercury demethylation rates (SpD) calculated from the tracer initial experiment with Mer Bleue sediments (calculated for t = 24h).

Microcosm	M (199-ambient) pmol g^{-1} h^{-1}	M (200) pmol g^{-1} h^{-1}	D(202) pmol g^{-1} h^{-1}	Specific ambient rate (199) (pmol g^{-1} h^{-1}) 100/ (Hg pmol g^{-1})	Specific methylation rate (200) (pmol g^{-1} h^{-1}) 100/ (add ^{200}Hg pmol g^{-1})	Specific demethylation rate (202) (pmol g^{-1} h^{-1}) 100/ (add $Me^{202}Hg$ pmol g^{-1})	M/D	[MeHg] / $[THg]_{t=0h}$	[MeHg] / $[THg]_{t=24h}$
N	0.01	n/a	n/a	0.00001	n/a	n/a	n/a	0.42%	0.4%
T1	0.21	1.06	0.037	0.00039	0.193	1.021	0.19	0.53%	3.8%
T2	-0.01	0.52	0.009	-0.00001	0.106	0.253	0.42	0.58%	1.6%
T3	0.06	1.46	0.030	0.00011	0.236	0.797	0.30	0.51%	3.3%
T4	-0.01	0.54	0.018	-0.00002	0.091	0.477	0.19	0.55%	1.5%

Table 3-7. Comparison of specific mercury methylation and methylmercury demethylation rate constants calculated from various tracer studies.

Site	Rate constant			$MeHg^+$		Reference
	Km (d-1)	Kd (d-1)	Half-life (d)	Predicted (ng/g)	Measured (ng/g)	
N - Mer Bleue, On	n/a	n/a	1.6	0.58	0.60	this study
T1 - Mer Bleue, On	0.046	0.284	2.4	1.42	1.56	this study
T2 - Mer Bleue, On	0.025	0.063	10.9	0.45	0.49	this study
T3 - Mer Bleue, On	0.057	0.219	3.2	0.81	0.85	this study
T4 - Mer Bleue, On	0.022	0.120	5.8	0.45	0.44	this study
Ranger Lake, On	0.012	0.42	1.7	2.8	1.8	Hintelmann et al., 2000
Lake Vernon, On	0.016	0.53	1.3	3	0.8	Hintelmann et al., 2000
Lake Vernon, On	0.012	0.48	1.5	2.5	0.8	Hintelmann et al., 1995
Brakish water estuary (Köp)	0.002	0.07				Drott et al., 2008
Brakish water estuary (Sku)	0.004	0.54				Drott et al., 2008
Low productive freshwater (Kar)	0.0004	0.05				Drott et al., 2008
Low productive lake (Ala)	0.002	0.02				Drott et al., 2008
High productive freshwaters	0.02	0.12				Drott et al., 2008
Adour River Estuary, France	0.034	0.07				Martin-Doimeadios et al., 2004 (biotic)
Adour River Estuary, France	0.002	0.24				Martin-Doimeadios et al., 2004 (abiotic)

Figures

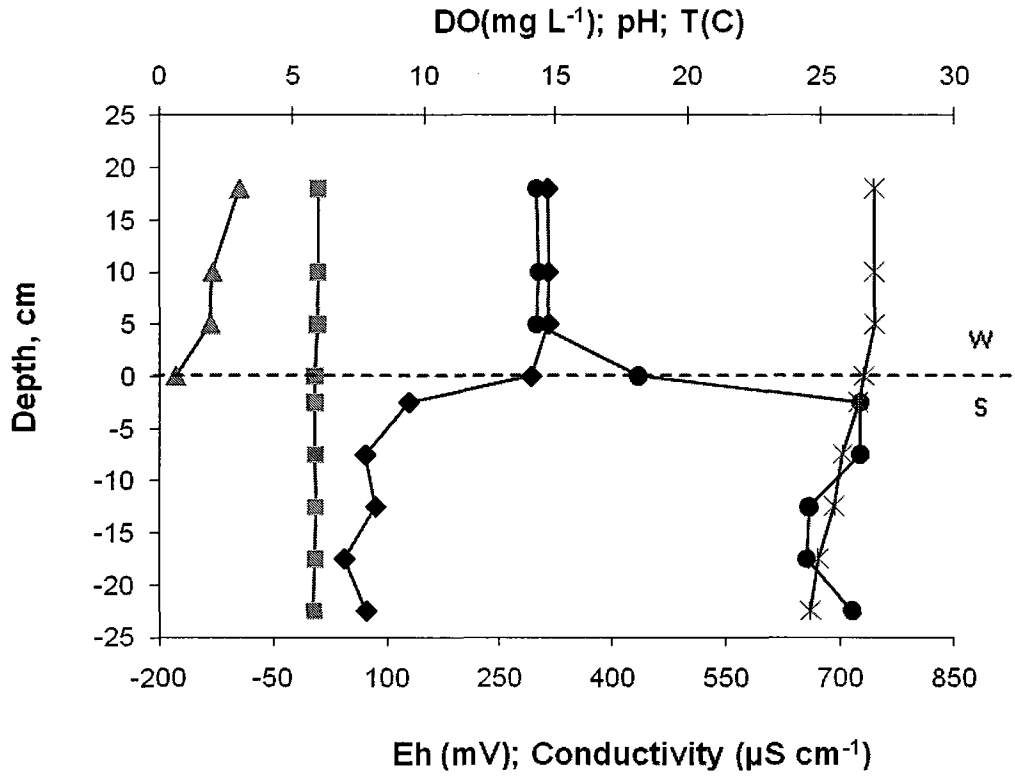

Figure 3-1. Physico-chemical characteristics of the porewaters and overlying water at Mer Bleue as a function of depth: Eh (mV,♦); conductivity (µS cm^{-1}, ●); temperature (^0C , ∗); pH (■); dissolved oxygen (mg L^{-1}, ▲). The dotted line represents the sediment (S) – water (W) interface.

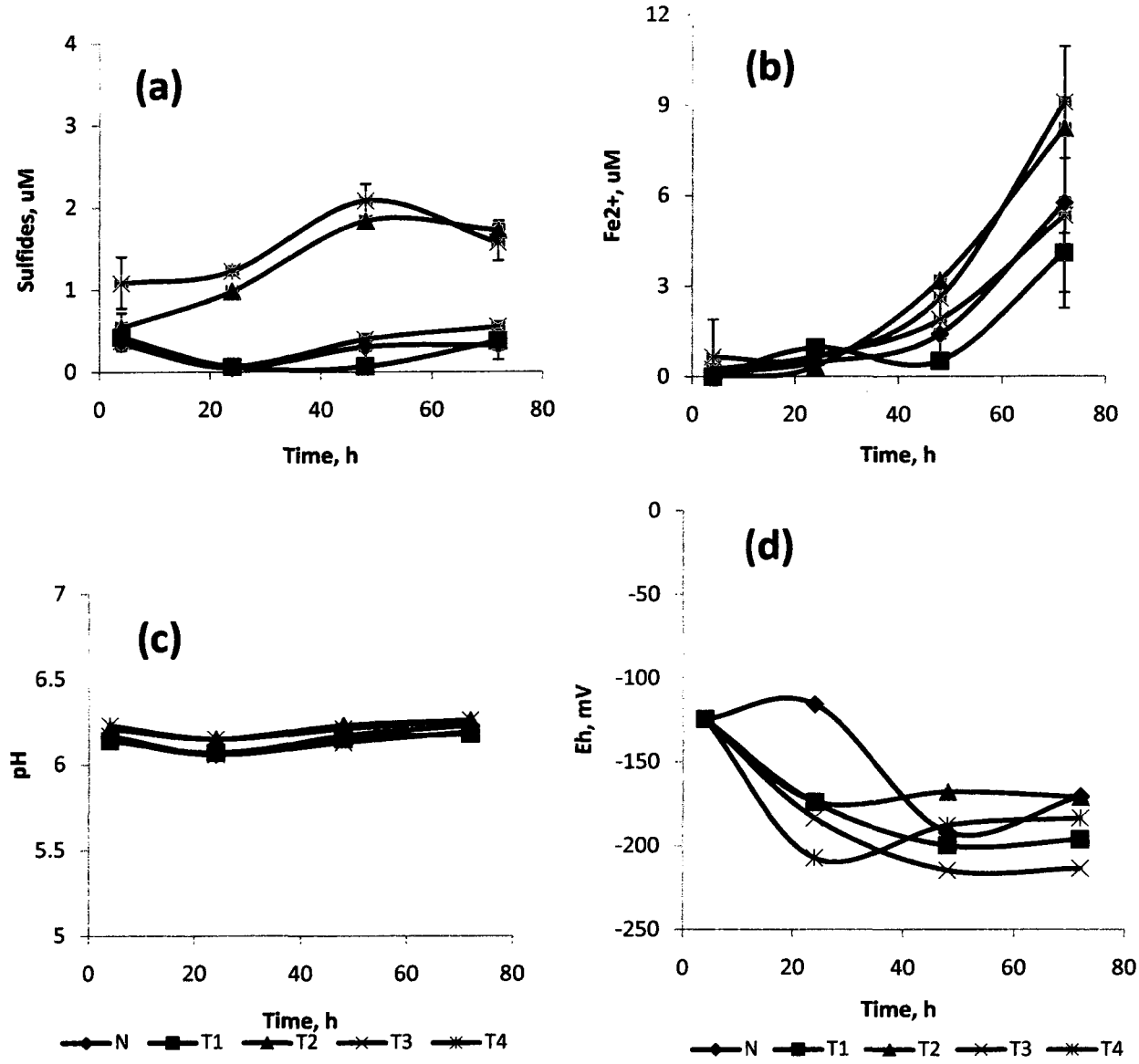

Figure 3-2. Porewater characteristics during the 72h microcosm incubations: N(♦), T1 (■), T2 (▲), T3 (×), T4 (∗) (sulfides (a), ferrous iron (b), pH (c), and Eh (d)). Error bars represent standard error (SE). The description of the microcosms is presented in Table 3-3.

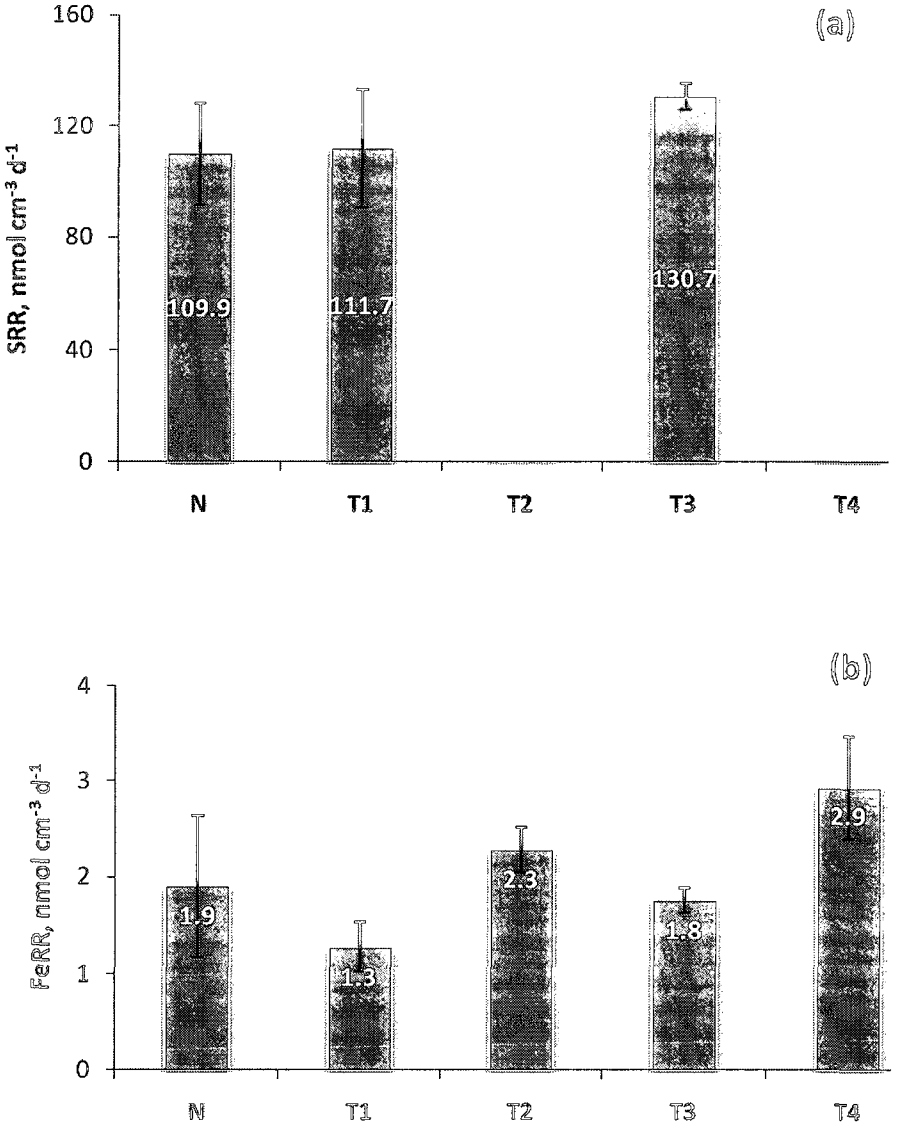

Figure 3-3. Sulfate Reduction Rates (a) and Iron Reduction Rates (b) in the Mer Bleue incubation microcosms. Error bars represent the standard error (SE) for n=3 replicates. The microcosms' description is in Table 3-3.

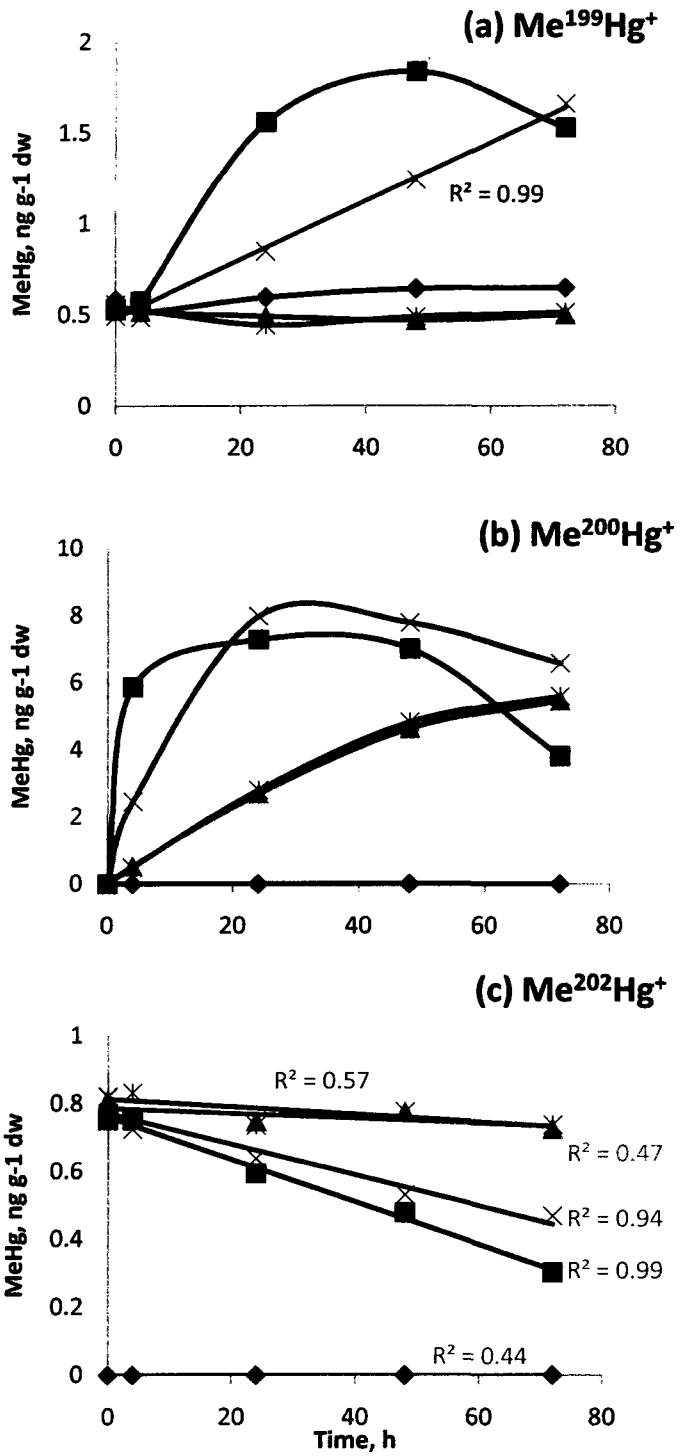

Figure 3-4. Ambient methylmercury trend (a) along with the evolution of MeHg produced (ng g^{-1} d.w., n=1) from the isotope enriched mercury spikes ^{200}Hg (b) and $Me^{202}Hg$ (c) during the 72h microcosm incubations: N (♦), T1 (■), T2 (▲), T3 (×), T4 (∗).The microcosms' description is in Table 3-3.

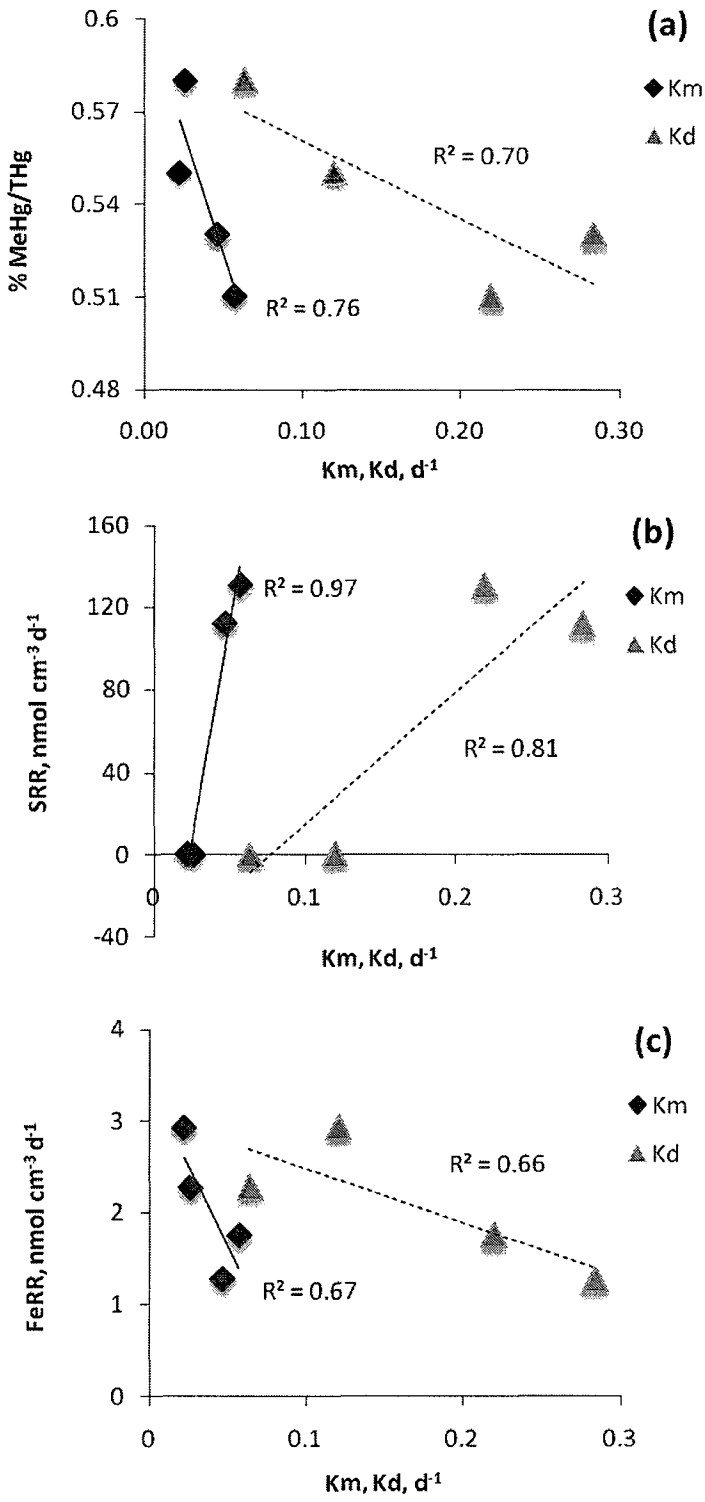

Figure 3-5. Relationship between Km (diamonds) or Kd (triangles) and percent MeHg to THg (a), Sulfate reduction rates (b), and Iron Reduction rates (c) for all microcosm. Km and Kd calculated for 24h as in Table 3-7.

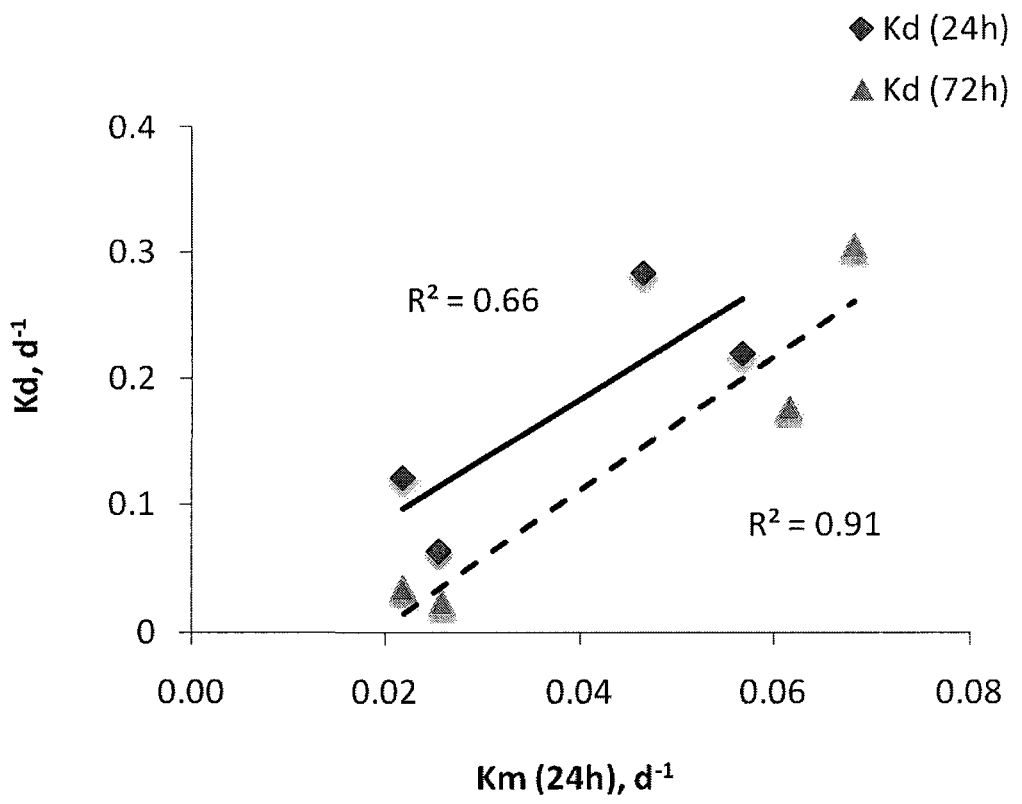

Figure 3-6. Relationship between Km and Kd for all microcosms. Kd calculated for 24h (dark diamonds) and for 72h (triangles).

Supporting Information

Five tables (Table S3-1 to S3-5) are presented as supporting information containing the statistical test results for FeRR calculation by linear regression, SRR and FeRR comparison among microcosms, XLfit results of curve fitting of ambient MeHg data for calculation of ambient Km and Kd, and Eh, dissolved iron and sulfides concentrations relationships with different MeHg isotope concentrations. We also provide a brief discussion of the inhibitory effect of Sodium molybdate and sodium 2-bromoethane sulfonate, an additional figure representing the relationship between porewater characteristics and different MeHg isotope concentrations, and a table containing the saturation indexes for all microcosms.

Inhibitory Effect of Sodium Molybdate and Sodium 2-Bromoethane Sulfonate

Naturally occurring SRB activity was inhibited by treating the sediment slurries with 1 mL of 1M sodium molybdate ($NaMoO_4$) to a final concentration of 2mM. The treatment is known to also prevent FeS formation. FeS formation may lead to an underestimation of iron reduction rates if rates are determined from the increase of dissolved Fe(II) concentrations. The efficiency of $NaMoO_4$ to inhibit sulfate reduction was determined by comparison of SRR in triplicate sub-samples (t=0h) from amended and not amended sediments.

The molybdate concentration was chosen taking into account the direct inhibitory effect of group VI anions on MeHg production [Chen et al., 1997] and based on the recommendations of Fleming et al. (2006), which pointed out that in previous research studies of freshwater sediments, excessive molybdate concentrations (20mM) might cause a more general inhibition of many sediment microbial processes. These authors found that a molybdate concentration of 0.2 mM was high enough to eliminate virtually all sulfate reduction activity and generally inhibited less than one-half of the total sediment activity for mercury methylation. This is in agreement with findings of Winfrey and Rudd, (1990), which also explored the impact of a range of molybdate concentrations on Hg methylation with freshwater sediments. Researchers have suggested that the appropriate concentration for molybdate application to sediments is equimolar to that of ambient sulfate [Oremland and Capone, 1988].

Naturally occurring methanogens were inhibited by treating the sediment slurries with 0.5 mL of 10mM of sodium 2-bromoethane sulfonate (BES, $BrCH_2CH_2SO_3Na$) (Pak and Bartha 1998) to give a final concentration of 10μM. The efficiency of BES to inhibit methane production was later tested by measuring methane concentrations in the headspace during the experiment.

BES is considered to be a "specific" inhibitor for methanogens because it is a structural analog of mercaptoehanesulfonic acid, the cofactor known as "HS-coenzyme M", which is found in all methanogens but not in other bacteria or Archaea (*Halobacterium halobium* or *Sulfolobus aidocaldarius*) [Oremland and Capone, 1988; Balch et al., 1979].

Coenzyme M (CoM) is associated with the terminal methylation reactions involved in methanogenesis, including the methyl-CoM reductase enzyme complex from which methane evolved [Oremland and Capone, 1988]. HS-Coenzyme M can be methylated via a methyltransferase reaction. BES acts like a competitive inhibitor of the methyl-CoM reductase complex, but it does not inhibit the methyltransferase system. Because the quantities of CoM in the environment are in nanomolar range, the authors pointed out that relatively small concentrations should be used. The BES concentration was chosen based on Oremland (1988) and Pak and Bartha (1998).

Table S3-1. Iron Reduction Rates (FeRR) determined by linear regression of the Fe^{2+} against sampling time (3 days)

H0: there is no relationship between Fe^{2+} (μM) and Time (day) results ; equation: y = a * x + b

Microcosm	ID	df	a	b	se	t-value	F	r^2	n	p-value	Statistical signification
Natural	N	10	1.90	-1.00	0.53	3.58	12.80	0.561	3	< 0.05	reject H0
Just Hg spikes	T1	10	1.27	-0.58	0.34	4.18	17.47	0.636	3	< 0.05	reject H0
Hg spikes + SRB inh.	T2	10	2.27	-0.76	0.57	3.97	15.75	0.612	3	< 0.05	reject H0
Hg spikes + MPA inh.	T3	10	1.75	-0.67	0.24	7.44	55.37	0.847	3	< 0.05	reject H0
Hg spikes + SRB and MPA inh	T4	10	2.93	-1.57	0.55	5.30	28.07	0.737	3	< 0.05	reject H0

Simple model I regression assumptions were checked using the plots resulting from the regression procedure (ANOVA):
Residuals vs fit plot: For any value of X, the Y's are independently and normally distributed (residuals are normally distributed)
Normal QQ plot of residuals: The variances of Y for fixed X are independent of X
Findlay, S. BIO 4118 course notes 2006 (p. 201 Linear correlations and simple linear regression).

Table S3-2. Statistical tests (two-Sample t-Test) results for SRR and FeRR comparison among microcosms.
(Findlay,S. BIO 4118 course notes 2006 , p. 143 Two samples comparison).

Rate	Procedure	mean X	mean Y	t	df	p	Statistical signification (H0: mean X = mean Y)		
SRR	N vs T1	109.9	111.7	-0.066	4	0.95	> 0.05	accept H0	
SRR	N vs T2	109.9	0.2	5.997	2	0.03	< 0.05	reject H0	significant difference
SRR	N vs T3	109.9	130.7	-1.099	2.3	0.37	> 0.05	accept H0	
SRR	N vs T4	109.9	0.4	5.988	2	0.03	< 0.05	reject H0	significant difference
SRR	T1 vs T2	111.7	0.2	5.240	2	0.03	< 0.05	reject H0	significant difference
SRR	T1 vs T3	111.7	130.7	-0.868	2.2	0.47	> 0.05	accept H0	
SRR	T1 vs T4	111.7	0.4	5.232	2	0.03	< 0.05	reject H0	significant difference
SRR	T2 vs T3	0.2	130.7	-27.242	2	0.00	< 0.05	reject H0	significant difference
SRR	T2 vs T4	0.2	0.4	-1.189	2.4	0.34	< 0.05	accept H0	
SRR	T3 vs T4	130.7	0.4	27.199	2	0.00	< 0.05	reject H0	significant difference
FeRR	N vs T1	1.9	1.3	0.816	2.5	0.4856	> 0.05	accept H0	
FeRR	N vs T2	1.9	2.9	-1.335	2.4	0.29	> 0.05	accept H0	
FeRR	N vs T3	1.9	1.8	0.203	2.12	0.86	> 0.05	accept H0	
FeRR	N vs T4	1.9	2.3	-0.408	3.7	0.71	> 0.05	accept H0	
FeRR	T1 vs T2	1.3	2.9	-4.790	4	0.01	< 0.05	reject H0	significant difference
FeRR	T1 vs T3	1.3	1.8	-1.676	3	0.19	> 0.05	accept H0	
FeRR	T1 vs T4	1.3	2.3	-1.694	2.9	0.19	> 0.05	accept H0	
FeRR	T2 vs T3	2.9	1.8	4.410	3	0.02	< 0.05	reject H0	significant difference
FeRR	T2 vs T4	2.9	2.3	1.127	3	0.35	> 0.05	accept H0	
FeRR	T3 vs T4	1.8	2.3	-0.948	2.4	0.43	> 0.05	accept H0	

Table S3-3. XL fit results of curve fitting of ambient MeHg data (199 isotope) for the calculation of ambient Km and Kd values.

	N	T1	T2	T3	T4
Km/Kd	0.0045	0.014	0.0037	0.013	0.0036
Kd	0.429	0.110	7273.28	0.027	2.6E+16
Km	0.0019	0.0015	27.17	0.0003	9.3E+13
Km/Kd	0.0045	0.014	0.004	0.013	0.004
F-test p	0.0240	0.744	0.007	0.605	0.010
T-test p	0.3920	0.468	0.377	0.284	0.368
r^2	0.0900	0.9040	0.721	0.9	0.028
$t_{1/2}$	1.6	6.3	0.0	25.7	0.0
km/kd ($1-e^{(-Kd*t)}$)	N	T1	T2	T3	T4
4	0.0037	0.005	0.0037	0.0013	0.0036
24	0.0045	0.013	0.0037	0.0061	0.0036
48	0.0045	0.014	0.0037	0.0094	0.0036
72	0.0045	0.014	0.0037	0.0110	0.0036
$[MeHg]_{predicted}$	N	T1	T2	T3	T4
4	0.47	0.55	0.46	0.18	0.46
24	0.58	1.42	0.45	0.81	0.45
48	0.58	1.52	0.45	1.23	0.44
72	0.58	1.58	0.44	1.46	0.44
$[MeHg]_{mesured}$	N	T1	T2	T3	T4
4	0.52	0.58	0.52	0.49	0.52
24	0.60	1.56	0.49	0.85	0.44
48	0.64	1.84	0.47	1.24	0.49
72	0.65	1.53	0.50	1.66	0.51

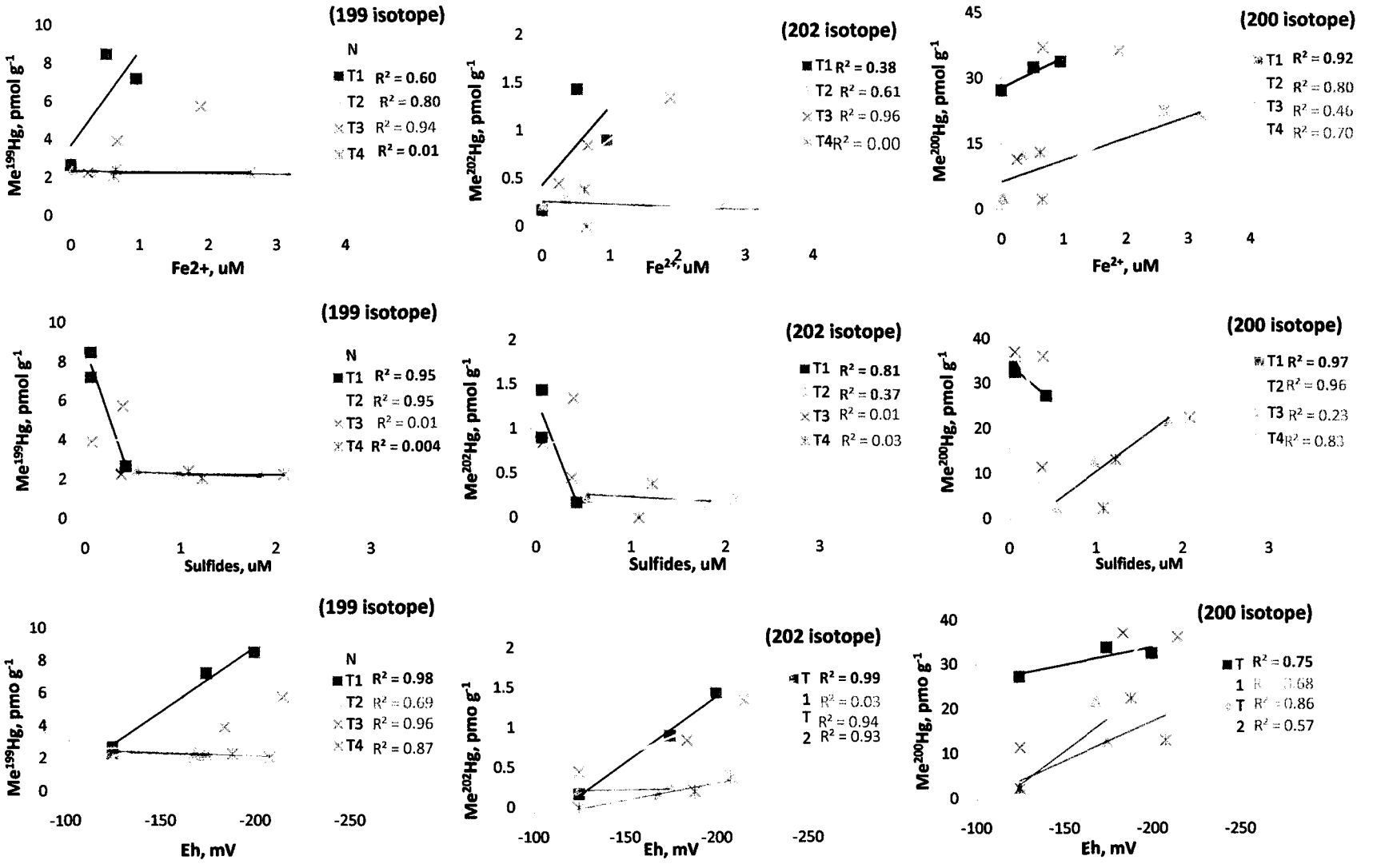

Figure S3-1. Relationship between porewater characteristics (μM, average n=3) and different MeHg isotope concentrations (pmol g^{-1} dw, n=1).

Table S3-4. Statistical analysis results for the relationship between porewater characteristics (pH, Eh, dissolved iron and sulfide) and different MeHg isotopes concentration in the microcosms. (H0: there is no relationship between pore water characteristics and MeHg concentration; linear regression for 48h)

Isotope	Porewater	ID	Linear regression					Pearson Correlation	
			Slope	Intercept	r^2	F	p	Coefficient	p
1	2	3	4	5	6	7	8	9	10
$Me^{199}Hg$	Eh	N	-0.01	1.98	0.502	1.01	0.50	-0.71	0.50
		T1	-0.08	-7.04	0.983	58.88	0.08	0.99	0.08
		T2	0.00	2.83	0.686	2.19	0.38	0.83	0.38
		T3	-0.04	-2.53	0.960	23.81	0.13	-0.98	0.13
		T4	0.00	2.93	0.869	6.61	0.24	0.93	0.24
$Me^{199}Hg$	Fe2+	N	0.40	2.43	0.830	4.87	0.27	0.91	0.27
		T1	4.93	3.66	0.602	1.51	0.43	0.78	0.43
		T2	-0.06	2.34	0.798	3.95	0.30	-0.89	0.30
		T3	1.97	2.10	0.941	15.97	0.16	0.97	0.16
		T4	0.01	2.22	0.008	0.01	0.94	0.09	0.94
$Me^{199}Hg$	pH	N	0.08	2.20	0.000	0.00	0.99	-0.02	0.99
		T1	-13.74	90.20	0.038	0.04	0.87	-0.20	0.87
		T2	-0.57	5.79	0.042	0.04	0.87	-0.20	0.87
		T3	-10.52	68.33	0.113	0.13	0.78	-0.34	0.78
		T4	4.34	-24.67	0.958	22.82	0.13	0.98	0.13
$Me^{199}Hg$	Sulfides	N	-0.49	2.81	0.072	0.08	0.83	-0.27	0.83
		T1	-14.36	8.77	0.952	19.69	0.14	-0.98	0.14
		T2	-0.17	2.46	0.953	20.25	0.13	-0.98	0.14
		T3	0.75	3.75	0.006	0.01	0.95	0.08	0.95
		T4	-0.02	2.27	0.004	0.00	0.96	-0.06	0.96
$Me^{200}Hg$	Eh	T1	-0.08	18.29	0.746	2.94	0.34	-0.86	0.34
		T2	-0.29	-33.38	0.681	2.13	0.38	-0.82	0.38
		T3	-0.30	-23.18	0.865	6.40	0.24	-0.93	0.24
		T4	-0.18	-17.93	0.573	1.34	0.45	-0.76	0.45
$Me^{200}Hg$	Fe2+	T1	6.90	27.83	0.92	11.76	0.18	0.96	0.18
		T2	4.91	6.37	0.803	4.07	0.29	0.90	0.29
		T3	11.56	17.39	0.462	0.86	0.52	0.68	0.52
		T4	7.42	2.99	0.704	2.38	0.37	0.84	0.37
$Me^{200}Hg$	pH	T1	-44.49	303.49	0.315	0.46	0.62	-0.56	0.62
		T2	48.20	-286.52	0.044	0.05	0.87	0.21	0.86
		T3	-207.98	1301.09	0.635	7.74	0.41	-0.80	0.41

		T4	-67.27	429.47	0.077	0.08	0.82	-0.28	0.82
$Me^{200}Hg$	Sulfides	T1	-16.38	34.28	0.969	31.22	0.11	-0.98	0.11
		T2	14.17	-3.70	0.955	21.23	0.14	0.98	0.14
		T3	-38.13	38.99	0.230	0.30	0.68	-0.48	0.68
		T4	16.93	-12.18	0.828	4.80	0.27	0.91	0.27
$Me^{202}Hg$	Eh	T1	-0.02	-1.91	0.991	112.40	0.06	-1.00	0.06
		T2	0.00	0.17	0.027	0.03	0.90	-0.16	0.89
		T3	-0.01	-0.77	0.941	16.07	0.16	-0.97	0.16
		T4	-0.01	-0.70	0.962	25.35	0.13	-0.98	0.12
$Me^{202}Hg$	Fe2+	T1	0.81	0.43	0.380	0.61	0.58	0.62	0.58
		T2	-0.03	0.26	0.610	1.57	0.43	-0.78	0.43
		T3	0.51	0.40	0.959	23.65	0.13	0.98	0.13
		T4	0.02	0.15	0.008	0.01	0.94	0.09	0.94
$Me^{202}Hg$	pH	T1	0.38	-1.51	0.001	0.00	0.98	0.03	0.98
		T2	-1.52	9.63	0.950	19.12	0.14	-0.97	0.14
		T3	-2.38	15.46	0.088	0.10	0.81	-0.29	0.81
		T4	-4.97	30.99	0.862	6.22	0.24	-0.92	0.24
$Me^{202}Hg$	Sulfides	T1	-2.76	1.35	0.815	4.39	0.28	-0.90	0.28
		T2	-0.06	0.29	0.366	0.58	0.59	-0.61	0.59
		T3	0.30	0.79	0.015	0.01	0.92	0.12	0.92
		T4	0.10	0.04	0.054	0.06	0.85	0.23	0.85
ΣMeHg	pH	N	0.08	2.20	0.000	0.00	0.99	0.02	0.99
		T1	-57.84	392.19	0.131	0.15	0.76	-0.36	0.76
		T2	46.12	-271.10	0.042	0.04	0.87	-0.20	0.87
		T3	-220.88	1384.88	0.563	1.29	0.46	-0.75	0.46
		T4	-67.90	435.78	0.078	0.08	0.82	-0.28	0.82
ΣMeHg	Eh	N	0.00	1.98	0.502	1.01	0.50	-0.71	0.50
		T1	-0.17	9.34	0.911	10.24	0.19	-0.95	0.19
		T2	-0.29	-30.39	0.686	2.19	0.38	-0.83	0.38
		T3	-0.34	-26.48	0.911	10.26	0.19	-0.95	0.19
		T4	-0.18	-15.70	0.575	1.35	0.45	-0.76	0.45
ΣMeHg	Fe2+	N	0.40	2.43	0.830	4.87	0.83	0.91	0.27
		T1	12.65	31.92	0.762	3.21	0.32	0.87	0.32
		T2	4.82	8.98	0.798	3.95	0.29	0.89	0.30
		T3	14.04	19.88	0.535	1.15	0.48	0.73	0.48
		T4	7.45	5.36	0.703	2.36	0.37	0.84	0.37
ΣMeHg	Sulfides	N	-0.49	2.81	0.072	0.08	0.07	-0.27	0.83
		T1	-33.50	44.40	0.998	426.70	0.03	-1.00	0.03
		T2	13.94	-0.95	0.952	20.02	0.14	0.98	0.14
		T3	-37.09	43.53	0.171	0.21	0.73	-0.41	0.73
		T4	17.01	-9.87	0.827	4.76	0.27	0.91	0.27

Table S3-5 Phreeqci Saturation index (SI) results for all microcosms incubated

Natural microcosm (N)

t=0h	Phase	SI	log IAP	log KT	
	Fe2(SO4)3	-38.37	-34.79	3.58	Fe2(SO4)3
	Fe3(OH)8	0.45	20.67	20.22	Fe3(OH)8
	Ferrihydrite	2.77	7.66	4.89	Fe(OH)3
	FeS(ppt)	-4.21	-8.12	-3.92	FeS
	Goethite	7.16	7.66	0.50	FeOOH
	Greigite	11.80	-33.23	-45.03	Fe3S4
	Hematite	19.33	15.32	-4.01	Fe2O3
	Jarosite-H	1.67	-10.43	-12.10	(H3O)Fe3(SO4)2(OH)6
	Lepidocrocite	6.29	7.66	1.37	FeOOH
	Mackinawite	-3.47	-8.12	-4.65	FeS
	Maghemite	8.93	15.32	6.39	Fe2O3
	Magnetite	16.94	20.67	3.74	Fe3O4
	Melanterite	-8.88	-11.35	-2.47	FeSO4:7H2O
	O2(g)	-21.77	61.35	83.12	O2
	Pyrite	27.55	9.07	-18.48	FeS2
	Sulfur	19.31	17.20	-2.11	S
t=24h	**Phase**	**SI**	**log IAP**	**log KT**	
	Fe2(SO4)3	-37.85	-34.27	3.58	Fe2(SO4)3
	Fe3(OH)8	0.59	20.81	20.22	Fe3(OH)8
	Ferrihydrite	2.64	7.53	4.89	Fe(OH)3
	FeS(ppt)	-4.63	-8.54	-3.92	FeS
	Goethite	7.03	7.53	0.50	FeOOH
	Greigite	8.66	-36.38	-45.03	Fe3S4
	Hematite	19.06	15.05	-4.01	Fe2O3
	Jarosite-H	1.80	-10.30	-12.10	(H3O)Fe3(SO4)2(OH)6
	Lepidocrocite	6.16	7.53	1.37	FeOOH
	Mackinawite	-3.89	-8.54	-4.65	FeS
	Maghemite	8.67	15.05	6.39	Fe2O3
	Magnetite	17.07	20.81	3.74	Fe3O4
	Melanterite	-8.22	-10.69	-2.47	FeSO4:7H2O
	O2(g)	-23.91	59.21	83.12	O2
	Pyrite	25.25	6.77	-18.48	FeS2
	Sulfur	17.42	15.31	-2.11	S
t=48h	**Phase**	**SI**	**log IAP**	**log KT**	
	Fe2(SO4)3	-38.71	-35.13	3.58	Fe2(SO4)3
	Fe3(OH)8	1.35	21.57	20.22	Fe3(OH)8
	Ferrihydrite	**2.66**	7.55	4.89	Fe(OH)3
	FeS(ppt)	-3.14	-7.05	-3.92	FeS
	Goethite	7.05	7.55	0.50	FeOOH
	Greigite	12.53	-32.51	-45.03	Fe3S4
	Hematite	19.11	15.10	-4.01	Fe2O3
	Jarosite-H	1.26	-10.84	-12.10	(H3O)Fe3(SO4)2(OH)6

Lepidocrocite 6.18 7.55 1.37 FeOOH
Mackinawite -2.41 -7.05 -4.65 FeS
Maghemite 8.72 15.10 6.39 Fe2O3
Magnetite 17.83 21.57 3.74 Fe3O4
Melanterite -7.81 -10.28 -2.47FeSO4:7H2O
O2(g) -26.64 56.48 83.12 O2
Pyrite 26.14 7.66 -18.48 FeS2
Sulfur 16.83 14.72 -2.11 S

t=72h Phase SI log IAP log KT

Fe2(SO4)3 -39.54 -35.96 3.58 Fe2(SO4)3
Fe3(OH)8 1.48 21.70 20.22 Fe3(OH)8
Ferrihydrite 2.36 7.25 4.89 Fe(OH)3
FeS(ppt) -2.39 -6.31 -3.92 FeS
Goethite 6.75 7.25 0.50 FeOOH
Greigite 12.73 -32.31 -45.03 Fe3S4
Hematite 18.51 14.51 -4.01 Fe2O3
Jarosite-H 0.21 -11.89 -12.10 (H3O)Fe3(SO4)2(OH)6
Lepidocrocite 5.88 7.25 1.37 FeOOH
Mackinawite -1.66 -6.31 -4.65 FeS
Maghemite 8.12 14.51 6.39 Fe2O3
Magnetite 17.96 21.70 3.74 Fe3O4
Melanterite -7.16 -9.63 -2.47FeSO4:7H2O
O2(g) -30.76 52.36 83.12 O2
Pyrite 24.85 6.37 -18.48 FeS2
Sulfur 14.79 12.68 -2.11 S

T1 microcosm

t=0h Phase SI log IAP log KT

Fe2(SO4)3 -37.92 -34.34 3.58 Fe2(SO4)3
Ferrihydrite 2.93 7.82 4.89 Fe(OH)3
Goethite 7.32 7.82 0.50 FeOOH
Hematite 19.64 15.63 -4.01 Fe2O3
Jarosite-H 2.24 -9.86 -12.10 (H3O)Fe3(SO4)2(OH)6
Lepidocrocite 6.45 7.82 1.37 FeOOH
Maghemite 9.25 15.63 6.39 Fe2O3
O2(g) -41.18 41.94 83.12 O2
Sulfur 9.71 7.60 -2.11 S

t=24h Phase SI log IAP log KT

Fe2(SO4)3 -37.90 -34.32 3.58Fe2(SO4)3
Fe3(OH)8 0.82 21.05 20.22 Fe3(OH)8
Ferrihydrite 2.59 7.49 4.89 Fe(OH)3
FeS(ppt) -4.23 -8.14 -3.92 FeS
Goethite 6.99 7.49 0.50 FeOOH
Greigite 9.21 -35.83 -45.03 Fe3S4
Hematite 18.98 14.97 -4.01 Fe2O3
Jarosite-H 1.69 -10.41 -12.10 (H3O)Fe3(SO4)2(OH)6
Lepidocrocite 6.11 7.49 1.37 FeOOH
Mackinawite -3.49 -8.14 -4.65 FeS

Maghemite 8.58 14.97 6.39 Fe2O3
Magnetite 17.31 21.05 3.74 Fe3O4
Melanterite -7.89 -10.36 -2.47FeSO4:7H2O
O2(g) -25.35 57.77 83.12 O2
Pyrite 25.00 6.52 -18.48 FeS2
Sulfur 16.78 14.67 -2.11 S

t=48h Phase SI log IAP log KT

Fe2(SO4)3 -39.15 -35.57 3.58 Fe2(SO4)3
Fe3(OH)8 0.52 20.74 20.22 Fe3(OH)8
Ferrihydrite 2.48 7.37 4.89 Fe(OH)3
FeS(ppt) -4.25 -8.17 -3.92 FeS
Goethite 6.87 7.37 0.50 FeOOH
Greigite 9.13 -35.91 -45.03 Fe3S4
Hematite 18.76 14.75 -4.01 Fe2O3
Jarosite-H 0.68 -11.42 -12.10 (H3O)Fe3(SO4)2(OH)6
Lepidocrocite 6.00 7.37 1.37 FeOOH
Mackinawite -3.52 -8.17 -4.65 FeS
Maghemite 8.36 14.75 6.39 Fe2O3
Magnetite 17.00 20.74 3.74 Fe3O4
Melanterite -8.31 -10.78 -2.47FeSO4:7H2O
O2(g) -25.48 57.64 83.12 O2
Pyrite 24.97 6.49 -18.48 FeS2
Sulfur 16.77 14.66 -2.11 S

t=72h Phase SI log IAP log KT

Fe2(SO4)3 -40.21 -36.63 3.58 Fe2(SO4)3
Fe3(OH)8 0.43 20.65 20.22 Fe3(OH)8
Ferrihydrite 1.96 6.85 4.89 Fe(OH)3
FeS(ppt) -2.57 -6.48 -3.92 FeS
Goethite 6.35 6.85 0.50 FeOOH
Greigite 11.96 -33.07 -45.03 Fe3S4
Hematite 17.71 13.70 -4.01 Fe2O3
Jarosite-H -0.90 -13.00 -12.10 (H3O)Fe3(SO4)2(OH)6
Lepidocrocite 5.48 6.85 1.37 FeOOH
Mackinawite -1.83 -6.48 -4.65 FeS
Maghemite 7.32 13.70 6.39 Fe2O3
Magnetite 16.92 20.65 3.74 Fe3O4
Melanterite -7.36 -9.83 -2.47FeSO4:7H2O
O2(g) -31.38 51.74 83.12 O2
Pyrite 24.43 5.95 -18.48 FeS2
Sulfur 14.55 12.44 -2.11 S

T2 microcosm (SRB inhibited)

t=0h Phase SI log IAP log KT

Fe2(SO4)3 -39.07 -35.49 3.58 Fe2(SO4)3
Fe3(OH)8 -0.84 19.38 20.22 Fe3(OH)8
Ferrihydrite 2.52 7.41 4.89 Fe(OH)3
FeS(ppt) -4.80 -8.71 -3.92 FeS
Goethite 6.91 7.41 0.50 FeOOH

	Greigite	11.32	-33.72	-45.03 Fe3S4
	Hematite	18.83	14.82	-4.01 Fe2O3
	Jarosite-H	0.79	-11.31	-12.10 (H3O)Fe3(SO4)2(OH)6
	Lepidocrocite	6.04	7.41	1.37 FeOOH
	Mackinawite	-4.07	-8.71	-4.65 FeS
	Maghemite	8.43	14.82	6.39 Fe2O3
	Magnetite	15.64	19.38	3.74 Fe3O4
	Melanterite	-9.74	-12.21	-2.47FeSO4:7H2O
	O2(g)	-19.59	63.53	83.12 O2
	Pyrite	28.25	9.78	-18.48 FeS2
	Sulfur	20.60	18.49	-2.11 S
t=24h	**Phase**	**SI**	**log IAP**	**log KT**
	Fe2(SO4)3	-37.14	-33.56	3.58 Fe2(SO4)3
	Fe3(OH)8	1.00	21.22	20.22 Fe3(OH)8
	Ferrihydrite	2.82	7.71	4.89 Fe(OH)3
	FeS(ppt)	-3.31	-7.22	-3.92 FeS
	Goethite	7.21	7.71	0.50 FeOOH
	Greigite	14.19	-30.85	-45.03 Fe3S4
	Hematite	19.44	15.43	-4.01 Fe2O3
	Jarosite-H	2.58	-9.52	-12.10 (H3O)Fe3(SO4)2(OH)6
	Lepidocrocite	6.34	7.71	1.37 FeOOH
	Mackinawite	-2.57	-7.22	-4.65 FeS
	Maghemite	9.04	15.43	6.39 Fe2O3
	Magnetite	17.48	21.22	3.74 Fe3O4
	Melanterite	-8.07	-10.54	-2.47FeSO4:7H2O
	O2(g)	-23.31	59.81	83.12 O2
	Pyrite	28.14	9.66	-18.48 FeS2
	Sulfur	19.00	16.89	-2.11 S
t=48h	**Phase**	**SI**	**log IAP**	**log KT**
	Fe2(SO4)3	-39.00	-35.42	3.58 Fe2(SO4)3
	Fe3(OH)8	1.41	21.64	20.22 Fe3(OH)8
	Ferrihydrite	2.46	7.35	4.89 Fe(OH)3
	FeS(ppt)	-1.90	-5.82	-3.92 FeS
	Goethite	6.85	7.35	0.50 FeOOH
	Greigite	15.65	-29.38	-45.03 Fe3S4
	Hematite	18.71	14.70	-4.01 Fe2O3
	Jarosite-H	0.74	-11.36	-12.10 (H3O)Fe3(SO4)2(OH)6
	Lepidocrocite	5.98	7.35	1.37 FeOOH
	Mackinawite	-1.17	-5.82	-4.65 FeS
	Maghemite	8.31	14.70	6.39 Fe2O3
	Magnetite	17.90	21.64	3.74 Fe3O4
	Melanterite	-7.30	-9.77	-2.47FeSO4:7H2O
	O2(g)	-29.33	53.79	83.12 O2
	Pyrite	26.80	8.32	-18.48 FeS2
	Sulfur	16.25	14.14	-2.11 S
t=72h	**Phase**	**SI**	**log IAP**	**log KT**
	Fe2(SO4)3	-37.79	-34.21	3.58 Fe2(SO4)3

Fe3(OH)8	2.64	22.86	20.22	Fe3(OH)8
Ferrihydrite	2.84	7.73	4.89	Fe(OH)3
FeS(ppt)	-1.48	-5.39	-3.92	FeS
Goethite	7.23	7.73	0.50	FeOOH
Greigite	16.74	-28.30	-45.03	Fe3S4
Hematite	19.47	15.47	-4.01	Fe2O3
Jarosite-H	2.18	-9.92	-12.10	(H3O)Fe3(SO4)2(OH)6
Lepidocrocite	6.36	7.73	1.37	FeOOH
Mackinawite	-0.75	-5.39	-4.65	FeS
Maghemite	9.08	15.47	6.39	Fe2O3
Magnetite	19.13	22.86	3.74	Fe3O4
Melanterite	-6.69	-9.16	-2.47	FeSO4:7H2O
O2(g)	-29.65	53.47	83.12	O2
Pyrite	27.03	8.55	-18.48	FeS2
Sulfur	16.06	13.95	-2.11	S

T3 microcosm (MPA inhibited)

t=0h	Phase	SI	log IAP	log KT
	Fe2(SO4)3	-38.53	-34.95	3.58 Fe2(SO4)3
	Fe3(OH)8	0.55	20.77	20.22 Fe3(OH)8
	Ferrihydrite	2.67	7.56	4.89 Fe(OH)3
	FeS(ppt)	-3.86	-7.77	-3.92 FeS
	Goethite	7.06	7.56	0.50 FeOOH
	Greigite	12.10	-32.94	-45.03 Fe3S4
	Hematite	19.12	15.11	-4.01 Fe2O3
	Jarosite-H	1.40	-10.70	-12.10 (H3O)Fe3(SO4)2(OH)6
	Lepidocrocite	6.19	7.56	1.37 FeOOH
	Mackinawite	-3.12	-7.77	-4.65 FeS
	Maghemite	8.73	15.11	6.39 Fe2O3
	Magnetite	17.03	20.77	3.74 Fe3O4
	Melanterite	-8.56	-11.03	-2.47 FeSO4:7H2O
	O2(g)	-23.38	59.74	83.12 O2
	Pyrite	27.15	8.67	-18.48 FeS2
	Sulfur	18.55	16.44	-2.11 S
t=24h	Phase	SI	log IAP	log KT
	Fe2(SO4)3	-38.01	-34.43	3.58 Fe2(SO4)3
	Fe3(OH)8	0.63	20.85	20.22 Fe3(OH)8
	Ferrihydrite	2.57	7.46	4.89 Fe(OH)3
	FeS(ppt)	-4.31	-8.22	-3.92 FeS
	Goethite	6.96	7.46	0.50 FeOOH
	Greigite	9.28	-35.75	-45.03 Fe3S4
	Hematite	18.93	14.93	-4.01 Fe2O3
	Jarosite-H	1.58	-10.52	-12.10 (H3O)Fe3(SO4)2(OH)6
	Lepidocrocite	6.09	7.46	1.37 FeOOH
	Mackinawite	-3.58	-8.22	-4.65 FeS
	Maghemite	8.54	14.93	6.39 Fe2O3
	Magnetite	17.11	20.85	3.74 Fe3O4
	Melanterite	-8.06	-10.53	-2.47 FeSO4:7H2O

	O2(g)	-24.85	58.27	83.12 O2
	Pyrite	25.24	6.76	-18.48 FeS2
	Sulfur	17.10	14.99	-2.11 S

t=48h	Phase	SI	log IAP	log KT
	Fe2(SO4)3	-38.63	-35.05	3.58 Fe2(SO4)3
	Fe3(OH)8	0.94	21.16	20.22 Fe3(OH)8
	Ferrihydrite	2.43	7.32	4.89 Fe(OH)3
	FeS(ppt)	-2.98	-6.89	-3.92 FeS
	Goethite	6.82	7.32	0.50 FeOOH
	Greigite	12.59	-32.45	-45.03 Fe3S4
	Hematite	18.66	14.65	-4.01 Fe2O3
	Jarosite-H	0.94	-11.16	-12.10 (H3O)Fe3(SO4)2(OH)6
	Lepidocrocite	5.95	7.32	1.37 FeOOH
	Mackinawite	-2.24	-6.89	-4.65 FeS
	Maghemite	8.26	14.65	6.39 Fe2O3
	Magnetite	17.43	21.16	3.74 Fe3O4
	Melanterite	-7.58	-10.05	-2.47FeSO4:7H2O
	O2(g)	-27.74	55.38	83.12 O2
	Pyrite	25.87	7.40	-18.48 FeS2
	Sulfur	16.40	14.29	-2.11 S

t=72h	Phase	SI	log IAP	log KT
	Fe2(SO4)3	-38.51	-34.93	3.58 Fe2(SO4)3
	Fe3(OH)8	1.95	22.17	20.22 Fe3(OH)8
	Ferrihydrite	2.66	7.55	4.89 Fe(OH)3
	FeS(ppt)	-2.28	-6.20	-3.92 FeS
	Goethite	7.05	7.55	0.50 FeOOH
	Greigite	14.11	-30.92	-45.03 Fe3S4
	Hematite	19.10	15.09	-4.01 Fe2O3
	Jarosite-H	1.39	-10.71	-12.10 (H3O)Fe3(SO4)2(OH)6
	Lepidocrocite	6.18	7.55	1.37 FeOOH
	Mackinawite	-1.55	-6.20	-4.65 FeS
	Maghemite	8.71	15.09	6.39 Fe2O3
	Magnetite	18.43	22.17	3.74 Fe3O4
	Melanterite	-7.13	-9.60	-2.47FeSO4:7H2O
	O2(g)	-29.12	54.00	83.12 O2
	Pyrite	26.01	7.53	-18.48 FeS2
	Sulfur	15.84	13.73	-2.11 S

T4 microcosm (SRB and MPA inhibited)

t=0h	Phase	SI	log IAP	log KT
	Fe2(SO4)3	-38.09	-34.51	3.58 Fe2(SO4)3
	Fe3(OH)8	0.94	21.16	20.22 Fe3(OH)8
	Ferrihydrite	2.66	7.55	4.89 Fe(OH)3
	FeS(ppt)	-2.99	-6.91	-3.92 FeS
	Goethite	7.05	7.55	0.50 FeOOH
	Greigite	14.31	-30.73	-45.03 Fe3S4
	Hematite	19.11	15.10	-4.01 Fe2O3
	Jarosite-H	1.68	-10.42	-12.10 (H3O)Fe3(SO4)2(OH)6

Lepidocrocite 6.18 7.55 1.37 FeOOH
Mackinawite -2.26 -6.91 -4.65 FeS
Maghemite 8.71 15.10 6.39 Fe2O3
Magnetite 17.43 21.16 3.74 Fe3O4
Melanterite -8.00 -10.47 -2.47FeSO4:7H2O
O2(g) -25.05 58.07 83.12 O2
Pyrite 27.63 9.15 -18.48 FeS2
Sulfur 18.17 16.06 -2.11 S

t=24h Phase SI log IAP log KT

Fe2(SO4)3 -37.36 -33.78 3.58 Fe2(SO4)3
Fe3(OH)8 1.23 21.45 20.22 Fe3(OH)8
Ferrihydrite 2.80 7.70 4.89 Fe(OH)3
FeS(ppt) -2.95 -6.86 -3.92 FeS
Goethite 7.20 7.70 0.50 FeOOH
Greigite 14.81 -30.22 -45.03 Fe3S4
Hematite 19.40 15.39 -4.01 Fe2O3
Jarosite-H 2.41 -9.69 -12.10 (H3O)Fe3(SO4)2(OH)6
Lepidocrocite 6.32 7.70 1.37 FeOOH
Mackinawite -2.21 -6.86 -4.65 FeS
Maghemite 9.00 15.39 6.39 Fe2O3
Magnetite 17.71 21.45 3.74 Fe3O4
Melanterite -7.86 -10.33 -2.47FeSO4:7H2O
O2(g) -24.44 58.68 83.12 O2
Pyrite 28.04 9.56 -18.48 FeS2
Sulfur 18.53 16.42 -2.11 S

t=48h Phase SI log IAP log KT

Fe2(SO4)3 -38.03 -34.45 3.58 Fe2(SO4)3
Fe3(OH)8 1.93 22.15 20.22 Fe3(OH)8
Ferrihydrite 2.78 7.67 4.89 Fe(OH)3
FeS(ppt) -1.98 -5.89 -3.92 FeS
Goethite 7.17 7.67 0.50 FeOOH
Greigite 16.39 -28.64 -45.03 Fe3S4
Hematite 19.36 15.35 -4.01 Fe2O3
Jarosite-H 1.92 -10.18 -12.10 (H3O)Fe3(SO4)2(OH)6
Lepidocrocite 6.30 7.67 1.37 FeOOH
Mackinawite -1.25 -5.89 -4.65 FeS
Maghemite 8.96 15.35 6.39 Fe2O3
Magnetite 18.42 22.15 3.74 Fe3O4
Melanterite -7.32 -9.79 -2.47FeSO4:7H2O
O2(g) -27.51 55.61 83.12 O2
Pyrite 27.69 9.21 -18.48 FeS2
Sulfur 17.21 15.10 -2.11 S

t=72h Phase SI log IAP log KT

Fe2(SO4)3 -38.17 -34.59 3.58 Fe2(SO4)3
Fe3(OH)8 2.63 22.85 20.22 Fe3(OH)8
Ferrihydrite 2.81 7.70 4.89 Fe(OH)3
FeS(ppt) -1.47 -5.39 -3.92 FeS

```
Goethite    7.20 7.70 0.50 FeOOH
Greigite    16.57 -28.47 -45.03 Fe3S4
Hematite    19.41 15.41 -4.01 Fe2O3
Jarosite-H  1.88 -10.22 -12.10 (H3O)Fe3(SO4)2(OH)6
Lepidocrocite  6.33 7.70 1.37 FeOOH
Mackinawite  -0.74 -5.39 -4.65 FeS
Maghemite   9.02 15.41 6.39 Fe2O3
Magnetite  19.11 22.85 3.74 Fe3O4
Melanterite  -6.75 -9.22 -2.47FeSO4:7H2O
O2(g)    -29.96 53.16 83.12 O2
Pyrite    26.85 8.37 -18.48 FeS2
Sulfur    15.86 13.75 -2.11 S
```

CHAPTER 4. BIOGEOCHEMICAL FACTORS INFLUENCING NET MERCURY METHYLATION IN CONTAMINATED FRESHWATER SEDIMENTS FROM THE ST. LAWRENCE RIVER IN CORNWALL, ONTARIO, CANADA[2]

[2] Adapted from M-L Avramescu, E. Yumvihoze, H. Hintelmann, D. Fortin, D.R.S.Lean, in prep.

Abstract

Mercury methylation in aquatic systems has been linked to the activity of various anaerobic microbes, including sulfate-reducers (SRB), iron-reducers (FeRP) and methanogens (MPA). Despite a large body of research with pure microbial cultures, little is known about the relative importance of each microbial group in the overall process in natural sediments. The present study on the contaminated sediments of the St. Lawrence River near Cornwall (Zone 1 SLR), Ontario, Canada, focused on the biogeochemical factors, i.e., the relative importance of the diverse groups of anaerobic microbes (FeRP, SRB, MPA), that affect net methylmercury formation in freshwater systems. Methylation and demethylation were measured separately by using enriched stable isotopes of mercury $^{200}Hg^{2+}$ and $Me^{199}Hg$ in microcosms treated with specific microbial inhibitors. Sediments from the St. Lawrence River in Cornwall, Ontario, were sampled in June and July 2007 and incubated in the dark at room temperature in an anaerobic chamber for 72-96h. The amount of $Me^{200}Hg$ produced and the amount of $Me^{199}Hg$ remaining were measured. During the first 48h, MeHg concentrations increased linearly for all treatments containing microbial inhibitors. Our results first indicate that the inhibition of certain groups of microbes clearly had an effect on methylation and demethylation. The Hg spike addition increased the availability of ambient Hg for methylation, with the exception of the SRB-inhibited microcosms. The highest calculated methylation percentage was in the microcosm where only MPA were inhibited, followed closely by the Hg spike control microcosm. The inhibition of methanogens stimulated net methylation, not only by inhibiting demethylation, but also by stimulating methylation (as demonstrated by M/D ratios), along with the stimulation of the SRB activity. Iron reduction might however be another important process in the production of MeHg in aquatic environments, because the inhibition of both SRB and MPA enhanced the iron reduction rate and MeHg production was not completely stopped. Moreover, the strong positive correlation between methylation rate constant (Km) and SRR and between demethylation rate constant (Kd) and MPA, clearly supports the fact that SRB are involved in Hg methylation and MPA in MeHg demethylation in the sediments. In contrast, the strong negative correlation between Kd and FeRR showed that the increase in FeRR corresponds to a decrease in demethylation, which

may indicate that iron reduction may influence net methylation in the Zone 1 SLR sediments by decreasing demethylation rather than favouring methylation in the long term.

Keywords: methylmercury, methylation, demethylation, SRB, MPA, FERP, sediments.

4.1. Introduction

Mercury methylation in aquatic systems has been linked to the activity of various anaerobic microbes, including sulfate-reducers, iron reducers and methanogens [i.e., Compeau and Bartha, 1985; Benoit et al., 2003; Fleming et al., 2006; Barkay et al., 2003, Wood 1968]. Despite a large body of research with pure microbial cultures, little is known about the relative importance of each microbial group in the overall process in natural sediments. The present study focussed on the contaminated sediments of the St. Lawrence River near Cornwall, Ontario, because the Moses-Saunders Dam downstream of the Beauharmois Dam in Quebec has been designated a Great Lakes "Area of Concern" (AOC) by the International Joint Commission (IJC) in 1985 [Ridal et al., 2009; Richman and Dreier, 2001]. The river's ecosystem has been affected by chemical pollution (heavy metals, such as Hg, Zn, Pb, Cu, etc. and organic compounds), which resulted in habitat degradation [Quemarais et al., 1998]. The main source of Hg in the river sediments originates from historical point source discharges from local industries (chemical, pulp and paper, mercury cell chlor-alkali and aluminum production) [Delongchamp et al., 2009; Richman and Dreier, 2001], but other sources, such as tributary discharging agricultural and wetland runoff, diffuse sources from Lake Ontario and long-range atmospheric transport and deposition, may also be important [Ridal et al., 2009]. Three main contaminated depositional zones (Zones 1, 2 and 3) were investigated along the Cornwall waterfront in response to the Remedial Action Plan (RAP). Within these zones, the Hg concentration of the sediments exceeded the sediment quality guidelines for the protection of aquatic organisms (Canadian Sediment Quality Guidelines for freshwater sediments-CSQG: Interim sediment quality guidelines-ISQL: 0.170 mg/Kg; Probable Effect Level-PEL: 0.486 mg/Kg) [Canadian Council of Ministers of the Environment, 2005], especially in Zone 1 where the highest levels of mercury in fish, methylmercury (MeHg) in sediments, % MeHg to total mercury (THg) in both sediments and porewater were found [Delongchamp et al., 2009]. There is also a high rate of methane production in the Zone 1 sediments [Poissant et al., 2001; Razavi, 2008]. The contaminated sediments have been found to be the net source of THg and the potential source of MeHg in the food web and the river system [Delongchamp et al., 2009], despite the closure of the main industrial

sources. A management strategy was adopted to leave the sediments in place, allowing the natural remediation through an eventual burial by sedimentation of low Hg content sediments. Investigation of the recently deposited surficial sediments indicated that even though they are less contaminated in THg, they are more contaminated in MeHg, with almost 6% MeHg in the top 1cm in Zone 1 [Delongchamp et al., 2009]. Elevated Hg concentrations in yellow perch, other fish species, and amphipods have also been found [Fowlie al., 2008; Razavi, 2008; Choy et al., 2008, Goulet et al., 2008]. Detailed data about the spread of contamination and the pathways for Hg transfer from the sediments to fish are the subject of the recent report summary of Ridal et al. (2009). There is therefore a crucial need to further characterize the factors affecting MeHg production, as well as the sediment-water interactions and concentrations of MeHg in biota in the Zone 1 of the St. Lawrence River near Cornwall.

What are the factors affecting methylmercury formation in surficial sediments of the Zone 1 of the St. Lawrence AOC? To answer this question, we investigated the biogeochemical factors that affect net methylmercury formation, more specifically the role played by methanogens (MPA), iron- (FeRP) and sulfate- (SRB) reducing bacteria in the St. Lawrence River sediments. River sediments were sampled during the summer of 2007 and incubated with enriched isotopes of mercury and specific microbial inhibitors. The MeHg formation and degradation rates were calculated and the data were correlated with anaerobic microbes (SRB, MPA, and FeRP) activity rates and geochemical parameters. The main objectives of the experiment with the St. Lawrence River sediments were: (a) to determine the rates of biotic methylmercury formation and demethylation and (b) to assess the relative contribution of the different groups of anaerobic microbes (SRB, MPA, and FeRP) to methylmercury formation and demethylation in freshwater sediments. Hypothesis and predictions tested in this chapter are:

H1: Abiotic methylation is the principal pathway for methyl mercury formation

P1: MeHg production rates in autoclaved microcosms will be similar to those in biotic experiments

H2: MeHg production and degradation are influenced by interspecific competition among SRB, MPA and FeRP for electron donors.

P2: MeHg production and degradation rates that can be related to microbial iron reduction should be higher in microcosms where sulfate reduction and/or methanogenesis are inhibited

4.2. Materials and Methods

4.2.1. Site Description

River sediments in the AOC have historically been contaminated with mercury (Hg) due to former Hg discharges from ICI Forest Products (mercury cell chlor-alkali plant, closed in 1995), Domtar Fine Papers Ltd. (pulp and paper mill, closed in 2006), Courtaulds chemicals (textile mill, closed in 1992), Cornwall Chemicals (which produced NaHS, HCl, CCl_4, and CS_2, closed in 1995) [Delongchamp et al., 2009, Richman and Dreier, 2001].

The reduction of the water flow along the Cornwall waterfront in the St. Lawrence River caused particulate matter to settle down in the depositional zones (Zones 1, 2 and 3) [Ridal et al., 2009; Biberhofer and Rukavina, 2002], which in return made these zones "Hg hotspots" [Ridal et al., 2009; Fathi, 2009]. Zone 1, the subject of this study, is characterized by a high spatial sediment heterogeneity characterized by large deposits of decaying bark and wood chips overlaid by fine-grained sediments with high concentrations of Hg [Biberhofer and Rukavina, 2002; Ridal et al., 2009]. The sediments are a composite of brown-black clayed mud with wood fibbers and oil patches resulting from the historical industrial contamination of the site [Ridal et al., 2009; Delongchamp et al., 2009; Biberhofer and Rukavina, 2002] and microbial decay. Microbial decomposition of the deposited wood fibbers from the Domtar pulp and paper mill has resulted in a high gas production (72% of the muddy deposit in this zone contains high gas content) [Biberhofer and Rukavina, 2002; Poissant et al., 2007]. It is also thought that gas production may cause sediment erosion and re-suspension in Zone 1, which in turn affects Hg bioavailability and distribution [Ridal et al., 2009; Fathi, 2009]. The increased bioavailability of Hg in zone 1 might therefore be an explanation for the elevated MeHg concentrations in Zone 1, as suggested by Razavi (2008). Zone 1 is composed of one site with high levels of deposited

wood fibbers (HWF, 18° 521′298″ E, 49°84′ 357″ N), and an adjacent site with a lower level of wood fibbers (LWF, 18°521′205″ E, 49° 84′295″ N) [Fathi, 2009; Razavi, 2008], the first one (HWF) being the focus of this study. The high sediment content of inorganic Hg and wood fibres and high gas evolution from the sediments make the Zone 1 HWF site a "hot spot" for Hg methylation. The increased supply and availability of nutrients, carbon sources and electrons acceptors, as well as bioavailable inorganic Hg to the methylating microbes by re-suspension of sediments due to gas bubbling in the sediment–water interface, might enhance the methylation potential of this zone, which in turn maintains a high %MeHg in sediments. Re-suspension may indirectly affect methylation rates in sediments by inducing a positive change in redox conditions (which allows dissolved oxygen to enter the sediments) and supplying nutrients and electrons acceptors that increase microbial activity. Heyes et al. (2004) and Kim et al. (2004) confirmed that methylation was increased by the secondary effect of re-suspension (i.e., decreasing sulfides levels). Moreover, Kim et al. (2006) observed a negative relationship between acid volatile species (AVS) and $Me^{199}Hg$ after re-suspension of anoxic sediments and concluded that that re-suspension can alter the association of Hg with binding phases.

4.2.2. Sample Collection

Surface water and sediment samples were collected from the Zone 1 of the St. Lawrence River in Cornwall, Ontario, Canada, in June, July, and August 2007. Surface sediments from Zone 1 were sampled using plastic tubes (10 cm in diameter and 1 m in length), sealed on site (to prevent oxygen contact) and kept cold during handling. The cores were taken at the same location (within a 1m X 1m area), sliced (0-5 cm) in the field and transferred into in 3-5 L pre-acid washed high density polyethylene (HDPE) bottles under nitrogen, in order to prevent contact with oxygen, and kept cold during their transport to the laboratory.

In the laboratory, the pooled sediments were homogenized and sediment sub-samples were transferred into sterile 500 mL brown HDPE bottles under nitrogen atmosphere and used for the microcosm incubations with enriched Hg isotopes and microbial inhibitors. The time lag between the sampling and the start of incubation was 24-

48 h (but it was 5 days for the June preliminary experiment due to the gamma radiation procedure), during which the samples were stored in the dark at 4^0C. Sub-samples were transferred under nitrogen atmosphere to centrifuge tubes and used for geochemical parameter analyses, microbial analyses, and total Hg (THg) and MeHg analyses.

Surface water from above the sediment-water interface was also sampled and collected in acid pre-washed high density polyethylene (HDPE) bottles. *In situ* pH and Eh measurements were performed for the July samples using a VWR portable pH meter with a VWR pH probe and Corning redox probe. Correction with respect to the hydrogen reference electrode was performed for each reading. Water conductivity was measured on site with a VWR conductivity and a YSI 54 oxygen meters. Samples were kept refrigerated and analyzed for sulfate, nitrate, and total phosphorus within two-three weeks of sampling.

4.2.3. Sample Analysis

Two categories of samples were analyzed: (a) water and sediment samples preserved in the field and (b) sediments and porewater samples taken from the microcosm incubation experiments designed to determine the potential Hg methylation and MeHg demethylation rates. Analyses performed on the samples preserved in the field included sediment THg, MeHg, water and organic carbon content (as loss on ignition (LOI)), porewater sulfate, sulfide, Fe^{2+} and Fe^{3+}. The analytical measurements associated with the samples originating from the microcosm incubations included sediment THg and MeHg isotopic analyses, sulfate reduction rate (SRR), iron reduction rates (FeRR), methane production rate (MPR), solid phase iron, water and organic carbon content (as LOI), pH and Eh, as well as pore water sulfate, sulfide, ferrous iron (Fe^{2+}), and ferric iron (Fe^{3+}). The pore water samples from the incubation experiment were extracted by centrifugation at 5000 rpm for 20 min, immediately transferred to a clean syringe, and filtered through 0.2μm syringe filters. All porewater analyses (i.e. Fe^{2+}, Fe^{3+}, sulfates, sulfides) were conducted during the day of sampling.

The total Hg and MeHg isotopic compositions were determined in the sediments from the incubation experiments, with the exception of the June 2007 experiment, where only total Hg and MeHg concentrations were measured. MeHg samples were analyzed in

duplicate, but for THg, only one replicate and only the initial samples (t=0h) were fully analyzed due to the high cost of the analyses. Total Hg and MeHg concentrations in all sediment samples were measured as wet weight and normalized to dry weight based on the water content of the samples in order to avoid sample loss and alteration during the drying process.

Methylmercury isotope analysis of wet sediment samples for the July microcosm incubation experiments was conducted using the new Thiosulfate method (TSE) [Avramescu et al., 2010] and the distillation-aqueous-ethylation method [Hintelmann and Ogrinc, 2003], for method comparison, as described in Chapter 2 [Avramescu et al., 2010]. To correct for procedural recoveries, each sample was spiked with $Me^{201}Hg$ prior to digestion or distillation, respectively. The Hg isotopes measured were ^{202}Hg (to calculate ambient MeHg concentrations), ^{200}Hg (methylation spike), ^{199}Hg (demethylation spike) and ^{201}Hg (internal standard). Peak areas were used to calculate the concentrations of individual isotopes using a programmed Excel spreadsheet used in Dr. Hintelmann's laboratory, which accounts for procedural blanks and the purity of the isotopes, as described in Hintelmann and Ogrinc (2003). Detailed description of the TSE method is given in Chapter 2, whereas the distillation-aqueous-ethylation method is described in Chapters 2 and 3, as well as their quality assurance.

The metabolic activity of methanogenic archaea (MPA) was determined by measuring the *in situ* methane production rates (MPR), using the headspace method adapted from [Koschorreck et al., 2000]. Immediately after adding the Hg spikes and inhibitors, 100mL sediment slurry was transferred in an anaerobic chamber into 125 ml serum glass bottles and sealed. The gas in the headspace was extracted at the same time as the aqueous sub-samples. After vigorous shaking (5 min.) and 30 minutes of headspace equilibration, 10 ml gas samples from the headspace were transferred into 12 ml vacutainers and analyzed using a SRI8610C Gas Chromatograph (with unheated splitless injector and a flame ionization detector (FID)). Sulfate reduction rates (SRR) were determined in triplicate for all microcosms (t=0h) according to Jørgensen (1978a) as described in Praharaj and Fortin (2004).

Details of the sediment analysis for total Hg and MeHg (isotopes and total) and their quality assurance, methods for the determination of DOC, DIC, sulfate, sulfide, Fe^{2+} and Fe^{3+} in porewater and methods for the determination of pH, Eh, water and organic carbon content (as loss on ignition (LOI)) in sediments, as well as of the metabolic activity of SRB (as SRR) and iron reducing microbes (FeRP) are described in Chapter 3. All chemical analyses run with reference to the method used are presented in Chapter 3, Table 3-1.

4.2.4. Hg Methylation - MeHg Demethylation Experiment Set-up

Environmental concentrations of MeHg reflect net methylation, which is the result of two simultaneous reactions: Hg methylation and MeHg degradation. Our experiments were designed to measure the rates of MeHg formation and demethylation and to assess the relative contribution of different types of anaerobic microbes involved in MeHg formation and demethylation, by combining the isotope enriched multilabeling technique [Hintelmann et al., 1995; 1997; 2000] with specific microbial inhibitors (SRB and MPA) following the experimental design described and validated in Chapter 3. In order to assess the relative contribution of different types of anaerobic microbes in methylmercury formation and demethylation, specific inhibitors of SRB (sodium molybdate, $NaMoO_4$) and MPA (sodium 2-bromoethane sulfonate, BES) were added prior to the addition of Hg enriched isotopes. There is no known inhibitor for iron reducing microbes (FeRP). The isotope enriched multilabeling technique (described in chapter 3 and the associated supporting information) using stable mercury-enriched isotopes allows us to determine the mercury species transformation rates (i.e., Hg methylation and MeHg demethylation rates).

The experimental set-up and the description of all microcosms incubated in June and July 2007 with sediment samples from the St. Lawrence River sediments (Cornwall, On) are presented in Tables 1 and 2, respectively. In the summer of 2007, three time series experiments were conducted with the St. Lawrence River sediments (Cornwall, On). The first experiment (June 2007) was a preliminary incubation experiment used to test the effect of ^{200}Hg isotope spike preparation (in Milli-Q water or porewater), the concentrations and efficiencies of microbial inhibitors used ($NaMoO_4$ and BES), and the use of gamma

radiation for sterilization of the sediments for the abiotic microcosm. Four microcosms in triplicate (three biotic and one abiotic) were incubated with ^{200}Hg spikes (in Milli-Q water or porewater) for 96h as described in Table 4-1. Results from the June 2007 experiment and tests are presented in the Support information of this chapter.

The second experiment (July 2007) was designed to test the two Hypotheses (H1 and H2). The whole experiment was identical to the one with the Mer Bleue sediments, with the difference that autoclaved abiotic microcosms were incubated along with five biotic ones (in triplicate) with 200Hg and Me199Hg spikes and microbial inhibitors for 96h. The description of the microcosms is given in Table 4-1.

Microcosms containing the St. Lawrence River sediment slurry (0-5cm) inoculated with stable mercury-enriched isotopes and treated with specific microbial inhibitors were incubated in dark HDPE bottles (cca. 500 g of homogenized sediments per replicate) at room temperature in an anaerobic chamber for 96h. Sub-samples were removed from replicate systems at regular time intervals (0, 24, 48, 72, 96 h) to measure the amount of $Me^{200}Hg$ produced and the amount of $Me^{199}Hg$ removed [Hintelmann et al., 1997; Martin-Doimeadios et al., 2004]. Temperature, pH, Eh, water and organic matter content (LOI), along with sulfate reduction rates (SRR) and methane production rates (MPR) were determined on separate sub-samples. The pore water was extracted immediately after sampling; subsequent analyses of Fe^{2+}, Fe^{3+}, sulfates, sulfides were conducted within minutes after the extraction in the anaerobic chamber, and sub-samples for Hg isotopic analyses were acidified and kept frozen until analysis. Sulfate reduction rates (SRR) were determined in parallel in triplicates for all microcosms (t=0) according to Jørgensen (1978). Methane production rates (MPR) were also determined in parallel in triplicate and/or duplicate for all microcosms using a modified method after Koschorreck et al. (2000).

The mercury species were enriched with $^{200}Hg^{+}$ and $Me^{199}Hg^{+}$. Stock solutions of 706 $\mu g\ mL^{-1}$ of $Me^{199}HgCl$ in 2-propanol and 911 $\mu g\ mL^{-1}$ $^{200}Hg^{2+}$ in 10% nitric acid were diluted appropriately on the day of spiking, using anoxic overlaying water from the sampling site, and their concentration was checked by GC-ICP-MS (Platform-ICP-MS, Micromass Ltd, Manchester, UK, [Hintelmann and Ogrnic 2003]) at Trent University,

Peterborough, Ontario, Canada. The added tracers were equilibrated in overlaying water for two hours before being added to the incubation bottles in order to achieve the same speciation as the ambient Hg(II) [Hintelmann et al., 2000; Drott et al., 2008b]. The additions of isotope enriched spikes of $^{200}Hg^{2+}$ and $Me^{199}Hg^{+}$ gave final incubation slurry concentrations of cca 77.7 ng g^{-1} ^{200}Hg and 4.7 ng g^{-1} $Me^{199}Hg$, respectively, for the July 2007 experiment. Details of the Hg spikes additions are given in Table 4-1. Isotope-enriched $^{200}Hg(NO_3)_2$ and $Me^{199}HgCl$ were kindly provided by Dr. Hintelmann (Trent University). $Me^{199}HgCl$ was prepared at Trent University from enriched ^{199}HgO.

Naturally occurring SRB activity was inhibited by treating the sediment slurries with 2 mL of 250 mM sodium molybdate ($NaMoO_4$) [Chen et al., 1996; Pak and Bartha, 1998] to a final concentration of cca 1.8 mM. This treatment also prevented FeS formation. FeS formation may lead to an underestimation of iron reduction rates if rates are determined from the increase of dissolved Fe(II) concentrations. The efficiency of $NaMoO_4$ to inhibit sulfate reduction was determined by comparison of SRR in triplicate subsamples (t=0h) from amended and not amended sediments. The molybdate concentration was chosen taking into account the results of the tests performed during the June 2007 experiments (presented in support information).

Naturally occurring methanogens were inhibited by treating the sediment slurries with 6.3mL of 2M of sodium 2-bromoethane sulfonate (BES, $BrCH_2CH_2SO_3Na$) [Compeau and Bartha, 1985; Balch and Wolfe, 1979] to a final concentration of cca 30 μM. The efficiency of BES as an inhibitor was later tested by measuring the headspace methane concentrations during all three experiments. The BES concentration was chosen based on the test results of the June 2007 experiments (presented in the Support Information along with the results of the June 2007 experiments).

4.2.5. Specific Potential Methylation Rate Constant Calculation

Pseudo-first order reactions were used to describe the potential methylation and demethylation rates following the procedure outlined in Hintelmann et al. (2000). The potential methylation and demethylation rates were calculated as specific potential methylation (Km) and demethylation (Kd) rate constants using the Equations 1-8 given in

Chapter 3. In addition, the methylation/demethylation (M/D) ratio, a measure of the relative importance of methylating and demethylating activities (which are useful to identify the potential conditions of accelerated methylmercury production [Ramlal et al., 1986]), was calculated using Equation 9 in Chapter 3.

4.2.6. Statistical Analyses

Simple linear regression was used to calculate FeRR for the different microcosms over a 72h incubation period, as well as relationships between the porewater characteristics and different MeHg isotope concentrations using the S-Plus 8.0 software for Windows [Morin and Findlay, 2006; Otto, 2007; Zar, 2006]. Student t-test was performed to assess if the differences between the SRR and FeRR were significant. The XLfit software was also used to determine ambient Km and Kd values by curve fitting the ambient MeHg data (202 isotope).

4.3. Results and Discussion

4.3.1. Field Data Results

The physico-chemical characteristics of the Zone 1 St. Lawrence River sampling site are presented in Figure 4-1. The river water (i.e., water above the sediment water interface) is slightly alkaline (pH = 8.11) and soft (conductivity = 280 $\mu S\ cm^{-1}$) and contains low levels of sulfate (25.63±1.01 mg L^{-1}, n=4), nitrate (0.22±0.04 $\mu gN\ L^{-1}$, n=4) and total phosphorous (38.6 $\mu gP\ L^{-1}$, n=2). The pH of the pore waters slightly decreases with sediment depth from 7.35 to 6.97 (0 – 15cm), whereas there is a sharp redox change at the sediment water interface. Pore waters (n=4) contain low levels of sulfate (20.63±4.5 μM), sulfide (1.54±0.32 μM), ferrous iron (14.49±3.21 μM) and ferric iron (4.34±2.81 μM).The surface sediments (0-5 cm, n=3) have a density of 1.19±0.01 g cm^{-3} and a porosity of 0.83±0.02 g cm^{-3}, contain on average ~9.8±0.4% of organic carbon (as LOI) and have a moisture content of 69.7±1.5%. Total mercury (THg) and methylmercury concentrations of the sediments vary between 807-1790 ng g^{-1} and 255–521 ng g^{-1} (n= 10), respectively. Our results are in agreement with previous geochemical studies of the St.

Lawrence River [Canario et al., 2009; Ridal et al., 2009; Fathi, 2009; Razavi, 2008; Delongchamp et al., 2009].

4.3.2. Hg Methylation – MeHg Demethylation: The July 2007 Experiment

The porewater characteristics, along with the sulfate- and iron reduction rates and methane production rates in the six systems tested (i.e., N1, T1, T2, T3, T4, and A1 as shown in Table 4-1) are presented in Figures 2 and 3. The statistics for the FeRR and MPR calculation by linear regression are shown in Table S4-2 (Supporting information). The statistical comparison test results for SRR, FeRR, and MPA among microcosms are presented in Table S4-3 (Supporting information). Geochemical analyses are presented as an average of the three replicates (±SD), although only two replicates were analyzed for the mercury isotopes due to the high cost of the isotope analyses. The saturation indices obtained with Phreeqci-2.15.0 are presented in Table S4-4 (Supporting information).

4.3.2.1. Aqueous Geochemistry of the Various Microcosms

The density and porosity of the pooled sediment slurries (n=18, three replicates per microcosm) used for the batch systems were 1.17 ± 0.03 g cm^{-3} and 0.84 ± 0.03g cm^{-3}, respectively, and the moisture and organic content were 71.04 ± 2.00% and 8.36 ± 0.61%, respectively.

In all biotic systems (n=5), the pH slightly increased from 6.9 ± 0.03 to7.0 ± 0.02 over the first 24h and remained constant thereafter, while the redox potential slightly declined over time (i.e. -199 ± 7 mV to -254 ± 4 mV), indicating the development of more reducing conditions in the systems (Figure 4-2a, 4-2b). In contrast, the abiotic microcosms (A1) exhibited different values when compared with the biotic microcosms. In the abiotic microcosms, the initial Eh was 40mV, which indicated slightly oxic conditions in the sediments as a result of sterilization (autoclaving), but the redox potential decreased to -218 mV after the 96h incubation period. The pH remained fairly stable (from 6.9 to 6.7) over the 96h incubation period.

The DIC concentration did not vary much for the N1 and T1 microcosms, but decreased in all systems treated with microbial inhibitors (T2, T3, and T4) by 16%, 25%,

and 60%, respectively (Figure 4-2d). In contrast, the DOC concentration decreased in 46h in all treatments (i.e. by 8-9% in N1, T2 and by 29-37% in T1, T4, and A1 microcosms), with the exception of T3 as illustrated in Figure 4-2c. The DOC values were higher in the microcosms treated with BES as well as in the autoclaved ones.

Sulfide concentrations (Figure 4-2e) slightly increased throughout the experiment in the N1 (from 0.30 to 0.45 μM) and T1 (from 0.29 to 0.71 μM) microcosms after an initial decrease over 24h. The SRB inhibited microcosms (T2 and T4) behaved differently with higher initial sulfide concentrations of 9.53 μM (T2) and 8.97 μM (T4), which decreased slightly over time to 8.35 and 7.11 μM, respectively, consistent with the measured SRR (T3: 0.1 nmol cm^{-3} d^{-1}, and T4: 0.9 nmol cm^{-3} d^{-1}), thus indicating the complete inhibition (99-100%) of the sulfate reducing activity by sodium molybdate. In the abiotic system (A1), the concentration slightly increased over 46h from 0.65 to 0.74 μM, which was inconsistent with the 100% inhibition of SRB activity (SRR= 0.1 nmol cm^{-3} d^{-1}). It is likely that the production of sulfides in the abiotic microcosm was caused by the dissolution of pre-existing iron sulfide minerals, as shown by the saturation index calculations (see Supporting Information, Table S4-4).

Ferrous iron (Fe^{2+}) concentrations increased constantly throughout the experiment in all microcosms (Figure 4-2g), with the lowest increase in the N1 and T1 microcosms (from 0.01 to 1.32 and 2.17 μM, respectively) and the highest increase in the T4 microcosm (from 0.14 to 28.15 μM), followed by the abiotic (A1: from 0.32 to 18.50 μM) and T3 (from 0.09 to 14.53 μM) microcosms.

The relatively high SRR (61.9 ± 7.2 nmol cm^{-3} d^{-1}) of the natural N1 microcosm was determined with the ^{35}S incubation technique and indicated the existence of an active SRB population in the Zone 1 of the St. Lawrence River sediments. The SRR increased slightly in the T1 (68.4 ± 12.9 nmol cm^{-3} d^{-1}) and T3 (65.14 ± 13.1 nmol cm^{-3} d^{-1}) microcosms, which represented an increase of 11 and 5%, respectively, when compared with the natural system (N1). The increase in SRR in the T3 microcosm proved that the BES inhibitor of MPA activity did not affect the activity of SRB (Figure 4-3). The differences among the SRR values of the N1, T1 and T3 microcosms were not statistically

significant ($p > 0.05$, Table S4-3), whereas in the case of the T2, T4 and A1 microcosms, these differences were statistically significant due to the complete inhibition of SRB activity in the molybdate inhibited (99-100%) and abiotic microcosms (100%).

The iron reduction rates (FeRR) were calculated from the linear increase of Fe^{2+} over 46h hours for all treatments (Figure 4-3b), and the statistical results of the regression analysis are presented in Table S4-2 (Supporting information). The FeRR of the natural (N1) microcosm was low (0.7 ± 0.1 nmol cm^{-3} d^{-1}) but indicated that iron reducers were active in the sediments of Zone 1 of the St. Lawrence River. A slight FeRR increase of 1.7 and 2.6 times, respectively, was observed for the T1 (1.1 ± 0.2 nmol cm^{-3} d^{-1}) and T2 (1.8 ± 0.6 nmol cm^{-3} d^{-1}) microcosms, but the differences were not statistically significant ($p < 0.05$, Table S4-3). The highest rate (14.7 ± 1.9 nmol cm^{-3} d^{-1}) was determined in the T4 microcosm where both SRB and MPA were inhibited, followed by T3 (7.6 ± 1.4 nmol cm^{-3} d^{-1}) and A1 (9.4 ± 1.3 nmol cm^{-3} d^{-1}). No statistical significant difference (Table S4-3 Supporting information) was observed between the FeRR of the T3 and A1 microcosms, but the differences were statistically significant ($p<0.05$) between the FeRR of those microcosms (T3, T4, A1) and the others. In general, the FeRR was stimulated by the inhibition of the other two microbial groups (SRB and MPA) when compared with the T1 and natural (N1) systems, respectively (Figure 4-3). It is known that iron reducers and sulfate reducers often compete for the same electron donors under environmental conditions [Fortin and Praharaj, 2005; Kusel et al., 1999]. Saturation index calculations (Supporting Information Table S4-4) did show that the N1, A1, and T1 systems were undersaturated with respect to FeS and mackinawite throughout the course of the experiment, indicating that the iron reduction rates were likely not biased by the precipitation of iron sulfides in those treatments. In contrast, the microcosms treated with microbial inhibitors (T2, T3, and T4) were all saturated with respect to mackinawite after 24h incubation (although all but T2 became undersaturated again after 46h), and just T4 and T2 were saturated with respect to FeS (after 24h and 46h, respectively), indicating the FeRR might be underestimated for those microcosms (Figure 4-3b). However, the calculations indicated that the microcosms were saturated with respect to more stable iron

sulfides, such as pyrite. Their formation cannot be ascertained here because kinetics is not taken into account in the thermodynamics calculations.

The relatively high methane production rates (MPR) (N1: 72.6 ± 4.3 nmol cm^{-3} d^{-1}) indicated the existence of an active MPA population in the Zone 1 St. Lawrence River sediments (Figure 4-3). The methanogenic activity of the T1 (89.5 ± 7.2 nmol cm^{-3} d^{-1}) and T2 microcosms (76.3 ± 5.8 nmol cm^{-3} d^{-1}) (with active SRB and FeRP activity) increased (23 and 5%, respectively) in comparison with the N1 microcosm, but the difference was not statistically significant (Table S4-3). In comparison, in the two systems (T3 and T4) treated with BES, the methanogenic activity was reduced with cca 90% (10 ± 0.3 nmol cm^{-3} d^{-1} and 9.2 ± 1.2 nmol cm^{-3} d^{-1}, respectively). Methane production was 100% inhibited in the abiotic microcosm (0.04 nmol cm^{-3} d^{-1}). The MPR differences between the inhibited (T3 and T4) and abiotic (A1) microcosms on one hand and the other microcosms on the other hand were statistically significant (Table S4-3, Supporting information).

In summary, all systems developed anoxic conditions during the course of the experiment, which represented suitable conditions for either iron or sulfate reduction, as well as for methanogenesis, as demonstrated by the measured iron-, sulfate reduction, and methane production rates. In addition, SRR values reported here are similar to those measured in aquatic environments, such as lake sediments (50-600 nmol cm^{-3} d^{-1}, [Ingvorsen et al., 1981; Meyer et al., 2000; Gough et al., 2008]). Regarding the calculated FeRR for the various microcosms, the values are in agreement with those reported for lake sediments (<0.1 μmol g^{-1} d^{-1}, [Blodau et al., 2002; 9.6-69.3 μmol g^{-1} d^{-1} , Wendt-Potthoff et al., 2002]). The results obtained for the St-Lawrence River sediments are in agreement with those of Mer Bleue (Chapter 3) in terms of the efficiency of the microbial inhibitors. Furthermore, the measurement of methane production in this experiment confirms the inhibition efficiency of BES.

Zone 1 of the St. Lawrence River near Cornwall (Zone 1 SLR) is known to be an ebullition site releasing many gases (i.e. CO_2, CO, H_2, methane) from the sediments to the water column and atmosphere [Canario et al., 2009; Poisson et al., 2007; Razavi, 2008]. Beside from being a significant mechanism for the release of gases from sediments to water

and atmosphere, ebullition is also involved in the recycling of nutrients and contaminants [Canario et al., 2009]. Measurements performed at the St. Lawrence River near Cornwall by Poissant and co-workers (2007) showed that the fluxes of gases released from the sediments were a mixture of CO_2, CO, H_2 and methane varying between 0.001 $\mu g\ m^{-2}\ h^{-1}$ (H_2) and 3.5 $mg\ m^{-2}\ h^{-1}$ (CH_4). Moreover, recent work of Razavi (2008) showed that the Zone 1 SLR bubbling rates ranged from < 1 to ~ 2800 $ml\ m^{-2}\ d^{-1}$ (< 4.9 to ~168.6 $mg\ m^{-2}\ h^{-1}$) and that the methane content in the gas ranged from 29 to 84% over their sampling season. The same authors showed that there were no significant differences among the sampling months, in either bubbling rates or mean CH_4 % in gas, though an apparent increase from July to September was observed. Those values translate in a range of methane production rates from <31 to 1054 $nmol\ cm^{-3}\ d^{-1}$ (assuming that 1g ww = 1ml = $1cm^3$) in the SLR Zone 1, which is comparable to the range the MPR range determined in the different microcosms (i.e., N1: 72.6 $nmol\ cm^{-3}\ d^{-1}$).

4.3.2.2. Isotope Enriched Hg Analysis Results

The analysis of the isotope enriched THg and MeHg in two replicate sets of the triplicate sediment samples was conducted at the University of Ottawa and Trent University using the methods described previously.

The minimum amount of isotope spikes was determined by backward calculation considering the initial THg and MeHg contents of the tested sediments and the detection limit for the isotope MeHg (approx. 1% of the ambient MeHg). The isotope enriched Hg spikes ($^{200}Hg^{2+}$ and $Me^{199}Hg^{+}$) used in this study were sufficient, i.e., the generated $Me^{200}Hg$ and the remaining $Me^{202}Hg$ (after demethylation) were greater than or at least equal to 1% of the ambient MeHg. However, the spike additions did increase the concentrations of total Hg and methylmercury by a factor of 1:1.1 and 2.7:3.5, respectively, when compared to the background ambient concentrations. Moreover, the addition of the isotope enriched spikes increased the % MeHg to THg from 0.2-0.3% to 0.4-0.9% (Table 4-3). The ambient background concentrations of the St-Lawrence sediments used for the incubation experiments along with the concentrations after the isotope addition are shown in Table 4-3.

Changes in the relative abundance of the 202 isotope followed the evolution of natural mercury (ambient), those of the 200 isotope followed the evolution of spiked enriched inorganic mercury (methylation), whereas changes of the 199 isotope followed the evolution of the spiked enriched methylmercury (demethylation) (Figure 4-4). The amounts of methylated mercury derived from the inorganic ^{200}Hg spike and demethylated mercury derived from the $Me^{199}Hg$ spike were calculated using Equations 3 and 6, respectively, (in Chapter 3). The trend of MeHg produced from the isotope enriched mercury spikes (^{200}Hg and $Me^{199}Hg$) along with the ambient MeHg trend during the 96h incubation time are presented in Figure 4-4. The microcosms however behaved differently with respect to the 199, 200, and 202 isotopes. A slight linear increase over 96h was observed for the $Me^{202}Hg$ concentrations (Figure 4-4a) in all microcosms, with T3 (r2 = 0.97) having the highest increase, followed by T1 (r2 = 0.88) and N1 (r2 = 0.68). No increase was observed in the T2, T4 and A1 microcosms (r2 = 0.54, 0.48, and 0.35, respectively). In contrast, the $Me^{200}Hg$ produced from the inorganic mercury spike had a linear increase for the first 46h in all treatments, after which steady state levels were achieved in all microcosms (Figure 4-4b), which is in agreement with the results obtained for Mer Bleue (Chapter 3). The observed decrease in MeHg production (equilibrium or steady state developed after 46 hour) was possible because demethylation may have slowed down the net increase in MeHg once sufficient MeHg was produced. Similar to Mer Bleue, the T3 and T1 microcosms showed the highest methylmercury increase (ng g^{-1}dw) of methylation tracer (200 isotope) with T1 also having the highest methylmercury decrease of the demethylation tracer (199 isotope), which might explain why the equilibrium was reached after 46h in the T1 system. In contrast to Mer Bleue, the T3 microcosm had the lowest MeHg (199 isotope) values among the Hg spiked microcosms (Figure 4-4c). The 199 isotope (demethylation tracer) results showed a linear decrease for 96h in the T1 and T2 microcosms, but almost no change was observed for the MPA inhibited (T3 and T4) and abiotic (A1) microcosms. In general, for all microcosms, the demethylation of $Me^{199}Hg$ took place very quickly with a linear decrease over the 96 hour incubation period. The similar trend observed for the 200 and 202 (ambient) isotopes during the incubation suggests that, similar to Mer Bleue, methylation of ambient mercury (202) and isotope enriched tracer (200) followed the same pathway. However, the different order of magnitude might be due to the different

availability of the two isotopes (ambient and tracer). A small increase of MeHg was observed in the natural microcosm (N1) suggesting that the addition of the spikes also increased the availability of ambient Hg for methylation in the spiked microcosms [Hintelmann et al., 2000; Drott et al., 2008a,b].

The total percentages of mercury methylated and methylmercury demethylated (46 and 96 h incubation) from the tracer spikes in the different microcosms are presented in Table 4-4. The highest methylation percentage was observed in the microcosms where MPA were inhibited (T3), followed closely by the T1 microcosm (Table 4-4). This trend was observed not only for the methylation (^{200}Hg) tracer (i.e 11.27 % T3 and 9.56 % T1), but also for the ambient (202) isotope (i.e. 0.51 % T3 and 0.44% T1), proving once again that the ambient (202 isotope) mercury and the methylation tracer (200 isotope) followed the same path despite of the availability differences between tracer and native Hg with methylation being a dominant process for the native Hg. Moreover, the elimination of the competition for organic substrate through the inhibition of methanogens, which favored the SRB and other microorganisms, might explain why the methylation percentage was slightly higher in the T3 microcosm than in T1. Regarding the demethylation potential (199 isotope), the T1 microcosm had a higher demethylation percent (40.41 %) than T3 (6.75%), which is in agreement with the cca 90% MPA inhibition (MPR = 10 nmol cm^{-3} d^{-1}) in the T3 assays.

With respect to the microcosms (T2 and T4) containing the SRB inhibitor, both systems had comparable methylating potential (2.56 % and 2.14 %, respectively), but very different demethylating potentials (96h) with T2, having the highest demethylation percentage (44.4 %) and the T4 microcosm, the lowest among all microcosms. This is in agreement with the microbial activity, MPA activity being was enhanced in the T2 microcosms (MPR = 76.3 nmol cm^{-3} d^{-1}) where SRB are inhibited, but it slowed down (90%) in the T4 microcosms (MPR = 9.2 nmol cm^{-3} d^{-1}) where BES inhibitor was applied along with molybdate. Moreover, the addition of BES (MPA inhibitor) stimulated not only the methylation of the 200 isotope tracer but also the methylation of ambient Hg in the T3 microcosm (0.51%), in contrast with the addition of sodium molybdate (SRB inhibitor), which inhibited the methylation of both the methylation tracer (200 isotope) and ambient

(202 isotope) mercury in the T2 (0.28%) and T4 (0.28%) microcosms (Table 4-4 and Figure 4-4). The decrease of the demethylation capacity by inhibition of MPA supports the importance of methanogens in MeHg demethylation in aquatic sediments, but the involvement of SRB in demethylation cannot be ruled out since the T4 microcosm had the lowest demethylation percent beside the abiotic microcosms (A1). Methanogens, as well as SRB, can use C1 organic compounds (i.e. MeHg) as carbon sources and they are involved in oxidative demethylation in anoxic sediments [Oremland et al., 1995; Marvin-Dipasquale and Oremland, 1998; Marvin-Dipasquale et al., 2000]. The methylation potentials for all isotopes (199, 200, 202) were highly decreased (the lowest values) in the abiotic (A1) microcosms (Table 4-5) showing that abiotic processes might have the lowest contribution to net MeHg production in those systems. In conclusion, the percentage of $Me^{200}Hg$ produced and $Me^{199}Hg$ demethylated varied with the type of microbes inhibited (Table 4-4). The values reported here are however in agreement with those reported by Hintelmann et al. (2000), i.e., ~ 40% demethylation.

4.3.2.3. Potential Rates of Methylation and Demethylation

Mercury methylation and methylmercury demethylation rates (pmol g^{-1} h^{-1}) along with the specific transformation rates calculated for the 46h incubation period with the isotope enriched tracers ($^{200}Hg^{2+}$ and $Me^{199}Hg^{+}$) are presented in Table 4-6.

The process of $^{200}Hg^{2+}$ methylation varied with the type of microbes inhibited, i.e., the highest calculated rate (among inhibited assays) was in the microcosms where methanogenesis was inhibited (T3: 0.72 pmol g^{-1} h^{-1}) and the lowest in the microcosm where both SRB and MPA were inhibited (T4: 0.12 pmol g^{-1} h^{-1}). No methylation of the 200 isotope was observed in the abiotic (A1) microcosms (Table 4-6). The specific methylation rate, calculated as the proportion of added isotope enriched tracers methylated or demethylated, was the highest in the T3-MPA inhibited microcosm, followed by the T1 microcosm. The SRB inhibited microcosms (T2 and T4) had rates four times lower than the other ones. In contrast, the specific demethylation rate ($Me^{199}Hg$) was the highest for the T2 – SRB inhibited microcosm followed by the T1 microcosm. The MPA inhibited microcosms had the lowest specific demethylation rates among all microcosms, which were in agreement with the methylation rates, i.e. higher methylation and lower

demethylation due to the inhibition of MPA. Moreover, the addition of inhibitors influenced not only the methylation and demethylation of the tracers in the four microcosms, but also the evolution of native MeHg. The rates were doubled in the T1 and T3 assays in comparison with the SRB inhibited (T2 and T4) and abiotic (A1) microcosms.

Ramlal et al. (1986) suggested that the methylation/demethylation (M/D) ratios (see Chapter 3 for description) were a good indicator of how environmental perturbations affected the net rate of mercury methylation and hence, MeHg concentrations in aquatic environments. The M/D ratios are a direct measure of the relative balance of methylating or demethylating activity in a specific system. Based on the M/D ratios showed in Table 4-6, we can conclude that all microcosms, with the exception of T3, favoured demethylation over methylation and the degree of magnitude of the ratios indicates that they varied with the type of active microbes. We observed that the inhibition of SRB (T2) alone largely decreased the M/D ratio due to the increase of the demethylation rate (44%), but also due to the decrease of the methylation one (63%). In contrast, the inhibition of MPA (T3) alone increased the M/D ratio by increasing the methylation rate (21%) and decreasing the demethylation one (22%). Moreover, the inhibition of both microbial groups (T4) changed the M/D ratios by reducing the magnitude of both processes (80% M and 64% D, respectively). These findings suggest that, similar to Mer Bleue, sulfate-reducers and methanogens play an important role in net MeHg formation and the inhibition of MPA stimulates net methylation not only by inhibition of demethylation but also by stimulation of methylation (see M/D ratios), along with the stimulation of the SRB activity. In addition, FeRR might be an important process in the production of MeHg in aquatic environments when SRB and MPA are not active since both processes were reduced, but not stopped, in the T4 microcosm (M/D ratio was 1.5 times lower than the one in T1). The M/D ratios in the abiotic microcosm indicate that no methylation took place.

The M/D ratios show that the activity of MPA is important for the demethylation process. For methylation, other processes, such as FeRP activity should be considered, beside SRB activity. The inhibition of both SRB and MPA (T4) enhanced the activity of iron reducing prokariots(FeRP) as demonstrated by the increase of FeRR in the inhibited microcosms with the highest rate in the T4 microcosm (Figure 4-3). It is known that iron

can affect mercury methylation by either altering the availability of Hg [Warner et al., 2003; Mehrotra et al., 2005] or enhancing the activity of FeRP with respect to other microorganisms, particularly SRB [Flemming et al., 2006; Kerin et al., 2006; Warner et al., 2003]. Hg methylation by FeRP may be important in sediments and soils where these organisms are dominant, e.g., iron-rich freshwater sediments [Fleming et al., 2006] and iron-rich sediments with low concentrations of sulfate [Kerin et al., 2006]. Moreover, Oremland et al. (1995) detected substantial oxidative demethylation at a site where sulfate reduction and methanogenesis rates were low, and suggested that other respiratory anaerobes (e.g., denitrifiers and Fe^{3+} and Mn^{4+} reducers) may also carry out oxidative demethylation, which can be an explanation for the higher demethylation rate measured in the T4 (SRB and MPA inhibited) microcosm when compared with the T2 microcosm.

4.3.2.4. Specific Methylation and Demethylation Rate Constants

In order to verify whether the methylation or demethylation rates were dependent on the amount of tracers added, as previously suggested by Hintelmann et al. (1995; 2000), we calculated the rate constants (Km and Kd), which by definition are independent of the amount spiked. The potential rate constants calculated from isotope enriched tracer trends over 46h (96 h for Kd due to linearity) are presented in Table 4-6 along with data from other studies.

Potential methylation rate constants (Km) differed significantly among microcosms, the MPA inhibited microcosm (T3) had the highest rate constant (0.016 d^{-1}), followed by the T1 microcosm (0.015 d^{-1}). The SRB inhibited microcosms had comparable specific methylation rate constants (T2: 0.003 d^{-1} and T4: 0.002 d^{-1}). The abiotic (A1) microcosm Km was almost zero (0.0001 d^{-1}). The trends observed for Km values in all microcosms are in agreement with the calculated potential methylation rates (M) presented in Table 4-5. In contrast with methylation, demethylation evolved linearly for 96h, and the Kd values were calculated for the whole period. With respect to the demethylation rate constants, the highest value (1.7 d^{-1}) was in the T2-SRB inhibited microcosm followed by the T1 microcosm (1.4 d^{-1}). Both MPA inhibited microcosms (T3 and T4) had similar low Kd rates (0.3 d^{-1} and 0.2 d^{-1}), which is in agreement with the high degree of inhibition of

methanogenesis (90% comparing with T1). The Kd values are in agreement with the Km values and also with the potential methylation rates (D) presented in Table 4-5.

Our results therefore indicate the importance of SRB in Hg methylation in freshwater systems, as reported in other studies [Compeau and Bartha, 1985; King et al., 2000; 2001; 2002; Fleming et al., 2006; Oremland et al., 1995]. For instance, Matilainen et al. (1995) observed that molybdate inhibited methylation in sediments from four lakes in Finland, and suggested that acetate-utilizing SRB were the main methylators under sulfate limiting conditions. In addition, in anoxic estuarine sediments, inhibition of methanogenesis stimulated the SRB activity and Hg methylation when sulfate was limiting [Compeau and Bartha, 1985]. Finally, Lovely and Klug (1983) showed that SRB were able to outcompete methanogens even in sulfate limited freshwater sediments.

The ambient rate constants Km and Kd were obtained by fitting the experimental data ($Me^{199}Hg$) to the curve derived from Equation 8 in Chapter 3 [Hintelmann et al., 2000]. The XLfit software was used o fit the curve and the results are presented in Table S4-5. The ambient MeHg concentrations in the microcosms were predicted by applying the calculated ambient rate constants (Table 4-7). In other tracer studies [Hintemann et al., 2000], discrepancies observed between the predicted and measured ambient MeHg concentrations (possibly due to differences in Km, Kd values being similar) were considered as an indication that the tracers were more bioavailable than the ambient mercury. As shown in Table 4-7, a relatively good agreement was obtained between the predicted and measured values of ambient methylmercury (202 isotope). In contrast, if we consider the fraction of Hg present as MeHg, the values were slightly higher for the tracer isotope (199 isotope: 0.24 – 0.50%) when compared to ambient Hg (202 isotope: 0.13 – 0.25%), and this supports the fact that the tracers were more available than the native Hg.

The demethylation rate constants translated into a relatively long half-life ($t_{½}$) of the native MeHg in sediments (i.e., 8.3 d^{-1}), higher than those for Mer Bleue or observed in other studies [Hintelmann et al., 2000; (1.8 d^{-1})], which indicated that the native MeHg had a longer residence time in the SLR sediments. The half-life of the added tracers varied from 0.4 and 0.5 d^{-1} in the T2 (SRB inhibited) and T1 microcosms, respectively, to 2.6 and 3.0 d^{-}

^{1} in the MPA inhibited microcosms (T3 and T4). In the abiotic microcosm, the half-life was 25.5 d^{-1}, which indicated that the abiotic process contributed less to the net methylation. As indicated by the half-life values, the added MeHg isotope (199: 0.5 d^{-1} in T1) was more available for demethylation than the ambient one (202: 8.3 d^{-1} in T1). The half-life values indicate that the native MeHg had a longer residence time and was more available for bioaccumulation. We also observed that for the St. Lawrence River system, the inhibition of MPA increased the residence time of MeHg in the sediments, which in turn might have increased the availability of MeHg for bioaccumulation. In contrast, the inhibition of SRB decreased the residence time of MeHg in sediments by increasing methanogenic activity and consequently, demethylation, thus reducing the availability of MeHg for bioaccumulation. Considering the decrease in demethylation rate constants in MPA inhibited microcosms (T3, T4) when compared to T1, we can conclude that oxidative demethylation (OD) may be an important pathway for MeHg demethylation in the SLR sediments. Given the long history of contamination of the investigated SLR sediments, we cannot ignore the importance of reductive demethylation (RD) by *mer* operon. In anaerobic sediment settings, the prevalence of either RD or OD is important, influencing the MeHg production especially in Hg-contaminated sediments since the mer operon process results in a net removal of Hg from the sediments (as Hg^{0}), whereas OD, with its end product (Hg^{2+}), may fuel re-methylation within the sediments [Barkay 2003]. Moreover, the methylation-demethylation cycle may exist in environments lacking the mer-mediated process [Barkay, 2003; Schaefer et al., 2002; Robinson and Tuovinen, 1984] and oxidative demethylation, mediated by anaerobic microbes, may prevail at lower Hg concentrations in anaerobic environments [Marvin-Dipasquale et al., 2000; Marvin-Dipasquale and Oremland, 1998; Oremland et al., 1991; 1995]. Whether the mer-mediated demethylation takes place at the same time in SLR sediments has yet to be determined.

The mer detoxification is extensive in aquatic environments, being induced at lower Hg^{2+} and oxygen concentrations (aerobic and facultative mercury resistant microbes). MeHg can be degraded reductively by *mer* operon fu nctions to CH_4 and elemental Hg^{0}, in contrast to OD, which degrades MeHg to CO_2, along with a small amount of CH_4 and ionic Hg^{2+}.

4.3.2.5. Relationship between the Rate Constants, SRR, FeRR, MPR, % MeHg and Porewater Geochemistry

We evaluated the relationship between the rate constants (Km and Kd) calculated under laboratory conditions and the percentage of MeHg (100*[MeHg]/[THg]) in sediments, sulfate reduction rates (SRR), methane production rates (MPR) and iron reduction rates (FeRR), as well as the pore water characteristics. Figure 4-5 presents the relationship between Km or Kd and the percentage of MeHg, SRR, and FeRR.

A strong positive relationship was observed between Kd and % MeHg ($r^2 = 0.66$), but not between Km and % MeHg ($r^2 = 0.10$). Therefore, our results (based on Figure 4-5a) indicate that the magnitude of Kd decreases with the increasing of % MeHg in sediments, limiting the detoxification mechanisms (which can be an indication of reductive demethylation by *mer* AB taking place in the SLR sediments). Our results are in agreement with the findings of Drott and co-workers (2008a), who reported positive significant correlations ($r^2 = 0.40$) between Kd and ambient concentrations of MeHg in surface sediments in Finland. Moreover, the authors reported positive significant correlation ($r^2 = 0.67 - 0.88$) between Km and % MeHg in some of the surface sediments investigated. The authors suggested that Km rates reflected a short term MeHg production, whereas % MeHg was an indication of the normalized long-term production of MeHg. They also found that Km can be used to estimate long-term MeHg production in the contaminated freshwater systems investigated. In marine surface sediments, Hammerschmit and Fitzgerald (2006) also reported a positive relationship between Km and the ratio [MeHg] to [Hg^{2+}], whereas Sunderland et al. (2004) concluded that % MeHg could be used to approximate the rate of methylation in estuarine sediments. In contrast to the published studies mentioned above, the absence of relationship in our case might be related to the fact that our data (i.e., Figure 4-5a) represent five microcosms, each equivalent to a different system (with different microbial activity), which are likely different from the ones reported in other studies [Drott et al., 2008a; b; Hammerschmit and Fitzgerald, 2006]. Also, the high variability of the SLR sediments with respect to THg can alter the relationship in our study.

Figure 4-5b shows that Km ($r^2 = 0.98$), but not Kd ($r^2 = 0.08$), is positively correlated with SRR (i.e. the higher the SRR, the higher the Km values), which indicates

that SRB are involved in Hg methylation, but may not be implicated in MeHg demethylation in SLR sediments. An inverse relationship was observed with MPR, with Kd (r^2 = 0.68) being positively correlated with MPR but not Km (r^2 = 0.11), showing that in contrast with SRB, methanogens are involved in MeHg demethylation in the Zone 1 SLR sediments (Fig 5c). As in the case of Mer Bleue, FeRR are negatively correlated with Km (r2=0.19) and Kd (r^2 = 0.60) (Figure 4-5d). The increase in FeRR therefore corresponds to a decrease in demethylation showing that the iron reduction may influence net methylation in the Zone 1 SLR sediments by decreasing demethylation rather than favouring methylation in the long term. This fact is supported by the negative relationship obtained between the porewater Fe^{2+} and Fe^{3+} and MeHg (199 isotope) concentrations (r^2 = 0.26 - 0.88) in the T1 and T3 microcosms; however the relationships are only significant ($p<0.05$, df=4) for T1 microcosm (Table S4-6). In addition, a positive relationship was obtained between the porewater Fe^{2+} and Fe^{3+} and MeHg (200 isotope) concentrations (Fe^{2+}: r^2 = 0.54-0.69; Fe^{3+}: r^2 = 0.53-0.64), as well as for the relationship with MeHg (202 isotope) (r^2: 0.53-0.66) in the T1 and T4 microcosms, but the statistical significance differed (Table S4-6). In contrast with Mer Bleue, no relationship (Table S4-6) was observed between the MeHg isotopes and Eh for all microcosms, except for the T3 (200 isotope: r^2=0.85; 202 isotope: r^2=0.82). However, higher variability was observed in the relationship between the 202 isotope and dissolved iron (Fe^{2+}) (r^2 = 0.38 – 0.96). The relationship between porewater sulfate and MeHg isotopes concentrations was highly variable (Table S4-6) with a strong positive relationship for T3 (200 isotope: r^2=0.88; 202 isotope: r^2=0.92) microcosms and a strong negative relationship for the A1 (200 isotope: r^2=0.82) microcosms. Also, no relationship was observed between the MeHg isotopes and sulfide concentrations for all microcosms. The strongest relationship (r^2=0. 76 -0.96, $p<0.05$) was obtained between pH and MeHg (200 isotope) concentrations, except for the A1 and N1 microcosms. However, the MeHg (199 isotope) and the natural MeHg (202 isotope) were not well correlated with the pH, except in the T3 microcosm (202 isotope: r^2 = 0.78), which shows that demethylation it less influenced by pH than methylation. In addition, little variation in pH alone does not affect the methylation of native Hg (202). Tentative stepwise multiple regression showed that MeHg concentrations for all isotopes were well

correlated with the cumulated actions of pH, Eh, Fe^{2+}(or Fe^{3+} or Fe total), and sulfate (data not shown).

The statistical analysis results of the linear regression (48h) of MeHg isotopes and porewater characteristics in the SLR Zone 1 microcosms are given in Table S4-6 (Support information). It is generally accepted that low pH values decrease the net MeHg production in anaerobic sediments [Ramlal et al., 1986; Steffan et al., 1988; Gilmour and Henry, 1991] and increase it at the sediment-water interface [Ullrich, 1991]. Demethylation rates in both sediments and water are less affected by pH than methylation rates, indicating that the changes observed in net MeHg production are largely due to an effect of pH on methylation rather than demethylation [Ramlal et al., 1986; Steffan et al., 1988; Matilainen et al., 1991]. The low pH variation in our microcosms, as mentioned previously, can be an explanation by the poor correlation observed for natural Hg isotope (202) and supports our findings of a strong correlation between the 200 Hg isotope (methylation) and pH.

Based on the results discussed above, we conclude that methylation and demethylation are dependent on the type of microbial inhibition treatment, which determines the type of microbes that are active in the specific systems, and the availability of Hg^{2+} for methylation. Demethylation and methylation are related to SRB and MPA activity, but another process might also be important in determining net Hg methylation levels and defining the MeHg concentration levels in the sediments. Further investigations are clearly needed to determine in which way those changes are critical for the long-term production of MeHg in aquatic systems. Iron-oxide amendments will hopefully show which way the FeRP are related to net methylmercury formation.

4.4. Conclusions and Future Work

Our results first indicate that Hg spike addition increased the availability of ambient Hg for methylation, with the exception of the SRB-inhibited microcosms (T2). The inhibition of certain groups of microbes clearly had an effect on methylation and demethylation. For instance, the highest calculated methylation percentage was in the microcosm where only MPA were inhibited (T3), followed closely by the T1 microcosm (Hg spike control). Given the fact that the methylation potential was greatly decreased in

the abiotic microcosms, we can conclude that methanogens play an important role in Hg methylation, but their inhibition in the microcosms favored SRB and/or FeRP.

In addition, it is generally accepted that methanogens, as well as SRB, are involved in oxidative demethylation in anoxic sediments, and our data indicate that in the St-Lawrence river sediments from Zone 1, methanogens might have had the leading role in MeHg demethylation. Results from our study also show that abiotic demethylation pathways have the lowest contribution to net MeHg production in the sediments.

The specific methylation rates corroborated the methylation and demethylation findings mentioned above. For instance, we observed that the specific methylation rates were far lower in the SRB and/or methanogen inhibited microcosms (T2 and T4) than in the control system (T1), whereas the specific demethylation rates were the lowest in methanogen inhibited systems (T3 and T4) and the highest in the SRB inhibited microcosm (T2) and control microcosm (T1).

In addition, the M/D ratios shown in Table 4-6 revealed that the inhibition of methanogens (T3) alone increased the M/D ratio by increasing the methylation rate and decreasing the demethylation one. Overall, all microcosms, with the exception of T3, favored demethylation over methylation and the degree of magnitude of the ratios indicates that they vary with the type of active microbes.

The findings for the St-Lawrence sediments are in agreement with the Mer Bleue ones with respect to the effect of sulfate-reducers and methanogens in net MeHg formation. The inhibition of methanogens stimulated net methylation, not only by inhibiting demethylation, but also by stimulating methylation (see M/D ratios), along with the stimulation of the SRB activity. Iron reduction (FeRR) might however be another important process in the production of MeHg in aquatic environments, because the inhibition of both SRB and MPA enhanced the iron reduction rate and MeHg production was not completely stopped. Alternatively, in the SRBs inhibited microcosms (T2 and T4), the increased sulfides production (Figure 4-2f) caused by the dissolution of pre-existing iron sulfide minerals (as shown by the saturation index calculations, Table S4-4), might stimulate the formation of charged Hg polisulfides complexes which are not available to

bacterial uptake (diffusive transport across microbial membranes) [Benoit et al . 1999] and determined the decrease in methylation.

Finally, the calculated demethylation rate constants translated into a relatively long half-life for the native MeHg in sediments (i.e., 8.3 d^{-1}), higher than those calculated for Mer Bleue or other studies [Hintelmann et al. 2000 (1.8 d^{-1})]. In contrast, the half-life of the added tracers was lower (0.4- 3 d^{-1}), decreasing with the SRB inhibition (T2: 0.4 d^{-1}) and increasing with the MPA inhibition (T3: 2.6 and T4: 3.0 d^{-1}). This is an important observation, since the residence time of MeHg in sediments affects its availability to biota. In the case of the St-Lawrence River Zone 1, if we consider the historical pollution with Hg and wood fibers in the area, and more recently the increased methanogenic activity, we can suggest that a natural remediation system evolved over time in the sediments in this area, in which increased methanogenic activity increased the demethylation processes (through OD) which in turn reduced the residence time of MeHg in the sediments, therefore reducing its availability to the biota. The existence of a well developed *mer* mediated detoxification system in the St-Lawrence river sediments cannot be ruled out, knowing that the *mer* detoxification is extensive in aquatic environments, especially in contaminated sediments.

In conclusion, the strong positive correlation between Km and SRR and between Kd and MPA, clearly supports the fact that SRB are involved in Hg methylation and MPA in MeHg demethylation in the sediments. In contrast, as it is the case in Mer Bleue, the strong negative correlation between Kd and FeRR showed that the increase in FeRR corresponds to a decrease in demethylation, which may indicate that iron reduction may influence net methylation in the Zone 1 SLR sediments by decreasing demethylation rather than favouring methylation in the long term. To clarify the role of FeRP in net Hg methylation, further experiments should be carried out with hydrous ferric oxide amendments to the sediments, along with Hg isotopes and microbial inhibitors.

4.5. References

Avramescu ML, Zhu J, Yumvihoze E, Hintelmann H, Fortin D, Lean DRS, 2010. A

simplified sample preparation procedure for measuring isotope enriched methylmercury. Environ. Toxicol. Chem., (in press).

Balch WE and Wolfe RS, 1979. Specific and biological distribution of coenzyme M (2-mercaptoethane sulfonic acid). Journal of Bacteriology, 137, 264-273.

Baldi F, Parati F, Filipelli M 1995. Dimethylmercury and dimethylmercury-sulfide of microbial origin in the biogeochemical cycle of Hg. Water Air Soil Pollut., 80, 805-811.

Barkay T, Miller SM, Summers AO, 2003. Bacterial mercury resistance from atoms to ecosystems. FEMS Microbiology Reviews, 27, 355-384.

Benoit JM, Gilmour CC, Heyes A, Mason RP, Miller CL, 2003. Geochemical and biological controls over methylmercury production and degradation in aquatic ecosystems. *ACS* Symposium Series 835, 262–297.

Benoit JM, Gilmour CC, Mason RP, 2001. The influence of sulfide on solid-phase mercury bioavailability for methylation by pure cultures of Desulfobulbus propionicus (1p3). Environ. Sci.Technol. 35, 127-132

Benoit JM, Gilmour CC, Mason RP, Heyes A, 1999. Sulfide controls on mercury speciation and bioavailability to methylating bacteria in sediment pore waters. Environ. Sci. Technol., 33, 951-957

Blodau C, Roehm CL, Moore TR, 2002. Iron, sulfur and dissolved carbon dynamics in a northern peatland. Archiv fur Hydrobiologie, 154, 561-583.

Cai Y, Tang G, Jaffé R, Jones R, 1997. Evaluation of some Isolation Methods for Organomercury Determination in Soil and Fish Samples by Capillary Gas Chromatography – Atomic Fluorescence Spectrometry. International Journal of Environmental Analytical Chemistry, 68, 331-345.

Canadian Council of Ministers of the Environment (CCME). Protocol for the derivation of Canadian sediment quality guidelines for the protection of aquatic life: summary tables — Update 2002. CCME EPC-98E; 2005; Prepared by Environment Canada, Guidelines Division, Technical Secretariat of the CCME Task Group on Water Quality Guidelines, Ottawa.

Canario J, Poissant L, O'Driscoll N, Vale C, Pilote M, Lean D 2009. Sediment processes and mercury transport in a frozen freshwater fluvial lake (Lake St. Louis, QC,

Canada). Environmental Pollution, 157, 1294–1300.

Celo V, Scott S, Lean DRS, 2006. Abiotic pathways of mercury methylation in the aquatic environment. The Science of the Total Environment, 368, 126-137.

Chen Y, Bonzongo JC, Miller GC, 1996. Inhibition of mercury methylation in anoxic freshwater sediment by group VI anions. ACS Division of Environmental Chemistry, Preprints 36, 55-57.

Choi S-C, Bartha R, 1994a. Environmental factors affecting mercury methylation in estuarine sediments. Bull. Environ. Contam Toxicol., 53, 805-812.

Choy ES, Hodson PV, Campbell LM, Fowlie AR, Ridal J. 2008. Spatial and temporal trends of mercury concentrations in young-of-the-year spottail shiners (notropis hudsonius) in the St. Lawrence River at Cornwall, ON. Arch Environ Contam Toxicol.,54, 473-81.

Compeau G, Bartha R, 1985. Sulfate-reducing bacteria: principal methylators of mercury in anoxic estuarine sediments. Appl. Environ. Microbiol., 50, 498-502.

Delongchamp TM, Lean DRS, Ridal JJ, Blais JM, 2009. Sediment mercury dynamics and historical trends of mercury deposition in the St. Lawrence River area of concern near Cornwall, Ontario, Canada. The Science of the Total Environment, 407, 4095-104.

Drott A, Lambertsson L, Björn E, Skyllberg U. 2007. Importance of dissolved neutral mercury sulfides for methyl mercury production in contaminated sediments. Environ. Sci. and Technol., 41, 2270-2276.

Drott A, Lambertsson L, Björn E, Skyllberg U. 2008a. Do Potential Methylation Rates Reflect Accumulated Methyl Mercury in Contaminated Sediments? Environ. Sci. Technol., 42, 153–158.

Drott A, Lambertsson L, Björn E, Skyllberg U. 2008b. Potential demethylation rate determinations in relation to concentrations of MeHg, Hg and pore water speciation of MeHg in contaminated sediments. Mar. Chem. 112, 93–101.

Falter R, 1999. Experimental study on the unintentional abiotic formation of inorganic mercury during analysis: Part 1: Localisation of the compounds effecting the abiotic mercury methylation. Chemosphere 39, 1051-1073.

Fathi M. 2009. Benthic flux of total mercury (THg) and methyl mercury (MeHg) between

contaminated sediments and the overlying water column in the St. Lawrence River. M.Sc. Thesis, University of Ottawa, Ottawa, ON, Canada.

Flemming EJ, Marck EE, Green PG, Nelson DC, 2006. Mercury methylation from unexpected sources: molybdate-inhibited freshwater sediments and an iron-reducing bacterium. Appl. Environ. Microbiol., 72, 457–464.

Fortin, D and Praharaj T, 2005. Role of microbial activity in Fe and S cycling in sub-oxic to anoxic sulfide-rich mine tailings: a mini-review., 6, 39-42.

Fowlie AR, Hodson PV, Hickey MBC, 2008. Spatial and seasonal patterns of mercury concentrations in fish from the St. Lawrence River at Cornwall, Ontario: Implications for monitoring. J. Great Lakes Res., 34, 72-85.

Gilmour CC and Henry EA, 1991. Mercury methylation in aquatic systems affected by acid deposition. Environ. Pollut., 71, 131-169.

Gough HL, Dahl AL, Tribou E, Noble PA, Gaillard J-F, Stahl DA. 2008. Elevated sulfate reduction in metal-contaminated freshwater lake sediments. Journal of Geophysical Research G: Biogeosciences 113 (4), art. no. G04037.

Goulet RR, Lalonde JD, Chapleau F, Findlay SC, Lean DRS, 2008. Temporal trends and spatial variability of mercury in four fish species in the Ontario segment of the St. Lawrence River, Canada. Arch Environ Contam Toxicol, 54, 716-29.

Hammerschmidt CR, FitzgeraldWF, Lamborg CH, Balcom PH, Visscher PT, 2004. Biogeochemistry of methylmercury in sediments of Long Island Sound. Mar. Chem. 90, 31–52

Hammerschmidt CR, Fitzgerald WF, 2006. Methylmercury cycling in sediments on the continental shelf of southern NewEngland. Geochim. Cosmochim. Acta, 70, 918–930.

Hammerschmidt CR, Fitzgerald WF, Balcom PH, Visscher PT 2008. Organic matter and sulfide inhibit methylmercury production in sediments of New York/New Jersey Harbor. Mar. Chem., 109, 165–182

Heyes A, Miller C, Mason RP, 2004. Mercury and methylmercury in Hudson River sediment: impact of tidal resuspension on partitioning and methylation. *Mar. Chem.* 90, 75–89.

Hintelmann H and Ogrinc N, 2003. Determination of stable mercury isotopes by ICP/MS

and their application in environmental studies. In: Cai, Y., Braids, C.O. (Eds.), Biogeochemistry of Environmentally Important Trace Elements. ACS Symp. Series 504, 835, 321–338.

Hintelmann H, Evans RD, Villeneuve JY, 1995. Measurement of mercury methylation in sediments by using enriched stable mercury isotopes combined with methylmercury determination by gas chromatography-inductively coupled plasma mass spectrometry. J Anal. Atom. Spectrom., 10,619–624.

Hintelmann H, Evans RD, 1997. Application of stable isotopes in environmental tracer studies—Measurement of monomethylmercury (CH_3Hg^+) by isotope dilution ICP-MS and detection of species transformation. Fresenius J. Anal. Chem., 358,378–385.

Hintelmann H, Keppel-Jones K, Evans RD, 2000. Constants of mercury methylation and demethylation rates in sediments and comparison of tracer and ambient mercury availability. Environ. Toxicol. Chem., 19, 2204– 2211.

Ingvorsen K, Zeikus JG, Brock TD, 1981. Dynamics of Bacterial Sulfate Reduction in a Eutrophic Lake. Appl. Environ. Microbiol., 42,1029-1036.

Kerin EJ, Gilmour CC, Roden E, Suzuki MT, Coates JD, Mason RP, 2006. Mercury Methylation by Dissimilatory Iron-Reducing Bacteria. Appl. Environ. Microbiol., 72, 7919–7921.

Kim E-H, Mason RP, Porter ET, Soulen HL, 2006. The impact of resuspension on sediment mercury dynamics, and methylmercury production and fate: A mesocosm study. Mar. Chem., 102, 300–315.

King JK, Harmon S, Michele S, Fu TT, Gladden JB, 2002. Mercury removal, methylmercury formation, and sulfate-reducing bacteria profiles in wetland mesocosms. Chemosphere, 46, 859-870.

King JK, Kostka JE, Frischer ME, Saunders FM, 2000. Sulfate-reducing bacteria methylate mercury at variable rates in pure culture and in marine sediments. Appl. Environ. Microbiol., 66, 2430-2437.

King JK, Kostka JE, Frisher ME, Saunders FM, Jahnke RA, 2001. A quantitative relationship that demonstrates mercury methylation rates in marine sediments are based on the community composition and activity of sulfate bacteria. Environ. Sci.

Technol., 35, 2492-2496.

Koschorreck M, 2000. Methane turnover in exposed sediments of an Amazon floodplain lake. Biogeochemistry, 50, 195–206.

Kusel K, Dorsch T, Acker G, Strackebrandt E, 1999. Microbial Reduction of Fe(III) in Acidic Sediments: Isolation of *Acidiphilium cryptum* JF-5 Capable of Coupling the Reduction of Fe(III) to the Oxidation of Glucose. Appl. Environ. Microbiol., 65,3633-3640.

Lovley, DR and Klug MJ, 1983. Sulfate reducers can outcompete methanogens at freshwater sulfate concentrations. Appl. Environ. Microbiol., 45, 187–192.

Martin-Doimeadios R, Tessier E, Amouroux D, Guyoneaud R, Duran R, Caumette P, Donard OFE, 2004. Mercury methylation/demethylation and volatilization pathways in estuarine sediment slurries using species-specific enriched stable isotopes. Mar. Chem., 90, 107– 123.

Marvin-Diapasquale MC and Oremland RS, 1998. Bacterial methylmercury degradation in Florida Everglades peat sediment. Environ. Sci. Technol., 32, 2556-2563.

Marvin-Diapasquale MC, Agee J, McGowan C, Oremland, RS, Thomas M, Krabbenhoft D, Gilmour CC, 2000. Methylmercury degradation pathways: a comparison among three mercury- impacted ecosystems. Environ. Sci. Technol., 34, 4908-4917.

Matilainen T, Verta M, Korhonen H, Niemi M, 1991. Specific rates of methylmercury production in lake sediments. *Water Air Soil Pollution*, 56, 595-605.

Matilainen T 1995. Involvement of bacteria in methylmercury formation in anaerobic lake waters. Water Air Soil Pollution, 80, 757-764.

Mehrotra AS, Sedlak DL, 2005. Decrease in net mercury methylation rates following iron amendment to anoxic wetland sediment slurries. Environ. Sci. Technol., 39, 2564–2570.

Meier J, Voigt A, Babenzien H-D, 2000. A comparison of 35S-SO42- radiotracer techniques to determine sulfate reduction rates in laminated sediments. J. Microbiol. Methods, 41, 9–18.

Morin A and Findlay CS, 2006. Course notes for BIO 4158 Applied Biostatistics.

University of Ottawa, Ottawa, On., Canada.

Nevin KP and Lovley DR, 2000. Potential for Nonenzymatic Reduction of Fe(III) via Electron Shuttling in Subsurface Sediments. The Science of the Total Environment, 34, 2472-2478.

Oremland RS, Miller LG, Dowdle P, Connell T, Barkay R, 1995. Methylmercury oxidative degradation potentials in contaminated and pristine sediments of the Carson River, Nevada. Appl. Environ. Microbiol., 61, 2745-2753.

Oremland RS and Capone DG, 1988. Use of specific inhibitors in biogeochemistry and microbial ecology. Adv. Microb. Ecol., 10,285–383.

Oremland RS, Culbertson CW, Winfrey MR, 1991. Methylmercury decomposition in sediments and bacterial cultures: involvement of methanogens and sulfate reducers in oxidative demethylation. Appl. Environ. Microbiol., 57, 130-137.

Otto M, 2007. Chemometrics. Statistics and Computer Application in Analytical Chemistry. Second Edition. Wiley-VCH Verlag GmbH & Co. KgaA.

Pak KR and Bartha R, 1998. Mercury methylation and demethylation in anoxic lake sediments and by strictly anaerobic bacteria. Appl. Environ. Microbiol., 64, 1013-1017.

Poissant L, Constant P, Pilote M, Canário J, O'Driscoll N, Ridal J, Lean DRS, 2007. The ebullition of hydrogen, carbon monoxide, methane, carbon dioxide and total gaseous mercury from the Cornwall area of concern. The Science of the Total Environment, 381,256-262.

Praharaj T, Fortin D, 2004. Indicators of microbial sulfate reduction in acidic sulfide-rich mine tailings. Geomicrobiology J., 21, 457-467.

Quemarais B, Cossa D, Rondeau B, Pham TT, Fortin B, 1998. Mercury distribution in relation to iron and manganese in the waters of the St. Lawrence River. The Science of the Total Environment, 213, 193–201.

Ramlal PS, Rudd JWM, Hecky RE, 1986. Methods for measuring specific rates of mercury methylation and degradation and their use in determining factors controlling net rates of mercury methylation. Appl. Environ. Microbiol., 51, 110-114.

Razavi NR, 2008. Role of bubbling from aquatic sediments in mercury transfer to a benthic invertebrate in the St. Lawrence River, Cornwall, Ontario. Master's Thesis,

Queen's University, Kingston, ON, Canada.

Richman LA and Dreier SI, 2001. Sediment contamination in the St. Lawrence River along the Cornwall, Ontario waterfront. J. Great Lakes Res., 27, 60-83.

Ridal JJ, Yanch LE, Fowlie AR, Razavi NR, Delongchamp TM, Choy ES, Fathi M, Hodson PV, Campbell LM, Blais JM, Hickey MBC, Yumvihoze E, Lean DRS. 2009. Potential causes of enhanced transfer of mercury to St. Lawrence River biota: Implications for sediment management strategies at Cornwall, Ontario, Canada. Hydrobiologia, 1-18 (in press).

Robinson JB and Tuovinen OH, 1984. Mechanisms of microbial resistance and detoxification of mercury and organomercury compounds-physiological, biochemical and genetic analyses. Microbiol. Reviews, 48, 95-124.

Schaefer J, Latowski J, Barkay T, 2002. mer-mediated resistance and volatilization of Hg(II) under anaerobic conditions. Geomicrobiol. J., 19, 87-102.

Steffan RJ, Korthals ET, Winfrey MR, 1988. Effect of acidification on mercury methylation, demethylation, and volatilization in sediments from an acid-susceptible lake. Appl. Environ. Microbiol., 54, 2003-2009.

Sunderland EM, Gobas FAPC, Heyes A, Branfireun BA, Bayer AK, Cranston RE, Parsons MB, 2004. Speciation and bioavailability of mercury in well-mixed estuarine sediments. Mar. Chem. 90, 91-105.

Ullrich SM, Tanton TW and Abdrashitova SA. 2001 Mercury in the aquatic environment: A review of factors affecting methylation. Critical Reviews in Environmental Science and Technol. 31:241–293.

Warner KA, Roden EE, Bonzongo JC, 2003. Microbial mercury transformation in anoxic freshwater sediments under iron-reducing and other electron-accepting conditions. Environ. Sci. Technol. 37: 2159–2165.

Weber JH.1993. Review of possible paths for abiotic methylation of mercury in the aquatic environment. Chemosphere 26: 2063-2077.

Wendt-Potthoff K, Frommichen R, Herzprung P, Koschorreck M, 2002. Microbial Fe(III) reduction in acidic mining lake sediments after addition of an organic substrate and lime. Water Air Soil Pollution, Focus, 2, 81-85.

Wood JM, Kennedy PS, Rosen CG, 1968. Synthesis of methylmercury compounds by

extracts of a methanogenic bacterium, Nature, 220, 173-174.

Zar JH. 2006. Biostatistical Analysis (5th edition). Prentice-Hall, Upper saddle River, New Jersey.

Tables

Table 4-1. St. Lawrence River (SLR) first preliminary experiment (June 2007) set up and microcosm description. Sampling times (t): 0, 24, 48, 96 h.

ID	Microcosm description (n=3 replicates)	Treatment added
N	Natural SLR sediments	Not spiked
B1	Biotic SLR sediments	^{200}Hg spike in Milli-Q water [1]
B2	Biotic SLR sediments	^{200}Hg spike in PW[1]
A	Abiotic SLR sediments (gamma radiated for 8h)	^{200}Hg spike in PW[1]

[1]: isotope enriched Hg solutions were added to give a final concentration of cca. 6.5 ng g^{-1} $^{200}Hg^{2+}$ in the sediments (1 mL of 1 μg mL^{-1} $^{200}Hg^{2+}$ prepared in ultrapure Milli-Q water or SLR porewater (PW); solutions were equilibrated for 2h at room temperature)

Table 4-2. Microcosm setup and description for the second St. Lawrence River (SLR) July 2007 experiment. The sampling times (t) were 0, 24, 48, 72 and 96 h.

ID	Microcosm description (n=3 replicate bottles)	Treatment			
		$^{200}Hg^{2+}$ and $Me^{199}Hg^{+}$ spikes	SRB inhibitor ($NaMoO_4$)	MPA inhibitor (BES)[2]	HFO[1]
N	Natural (unspiked control)	no	no	no	no
T1	Hg spiked control	yes[3]	no	no	no
T2	SRB inhibited	yes[3]	yes[4]	no	no
T3	MPA inhibited	yes[3]	no	yes[5]	no
T4	SRB and MPA inhibited	yes[3]	yes[4]	yes[5]	no
A1	Hg spiked Abiotic control (Autoclaved sediments at 105°C three times for 45 min)	yes[3]	no	no	no

[1]:HFO: ferrihydrte

[2]:BES: sodium 2-bromoethane sulfonate

[3]:isotope enriched Hg solutions were added to give a final concentration of cca. 77.7 ng g^{-1} $^{200}Hg^{2+}$ (1.1 mL of 10.743 μg mL^{-1} $^{200}Hg^{2+}$) and cca 4.7 ng g^{-1} $Me^{199}Hg^{+}$ (1.1 mL of 647.2 ng mL^{-1} $Me^{199}Hg$) in the sediment slurry.

[4]:1.4mM final concentration of molybdate in the sediments (2.5 mL of 250mM $NaMoO_4$)

[5]:28mM final concentration of BES in the sediments (6.3 mL of cca 2M BES)

Table 4-3. Sediment ambient background concentrations and percent increases due to isotope enriched Hg ($^{200}Hg^{2+}$ and $Me^{199}Hg^{+}$) additions in the St. Lawrence River incubation experiment July 2007. Standard errors are given (±SE) where n ≥ 2.

Parameter	N1	T1	T2	T3	T4	A1
Organic content (±SE), (%) n=3	7.7 (0.1)	7.9 (0.1)	7.9 (0.1)	9.2 (0.1)	9.0 (0.1)	8.2 (0.1)
Water content (±SE), (%) n=3	73.3 (2.6)	70.4 (0.1)	70.8 (0.1)	70.9 (0.0)	70.9 (0.1)	72.4 (1.2)
Ambient (202) THg, ng g^{-1} d.w, n=1	1079	1593	866	1790	1790	982
Ambient (202) MeHg(±SD), ng g^{-1} d.w, n=2	2.9 (0.0)	2.5 (0.1)	2.6 (0.1)	3.3 (0.8)	2.9 (0.2)	1.8 (0.2)
THg (±SD) after spike additions, ng g^{-1} d.w, n=2	751 (280)	820 (140)	1106	907 (11)	1212 (70)	2018 (1538)
MeHg (±SD) after $Me^{199}Hg$ addition, ng g^{-1} d.w, n=2	2.6 (0.0)	7.0 (0.01)	8.2 (0.7)	8.9 (0.5)	8.4 (1.1)	6.2 (0.3)
^{200}Hg addition (±SD)	n.a.[1]	61.5 (0.3)	72.2 (18.6)	66.2 (0.4)	76.7 (8.6)	67.7 (6.0)
$Me^{199}Hg$ addition (±SD)	n.a	4.1 (0.1)	5.1 (0.5)	5.4 (0.3)	5.2 (0.5)	4.3 (0.2)
Factor increase[2] in THg due to ^{200}Hg and $Me^{199}Hg$	n.a	1 times	1.1 times	1 times	1 times	1.1 times
Factor increase in MeHg due to $Me^{199}Hg$	n.a	2.8 times	3.2 times	2.7 times	2.9 times	3.5 times
% MeHg initial	n.a	0.2%	0.3%	0.2%	0.2%	0.2%
% MeHg after spiking	n.a	0.4%	0.9%	0.5%	0.5%	0.6%
increase in % MeHg	n.a	0.3%	0.6%	0.3%	0.3%	0.4%

[1]: not available

[2]: Due to the high variability of the ambient THg in the SLR sediments (751÷2018 ng/g dw), the increase in THg due to Hg spike addition was calculated considering: $[THg]_{(after\ spike\ addition)} = [THg]_{(before\ spike\ additions)} + [^{200}Hg] + [^{199}Hg]$.

Table 4-4. Total percentage of mercury methylated and methylmercury demethylated from the spikes in the different systems (calculated by dividing the amount measured by the amount spiked x100).

Microcosm	^{202}Hg methylated (%)[1]		^{200}Hg methylated (%)		Me^{199}Hg demethylated (%)	
	46h	96h	46h	96h	46h	96h
N	0.33	0.32	n/a	n/a	n/a	n/a
Ab	0.13	0.20	0.45	0.43	-8.75	-10.39
T1	0.41	0.44	9.39	9.56	14.29	40.41
T2	0.29	0.28	2.7	2.56	16.22	44.44
T3	0.43	0.51	10.5	11.27	8.09	6.75
T4	0.25	0.28	1.88	2.14	4.16	1.55

[1]: Percent of the ambient (202 isotope) Hg methylated (%[MeHg] / [Hg^{2+}]) was calculated considering Hg^{2+} = [THg] – [ΣMeHg].

Table 4-5. Comparison of specific mercury methylation (SpM) and methylmercury demethylation rates (SpD) calculated from the tracer July 2007 experiment with the St. Lawrence River sediments (calculated for t = 46h).

Microcosm	M (202-ambient) pmol g^{-1} h^{-1}	M (200) pmol g^{-1} h^{-1}	D(199) pmol g^{-1} h^{-1}	Specific ambient rate (202) (pmol g^{-1} h^{-1}) 100/(Hg pmol g^{-1})	Specific methylation rate (200) (pmol g^{-1} h^{-1}) 100 / (add ^{200}Hg pmol g^{-1})	Specific demethylation rate (199) (pmol g^{-1} h^{-1}) 100/(add $Me^{199}Hg$ pmol g^{-1})	M/D	[MeHg] / [THg]t=0h	[MeHg] / [THg]t=46h
N	0.08	n/a	n/a	0.002	nd	nd	n/a	0.2%	0.3%
T1	0.09	0.59	0.05	0.002	0.19	0.31	0.6	0.4%	0.7%
T2	0.04	0.22	0.07	0.001	0.05	0.36	0.2	0.8%	1.0%
T3	0.08	0.72	0.04	0.002	0.22	0.17	1.2	0.4%	0.8%
T4	0.01	0.12	0.02	0.0003	0.03	0.09	0.4	0.4%	0.5%
A1	0.05	0.00	-0.04	0.001	0.00	-0.19	0.0	0.6%	0.6%

Table 4-6. Comparison of specific mercury methylation and methylmercury demethylation rate constants calculated from various tracer studies.

Site	Rate constant			$MeHg^+$		Reference
	Km (d^{-1})	Kd (d^{-1})	Half-life (d)	Predicted (ng g^{-1})	Measured (ng g^{-1})	
N1 –SLR July 2007	n/a	n/a	n/a	2.12	2.86	this study
T1 –SLR July 2007	0.015	1.4	0.5	2.64	2.80	this study
T2 –SLR July 2007	0.003	1.7	0.4	2.49	2.64	this study
T3 –SLR July 2007	0.016	0.3	2.6	3.33	3.70	this study
T4 –SLR July 2007	0.002	0.2	3.0	2.97	3.30	this study
A1 –SLR July 2007	0.000	0.0	25.5	0.98	1.69	this study
N - Mer Bleue, On	n/a	n/a	1.6	0.58	0.60	this study, chapter 3
T1 - Mer Bleue, On	0.046	0.284	2.4	1.42	1.56	this study chapter 3
T2 - Mer Bleue, On	0.025	0.063	10.9	0.45	0.49	this study chapter 3
T3 - Mer Bleue, On	0.057	0.219	3.2	0.81	0.85	this study chapter 3
T4 - Mer Bleue, On	0.022	0.120	5.8	0.45	0.44	this study chapter 3
Ranger Lake, On	0.012	0.42	1.7	2.8	1.8	Hintelmann et al., 2000
Lake Vernon, On	0.016	0.53	1.3	3	0.8	Hintelmann et al., 2000
Lake Vernon, On	0.012	0.48	1.5	2.5	0.8	Hintelmann et al., 1995

Figures

Figure 4-1. Physico-chemical characteristics of the porewaters and overlying water at the St. Lawrence River site (Cornwall, On., June 2007) as a function of depth: Eh (mV,♦); conductivity (μS cm^{-1}, ●); temperature (^0C , ∗); pH (■). The dotted line represents the sediment (S) – water (W) interface.

Figure 4-2. Porewater characteristics during the 96h microcosm incubations: N (∗),T1 (■), T2 (▲), T3 (×), T4 (▼), A1 (●). (pH (a), and Eh (b), ferrous iron (c), ferric iron (d), sulfides (e), sultate (f), DOC (g), DIC (h)). Error bars represent standard error (SE). The description of the microcosms is presented in Table 4-1.

Figure 4-3. Sulfate Reduction Rates (a), Iron Reduction Rates (b), and Methane Production rates (c) in the St. Lawrence River incubation microcosms (July 2007). Error bars represent the standard error (SE) for n=3 replicates. The microcosms' description is in Table 4-3.

Figure 4-4. Ambient MeHg trend (a) along with the evolution of MeHg produced (ng g^{-1} d.w., n=1) from the isotope enriched mercury spikes ^{200}Hg (b) and $Me^{199}Hg$ (c) during the 96h microcosm incubations (July 2007): N (◆),T1 (■), T2 (▲), T3 (×), T4 (∗), A1 (●).The microcosms' description is in Table 4-1.

Figure 4-5. Relationship between Km (diamonds) or Kd (squares) and percent MeHg to THg (a), Sulfate reduction rates (b), Methane production Rates (c), and Iron Reduction rates (c) for all microcosm. Km and Kd calculated for 46h as in Table 4-6.

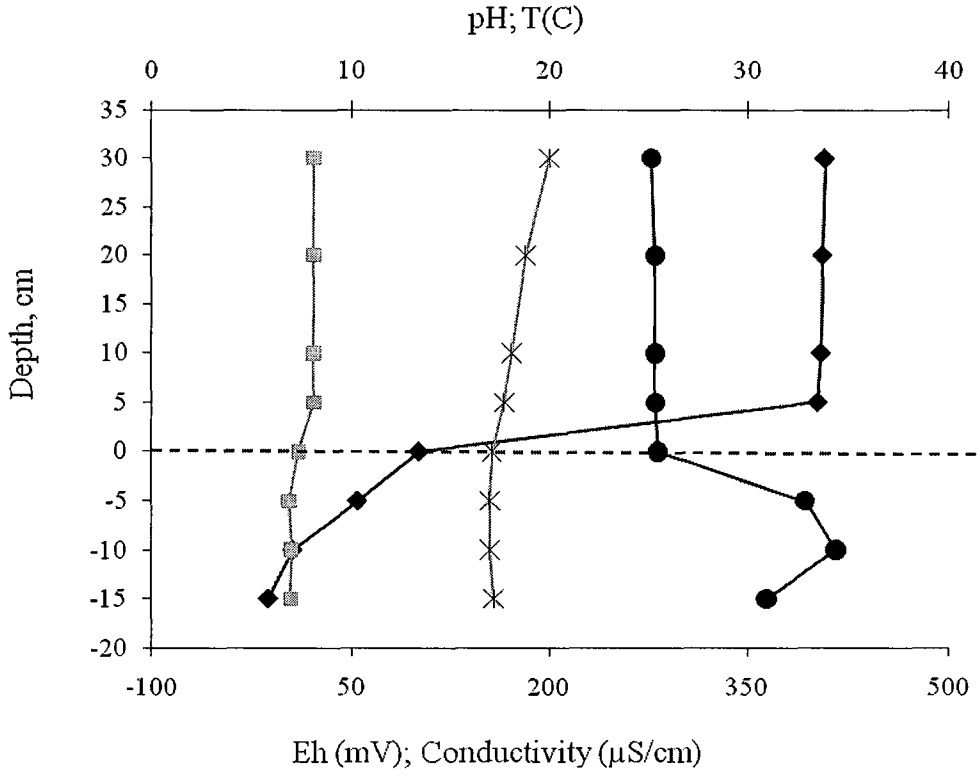

Figure 4-1. Physico-chemical characteristics of the porewaters and overlying water at the St. Lawrence River site (Cornwall, On., June 2007) as a function of depth: Eh (mV,♦); conductivity (µS cm^{-1}, ●); temperature (^{0}C , ∗); pH (■). The dotted line represents the sediment (S) – water (W) interface.

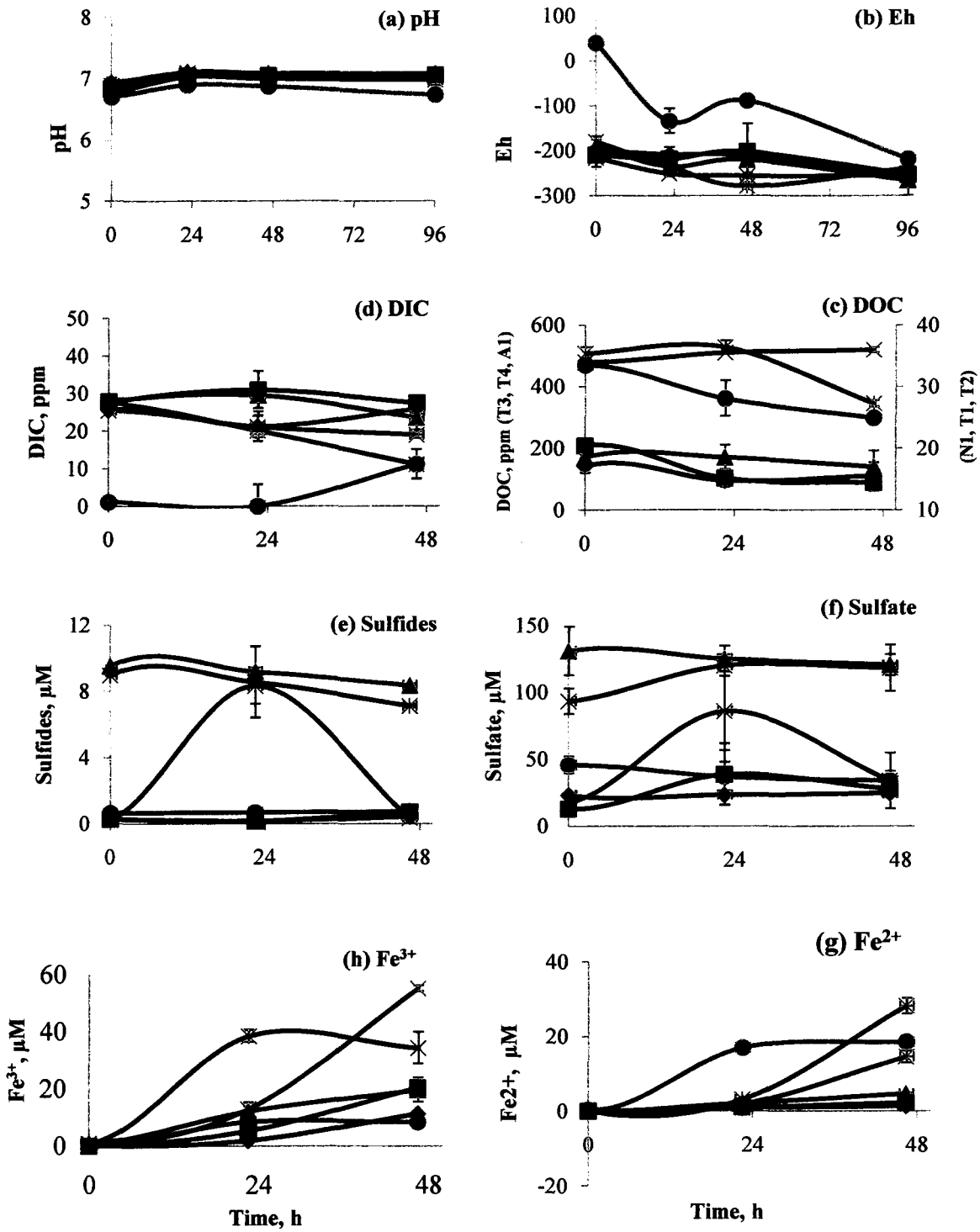

Figure 4-2. Porewater characteristics during the 96h microcosm incubations: N (∗),T1 (■), T2 (▲), T3 (×), T4 (▼), A1 (●). (pH (a), and Eh (b), ferrous iron (c), ferric iron (d), sulfides (e), sultate (f), DOC (g), DIC (h)). Error bars represent standard error (SE). The description of the microcosms is presented in Table 4-1.

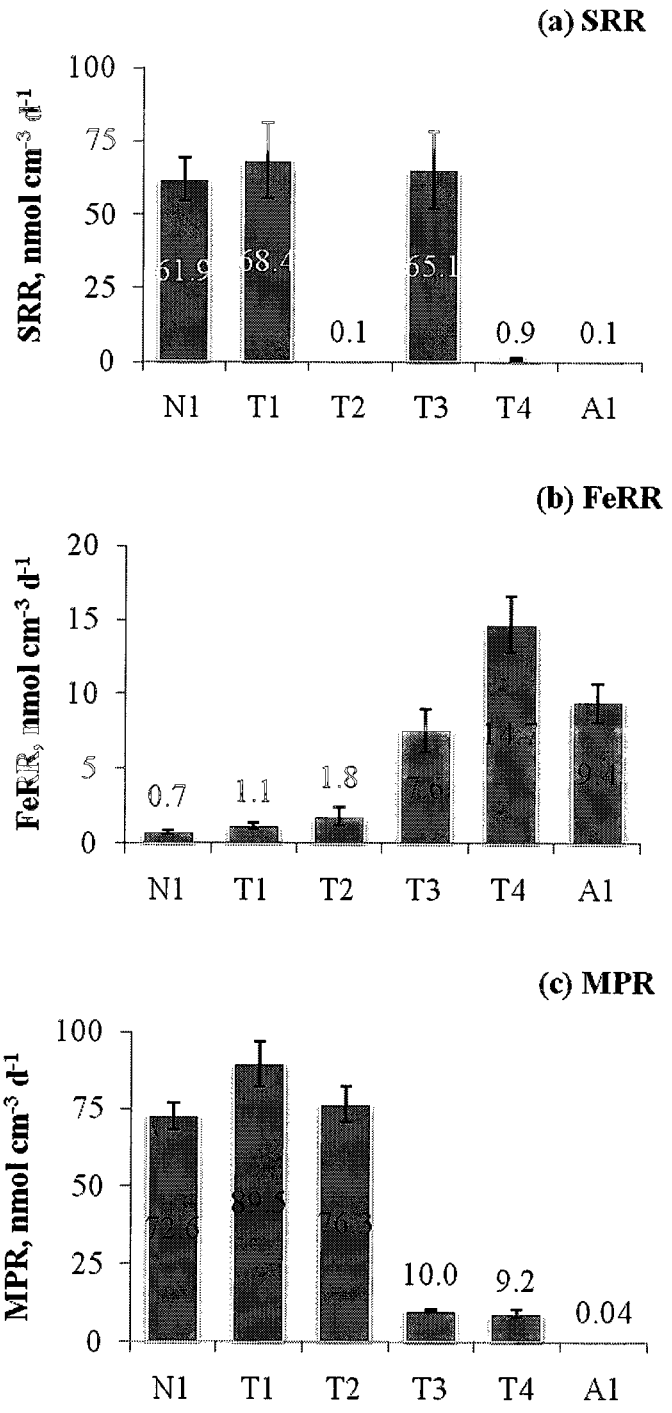

Figure 4-3. Sulfate Reduction Rates (a), Iron Reduction Rates (b), and Methane Production rates (c) in the St. Lawrence River incubation microcosms (July 2007). Error bars represent the standard error (SE) for n=3 replicates. The microcosms' description is in Table 4-3.

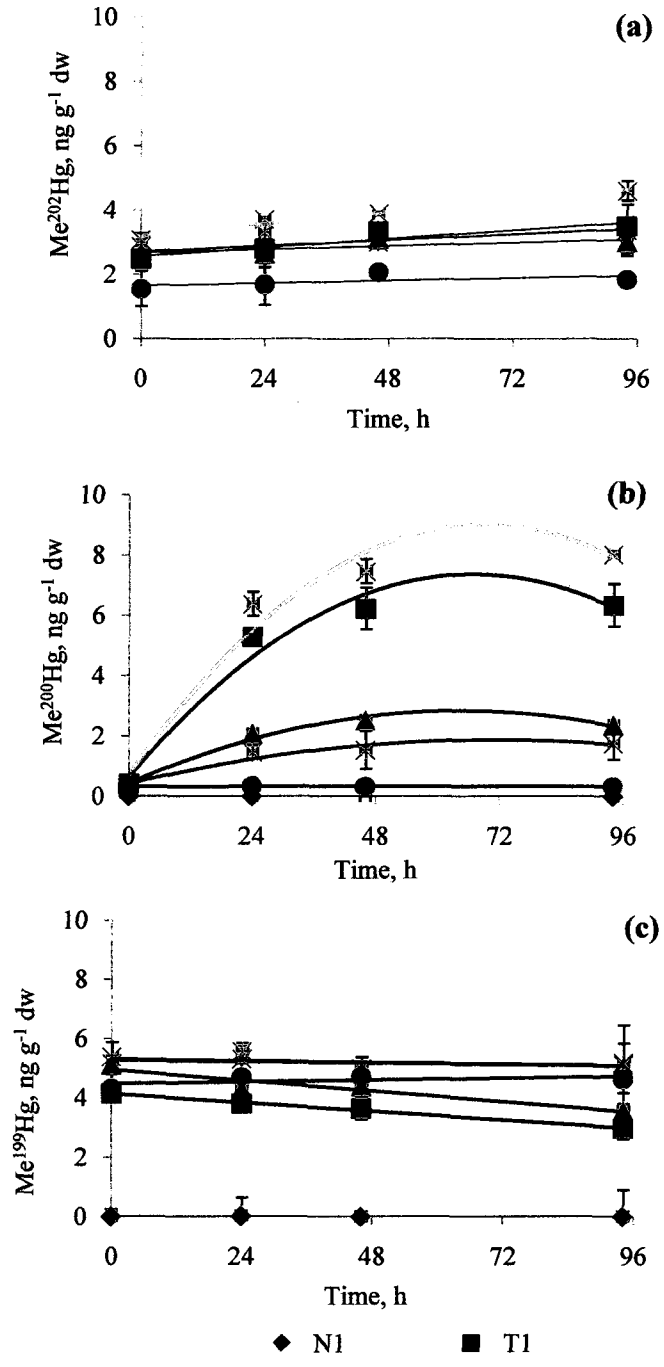

Figure 4-4. Ambient MeHg trend (a) along with the evolution of MeHg produced (ng g^{-1} d.w., n=2) from the isotope enriched mercury spikes ^{200}Hg (b) and $Me^{199}Hg$ (c) during the 96h microcosm incubations (July 2007): N (◆),T1 (■), T2 (▲), T3 (×), T4 (✶), A1 (●).The microcosms' description is in Table 4-1.

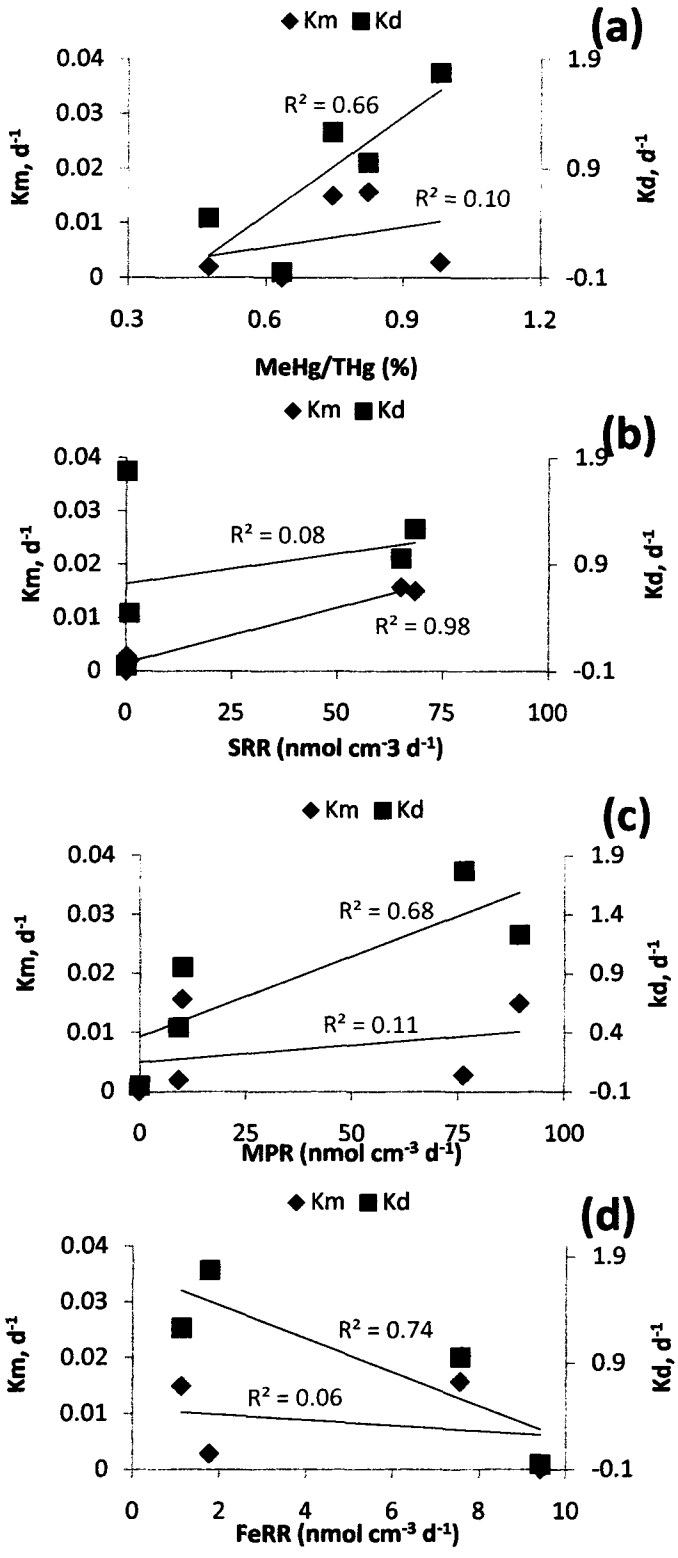

Figure 4-5. Relationship between Km (diamonds) or Kd (squares) and percent MeHg to THg (a), Sulfate reduction rates (b), Methane production Rates (c), and Iron Reduction rates (c) for all microcosm. Km and Kd calculated for 46h as in Table 4-6.

Supporting information

We present as supporting information the following data:

- The initial experiments with the St. Lawrence River sediments (June 2007) when we tested the preparation of the isotope enriched Hg spikes (in MilliQ-water or porewater), as well as the efficiency of the microbial inhibitors (sodium molybdate and BES).
- Five Figures (Figure S4-1 to S4-5) containing average total MeHg, mercury methylation rates, Sulfate Reduction Rates (SRR), Methane Production Rates (MPA), and porewater characteristics in St. Lawrence River incubation microcosms, June 2007; Sulfate Reduction Rates and Methane Production Rates measured during inhibitor concentration tests performed with the St. Lawrence River sediments in June 2007.
- Two tables (Table S4-1) containing St. Lawrence River (SLR) first preliminary experiment (June 2007) set up and microcosm description and statistical test results for the mercury methylation rate comparison among microcosms; as well as
- Five tables (Table S4-2 – S4-7) containing the statistical test results for FeRR and MPR calculation by linear regression; SRR, FeRR, and MPR comparison among microcosms; XLfit results of curve fitting of ambient MeHg data for the calculation of ambient Km and Kd; Eh, dissolved iron and sulfides concentrations relationships with different MeHg isotope concentrations and the saturation indexes for all microcosms.
- An additional figure representing the relationship between porewater characteristics and different MeHg isotope concentrations

Zone 1 St. Lawrence River sediment initial Experiments (June 2007)

As previously described in the materials and methods section of this chapter, the first experiment (June 2007) was a preliminary incubation experiment used to test the effect of ^{200}Hg isotope spike preparation (in Milli-Q water or porewater), the concentrations and efficiencies of microbial inhibitors used ($NaMoO_4$ and BES), and the use of gamma radiation for sterilization of the sediments for the abiotic microcosm. Abiotic control is necessary since abiotic reactions might be important for net Hg methylation in aquatic environment [Cello et al., 2006, Falter 1999, Baldi et al., 1995, Weber 1996] as explained in Chapter 1. Moreover, beside microbial iron reduction, the abiotic iron reduction is an important process in aquatic environment [Nevin and Lovley 2000, Fortin et al., 2005] contributing to calculated FeRR and making necessary to differentiate its contribution to FeRR when we look at the correlation between Hg methylation and iron reducing microbes activity (expressed as FeRR). Nevin and Lovley [2000] demonstrated that microbially reduced humics or other microbially generated hydroquinones were able to reduce abiotically (nonenzymatic) ferric iron in subsurface sediment.

Four microcosms (three biotic and one abiotic) in triplicate were spiked with 1 mL of 1 μg mL^{-1} ^{200}Hg spikes (in Milli-Q water or SLR porewater) and incubated in the dark in an anaerobic chamber for 96h as described in Table S4-1. Isotope enriched Hg solutions were added to give a final concentration of cca. 6.5 ng g^{-1} $^{200}Hg^{2+}$ in the sediments. The added tracers were equilibrated in overlaying water for two hours before being added to the incubation tubes in order to achieve the same speciation as the ambient Hg(II) [Hintelmann et al., 2000; Drott et al., 2008b].

Sub-samples were removed from replicate systems at regular time intervals (0, 24, 48, 96 h) to measure the amount of total MeHg produced. Temperature, pH, Eh, water and organic matter content (LOI), porewater analyses (Fe^{2+}, Fe^{3+}, sulfates, sulfides, DOC, DIC, nitrates), along with sulfate reduction rates (SRR) and methane production rates (MPR) were determined on separate sub-samples as described in materials and method section. Sub-samples for Hg isotopic analyses were acidified and kept frozen until analysis. The sediment samples were analyzed for total MeHg (ΣMeHg - all isotopes) according to Cai et al., 1996. (H_2SO_4-KBr-$CuSO_4$ leaching /CH_2Cl_2 extraction / $Na_2S_2O_3$ purification / CH_2Cl_2 extraction / GC-AFS detection).

Spike Preparation Test Results

Mercury methylation rates (pmol g^{-1} h^{-1}) were calculated in triplicate for all four microcosms for the 48h incubation period. To determine if there was a difference in rates between the microcosms treated with the spike prepared in Milli-Q water (B1) or porewater (B2), comparison tests (student t-tests) were performed using MS Excel (adds in functions). It is generally accepted that the rate of methylmercury production is not only influenced by the activity of methylating microbes but also by the availability of Hg(II) for uptake and methylation, and the dissolved neutral HgS^0 complexes are easily uptaken through passive diffusion by methylating microbes [Benoit et al 1999a].

The tested hypothesis (H) and the prediction (P) are: (H1) Spike preparation in anoxic porewater will enhance Hg methylation due to formation of neutral Hg sulfides; (P1) MeHg production rates (pmol g^{-1} h^{-1}) will be higher in the B2 microcosm than in the B1 one.

The trend of total MeHg (sum of all isotopes) produced from the isotope enriched mercury spikes during the 96h incubation time are presented in Figure S4-1. The microcosms behaved differently during the 96h incubation period. A slightly linear increase (2.94 to 3.32 ng g^{-1} dw) was observed in the natural (N) microcosm over 96h. Similar linear increase in the first 24h followed by steady state levels (Figure S4-1) was observed for total MeHg in both biotic microcosms (B1: 2.88 – 4.16 ng g^{-1} dw and B2: 2.87 – 4.19 ng g^{-1} dw). The abiotic (A) microcosm behaved differently with no increase in the first 24h followed by a sharp increase that reached a steady state after 46h, which may suggest that this sediment may require a longer period of gamma-radiation, which in the future may delay the beginning of the experiments. Given these findings and the larger amount of sediments necessary for the next incubations (July 2007) with SLR sediments, the autoclaving method (105^0C for 2 x 45 min) was used to prepare the abiotic microcosms.

For comparison, mercury methylation rates (pmol g^{-1} h^{-1}) were calculated by linear regression for 24h and 48h. The results are presented in Figure S4-2. The B1 and B2 microcosms have slightly different potential methylation rates, but comparison tests (student t-tests) proved that the difference was not statistically significant ($p > 0.05$). This was also the case of the natural (N) system and the abiotic (A) one. When considering the rates for 24h, significant differences were

observed between the natural (N) and B1, and also B2 microcosms ($p < 0.05$), but not between the natural and abiotic microcosms. In conclusion, the small difference in rates between the microcosm B1 treated with the spike prepared in Milli-Q water and the microcosm B2 treated with the Hg spiked prepared in pore water was not significant, which proved that our methylation results for Mer Bleue experiment, where the spike was prepared in Milli-Q water, were not biased. Taking in consideration previous studies [Hintelmann et al., 2000; Hammerschmidt et al., 2004] which suggested the added tracers to have if possible the same speciation as the ambient Hg(II), for the next experiments (July 2007) the isotope enhanced Hg spikes were prepared with water overlying the sediments and allowed to react with natural ligands for 2–4 h before aliquots were added to the incubation bottles. The same approach was also used in more recent studies [Drott et al., 2008b; Hammerschmidt et al., 2008]. This approach was used considering previous studies of Benoit and collaborators (1999; 2001) who found that, to be available for methylation, the Hg^{2+} must be dissolved and enter the microbial cell presumably by passive diffusion as a neutrally charged complex, possibly HgS^0 in pore water. Also, Hammerschmidt and Fitzgerald (2004) suggested that HgS^0 was the dominant complex of Hg^{2+} when S^{2-} was less than about 10 μM, whereas $HgHS^{2-}$ was the dominant complex at greater levels of dissolved sulfide. Recent studies of Hammerschmidt et al. [2008] demonstrate the positive correlation between the potential gross rates of Hg methylation in sediments and the level of Hg^{2+} presumably as HgS^0, in deposits with less than 10 μM dissolved sulfide. The authors also find that the Hg methylation rates are reduced greatly in deposits with greater levels of dissolved sulfide.

Porewater characteristics are presented in Figure S4-3. The decrease in sulfate concentrations in the first 24h in the biotic microcosms (N, B1, B2) was in agreement with the linear increase in sulfides, suggesting that sulfate reducing bacteria were active in those microcosms. In contrast, in the abiotic microcosm no sulfide increase was observed in the first 24h, after which the sulfide concentration doubled (from 0.8 to 1.65 μM, Figure S4-3), which is in agreement with the methylmercury evolution (Figure S4-1) and supports the conclusion that the gamma-radiation method used did not sterilize the sediment completely, and longer irradiation is necessary for these sediments. Moreover, the SRR presented in Figure S4-4 also confirmed this statement, a highly increased rate being measured in the irradiated sediment (i.e. 277 nmol cm^{-3} d^{-1} after 24h). The MPR in the abiotic (A) microcosm was not different from the one in the B1 microcosm and just slightly decreased when compared with the natural (N) one, which proved that microbes were not inhibited

in this treatment. Also, for this experiment the MPR were measured by headspace method but using 5 ml sediment transferred at t=0h in 20 mL serum vials and sealed. For further experiments a higher amount (i.e. 100 mL) is recommended to reduce the variability of results.

Inhibitor Concentration Test Description and Results

In parallel, the SRB and MPA inhibitor concentrations were tested on different samples by measuring the SRR and methane concentrations at the beginning and after 24h incubation, using the methods described in the materials and methods section of this chapter. In case of MPR, a smaller sample amount (5mL) was transferred in serum vials and incubated for 24h, this being a preliminary experiment. The headspace gas was sampled at the beginning (T=0h) and after 24h, and transferred in 10 mL exetainers for GC analysis.

Regarding the sodium molybdate (SRB inhibitor), a wide range of concentrations varying between 0.1 and 20 mM was tested. Previously, Pak and Bartha (1998) used concentrations of 20 mM sodium molybdate in their inhibition experiment with marine sediments. Researchers have suggested that the appropriate concentration for molybdate application to sediments is equimolar to that of ambient sulfate [Oremland and Capone, 1988]. Fleming et al. (2006) pointed out that in previous research studies of freshwater sediments, excessive molybdate concentrations (20 mM) might cause a more general inhibition of many sediment microbial processes. These authors found that a molybdate concentration of 0.2 mM was high enough to eliminate virtually all sulfate reduction activity and generally inhibited less than one-half of the total sediment activity for mercury methylation. This is in agreement with findings of Winfrey and Rudd (1990) who also explored the impact of a range of molybdate concentrations on Hg methylation with freshwater sediments.

For sodium 2-bromoethane sulfonate (BES, $BrCH_2CH_2SO_3Na$), "specific" inhibitor for methanogens, the concentrations tested were between 2 and 20 mM based on studies by Oremland (1988) and Compeau and Bartha (1985).

Figure S4-5 presents the molybdate (a) and BES (b) inhibition test results obtained with SLR sediments in June 2007. We observed that in SLR sediments concentrations as low as 0.1 mM produced an inhibition of sulfate reducing activity by 95%, and concentrations between 1 and –20 mM caused an inhibition of almost 100%. Consequently, considering these results and to ensure the

coverage of a wider range of sulfate concentrations, the 2 mM sodium molybdate concentration was chosen for the next experiments (July 2007) with SLR sediments. This was also in agreement with other studies [Flemming et al., 2006] that used concentrations between 0.2 and 4 mM of molybdate for SRB inhibition in experiments performed with Clare Lake sediment.

As shown in Figure S4-3, the lowest methane production rate (12 nmol cm^{-3} d^{-1}) was obtained with a concentration of 20 mM BES applied, corresponding to an inhibition of cca 80% of methane production in sediments. The concentration of BES varied with the type of the sediment and even with the time of sampling as suggested by Oremland (1988), a critical amount being more efficient than higher concentrations. To ensure an effective inhibition, many authors used a concentration of 30 mM BES for inhibition of methanogens in sediments [i.e., Compeau and Bartha, 1985]. Considering our tests results and other study recommendations, we considered BES concentrations of 10 and 20 mM for our next incubation experiments.

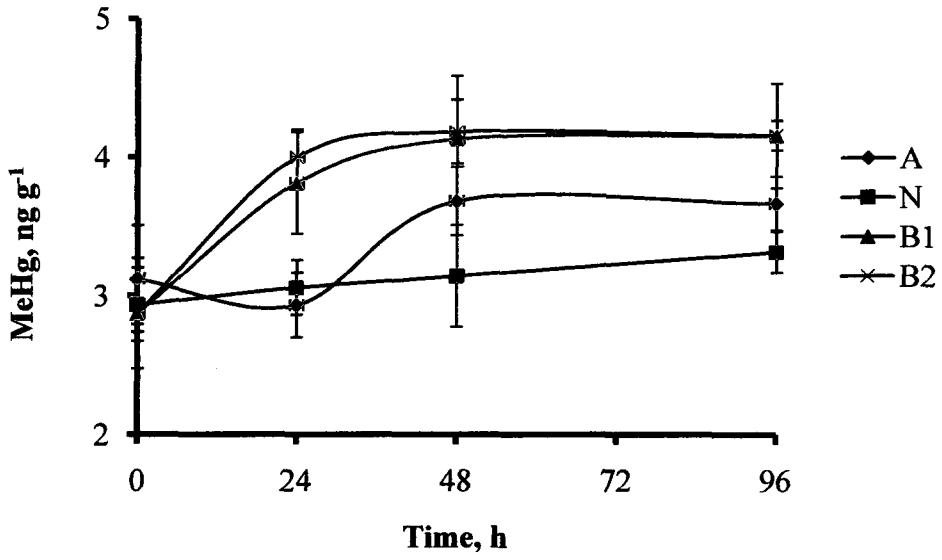

Figure S4-1. Average total MeHg trend (ng g^{-1} d.w., n=3) during the 96h microcosm incubations (June 2007): A (◆), N (■), B1 (▲), B2 (×). The microcosms' description is in Table S4-1.

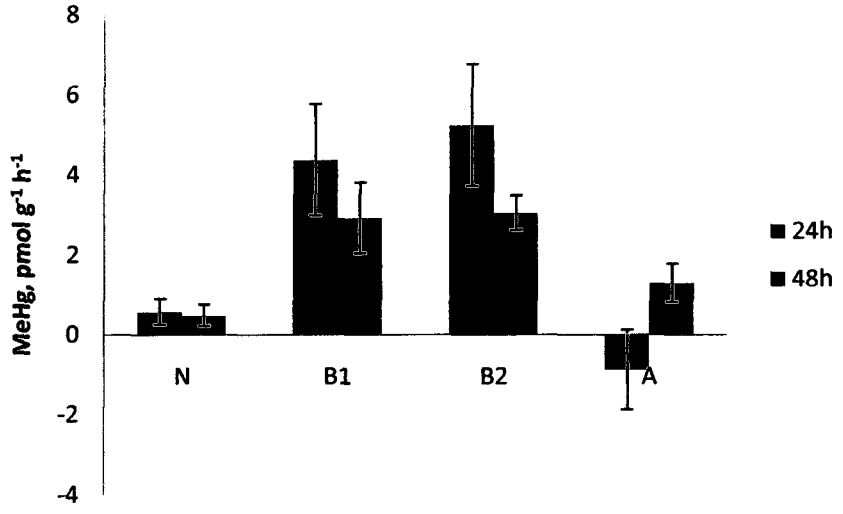

Figure S4-2. Mercury methylation rates (pmol g^{-1} h^{-1}) in St Lawrence River incubation microcosms (June 2007). Error bars represent the standard error (SE) for n=3 replicates. The microcosm's description is in Table S4-1.

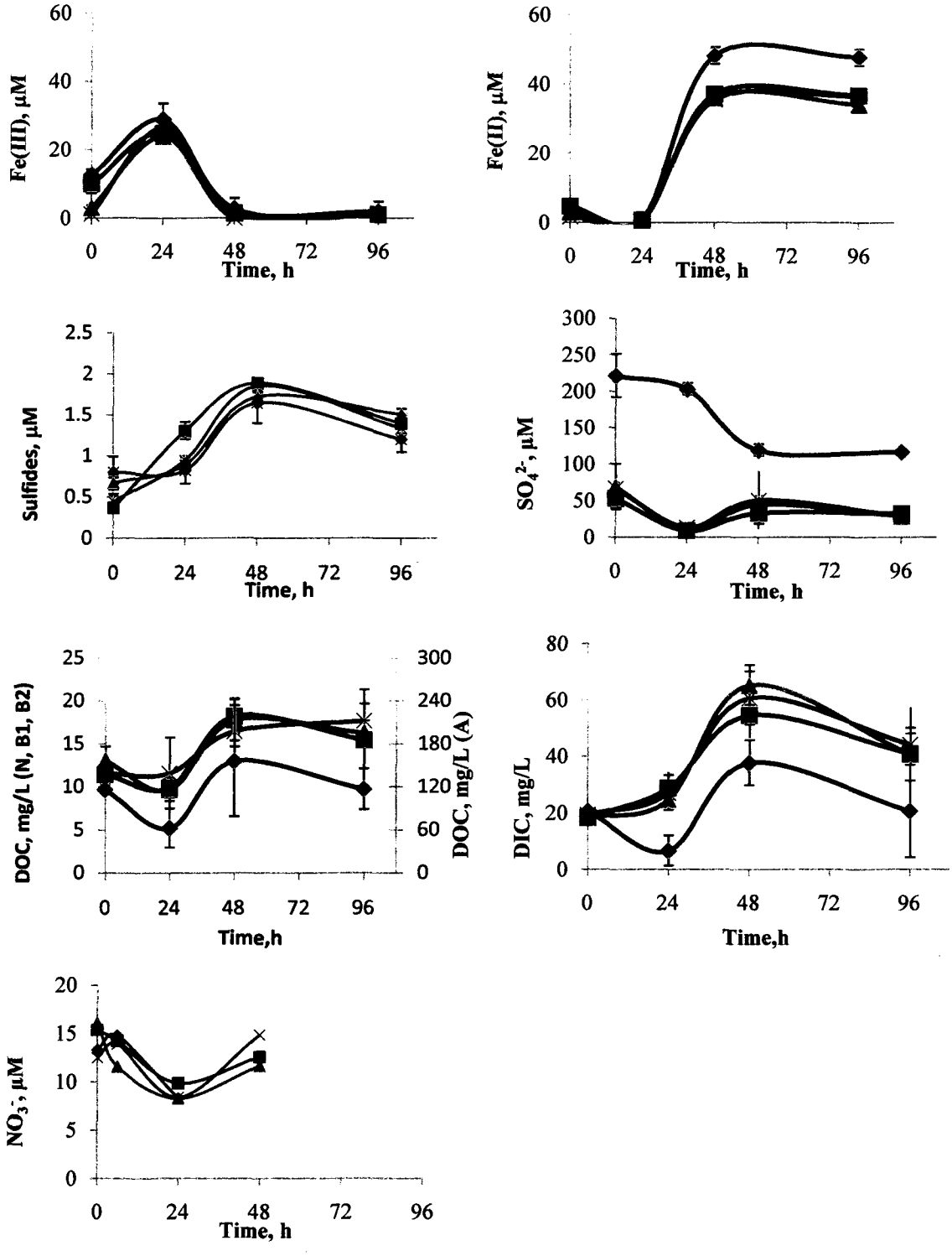

Figure S4-3. Porewater characteristics during the 96h microcosm incubations: N(×), B1(■), B2(▲), A(◆) (ferrous iron (a), ferric iron (b), sulfides (c), sulfates (d), DOC (e), DIC (f), NO^{3-} (g). Error bars represent standard error (SE). The description of microcosms is presented in Table S4-1.

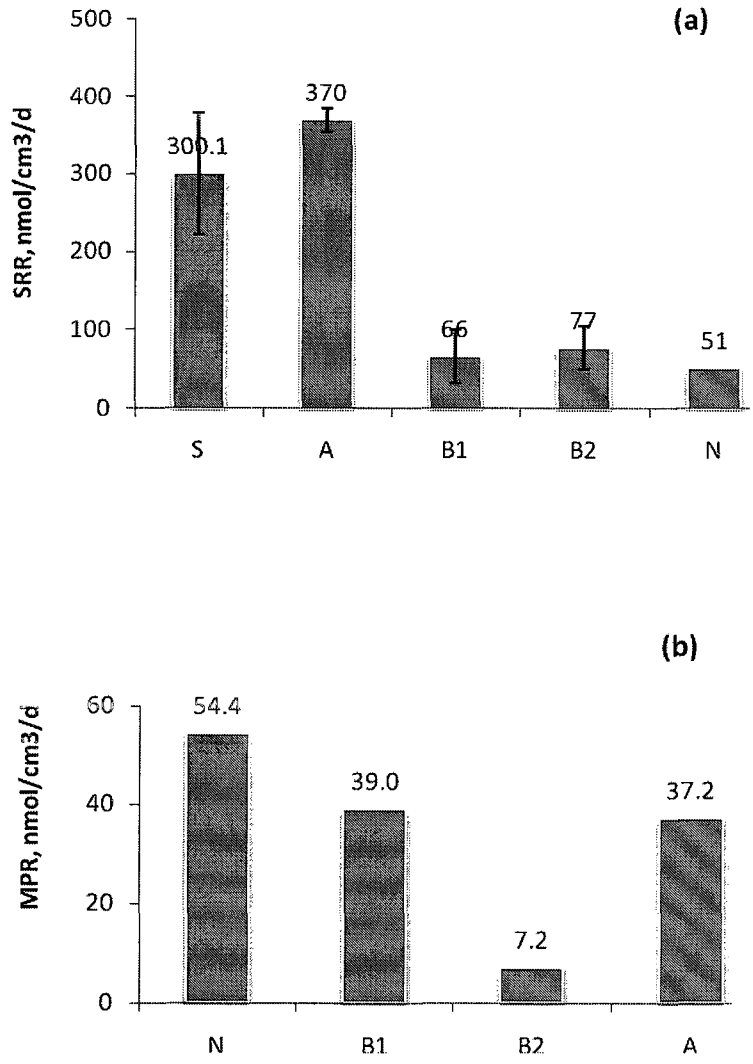

Figure S4-4. Sulfate Reduction Rates (a) and Methane Production Rates (b) in the St. Lawrence River incubation microcosms (June 2007). Error bars represent the standard error (SE) for n=3 replicates. The microcosms' description is presented in Table S4-1.

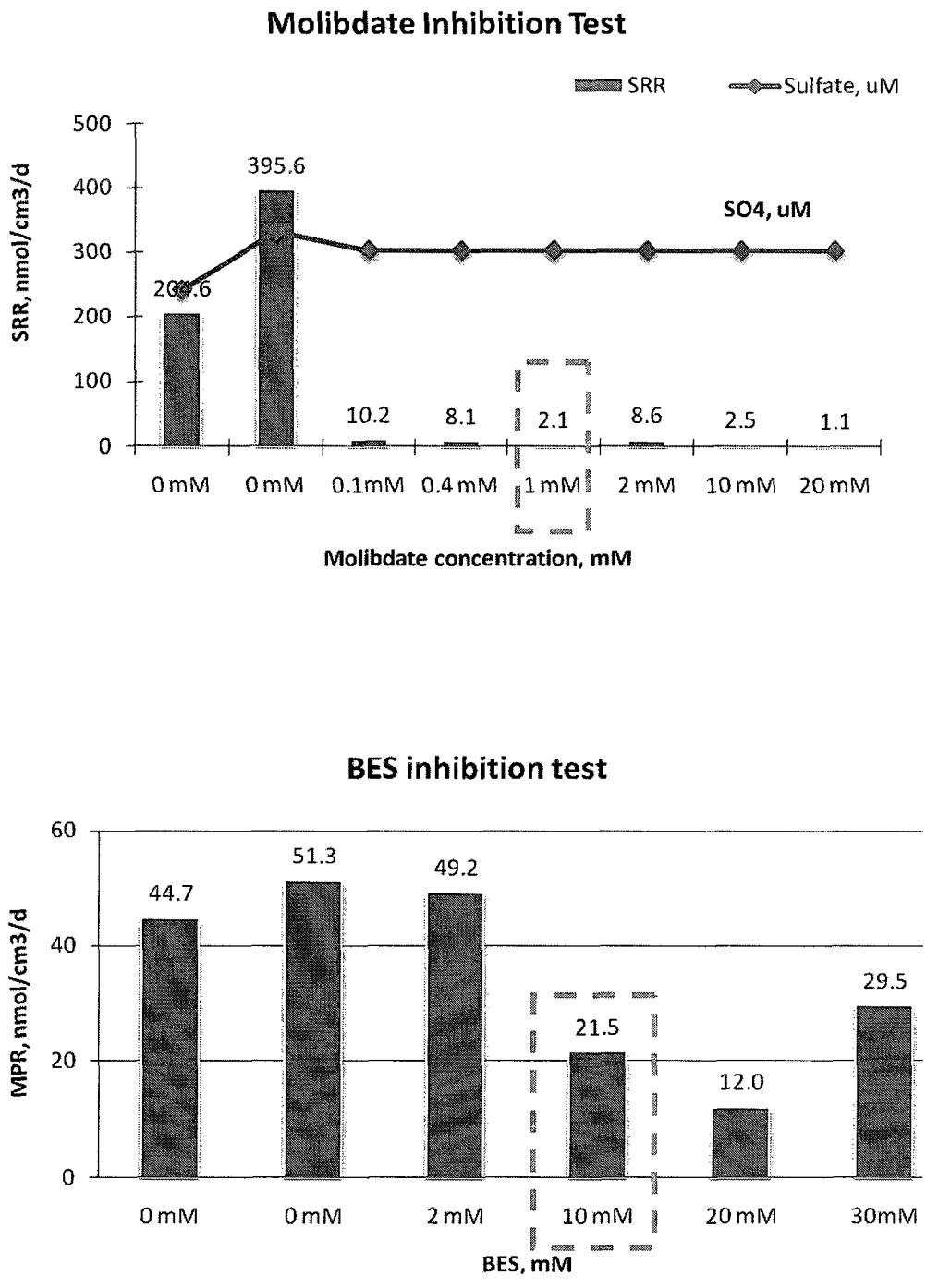

Figure S4-5. Sulfate Reduction Rates and sulfate concentrations (a) and Methane Production Rates (b) measured during inhibitor concentration tests performed with the St. Lawrence River sediments (June 2007). The chosen concentration is marked by the green rectangle.

Table S4-1. Statistical test (student t-test) results for the mercury methylation rate comparison among microcosms (H0: mean X = mean Y)

X vs Y	mean X	mean Y	t Stat	df	n	p	Statistical significance	
N vs B1	0.55	4.37	-2.67	2	3	0.056	< 0.04	significant difference
N vs B2	0.55	5.25	-3.01	2	3	0.040	< 0.05	significant difference
N vs A	0.55	-0.88	1.35	2	3	0.247	> 0.05	
B1 vs B2	4.37	5.25	-0.42	2	3	0.693	> 0.05	
B1 vs A	4.37	-0.88	3.07	2	3	0.037	< 0.04	significant difference
B2 vs A	5.25	-0.88	3.36	2	3	0.028	< 0.05	significant difference

Table S4-2. Iron Reduction Rates (FeRR) and Methane Production Rates (MPR) determined by linear regression (y = a * x + b) of the produced Fe^{2+} and methane, respectively, against sampling time (3 days). (H0: there is no relationship between CH4 (mmol/cm3) and Time (day) results)

Microcosm ID	df	Slope	Intercept	se	t-value	F	r^2	p-value	Statistical signification	Regression Equation
Iron Reduction Rates (FeRR) determined by linear regression (y = a * x + b) of the Fe^{2+} against sampling time (3 days)										
N1	7	**0.69**	0.08	0.12	5.54	30.70	0.81	p< 0.05	reject H0	[Fe^{2+}, uM] = 0.69* time(d) + 0.08
T1	7	**1.12**	0.00	0.17	6.73	45.25	0.87	p < 0.05	reject H0	[Fe^{2+}, uM] = 1.12* time(d)
T2	7	**1.74**	0.22	0.51	3.39	11.48	0.62	p < 0.05	reject H0	[Fe^{2+}, uM] = 1.74* time(d) + 0.22
T3	7	**7.53**	-1.69	1.56	4.83	23.33	0.77	p < 0.05	reject H0	[Fe^{2+}, uM] = 7.53* time(d) -1.69
T4	7	**14.60**	-3.48	2.71	5.38	28.99	0.81	p < 0.05	reject H0	[Fe^{2+}, uM] = 14.6* time(d) - 3.48
A1	7	**9.09**	2.84	1.92	4.72	22.32	0.76	p < 0.05	reject H0	[Fe^{2+}, uM] = 9.09* time(d) + 2.84
Methane Production Rates (MPR) determined by linear regression (y = a * x + b) of the methane produced against sampling time (3 days)										
N1	13	**72.55**	-0.24	2.42	30.03	901.50	0.99	< 0.05	reject H0	[CH4, uM] = 72.55 * time(d) - 0.24
T1	13	**89.53**	-3.30	4.48	19.98	399.20	0.97	< 0.05	reject H0	[CH4, uM] = 89.53 * time(d) - 3.30
T2	13	**76.27**	-0.69	3.46	22.03	485.10	0.97	< 0.05	reject H0	[CH4, uM] = 76.27 * time(d) - 0.69
T3	13	**10.03**	6.99	0.65	15.46	239.10	0.95	< 0.05	reject H0	[CH4, uM] = 10.03 * time(d)+ 6.99
T4	13	**9.18**	6.81	0.82	11.22	126.00	0.91	< 0.05	reject H0	[CH4, uM] = 9.18 * time(d) + 6.18
A1	13	**0.02**	0.47	0.04	0.51	0.26	0.02	> 0.05	accept H0	

Simple model I regression assumptions were checked using the plots resulting from the regression procedure (ANOVA):

Residuals vs fit plot: For any value of X, the Y's are independently and normally distributed (residuals are normally distributed)

Normal QQ plot of residuals: The variances of Y for fixed X are independent of X

Table S4-3. Statistical tests (two-Sample t-Test) results for SRR, FeRR, and MPA comparison among microcosms.

Rate	Procedure (X vs Y)	mean X	mean Y	t	df	p	Statistical signification (H0: mean X = mean Y)		
SRR	N1 vs T1	61.9	68.4	-0.442	3	0.69	> 0.05	accept H0	
SRR	N1 vs T2	61.9	0.1	8.627	2	0.01	< 0.05	reject H0	significant difference
SRR	N1 vs T3	61.9	65.1	-0.214	3	0.84	> 0.05	accept H0	
SRR	N1 vs T4	61.9	0.9	8.508	2	0.01	< 0.05	reject H0	significant difference
SRR	N1 vs A1	61.9	0.1	8.633	2	0.01	< 0.05	reject H0	significant difference
SRR	T1 vs T2	68.4	0.1	5.299	2	0.03	< 0.05	reject H0	significant difference
SRR	T1 vs T3	68.4	65.1	0.182	4	0.86	> 0.05	accept H0	
SRR	T1 vs T4	68.4	0.9	5.237	2	0.03	< 0.05	reject H0	significant difference
SRR	T1 vs A1	68.4	0.1	5.302	2	0.03	< 0.05	reject H0	significant difference
SRR	T2 vs T3	0.1	65.1	-4.976	2	-0.04	< 0.05	reject H0	significant difference
SRR	T2 vs T4	0.1	0.9	-1.9594	2	0.17	> 0.05	accept H0	
SRR	T2 vs A1	0.1	0.1	0.3109	3	0.78	> 0.05	accept H0	
SRR	T3 vs T4	65.1	0.9	4.915	2	0.04	< 0.05	reject H0	significant difference
SRR	T3 vs A1	65.1	0.1	4.9791	2	0.04	< 0.05	reject H0	significant difference
SRR	T4 vs A1	0.9	0.1	2.11	2	0.16	> 0.05	accept H0	
FeRR	N1 vs T1	0.68	1.13	-1.91	4	0.13	> 0.05	accept H0	
FeRR	N1 vs T2	0.68	1.77	-1.71	2	0.22	> 0.05	accept H0	
FeRR	N1 vs T3	0.68	7.56	-4.84	2	0.04	< 0.05	reject H0	significant difference
FeRR	N1 vs T4	0.68	14.66	-7.34	2	0.02	< 0.05	reject H0	significant difference
FeRR	N1 vs A1	0.68	9.41	-6.68	2	0.02	< 0.05	reject H0	significant difference
FeRR	T1 vs T2	1.13	1.77	-0.99	2	0.41	> 0.05	accept H0	

Table S4-3 (continued)

FeRR	T1 vs T3	1.13	7.56	-4.50	2	0.04	< 0.05	reject H0	significant difference
FeRR	T1 vs T4	1.13	14.66	-7.08	2	0.02	< 0.05	reject H0	significant difference
FeRR	T1 vs A1	1.13	9.41	-6.31	2	0.02	< 0.05	reject H0	significant difference
FeRR	T2 vs T3	1.77	7.56	-3.74	3	0.04	< 0.05	reject H0	significant difference
FeRR	T2 vs T4	1.77	14.66	-6.44	2	0.01	< 0.05	reject H0	significant difference
FeRR	T2 vs A1	1.77	9.41	-5.31	3	0.01	< 0.05	reject H0	significant difference
FeRR	T3 vs T4	7.56	14.66	-3.00	4	0.04	< 0.05	reject H0	significant difference
FeRR	T3 vs A1	7.56	9.41	-0.96	4	0.39	> 0.05	accept H0	
FeRR	T4 vs A1	14.66	9.41	2.28	4	0.09	> 0.06	accept H0	
MPR	N vs T1	72.6	89.5	-2.02	3	0.13	> 0.05	accept H0	
MPR	N vs T2	72.6	76.3	-0.51	4	0.64	> 0.05	accept H0	
MPR	N vs T3	72.6	10.0	14.42	2	0.005	< 0.05	reject H0	significant difference
MPR	N vs T4	72.6	9.2	14.13	2	0.003	< 0.05	reject H0	significant difference
MPR	N vs A1	72.6	0.0	16.78	2	0.004	< 0.05	reject H0	significant difference
MPR	T1 vs T2	89.5	76.3	1.43	4	0.23	> 0.05	accept H0	
MPR	T1 vs T3	89.5	10.0	11.01	2	0.01	< 0.05	reject H0	significant difference
MPR	T1 vs T4	89.5	9.2	10.99	2	0.01	< 0.06	reject H0	significant difference
MPR	T1 vs A1	89.5	0.0	12.41	2	0.01	< 0.07	reject H0	significant difference
MPR	T2 vs T3	76.3	10.0	11.35	2	0.01	< 0.08	reject H0	significant difference
MPR	T2 vs T4	76.3	9.2	11.28	2	0.01	< 0.09	reject H0	significant difference
MPR	T2 vs A1	76.3	0.0	13.09	2	0.01	< 0.10	reject H0	significant difference
MPR	T3 vs T4	10.0	9.2	0.69	2	0.55	> 0.05	accept H0	
MPR	T3 vs A1	10.0	0.0	28.78	2	0.001	< 0.12	reject H0	significant difference
MPR	T4 vs A1	9.2	0.0	7.67	2	0.02	< 0.13	reject H0	significant difference

Table S4-4 Phreeqci Saturation index (SI) results for all microcosms incubated (July 2009)

Natural (N1) microcosm, T=0h

Phase	SI	log IAP	log KT	
Cinnabar	**6.20**	-38.99	-45.19	HgS
Fe2(SO4)3	-48.00	-44.42	3.58	Fe2(SO4)3
Fe3(OH)8	-3.27	16.95	20.22	Fe3(OH)8
Ferrihydrite	0.66	5.55	4.89	Fe(OH)3
FeS(ppt)	-4.07	-7.99	-3.92	FeS
Goethite	5.05	5.55	0.50	FeOOH
Greigite	6.66	-38.38	-45.03	Fe3S4
Hematite	15.11	11.10	-4.01	Fe2O3
Hg(OH)2	-21.66	-25.16	-3.50	Hg(OH)2
HgSO4	-34.25	-43.67	-9.42	HgSO4
Jarosite-H	-8.26	-20.36	-12.10	(H3O)Fe3(SO4)2(OH)6
Lepidocrocite	4.18	5.55	1.37	FeOOH
Mackinawite	-3.34	-7.99	-4.65	FeS
Maghemite	4.72	11.10	6.39	Fe2O3
Magnetite	**13.21**	16.95	3.74	Fe3O4
Melanterite	-10.19	-12.66	-2.47	FeSO4:7H2O
Metacinnabar	5.83	-38.99	-44.82	HgS
Montroydite	-21.51	-25.16	-3.65	HgO
O2(g)	-32.16	50.96	83.12	O2
Pyrite	22.14	3.66	-18.48	FeS2
Sulfur	13.76	11.65	-2.11	S

N1, t=24h

Phase	SI	log IAP	log KT	
Cinnabar	5.61	-39.58	-45.19	HgS
Fe2(SO4)3	-46.15	-42.57	3.58	Fe2(SO4)3
Fe3(OH)8	1.87	22.09	20.22	Fe3(OH)8
Ferrihydrite	2.09	6.98	4.89	Fe(OH)3
FeS(ppt)	-2.08	-5.99	-3.92	FeS
Goethite	6.48	6.98	0.50	FeOOH
Greigite	10.67	-34.37	-45.03	Fe3S4
Hematite	17.97	13.97	-4.01	Fe2O3
Hg(OH)2	-21.97	-25.46	-3.50	Hg(OH)2
HgSO4	-34.89	-44.31	-9.42	HgSO4
Jarosite-H	-4.64	-16.74	-12.10	(H3O)Fe3(SO4)2(OH)6
Lepidocrocite	5.61	6.98	1.37	FeOOH
Mackinawite	-1.34	-5.99	-4.65	FeS
Maghemite	7.58	13.97	6.39	Fe2O3
Magnetite	18.35	22.09	3.74	Fe3O4
Melanterite	-8.25	-10.72	-2.47	FeSO4:7H2O
Metacinnabar	5.24	-39.58	-44.82	HgS
Montroydite	-21.81	-25.46	-3.65	HgO
O2(g)	-35.55	47.57	83.12	O2
Pyrite	22.16	3.68	-18.48	FeS2
Sulfur	11.78	9.67	-2.11	S

N, t=46h

Phase	SI	log IAP	log KT	
Cinnabar	5.07	-40.11	-45.19	HgS
Fe2(SO4)3	-44.38	-40.80	3.58	Fe2(SO4)3
Fe3(OH)8	3.43	23.66	20.22	Fe3(OH)8
Ferrihydrite	2.83	7.72	4.89	Fe(OH)3
FeS(ppt)	-1.53	-5.45	-3.92	FeS
Goethite	7.22	7.72	0.50	FeOOH
Greigite	14.01	-31.03	-45.03	Fe3S4
Hematite	19.44	15.43	-4.01	Fe2O3
Hg(OH)2	-22.95	-26.44	-3.50	Hg(OH)2
HgSO4	-35.77	-45.19	-9.42	HgSO4
Jarosite-H	-2.24	-14.34	-12.10	(H3O)Fe3(SO4)2(OH)6
Lepidocrocite	6.35	7.72	1.37	FeOOH
Mackinawite	-0.80	-5.45	-4.65	FeS
Maghemite	9.05	15.43	6.39	Fe2O3
Magnetite	19.92	23.66	3.74	Fe3O4
Melanterite	-8.05	-10.52	-2.47	FeSO4:7H2O
Metacinnabar	4.71	-40.11	-44.82	HgS
Montroydite	-22.79	-26.44	-3.65	HgO
O2(g)	-33.01	50.11	83.12	O2
Pyrite	24.41	5.94	-18.48	FeS2
Sulfur	13.49	11.38	-2.11	S

Abiotic (A1) microcosm

A1, t=0h

Phase	SI	log IAP	log KT	
Cinnabar	15.77	-29.42	-45.19	HgS
FeS(ppt)	-10.99	-14.90	-3.92	FeS
Hg(OH)2	-4.14	-7.64	-3.50	
HgSO4	-15.98	-25.40	-9.42	HgSO4
Mackinawite	-10.25	-14.90	-4.65	FeS
Melanterite	-8.41	-10.88	-2.47	FeSO4:7H2O
Metacinnabar	15.40	-29.42	-44.82	HgS
Montroydite	-3.99	-7.64	-3.65	HgO
O2(g)	-53.64	29.48	83.12	O2
Pyrite	-3.47	-21.95	-18.48	FeS2
Sulfur	-4.93	-7.04	-2.11	S

A1, t=24h

Phase	SI	log IAP	log KT	
Cinnabar	15.79	-29.40	-45.19	HgS
Fe2(SO4)3	-43.43	-39.85	3.58	Fe2(SO4)3
Fe3(OH)8	3.69	23.91	20.22	Fe3(OH)8
Ferrihydrite	2.56	7.45	4.89	Fe(OH)3
FeS(ppt)	-9.23	-13.14	-3.92	FeS
Goethite	6.95	7.45	0.50	FeOOH
Greigite	-19.64	-64.68	-45.03	Fe3S4
Hematite	18.91	14.91	-4.01	Fe2O3
Hg(OH)2	-3.76	-7.25	-3.50	Hg(OH)2
HgSO4	-16.09	-25.50	-9.42	HgSO4
Jarosite-H	-2.05	-14.15	-12.10	(H3O)Fe3(SO4)2(OH)6
Lepidocrocite	6.08	7.45	1.37	FeOOH
Mackinawite	-8.49	-13.14	-4.65	FeS
Maghemite	8.52	14.91	6.39	Fe2O3
Magnetite	20.17	23.91	3.74	Fe3O4
Melanterite	-6.78	-9.25	-2.47	FeSO4:7H2O
Metacinnabar	15.42	-29.40	-44.82	HgS
Montroydite	-3.60	-7.25	-3.65	HgO
O2(g)	-37.20	45.92	83.12	O2
Pyrite	6.15	-12.33	-18.48	FeS2
Sulfur	2.92	0.81	-2.11	S

A1 t=46h

Phase	SI	log IAP	log KT	
Cinnabar	16.05	-29.14	-45.19	HgS
Fe2(SO4)3	-43.56	-39.98	3.58	Fe2(SO4)3
Fe3(OH)8	3.71	23.94	20.22	Fe3(OH)8
Ferrihydrite	2.56	7.45	4.89	Fe(OH)3
FeS(ppt)	-9.42	-13.33	-3.92	FeS
Goethite	6.95	7.45	0.50	FeOOH
Greigite	-20.52	-65.56	-45.03	Fe3S4
Hematite	18.90	14.89	-4.01	Fe2O3
Hg(OH)2	-3.27	-6.77	-3.50	Hg(OH)2
HgSO4	-15.64	-25.06	-9.42	HgSO4
Jarosite-H	-2.14	-14.24	-12.10	(H3O)Fe3(SO4)2(OH)6
Lepidocrocite	6.08	7.45	1.37	FeOOH
Mackinawite	-8.68	-13.33	-4.65	FeS
Maghemite	8.51	14.89	6.39	Fe2O3
Magnetite	20.20	23.94	3.74	Fe3O4
Melanterite	-6.78	-9.25	-2.47	FeSO4:7H2O
Metacinnabar	15.68	-29.14	-44.82	HgS
Montroydite	-3.12	-6.77	-3.65	HgO
O2(g)	-37.38	45.74	83.12	O2
Pyrite	5.65	-12.83	-18.48	FeS2
Sulfur	2.61	0.50	-2.11	S

T1 (Just Hg spikes added) microcosm

T1, t=0h

Phase	SI	log IAP	log KT	
Cinnabar	15.93	-29.25	-45.19	HgS
Hg(OH)2	-3.28	-6.78	-3.50	Hg(OH)2
HgSO4	-15.86	-25.27	-9.42	HgSO4
Metacinnabar	15.57	-29.25	-44.82	HgS
Montroydite	-3.13	-6.78	-3.65	HgO
O2(g)	-69.36	13.76	83.12	O2
Sulfur	-13.48	-15.59	-2.11	S

T1, t=24h

Phase	SI	log IAP	log KT	
Cinnabar	15.59	-29.60	-45.19	HgS
Fe2(SO4)3	-44.62	-41.04	3.58	Fe2(SO4)3
Fe3(OH)8	2.82	23.04	20.22	Fe3(OH)8
Ferrihydrite	2.53	7.42	4.89	Fe(OH)3
FeS(ppt)	-10.89	-14.81	-3.92	FeS
Goethite	6.92	7.42	0.50	FeOOH
Greigite	-23.91	-68.95	-45.03	Fe3S4
Hematite	18.86	14.85	-4.01	Fe2O3
Hg(OH)2	-3.10	-6.60	-3.50	Hg(OH)2
HgSO4	-15.81	-25.23	-9.42	HgSO4
Jarosite-H	-2.89	-14.99	-12.10	(H3O)Fe3(SO4)2(OH)6
Lepidocrocite	6.05	7.42	1.37	FeOOH
Mackinawite	-10.16	-14.81	-4.65	FeS
Maghemite	8.46	14.85	6.39	Fe2O3
Magnetite	19.30	23.04	3.74	Fe3O4
Melanterite	-7.97	-10.44	-2.47	FeSO4:7H2O
Metacinnabar	15.23	-29.60	-44.82	HgS
Montroydite	-2.95	-6.60	-3.65	HgO
O2(g)	-34.06	49.06	83.12	O2
Pyrite	5.21	-13.27	-18.48	FeS2
Sulfur	3.65	1.54	-2.11	S

T1, t=46h

Phase	SI	log IAP	log KT	
Cinnabar	7.44	-37.74	-45.19	HgS
Fe2(SO4)3	-43.88	-40.30	3.58	Fe2(SO4)3
Fe3(OH)8	4.31	24.53	20.22	Fe3(OH)8
Ferrihydrite	3.12	8.01	4.89	Fe(OH)3
FeS(ppt)	-1.82	-5.74	-3.92	FeS
Goethite	7.51	8.01	0.50	FeOOH
Greigite	12.55	-32.48	-45.03	Fe3S4
Hematite	20.02	16.02	-4.01	Fe2O3
Hg(OH)2	-19.99	-23.49	-3.50	Hg(OH)2
HgSO4	-32.84	-42.26	-9.42	HgSO4
Jarosite-H	-1.42	-13.52	-12.10	(H3O)Fe3(SO4)2(OH)6
Lepidocrocite	6.64	8.01	1.37	FeOOH
Mackinawite	-1.09	-5.74	-4.65	FeS
Maghemite	9.63	16.02	6.39	Fe2O3
Magnetite	20.80	24.53	3.74	Fe3O4
Melanterite	-7.79	-10.26	-2.47	FeSO4:7H2O
Metacinnabar	7.08	-37.74	-44.82	HgS
Montroydite	-19.84	-23.49	-3.65	HgO
O2(g)	-33.02	50.10	83.12	O2
Pyrite	23.54	5.06	-18.48	FeS2
Sulfur	12.90	10.79	-2.11	S

T2 (Hg spikes and SRB inhibitor) microcosm

T2, t=0h

Phase	SI	log IAP	log KT	
Cinnabar	6.02	-39.17	-45.19	HgS
Fe2(SO4)3	-43.66	-40.08	3.58	Fe2(SO4)3
Fe3(OH)8	-0.70	19.52	20.22	Fe3(OH)8
Ferrihydrite	1.64	6.53	4.89	Fe(OH)3
FeS(ppt)	-1.93	-5.84	-3.92	FeS
Goethite	6.03	6.53	0.50	FeOOH
Greigite	15.38	-29.65	-45.03	Fe3S4
Hematite	17.08	13.07	-4.01	Fe2O3
Hg(OH)2	-23.38	-26.87	-3.50	Hg(OH)2
HgSO4	-35.17	-44.59	-9.42	HgSO4
Jarosite-H	-3.73	-15.83	-12.10	(H3O)Fe3(SO4)2(OH)6
Lepidocrocite	5.16	6.53	1.37	FeOOH
Mackinawite	-1.19	-5.84	-4.65	FeS
Maghemite	6.68	13.07	6.39	Fe2O3
Magnetite	15.78	19.52	3.74	Fe3O4
Melanterite	-8.79	-11.26	-2.47	FeSO4:7H2O
Metacinnabar	5.65	-39.17	-44.82	HgS
Montroydite	-23.22	-26.87	-3.65	HgO
O2(g)	-30.66	52.46	83.12	O2
Pyrite	26.57	8.09	-18.48	FeS2
Sulfur	16.05	13.94	-2.11	S

T2, t=24h

Phase	SI	log IAP	log KT	
Cinnabar	5.60	-39.59	-45.19	HgS
Fe2(SO4)3	-42.42	-38.84	3.58	Fe2(SO4)3
Fe3(OH)8	3.82	24.04	20.22	Fe3(OH)8
Ferrihydrite	2.89	7.78	4.89	Fe(OH)3
FeS(ppt)	-0.02	-3.93	-3.92	FeS
Goethite	7.28	7.78	0.50	FeOOH
Greigite	19.43	-25.61	-45.03	Fe3S4
Hematite	19.57	15.56	-4.01	Fe2O3
Hg(OH)2	-23.68	-27.18	-3.50	Hg(OH)2
HgSO4	-35.89	-45.31	-9.42	HgSO4
Jarosite-H	-0.82	-12.92	-12.10	(H3O)Fe3(SO4)2(OH)6
Lepidocrocite	6.41	7.78	1.37	FeOOH
Mackinawite	0.71	-3.93	-4.65	FeS
Maghemite	9.18	15.56	6.39	Fe2O3
Magnetite	20.31	24.04	3.74	Fe3O4
Melanterite	-7.18	-9.65	-2.47	FeSO4:7H2O
Metacinnabar	5.23	-39.59	-44.82	HgS
Montroydite	-23.53	-27.18	-3.65	HgO
O2(g)	-33.79	49.33	83.12	O2
Pyrite	26.80	8.32	-18.48	FeS2
Sulfur	14.36	12.25	-2.11	S

T2, t=46h

Phase	SI	log IAP	log KT	
Cinnabar	5.72	-39.47	-45.19	HgS
Fe2(SO4)3	-42.06	-38.48	3.58	Fe2(SO4)3
Fe3(OH)8	4.57	24.79	20.22	Fe3(OH)8
Ferrihydrite	3.10	7.99	4.89	Fe(OH)3
FeS(ppt)	0.27	-3.65	-3.92	FeS
Goethite	7.49	7.99	0.50	FeOOH
Greigite	19.96	-25.07	-45.03	Fe3S4
Hematite	19.98	15.98	-4.01	Fe2O3
Hg(OH)2	-23.51	-27.00	-3.50	Hg(OH)2
HgSO4	-35.74	-45.16	-9.42	HgSO4
Jarosite-H	-0.24	-12.34	-12.10	(H3O)Fe3(SO4)2(OH)6
Lepidocrocite	6.62	7.99	1.37	FeOOH
Mackinawite	1.00	-3.65	-4.65	FeS
Maghemite	9.59	15.98	6.39	Fe2O3
Magnetite	21.06	24.79	3.74	Fe3O4
Melanterite	-6.86	-9.33	-2.47	FeSO4:7H2O
Metacinnabar	5.35	-39.47	-44.82	HgS
Montroydite	-23.35	-27.00	-3.65	HgO
O2(g)	-34.31	48.81	83.12	O2
Pyrite	26.77	8.29	-18.48	FeS2
Sulfur	14.05	11.94	-2.11	S

T3 (Hg spikes and MPA inhibitor) microcosm

T3, t=0h

Phase	SI	log IAP	log KT	
Cinnabar	15.95	-29.24	-45.19	HgS
Fe2(SO4)3	-46.23	-42.65	3.58	Fe2(SO4)3
Fe3(OH)8	-1.24	18.98	20.22	Fe3(OH)8
Ferrihydrite	1.33	6.22	4.89	Fe(OH)3
FeS(ppt)	-12.10	-16.02	-3.92	FeS
Goethite	5.72	6.22	0.50	FeOOH
Greigite	-26.22	-71.25	-45.03	Fe3S4
Hematite	16.45	12.44	-4.01	Fe2O3
Hg(OH)2	-3.18	-6.68	-3.50	Hg(OH)2
HgSO4	-15.62	-25.04	-9.42	HgSO4
Jarosite-H	-5.97	-18.07	-12.10	(H3O)Fe3(SO4)2(OH)6
Lepidocrocite	4.85	6.22	1.37	FeOOH
Mackinawite	-11.37	-16.02	-4.65	FeS
Maghemite	6.05	12.44	6.39	Fe2O3
Magnetite	15.24	18.98	3.74	Fe3O4
Melanterite	-9.35	-11.82	-2.47	FeSO4:7H2O
Metacinnabar	15.59	-29.24	-44.82	HgS
Montroydite	-3.03	-6.68	-3.65	HgO
O2(g)	-32.27	50.85	83.12	O2
Pyrite	5.33	-13.15	-18.48	FeS2
Sulfur	4.97	2.86	-2.11	S

T3, t=24h

Phase	SI	log IAP	log KT	
Cinnabar	5.88	-39.31	-45.19	HgS
Fe2(SO4)3	-42.41	-38.83	3.58	Fe2(SO4)3
Fe3(OH)8	3.45	23.67	20.22	Fe3(OH)8
Ferrihydrite	2.83	7.72	4.89	Fe(OH)3
FeS(ppt)	-0.26	-4.18	-3.92	FeS
Goethite	7.22	7.72	0.50	FeOOH
Greigite	19.08	-25.95	-45.03	Fe3S4
Hematite	19.45	15.44	-4.01	Fe2O3
Hg(OH)2	-23.40	-26.90	-3.50	Hg(OH)2
HgSO4	-35.57	-44.99	-9.42	HgSO4
Jarosite-H	-0.92	-13.02	-12.10	(H3O)Fe3(SO4)2(OH)6
Lepidocrocite	6.35	7.72	1.37	FeOOH
Mackinawite	0.47	-4.18	-4.65	FeS
Maghemite	9.06	15.44	6.39	Fe2O3
Magnetite	19.94	23.67	3.74	Fe3O4
Melanterite	-7.39	-9.86	-2.47	FeSO4:7H2O
Metacinnabar	5.52	-39.31	-44.82	HgS
Montroydite	-23.25	-26.90	-3.65	HgO
O2(g)	-33.02	50.10	83.12	O2
Pyrite	26.94	8.47	-18.48	FeS2
Sulfur	14.75	12.64	-2.11	S

T3, t=46h

Phase	SI	log IAP	log KT	
Cinnabar	15.86	-29.33	-45.19	HgS
Fe2(SO4)3	-42.35	-38.77	3.58	Fe2(SO4)3
Fe3(OH)8	5.62	25.84	20.22	Fe3(OH)8
Ferrihydrite	3.46	8.35	4.89	Fe(OH)3
FeS(ppt)	-9.66	-13.57	-3.92	FeS
Goethite	7.85	8.35	0.50	FeOOH
Greigite	-19.95	-64.99	-45.03	Fe3S4
Hematite	20.71	16.71	-4.01	Fe2O3
Hg(OH)2	-3.12	-6.62	-3.50	Hg(OH)2
HgSO4	-15.69	-25.11	-9.42	HgSO4
Jarosite-H	0.17	-11.93	-12.10	(H3O)Fe3(SO4)2(OH)6
Lepidocrocite	6.98	8.35	1.37	FeOOH
Mackinawite	-8.92	-13.57	-4.65	FeS
Maghemite	10.32	16.71	6.39	Fe2O3
Magnetite	22.11	25.84	3.74	Fe3O4
Melanterite	-6.89	-9.36	-2.47	FeSO4:7H2O
Metacinnabar	15.49	-29.33	-44.82	HgS
Montroydite	-2.97	-6.62	-3.65	HgO
O2(g)	-34.13	48.99	83.12	O2
Pyrite	6.70	-11.78	-18.48	FeS2
Sulfur	3.90	1.79	-2.11	S

T4 (Hg spikes, SRB and MPA inhibitor) microcosm

T4, t=0h

Phase	SI	log IAP	log KT	
Cinnabar	6.00	-39.18	-45.19	HgS
Fe2(SO4)3	-44.14	-40.56	3.58	Fe2(SO4)3
Fe3(OH)8	-0.31	19.91	20.22	Fe3(OH)8
Ferrihydrite	1.61	6.50	4.89	Fe(OH)3
FeS(ppt)	-1.50	-5.41	-3.92	FeS
Goethite	6.00	6.50	0.50	FeOOH
Greigite	15.68	-29.35	-45.03	Fe3S4
Hematite	17.02	13.01	-4.01	Fe2O3
Hg(OH)2	-23.37	-26.87	-3.50	Hg(OH)2
HgSO4	-35.31	-44.72	-9.42	HgSO4
Jarosite-H	-4.10	-16.20	-12.10	(H3O)Fe3(SO4)2(OH)6
Lepidocrocite	5.13	6.50	1.37	FeOOH
Mackinawite	-0.76	-5.41	-4.65	FeS
Maghemite	6.62	13.01	6.39	Fe2O3
Magnetite	16.18	19.91	3.74	Fe3O4
Melanterite	-8.48	-10.95	-2.47	FeSO4:7H2O
Metacinnabar	5.64	-39.18	-44.82	HgS
Montroydite	-23.22	-26.87	-3.65	HgO
O2(g)	-32.60	50.52	83.12	O2
Pyrite	26.01	7.53	-18.48	FeS2
Sulfur	15.05	12.94	-2.11	S

T4, t=24h

Phase	SI	log IAP	log KT	
Cinnabar	5.81	-39.38	-45.19	HgS
Fe2(SO4)3	-41.48	-37.90	3.58	Fe2(SO4)3
Fe3(OH)8	4.98	25.20	20.22	Fe3(OH)8
Ferrihydrite	3.39	8.28	4.89	Fe(OH)3
FeS(ppt)	0.09	-3.82	-3.92	FeS
Goethite	7.78	8.28	0.50	FeOOH
Greigite	20.39	-24.65	-45.03	Fe3S4
Hematite	20.57	16.56	-4.01	Fe2O3
Hg(OH)2	-23.42	-26.92	-3.50	Hg(OH)2
HgSO4	-35.65	-45.07	-9.42	HgSO4
Jarosite-H	0.63	-11.47	-12.10	(H3O)Fe3(SO4)2(OH)6
Lepidocrocite	6.91	8.28	1.37	FeOOH
Mackinawite	0.83	-3.82	-4.65	FeS
Maghemite	10.17	16.56	6.39	Fe2O3
Magnetite	21.47	25.20	3.74	Fe3O4
Melanterite	-7.04	-9.51	-2.47	FeSO4:7H2O
Metacinnabar	5.44	-39.38	-44.82	HgS
Montroydite	-23.27	-26.92	-3.65	HgO
O2(g)	-32.44	50.68	83.12	O2
Pyrite	27.54	9.06	-18.48	FeS2
Sulfur	14.99	12.88	-2.11	S

T4, t=46h

Phase	SI	log IAP	log KT	
Cinnabar	5.81	-39.37	-45.19	HgS
Fe2(SO4)3	-41.61	-38.03	3.58	Fe2(SO4)3
Fe3(OH)8	5.84	26.06	20.22	Fe3(OH)8
Ferrihydrite	3.34	8.23	4.89	Fe(OH)3
FeS(ppt)	0.94	-2.97	-3.92	FeS
Goethite	7.73	8.23	0.50	FeOOH
Greigite	20.81	-24.23	-45.03	Fe3S4
Hematite	20.47	16.46	-4.01	Fe2O3
Hg(OH)2	-23.31	-26.80	-3.50	Hg(OH)2
HgSO4	-35.55	-44.97	-9.42	HgSO4
Jarosite-H	0.46	-11.64	-12.10	(H3O)Fe3(SO4)2(OH)6
Lepidocrocite	6.86	8.23	1.37	FeOOH
Mackinawite	1.68	-2.97	-4.65	FeS
Maghemite	10.07	16.46	6.39	Fe2O3
Magnetite	22.32	26.06	3.74	Fe3O4
Melanterite	-6.09	-8.56	-2.47	FeSO4:7H2O
Metacinnabar	5.45	-39.37	-44.82	HgS
Montroydite	-23.15	-26.80	-3.65	HgO
O2(g)	-36.48	46.64	83.12	O2
Pyrite	26.26	7.78	-18.48	FeS2
Sulfur	12.86	10.75	-2.11	S

Table S4-5. XL fit results of curve fitting of ambient MeHg data (202 isotope) for the calculation of ambient Km and Kd values.

	N1	T1	T2	T3	T4	A1
Km/Kd	0.003	0.004	0.003	0.005	0.003	0.0014
Kd	0.084	0.067	0.084	0.071	7.6E+37	7.0E-02
Km	0.0003	0.0003	0.0002	0.0003	2.0E+35	9.9E-05
F-test p	0.007	0.027	0.001	0.021	0.012	0.874
T-test p	0.1850	0.193	0.181	0.189	0.173	0.387
r^2	0.517	0.467	0.272	0.576	0.150	0.038
t ½	8.3	10.3	8.2	9.8	0.0	9.9
km/kd (1-exp$^{(-kd*t)}$)	**N1**	**T1**	**T2**	**T3**	**T4**	**A1**
24	0.0028	0.0035	0.0025	0.0040	0.0026	0.0012
24	0.0028	0.0035	0.0025	0.0040	0.0026	0.0012
46	0.0032	0.0042	0.0028	0.0047	0.0026	0.0014
46	0.0032	0.0042	0.0028	0.0047	0.0026	0.0014
94	0.0033	0.0044	0.0028	0.0049	0.0026	0.0014
94	0.0033	0.0044	0.0028	0.0049	0.0026	0.0014
[MeHg]predicted	**N1**	**T1**	**T2**	**T3**	**T4**	**A1**
24	2.1	2.6	2.5	3.3	3.0	1.0
24	2.1	2.6	2.5	3.3	3.0	1.0
46	2.4	3.1	2.8	3.9	3.0	1.2
46	2.4	3.1	2.8	3.9	3.0	1.2
94	2.4	3.3	2.9	4.1	3.0	1.2
94	2.4	3.3	2.9	4.1	3.0	1.2
[MeHg]measured	**N1**	**T1**	**T2**	**T3**	**T4**	**A1**
24	2.6	2.8	2.6	3.5	3.8	1.7
24	3.2	2.8	2.7	3.9	2.8	1.7
46	3.2	3.1	3.1	4.0	2.9	2.4
46	3.5	3.5	3.1	3.7	3.1	1.8
94	3.5	3.4	3.2	5.2	3.5	2.9
94	3.0	3.6	2.8	4.0	3.2	1.8

Table S4-6. Statistical analysis results for the relationship between porewater characteristics (pH, Eh, dissolved iron, sulfate, and sulfide) and different MeHg isotope concentrations in the microcosms. (H0: there is no relationship between pore water characteristics and MeHg concentration; linear regression for 46h).

MeHg Isotope	Characteristic	Assay	slope	r^2	F	Df	p	Significance
200	pH	A1	0.062	0.06	0.26	4	0.27	
200	pH	N1	-0.005	0.00	0.01	4	0.92	
200	pH	T1	23.428	0.96	93.10	4	0.00	< 0.05
200	pH	T2	8.578	0.88	28.50	4	0.01	< 0.05
200	pH	T3	18.030	0.76	12.97	4	0.02	< 0.05
200	pH	T4	4.952	0.88	28.03	4	0.01	< 0.05
200	Eh	A1	0.000	0.14	0.65	4	0.11	
200	Eh	N1	0.000	0.11	0.49	4	0.52	
200	Eh	T1	-0.060	0.05	0.23	4	0.65	
200	Eh	T2	-0.034	0.51	4.22	4	0.11	
200	Eh	T3	-0.138	0.85	23.53	4	0.01	< 0.05
200	Eh	T4	-0.010	0.65	7.57	4	0.05	< 0.05
200	Fe^{2+}	A1	0.001	0.18	0.89	4	0.40	
200	Fe^{2+}	N1	-0.004	0.10	0.43	4	0.55	
200	Fe^{2+}	T1	2.183	0.69	8.99	4	0.04	< 0.05
200	Fe^{2+}	T2	0.393	0.64	6.97	4	0.06	
200	Fe^{2+}	T3	0.440	0.54	4.68	4	0.10	
200	Fe^{2+}	T4	0.022	0.34	2.09	4	0.22	
200	Fe^{3+}	A1	0.002	0.16	0.76	4	0.43	
200	Fe^{3+}	N1	0.000	0.20	0.97	4	0.38	
200	Fe^{3+}	T1	0.250	0.64	7.10	4	0.06	< 0.05
200	Fe^{3+}	T2	0.063	0.56	5.07	4	0.09	< 0.05
200	Fe^{3+}	T3	0.093	0.53	4.48	4	0.10	
200	Fe^{3+}	T4	0.027	0.90	36.96	4	0.00	< 0.05
200	Sulfate	A1	-0.001	0.33	1.96	4	0.23	
200	Sulfate	N1	0.002	0.56	5.08	4	0.09	
200	Sulfate	T1	0.201	0.33	1.95	4	0.24	
200	Sulfate	T2	-0.029	0.34	2.08	4	0.22	
200	Sulfate	T3	0.121	0.88	30.13	4	0.01	< 0.05
200	Sulfate	T4	0.008	0.08	0.37	4	0.58	
200	Sulfides	A1	-0.168	0.12	0.57	4	0.49	
200	Sulfides	N1	-0.054	0.35	2.17	4	0.22	
200	Sulfides	T1	4.037	0.16	0.79	4	0.43	
200	Sulfides	T2	-0.510	0.20	1.02	4	0.37	
200	Sulfides	T3	0.270	0.13	0.59	4	0.49	
200	Sulfides	T4	-0.465	0.53	4.55	4	0.10	
199	pH	A1	0.945	0.08	0.34	4	0.19	
199	pH	N1	0.055	0.13	0.59	4	0.49	
199	pH	T1	-1.728	0.48	3.76	4	0.13	

199	pH	T2	-3.086	0.53	4.44	4	0.10	
199	pH	T3	-0.088	0.00	0.01	4	0.93	
199	pH	T4	0.344	0.00	0.02	4	0.91	
199	Eh	A1	-0.002	0.23	1.19	4	0.50	
199	Eh	N1	0.055	0.13	0.59	4	0.25	
199	Eh	T1	-0.002	0.00	0.01	4	0.91	
199	Eh	T2	0.020	0.80	15.62	4	0.13	
199	Eh	T3	0.006	0.18	0.91	4	0.40	
199	Eh	T4	-0.001	0.01	0.05	4	0.83	
199	Fe^{2+}	A1	0.022	0.37	2.38	4	0.20	
199	Fe^{2+}	N1	0.001	0.00	0.00	4	0.95	
199	Fe^{2+}	T1	-0.255	0.88	28.71	4	0.01	< 0.05
199	Fe^{2+}	T2	-0.117	0.26	1.43	4	0.30	
199	Fe^{2+}	T3	-0.030	0.34	2.04	4	0.23	
199	Fe^{2+}	T4	-0.011	0.08	0.36	4	0.58	
199	Fe^{3+}	A1	0.041	0.28	1.54	4	0.28	
199	Fe^{3+}	N1	-0.001	0.11	0.50	4	0.52	
199	Fe^{3+}	T1	-0.025	0.60	6.00	4	0.07	
199	Fe^{3+}	T2	-0.018	0.21	1.09	4	0.35	
199	Fe^{3+}	T3	-0.007	0.43	3.02	4	0.16	
199	Fe^{3+}	T4	0.005	0.03	0.11	4	0.76	
199	Sulfate	A1	-0.020	0.82	18.10	4	0.01	< 0.05
199	Sulfate	N1	-0.004	0.62	6.57	4	0.06	
199	Sulfate	T1	-0.017	0.22	1.12	4	0.35	
199	Sulfate	T2	0.004	0.03	0.14	4	0.73	
199	Sulfate	T3	-0.006	0.31	1.79	4	0.25	
199	Sulfate	T4	0.008	0.08	0.35	4	0.58	
199	Sulfides	A1	0.084	0.00	0.00	4	0.98	
199	Sulfides	N1	-0.078	0.27	1.46	4	0.29	
199	Sulfides	T1	-0.608	0.35	2.12	4	0.22	
199	Sulfides	T2	0.153	0.09	0.37	4	0.57	
199	Sulfides	T3	0.019	0.08	0.37	4	0.58	
199	Sulfides	T4	0.105	0.03	0.10	4	0.76	
202	pH	A1	0.020	0.00	0.00	4	0.40	
202	pH	N1	2.618	0.31	1.78	4	0.25	
202	pH	T1	2.604	0.56	5.03	4	0.09	
202	pH	T2	0.964	0.19	0.96	4	0.39	
202	pH	T3	2.275	0.78	14.24	4	0.02	
202	pH	T4	0.895	0.05	0.23	4	0.66	
202	Eh	A1	-0.002	0.40	2.68	4	0.02	< 0.05
202	Eh	N1	0.000	0.00	0.00	4	0.99	
202	Eh	T1	0.004	0.01	0.05	4	0.83	
202	Eh	T2	0.000	0.00	0.00	4	1.00	
202	Eh	T3	-0.017	0.82	17.88	4	0.01	< 0.05
202	Eh	T4	-0.003	0.13	0.59	4	0.49	
202	Fe^{2+}	A1	0.024	0.55	4.82	4	0.09	
202	Fe^{2+}	N1	0.474	0.66	7.60	4	0.05	< 0.05

202	Fe^{2+}	T1	0.281	0.54	4.66	4	0.10	
202	Fe^{2+}	T2	0.096	0.66	7.75	4	0.05	
202	Fe^{2+}	T3	0.055	0.53	4.54	4	0.10	
202	Fe^{2+}	T4	-0.002	0.00	0.02	4	0.90	
202	Fe^{3+}	A1	0.044	0.41	2.76	4	0.17	
202	Fe^{3+}	N1	0.045	0.72	10.12	4	0.03	< 0.05
202	Fe^{3+}	T1	0.038	0.71	9.78	4	0.04	< 0.05
202	Fe^{3+}	T2	0.017	0.72	10.38	4	0.03	
202	Fe^{3+}	T3	0.011	0.47	3.61	4	0.13	
202	Fe^{3+}	T4	0.008	0.14	0.66	4	0.46	
202	Sulfate	A1	-0.011	0.31	1.84	4	0.25	
202	Sulfate	N1	0.074	0.19	0.93	4	0.39	
202	Sulfate	T1	0.037	0.53	4.48	4	0.10	
202	Sulfate	T2	-0.006	0.30	1.69	4	0.26	
202	Sulfate	T3	0.015	0.92	49.04	4	0.00	< 0.05
202	Sulfate	T4	0.004	0.04	0.15	4	0.71	
202	Sulfides	A1	-0.248	0.00	0.01	4	0.93	
202	Sulfides	N1	1.300	0.08	0.34	4	0.59	
202	Sulfides	T1	0.992	0.47	3.49	4	0.14	
202	Sulfides	T2	-0.009	0.00	0.00	4	0.95	
202	Sulfides	T3	0.013	0.02	0.08	4	0.79	
202	Sulfides	T4	-0.075	0.03	0.11	4	0.76	
ΣMeHg	pH	A1	1.028	0.04	0.15	4	0.43	
ΣMeHg	pH	N1	2.668	0.33	1.95	4	0.24	
ΣMeHg	pH	T1	24.304	0.92	47.76	4	0.00	< 0.05
ΣMeHg	pH	T2	6.456	0.67	8.12	4	0.05	< 0.05
ΣMeHg	pH	T3	20.216	0.82	18.37	4	0.01	< 0.05
ΣMeHg	pH	T4	6.190	0.30	1.68	4	0.26	
ΣMeHg	Eh	A1	-0.004	0.43	3.01	4	0.03	
ΣMeHg	Eh	N1	-0.001	0.00	0.00	4	0.97	
ΣMeHg	Eh	T1	-0.057	0.04	0.19	4	0.69	
ΣMeHg	Eh	T2	-0.014	0.12	0.56	4	0.49	
ΣMeHg	Eh	T3	-0.150	0.85	23.44	4	0.01	< 0.05
ΣMeHg	Eh	T4	-0.015	0.30	1.74	4	0.26	
ΣMeHg	Fe^{2+}	A1	0.048	0.63	6.93	4	0.06	< 0.05
ΣMeHg	Fe^{2+}	N1	0.471	0.66	7.90	4	0.05	< 0.05
ΣMeHg	Fe^{2+}	T1	2.209	0.63	6.91	4	0.06	< 0.05
ΣMeHg	Fe^{2+}	T2	0.371	0.76	12.99	4	0.02	< 0.05
ΣMeHg	Fe^{2+}	T3	0.464	0.51	4.21	4	0.11	
ΣMeHg	Fe^{2+}	T4	0.009	0.01	0.05	4	0.83	
ΣMeHg	Fe^{3+}	A1	0.087	0.47	3.62	4	0.13	
ΣMeHg	Fe^{3+}	N1	0.044	0.70	9.41	4	0.04	< 0.05
ΣMeHg	Fe^{3+}	T1	0.263	0.63	6.94	4	0.06	< 0.05
ΣMeHg	Fe^{3+}	T2	0.062	0.73	10.80	4	0.03	< 0.05
ΣMeHg	Fe^{3+}	T3	0.097	0.49	3.81	4	0.12	
ΣMeHg	Fe^{3+}	T4	0.040	0.42	2.88	4	0.17	

ΣMeHg	Sulfate	A1	-0.033	0.79	14.64	4	0.02	< 0.05
ΣMeHg	Sulfate	N1	0.072	0.18	0.90	4	0.40	
ΣMeHg	Sulfate	T1	0.221	0.36	2.20	4	0.21	
ΣMeHg	Sulfate	T2	-0.031	0.54	4.63	4	0.10	
ΣMeHg	Sulfate	T3	0.130	0.87	27.65	4	0.01	< 0.05
ΣMeHg	Sulfate	T4	0.020	0.11	0.52	4	0.51	
ΣMeHg	Sulfides	A1	-0.332	0.00	0.00	4	0.95	
ΣMeHg	Sulfides	N1	1.168	0.07	0.28	4	0.62	
ΣMeHg	Sulfides	T1	4.420	0.18	0.86	4	0.41	
ΣMeHg	Sulfides	T2	-0.366	0.14	0.66	4	0.46	
ΣMeHg	Sulfides	T3	0.302	0.14	0.64	4	0.47	
ΣMeHg	Sulfides	T4	-0.434	0.10	0.45	4	0.54	

CHAPTER 5: CONCLUSIONS AND PERSPECTIVES ON FUTURE RESEARCH

This study shows the importance of biotic pathways in net methylmercury production in freshwater systems, but abiotic pathways were also investigated. The net amount of methylmercury formed and the rates of methylation and demethylation depend on mercury speciation under certain conditions, the activity of methylating microbes, as well as several environmental factors such as pH, temperature, presence of complexing agents, especially sulfides and organic matter.

Chapter 2 shows a new modified procedure for measuring mercury isotopes in sediment samples. This procedure uses acid leaching-ion exchange-thiosulfate extraction (TSE) to isolate and purify the methylated mercury from the matrix. The new TSE procedure offers the advantages of artefact-free formation and low detection limits, as well as the possibility of quantification of individual isotopes of mercury. Other important advantages of the TSE procedure include the extraction and analysis of a large number of samples in a short time and excellent analyte recoveries (94-106%). Moreover, the high sensitivity of the ethylation step and the use of ICP-MS offer the advantage of a low detection limit which allows the application of this new method to analyze samples bearing trace levels of MeHg as presented in this study.

Chapter 3 demonstrates that specific inhibitors and enriched isotope additions are a useful methodology for studying the role of various microbes in Hg methylation. The combined use of specific inhibitors (sodium molybdate and sodium 2-bromoethan sulfonate) indicated that iron reducing microbes (FeRP) may be responsible for some mercury methylation although future experiments are necessary. In Mer Bleue sediments, mercury methylation proceeded very fast, in some cases reaching an equilibrium or steady state within 24 hours. In contrast, methylmercury demethylation evolved linearly for 72h. Inhibition of both sulfate reducers and methanogens slowed down the net methylmercury production but did not completely stop it (it continued throughout the 72h period) indicating that other processes, biotic (iron reducing microbes) or abiotic, may also be very important. Our results also showed that newly added tracers were more available for transformation than ambient species, and low spike concentrations (<100% increase in THg) should be used in future experiments to be closer to natural conditions. The strong positive correlation of

both methylation (Km) and demethylation (Kd) rate constants with sulfate reducing rates (SRR) indicates that sulfate reducing bacteria (SRB) are involved in both methylation and demethylation processes in the Mer Bleue sediments. In contrast, the negative relationship between Km or Kd and iron reduction rates (FeRR) shows that the increase in FeRR affects both methylation and demethylation processes, but to a different degree, which was reflected in the observed increase in M/D ratios. The strong positive relationship obtained in all microcosms between methylmercury concentrations (200 isotope) and porewater ferrous iron also supports the influence of iron reduction on net methylation in Mer Bleue sediments in the long term. Moreover, a strong negative relationship between methylmercury isotopes and Eh for all microcosms except for the SRB inhibited (202 isotope) one also shows that SRB are involved in the methylation process in the Mer Bleue wetland. The increase in demethylation with the increase in SRR shows that SRB are also involved in demethylation processes in the Mer Bleue sediments, presumably by oxidative demethylation (OD). In addition, the decrease in demethylation rate constants in all microcosms treated with inhibitors indicate that oxidative demethylation may be an important pathway for methylmercury demethylation in the Mer Bleue sediments in which both sulfate reducers and methanogens are involved. Their separate or simultaneous involvement in the process may be driven by the redox conditions in the Mer Bleue sediments, as methylmercury concentrations are strong correlated to the redox potential (Eh). Future experiments with abiotic and iron oxide spiked microcosms should be set up to assess the contribution of abiotic processes and the importance of iron-reducers on methylmercury formation or demethylation. All those findings are in agreement with the hypothesis that MeHg production and degradation are influenced by interspecific competition among SRB, MPA and FeRP for electron donors.

Chapter 4 demonstrated that in the St. Lawrence River (Zone 1) sediments, as in the Mer Bleue case, the inhibition of certain groups of microbes clearly had an effect on methylation and demethylation processes which answers the second hypothesis (Chapter 4, H2), methylmercury production and degradation are influenced by interspecific competition among SRB, MPA and FeRP for electron donors. Our data indicate that in the St. Lawrence River, SRB are the primary methylators and methanogens might have the leading role in

MeHg demethylation, while the abiotic pathways have the lowest contribution to net MeHg production in the sediments, contradicting the first hypothesis (Chapter 4, H1) that abiotic methylation is the principal pathway for methyl mercury formation.

The findings for the SLR sediments are in agreement with the Mer Bleue ones with respect to the effect of sulfate-reducers and methanogens in net MeHg formation. The inhibition of methanogens stimulated net methylation, not only by inhibiting demethylation, but also by stimulating methylation, along with the stimulation of the SRB activity. Iron reduction (FeRR) might however be another important process in the production of MeHg in aquatic environments because the inhibition of both SRB and MPA enhanced the iron reduction rate and MeHg production was not completely stopped. The strong positive correlation between Km and sulfate reducing rates, and between Kd and methane production rates, clearly supports the fact that sulfate-reducing bacteria are involved in mercury methylation and methanogens in methylmercury demethylation in the Zone 1 SLR sediments. In contrast, as it was the case in Mer Bleue, the strong negative correlation between Kd and FeRR shows that the increase in FeRR corresponds to a decrease in demethylation, which may indicate that iron reduction may influence net methylation in the Zone 1 SLR sediments by decreasing demethylation rather than favouring methylation in the long term.

Overall, all microcosms, with the exception of the methanogen inhibited one, favored demethylation over methylation, and the degree of magnitude of the ratios indicated that they varied with the type of active microbes. The calculated demethylation rate constants translated into a relatively long half-life (8.3 d^{-1}) for the native MeHg in sediments, higher than that (1.6 d^{-1}) calculated for Mer Bleue. In contrast, the half-life of the added tracers was lower (0.4 - 3 d^{-1}), decreasing with the SRB inhibition (T2: 0.4 d^{-1}) and increasing with the MPA inhibition (T3: 2.6 and T4: 3.0 d^{-1}). This is an important observation since the residence time of MeHg in sediments affects its availability to biota. In the case of the St. Lawrence River Zone 1, if we consider the historical pollution with Hg and wood fibbers in the area and the recent increase in methanogenic activity, we can suggest that a natural remediation system has evolved over time in the sediments in which increased methanogenic activity will increase the demethylation processes (through OD) which in turn will reduce the residence

time of MeHg in the sediments, therefore reducing its availability to biota. The existence of a well developed *mer* mediated detoxification system in the SLR sediments cannot be ruled out knowing that the *mer* detoxification is extensive in aquatic environments, especially in contaminated sediments.

To clarify the role of FeRP in net Hg methylation, further experiments should be carried out with hydrous ferric oxide amendments to the sediments, along with Hg isotopes and microbial inhibitors for shorter incubation periods (24h) and more frequent sampling (i.e. 6h, 12h, 24h). Also, *mer* mediated demethylation should be investigated to clarify the importance and role of *mer* mediated detoxification in this system. Considering the influence of different anaerobic microbes on methylmercury production and degradation, as well as the importance of redox conditions and dissolved iron on net methylmercury production observed in this study, monitoring the seasonal changes in pH, redox potential, dissolved iron and sulfate, along with changes in Hg concentration and microbial activity (SRB, MPA, FeRP) would give more information on the methylation potential variation in those sediments, as well as factors affecting mercury availability for methylation and accumulation in this zone of the St. Lawrence River.